ON THE MECHANISM OF TITANIUM-TARTRATE CATALYZED ASYMMETRIC EPOXIDATION

M.G. FINN

SUBMITTED TO THE DEPARTMENT OF
CHEMISTRY IN PARTIAL
FULFILLMENT OF THE
REQUIREMENTS FOR THE
DEGREE OF

DOCTOR OF PHILOSOPHY IN
INORGANIC CHEMISTRY

at the

MASSACHUSETTS INSTITUTE OF TECHNOLOGY

December, 1985

Signature of Author .. ..
Department of Chemistry
December 24, 1985

Certified by ....
K. Barry Sharpless
Thesis Supervisor

Accepted by ... .
Glenn A. Berchtold
Chairman, Department Committee

This doctoral thesis has been examined by a Committee of the Department of Chemistry as follows:

Professor Satoru Masamune _____
Chairman

Professor K. Barry Sharpless _____
Thesis Supervisor

Professor Frederick D. Greene _____

ON THE MECHANISM OF TITANIUM-TARTRATE CATALYZED ASYMMETRIC EPOXIDATION

by

M.G. FINN

Submitted to the Department of Chemistry on
December 24, 1985, in partial fulfillment of the
requirements for the Degree of Doctor of Philosophy
in Inorganic Chemistry

An exploration of the structures and properties of titanium-tartrate complexes in solution was undertaken in order to develop a detailed understanding of the mechanism of the asymmetric epoxidation reaction.

The equilibrium constants for exchange of alkyl hydroperoxides for alkoxides in Ti(IV) complexes were found to be sensitive to the steric natures of both the hydroperoxide and the titanium complex.

Molecular weight measurements showed $[Ti(tartrate)(OR)_2]_x$ to be dimeric in solution. Proton and ^{13}C NMR studies demonstrated that the asymmetric epoxidation system is not composed of only one Ti-tartrate species; small amounts of Ti-tartrate species of other than a 1:1 stoichiometry are present in such solutions. However, pseudo-first order kinetics measurements provided evidence that $[Ti(tartrate)(OR)_2]_2$ is by far the most active catalyst in the mixture. To explore the solvent dependence of the reaction, rates of asymmetric epoxidation were measured in CH_2Cl_2, pentane, and ether. Both the polar, coordinating solvent (ether) and the nonpolar solvent (pentane) were found to decrease the rate of reaction relative to that in CH_2Cl_2. The experimental rate law was found to be different in pentane than in the other two solvents tested.

Proton, carbon, and oxygen NMR studies of $[Ti(tartrate)(OR)_2]_2$ in solution, along with difference FTIR measurements of deuterium-labeled alkoxide complexes, were found to be consistent with structures of Ti-tartrate derivatives previously found by x-ray crystallography. A secondary deuterium isotope effect study was performed, indicating that epoxidation occurs with simultaneous formation of C-O bonds in the transition state. Using a proposed catalyst structure analogous to those found by x-ray crystallography, a detailed mechanism for asymmetric epoxidation was suggested, with several possibile sources of asymmetric induction defined.

Thesis Supervisor: K. Barry Sharpless

Title: Professor of Chemistry

Acknowledgements

If you're lucky, doing graduate research is like building a house with your family: they see you day in and day out in every mood and temper, and they like you anyway. I have been very lucky, and the Sharpless group "family" has been unstinting with their comraderie, assistance, and support. Indeed, the reader will notice that I have included results from many group members in this thesis. One of my chief joys has been the fact that my investigation of the asymmetric epoxidation mechanism has allowed me to stick my nose into everybody else's business, and thus have I been patiently taught chemistry by everyone in the laboratory.

I spare a small measure of pity for you, gentle reader, when you peruse the following list of individuals to whom I am indebted. For me, every name carries with it rich images and many stories, but for you it's just a list. If you're one of the names, I hope your images and stories are as delightful as mine. Thanks to:

Scott Woodard, for his excellent work (much quoted here) and careful teaching. Victor Martin and Tsutomu Katsuki, for many compounds borrowed and much advice rendered, and also for the inspiration of their remarkable bay (if not their notebooks). Teruhiko Ishii and Muneo Takatani, for things adamantyl. Uttam and Mitaly Pati, for great food. Albert Lee, for useful techniques; Fred and Ann Walker, for helpful discussions and a good cookout or two. The late Larry Reed III, whose most untimely passing has robbed us of a man of intellectual excellence and buoyant spirit, and to Ann Carr. Linda Lu Chang, for a rewarding collaboration on tartrate analogues and tartramides (meaning that she did most of the work).

Carl Behrens, for patience with silly questions, nmr dissections, many rides home, and discussions of philosophy. Mary Jean Schweiter, for items borrowed and for her chemical and philosophical contributions. Tom Erickson and Dave Tuddenham, for Coarse Golf. Curtis Adams and Toni Chancellor, for chemical advice and hot salsa, respectively. Steve Viti, for tee-offs, taxes, and tip-ins. Roy and Jian Johnson, for an enjoyable collaboration. Sotaro and Yasuko Miyano, for bringing good advice and great sukiyaki to our bay. Mamoru Uchiyama, for caricatures. Ken and Rena Kirshenbaum, for good chemistry, welcome dinners, and especially for the Beagle Fund. Maurice Caron and Micheline Collin, for advice, chemicals,

and the punk party, all "Caron-Grade". Rob Ronald, for his wisdom in chemistry and food, and for Rigoletto. David and Sally Hollinshead, for patience in explaining organic chemistry, much laughter, and for showing me how to dunk.

Drew Burns, for much discussion and useful results and far too many four-putts. J. Gordon Hill, for very interesting chemistry and for being unguardable on the court. Pui Tong Ho, for many drybox favors. Janice Klunder and Soo Ko, for informative and enjoyable talks. Paul Carlier, for the same, plus feeding the cat. Yun Gao, for showing us all how to learn, be it chemistry, basketball, or skiing. Chris Burns and Cheryl Martin, for delightful companionship in the late night hours. Jon Ellman, for producing good humor and excellent chemistry through a long series of reactions. Pam Shapiro, for persevering through a difficult project to a successful conclusion, and for her wonderful support. Mike Chong and Rosie Armstrong, for good advice and amazing deserts. Bob Hanson, for Flatland and much advice. Dave Borhani, for many interesting discussions. Joel Hawkins and Mary Stone, for fascinating chemistry and timely encouragement. Hiroko Masamune, for a friendship of shared interests in science, politics, and music, and for proofreading this thesis. Marie Martin, without whom the Sharpless group would not function, for kindness, encouragement, and favors too numerous to count.

Many outside the Sharpless group have been helpful and encouraging in this work. First and foremost is the excellent staff of the Spectroscopy Laboratory: Jim Symmes, Jeanne Owens, Debbie Western, and Matt Ziegler. I cannot thank them enough for their enthusiasm, expertise, and kindness, displayed in their response to my many requests for NMR and mass spec assistance. For instruction in the art of Fourier transform IR spectroscopy, I am grateful to Jim Bentsen. For enlightening conversations, I thank Mike and Marianna Adam, Alan Walts, Professor William Roush, Marc Walters, Professor Frederick Greene and Professor Satoru Masamune. I am indebted to Professors Greene and Masamune for their review of this thesis at a time of year usually reserved for somewhat lighter pursuits. I also thank Professors Ken Houk, Andrzej Cieplak, and Wilfred Nelson for discussions and assistance at various times. The work of Professor Robert Bach features prominently in our thinking, and I thank him for his enthusiastic participation in many discussions.

For friendship and support out of the laboratory, I am most grateful to Lynne Moulton, Jon Teich, Margaret Orr, Beth Landau, and, always, Christine Kuranishi.

As the reader will perceive, the x-ray crystal structures obtained by Dr. Steven Pedersen form the cornerstone of our mechanistic proposals. However, from the body of this thesis the reader cannot perceive the considerable amount of instruction and inspiration that I have taken from him. This work would have been far less rewarding had Steve not been involved.

Professor K. Barry Sharpless has sponsored my research in financial, scientific, and philosophical terms. It is rare to meet a person in any field whose expertise and enthusiasm meet the Sharpless standard; it makes research an awful lot of fun. I count myself privilaged to have worked with him on this fascinating chemistry, and I thank Barry, Jan, Hannah, Will, and Ike for their warmth and thoughtfulness that have made my graduate work so enjoyable.

Lastly, I thank Mrs. Adelle Hechter and Dr. M. Edward Kaighn for their love and support. This work is lovingly dedicated to Sivia Finn, which is all the thanks I can offer her short of writing a book on the subject.

Table of Contents

Section V. Experimental Section

To Sivia Finn

By Thinking is Humans making big edvences on Enimals.
This we call Progriss.

- Hyman K*a*p*l*a*n[1]

Section I

Introduction

A. Prologue

The enantioselective preparation of asymmetric compounds comprises a rapidly expanding area of chemical science and technology.[2] The discovery by Katsuki and Sharpless of an efficient asymmetric epoxidation reaction for allylic alcohol substrates[3] represents one of the most significant addition to that field of the past several years.[4] The reaction mixture includes a titanium tetraalkoxide, a chiral tartrate diester, the allylic alcohol substrate, and an alkyl hydroperoxide as the oxidant. The enantioselectivity pattern of the reaction is introduced below in Figure 1. To date, no exception has been found among prochiral substrates to the enantiofacial selection rule shown: when drawn with the hydroxymethyl group at the lower right, L-tartrate directs epoxidation to the bottom face of the olefin, D-tartrate to the top face.[4]

Figure 1. Asymmetric epoxidation of prochiral allylic alcohols.

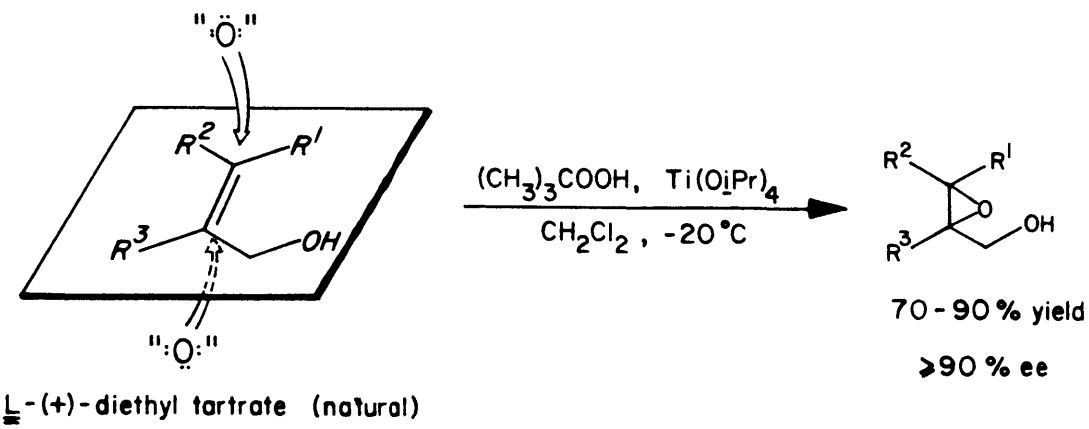

That the asymmetric epoxidation process has been of very great utility in the synthesis of natural products[5] is due primarily to one remarkable feature of the reaction: high enantiofacial selection is obtained for allylic alcohol substrates of widely varying structure. Table 1 presents examples from the Sharpless and Masamune laboratories of prochiral allylic alcohols successfully accomodated by the reaction. It is not our intention to show all the successful substrates known (of which there are many others), but rather to give an indication of the scope of the asymmetric epoxidation process.

Table 1. Allylic alcohols successfully accomodated by the titanium-tartrate asymmetric epoxidation process.

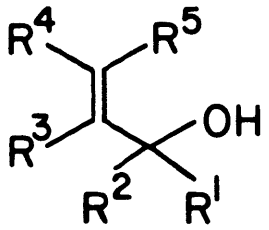

Entry		% e.e.	% Yield	Reference
Unsubstituted				
1	$R^1=R^2=R^3=R^4=R^5$ = H	95	15	b
trans-Disubstituted [$R^1=R^2=R^3=R^5$ = H]				
2	R^4 = CH_3	>95	45	c
3	R^4 = n-$C_{10}H_{21}$	>95	79	d
4	R^4 = $(CH_2)_3CH=CH_2$	>95	80	c
5	R^4 = Me_3Si	>95	60	e
6	R^4 = t-Bu	>95		f
7	R^4 = Ar	≥95	0-90	g
8	R^4 = CH_2OCH_2Ph	98	85	h
9	R^4 = 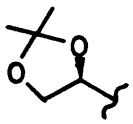	>95	78-85	h
10	R^4 = 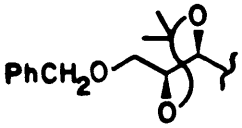	>95	70	h
11	R^4 = 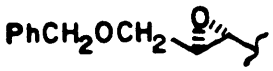	>99	76	(+)-DET used[i,j]
12	R^4 = 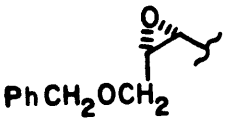	>99	70	(+)-DET used[i,k]
13	R^4 = 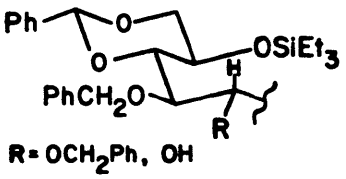	>93	70-88	l

Table 1. Continued.

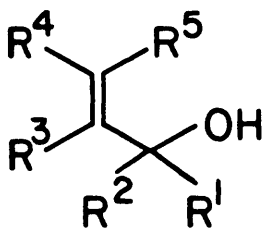

Entry		% e.e.[a]	% Yield	Reference
cis-Disubstituted $R^1=R^2=R^3=R^4$ = H				
14	R^5 = n-$C_{10}H_{21}$	90	82	c,d
15	R^5 = CH_2Ph	91	83	e
16	R^5 = CH_2OCH_2Ph	92	84	h
17	R^5 = 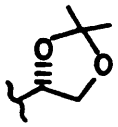	96 85	55	(+)-tartrate only[h] m
1,1-Disubstituted $R^1=R^2=R^4=R^5$ = H				
18	R^3 = -cyclohexyl	>95	81	d
19	R^3 = n-$C_{14}H_{29}$	>95	51	n
20	R^3 = t-Bu	85		f
trans-1,1,2-Trisubstituted $R^1=R^2=R^5$ = H				
21	R^3 = R^4 = Ph	>95	87	d
22	R^3 = Me, R^4 = Et	>95	79	c
23	R^3 = Me, R^4 = 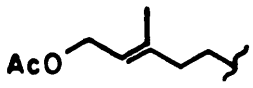	>95	70	d
24	R^3 = Me, R^4 = 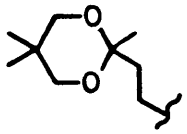	>95	92	e
cis-1,1,2-Trisubstituted $R^1=R^2=R^4$ = H				
25	R^3 = Me, R^5 = CH_2Ph	91	90	e

Table 1. Continued.

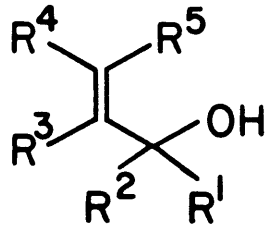

Entry		% e.e.	% Yield	Reference
1,2,2-Trisubstituted	$R^1=R^2=R^3$ = H			
26	$R^4 = CH_2CH_2CH=C(CH_3)_2$, R^5 = Me	>95	77	d
27	R^4 = Me, $R^5 = CH_2CH_2CH=C(CH_3)_2$	94	79	d
Tetrasubstituted	$R^1=R^2$ = H			
28	R^3 = Me, R^4 = Ph, $R^5 = CH_2Ph$	94	90	e
29	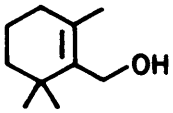	94	90	o

a) Unless otherwise noted, epoxidations involving either tartrate enantiomer are effective. b) Reference 3e. c) Reference 3b. d) Reference 3a. e) Reference 3d. f) Reference 3j.

g) Yields depend on the electron donating or withdrawing properties of the substituents on the phenyl ring. h) Reference 6a.

i) The enantiofacial selectivity of the epoxidation was not directly measured, since the diastereomeric product was purified by chromatography. The yield reported is that of the pure bisepoxy alcohol product. Reference 6b. DET = diethyl tartrate.

j) Epoxidation with (+)-DET afforded approximately 50% yield of the expected diastereomeric bisepoxy alcohol after chromatography. Tuddenham, D.; Sharpless, K.B., unpublished results.

k) Viti, S.M.; Sharpless, K.B., unpublished results.

l) Reference 6c. This reaction required the use of Ti:tartrate:substrate in a ratio of 3.6:5:1. Use of the standard (i.e. 1.2:1.5:1) conditions afforded significant amounts of the , - unsaturated aldehyde. m) Reference 7. n) Reference 8.

o) Erickson, T.J.; Sharpless, K.B., unpublished results. The absolute configuration of the product epoxy alcohol was not determined.

Thus, in the asymmetric epoxidation is found the first truly successful blend of substrate generality and high enantioselectivity. In addition, structures of the other components of the reaction can also be varied without diminishing enantiomeric excess or chemical yield. For example, while the tartrate esters most commonly used are dimethyl tartarte (DMT), diethyl tartrate (DET), and diisopropyl tartrate (DIPT), the ester group can also be stearyl, benzyl, or neopentyl with no loss in enantiomeric excess for epoxidation of a standard substrate. As discussed in Section III.B., the structure of the alkyl hydroperoxide can also be varied from tert-butyl hydroperoxide (TBHP, the most commonly used oxidant) to triphenylmethyl hydroperoxide with little adverse effect.

The lure of this reaction for the mechanistic investigator is powerful: how can high levels of asymmetric induction consistently be achieved in a system that tolerates wide variations in the steric features of its components? The degree of structural tolerance is of such magnitude that we suspect that purely steric interactions are not responsible for the stereoselectivity of the reaction.

For the student of epoxidation processes in general, the asymmetric epoxidation provides an important mechanistic opportunity. With the added variable of asymmetric induction (and, therefore of diastereomeric interactions in the transition state), information about the course of the reaction can be obtained at a level of detail that is impossible to realize in an achiral context. Asymmetric modifications of the attack of nucleophiles on carbonyl groups have similarly given rise to detailed transition state models[9] that are now routinely used to rationalize and predict reactivity patterns.

Studies of the asymmetric epoxidation mechanism detailed here are divided into four areas: catalyst structure, kinetics, "mapping" of the transition state by changing reaction components, and modifications of the "parent" asymmetric epoxidation system.

It is no accident that the title for this thesis closely resembles that of Dr. Scott Woodard's in 1981, since much of the work presented here follows directly from his studies. We will attempt to answer the following questions:

(1) Is the asymmetric epoxidation reaction performed by one dominant catalyst in solution, or are there many active species present?

(2) What is the structure of each catalyst (if there are more than one), and what are their relative activities?

(3) What is the detailed mechanism for oxygen transfer that accounts for the high enantio- and diastereoselectivity of the reaction?

(4) What factors are responsible for loss of catalyst activity?

(5) How does the introduction of extra additives or the use of reagents in non-standard ratios affect the reaction?

There are many other interesting questions that can be posed. Our first concern is to identify the interactions that give rise to high enantioselectivity without strict restrictions on the structure of the substrate. Until recently, the achievement of high enantioselectivity has been designed and rationalized largely on the basis of steric factors alone.[10] Enzymes employ lock-and-key interactions for asymmetric induction with unmatched success, but this does not have to be the only way to achieve such a result. Perhaps the asymmetric epoxidation reaction, with its remarkable scope, is the product of nonsteric elements for the control of enantioselectivity; it is important to see if this is true.

B. Epoxidation Mechanisms

Several reviews have been published on the scope and mechanism of epoxidation of alkenes by peroxy acids[11] and metal-hydroperoxide systems.[12] We shall summarize the most important mechanistic features of these reactions and we urge the reader to refer to the review papers for a more complete historical account. We will deal only with epoxidation by electrophilic peroxidic oxidants, of which the titanium-tartrate-hydroperoxide system is one. There are of course many other methods for preparing the epoxide group, including epoxidation of electron-poor olefins by nucleophilic peroxidic reagents (e.g. basic hydrogen peroxide),[11b] the Darzens reaction,[13] and condensation reactions of carbonyl compounds with the ylides of some main group elements.[14]

1. Peracids.

That the olefinic unit appears to be the nucleophile and the peroxy acid the electrophile has been known since the discovery of the reaction in 1909 by the Russian chemist N. Prileschajew.[15] Thus, either increasing the

electron density of the olefin or decreasing that of the peracid serves to boost the rate of the reaction.[11,16] Recent theoretical treatments have addressed this seeming paradox of how an oxygen atom equipped with lone pairs can act as an electrophile.[17] In keeping with this trend, Henbest[18] observed that substitution of an electron-withdrawing substituent in the allylic position of an olefin decreases the rate of its epoxidation; i.e., 3-methoxycyclohexene is epoxidized by peracid almost 15 times slower than cyclohexene itself. He also made the extremely important observation that 3-hydroxycyclohexene is epoxidized at half the rate of cyclohexene, that is, about seven times faster than its methyl ether. Epoxidation rates are relatively insensitive to steric hindrance,[19] and ring strain.[20] For example, the increased nucleophilicity of tetraalkyl-substituted olefins boosts their reactivity relative to less substituted olefins despite the increased steric hindrance about the double bond.[11a,12a] The epoxidation reaction is bimolecular - first order in substrate and peracid. It proceeds in a wide variety of solvents, with a small and roughly inverse dependence of rate on solvent polarity. The many determinations of activation parameters that have been made agree that the reaction proceeds with a large negative entropy of activation, implying the existence of a highly-ordered transition state.[11,16]

As first observed by Henbest,[18] an allylic hydroxyl group can also be responsible for directing the stereochemical course of an epoxidation by peracid reagents (and also for increasing its rate as noted above for 3-hydroxycyclohexene relative to the corresponding methyl ether). The authors proposed that an association of the hydroxyl functionality with the peracid reagent is responsible for the syn-selectivities and rates observed, an idea that has received much support and utilization in the literature.[21]

In 1950, Bartlett[22] proposed the "butterfly" mechanism involving interaction of the peroxy oxygen distal to the carbonyl group of a peracid with the olefin accompanied by a concerted rearrangement of bonds to afford epoxide and carboxylic acid. It has remained the basis for most mechanistic proposals of epoxidation through the present day. The ordered, bimolecular transition state is consistent with the observed characteristics of the reaction.

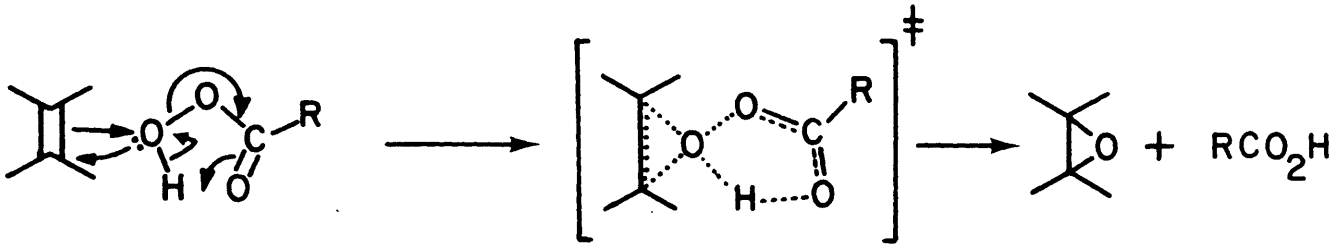

Another early mechanistic proposal, involving a 1,3-dipolar addition reaction of olefin with peracid as suggested by Kwart[23], has not been rigorously disproved, but the experimental evidence[11a,c,24] and theoretical calculations[27a,b] suggest that it is not operative.

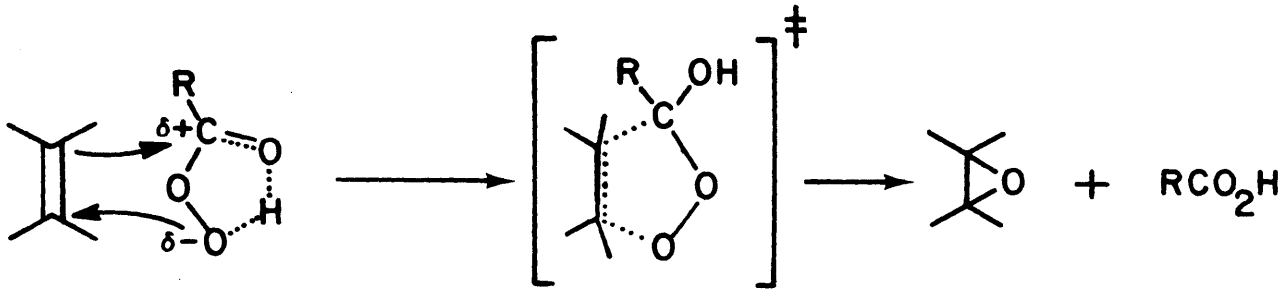

An important modification of the butterfly mechanism is the suggestion that attack of the olefin on the peroxy acid takes place along the O-O axis in an S_N2-type fashion.[27a,c,d,28] With this assumption, Sharpless has proposed that the hydroxyl group of an allylic alcohol can only participate in a hydrogen bond with the distal peroxy oxygen of a peracid, as shown in Figure 2.[12f] Prior to this suggestion, the allylic alcohol was generally assumed to interact with the peracid through a hydrogen bond to the proximal peracid oxygen.

Figure 2. Proposed transition state geometry for epoxidation of allylic alcohols by peracid.

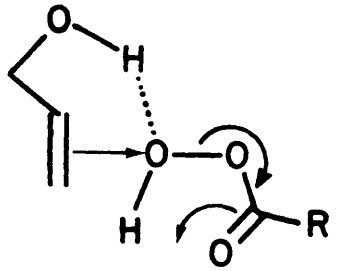

2. Epoxidation by Transition Metal--Hydroperoxide Systems.

As with peroxy acids, the dependence of oxidation rate on olefin and hydroperoxide structures is in accord with the attack of nucleophilic olefin on electrophilic peroxide: greater alkyl substitution on the

olefin[12b,29,25] and greater electron withdrawing power in the hydroperoxide[30] both increase the rate. Radical initiators or inhibitors have no effect on the epoxidation reaction.[11a,29]

The hydroperoxide and the metal participate in a fast, reversible association that activates the hydroperoxide to nucleophilic attack by the olefin.[29,31,12h] The rate-determining epoxidation step is bimolecular for unfunctionalized olefins, and the reaction is inhibited by polar, coordinating solvents and alcohols.[31,12h] Thus, epoxidation with d^0 metal catalysts is first order in each of the reactive components -- olefin, hydroperoxide, and catalyst.[29,31,12b,h] The activation parameters of metal-catalyzed epoxidations have been reported;[31] $\Delta H^{\ddagger}$ = 12-15 kcal/mole and $\Delta S^{\ddagger}$ = -14 - -20 eu, comparable to the values reported for peroxy acid epoxidations (vide supra).

Consistent with this data, the early mechanistic proposals were of the form shown in Figure 3, with metal M = V or Mo. The metal-hydroperoxide coordination was assumed to be a dative one through the oxygen proximal to the alkyl group.

Figure 3. First proposed transition state structure for olefin epoxidation by metal alkylperoxide reagents.

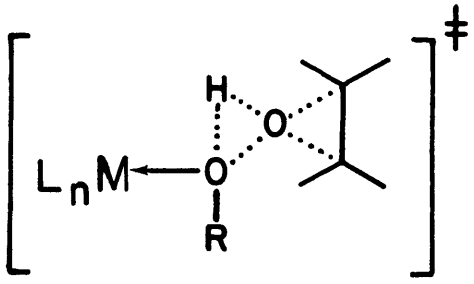

In 1970, Mimoun and coworkers found that covalent peroxo complexes of molybdenum stoichiometrically epoxidize olefins under mild conditions.[32] This finding raised the possibility that metal peroxo complexes formed from hydroperoxides were the active oxidants. However, Chong and Sharpless later provided evidence through ^{18}O labelling experiments that the hydroperoxide remains intact during the reaction.[33] In addition, the peroxo group of covalent oxo-peroxo complexes of Mo[34] and Cr[35] has been shown to undergo no exchange with the oxo oxygen,[34] and labeling of the oxo group has demonstrated that it is a peroxo- and not the oxo-oxygen that is transferred to the olefin undergoing epoxidation.[34a]

The epoxidation of allylic alcohols on d^0 transition metal templates proceeds more rapidly and under milder conditions than the epoxidation of olefins lacking a nearby hydroxyl group[36,29,37]. This effect is much more pronounced in metal-catalyzed reactions than in peracid oxidations due to the propensity of high valent transition metals to rapidly form covalent metal-oxygen bonds. The epoxidation step therefore proceeds in a unimolecular fashion, with both allylic alcohol and hydroperoxide bound to the metal center. It has been estimated that the conversion of a reaction step from intermolecular to intramolecular (i.e. a reduction in kinetic order by one) results in a favorable change in $T\Delta S^{\ddagger}$ of about 5 kcal/mole, corresponding to a rate acceleration of about 1000-fold at 25 °C.[38]

Since the epoxidation of cyclic allylic alcohols on metal catalysts invariably gives a syn epoxy alcohol product,[36,12f] it is likely that the extremely rapid epoxidation of cyclic allylic alcohols occurs on a single metal center. Most proposals in the literature concerning the mechanism of epoxidation of acyclic cases are also based on this concept. Since it is also likely that the detailed mechanism of oxygen transfer to these substrates is the same as for isolated olefins, the geometric constraints of the allylic alcohol epoxidation make it seem unlikely that the hydroperoxide is bound to the metal by the proximal oxygen, as indicated in Figure 3. Rather, Sharpless has proposed the arrangement in Figure 4, whereby the hydroperoxide is bound covalently to the metal through the oxygen atom distal to the alkyl group.[33] The proximal oxygen atom is then thought to interact with the metal in the transition state, further activating the hydroperoxide toward nucleophilic attack.[30]

Figure 4. General transition state structure for metal alkylperoxide epoxidation of allylic alcohols.

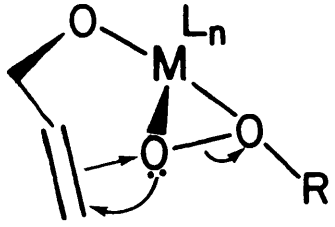

In support of this general scheme for epoxidation of an allylic alkoxide by an alkylperoxide bound to the same metal center is a recent observation by Wolczanski.[39] Under anhydrous conditions, the following

epoxidation reaction occurs in high yield:

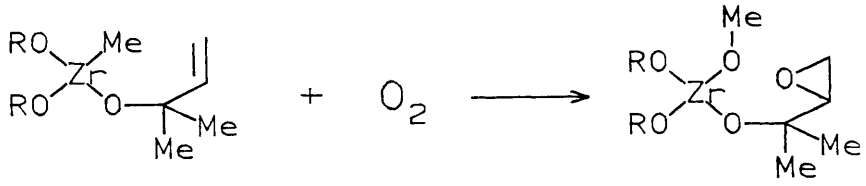

presumably through formation of the alkylperoxy complex $(RO)_2Zr(OOMe)(OCMe_2CH{=}CH_2)$ followed by intramolecular oxygen transfer.

The notion of oxygen transfer through a bidentate alkylperoxide moiety is supported by an x-ray crystal structure of a vanadium(V)-TBHP complex 1 by Mimoun and coworkers.[40a] It clearly shows bonding of the oxygen proximal to the tert-butyl group with the metal. Note that this oxygen center displays a nearly tetrahedral geometry.

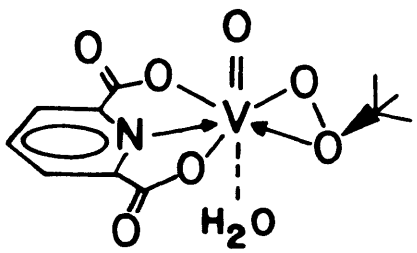

1

TBHP has also been shown to bind in a monodentate fashion, in the crystal structure of the Hf(IV)-TBHP complex 2.[40b] This complex undergoes oxygen transfer too, producing $Cp^*_2Hf(OEt)(OtBu)$ in a first order reaction, indicating that oxygen transfer is intramolecular.[40b] It seems necessary for both oxygens of the alkylperoxide to be associated with the metal in the transition state of such a reaction.

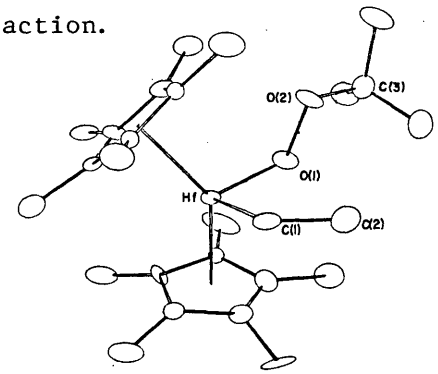

2

The general scheme of olefin attack on a bound alkyl peroxide has been

used by several authors to rationalize their observed diastereoselectivities: Oshima for aluminum alkoxide catalyzed epoxidations,[41] Mihelich for vanadium catalyzed epoxidations of homoallylic alcohols (to extremely high diastereomeric ratios),[42] Narula[39a] and Mihelich [39c] for epoxidation of allylic alcohols on vanadium, Modena for oxidations with vanadium catalysts and hydrogen peroxide,[43] Rebek for intramolecular epoxidation of alkene-substituted peroxy acids and peroxy ethers,[44] and Teranishi for vanadium-catalyzed epoxidations of cyclic allylic alcohols of varying ring sizes.[36a]

Teranishi and coworkers proposed optimum dihedral angles of 150, 150, and 90 degrees for peracid, molybdenum-catalyzed, and vanadium-catalyzed epoxidations, respectively. Sharpless and Verhoeven reviewed many examples of diastereoselective epoxidation of hydroxyl-substituted alkenes in 1979.[12f] They extended the application of the model of Figure 4 to considerations of the detailed geometry of the transition state. As a result of the geometrical requirements of a backside S_N2 displacement on the O-O bond, they predicted an optimum O-C-C=C dihedral angle for the allylic alcohol of about 50 degrees in vanadium-catalyzed epoxidations, and about 120 degrees for peracid reactions.[37b]

3. Peroxymetallation.

In conjunction with their excellent work on metal-peroxo oxidations of organic substrates, Mimoun and colleagues have proposed a different mechanism for epoxidation by peroxidic reagents.[45] The ability of olefins to act as ligands for transition metals of group VIII (e.g. Rh and Pt) suggests that such an interaction is the first step in oxidation reactions of olefins on these metals. Insertion of coordinated olefin into a metal-peroxo oxygen bond would then give a five-membered peroxymetallocycle intermediate, shown below in Figure 5. Such an intermediate has actually been isolated from reactions of Pt[46] and Rh[47] peroxo complexes with cyano-substituted olefins. With metal-hydroperoxide complexes, the authors postulate a pseudo-cyclic five-membered metallocycle. The metallocycle can then decompose to give an epoxide or a carbonyl compound.

Since the intermediates have been isolated and characterized, peroxymetallation is well supported in the group VIII cases. However, we believe

Figure 5. The peroxymetallation mechanism.

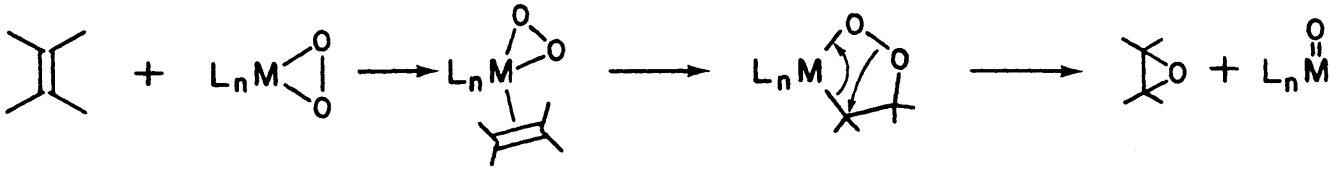

that the mechanism is not operative with d^0 early transition metals (group IV, group V, and group VI) for the following reasons. (1) The formation of the peroxymetallocycle should be easiest for olefins well suited to 1,3-dipolar additions (as is observed with Pt peroxides). Such electron deficient olefins have not been observed to react in these metal-catalyzed epoxidations with alkyl hydroperoxides. Other strained olefins (e.g. norbornene) that do undergo epoxidation react much more slowly than would be expected if the reaction proceeded through a 1,3-dipolar-like transition state.[34a] (2) With allylic alcohols, peroxymetallation demands the formation of a strained bicyclic intermediate. (3) Molybdenum porphyrin complexes have been shown to catalyze the epoxidation of alkenes by t-butylhydroperoxide.[48] In this case, the steric constraints imposed by the macrocyclic ligand make it difficult for both olefin and hydroperoxide to be bound to the metal at the same time. (4) A coordinative interaction of an olefin with the metal, required by the peroxymetallation scheme, has not been spectroscopically observed for d^0 elements of groups IV or V, to our knowledge. It must be emphasized, however, that definitive evidence for support or rejection of the peroxymetallation mechanism for these early transition metal catalyzed epoxidations has not yet been found.

4. Theoretical Investigations.

Because of the complexity of the reaction, relatively few calculations on the transition states of epoxidations have been published,[49] though the conformation and rotational barriers of hydrogen peroxide[52] have been well studied. Most of the published work has been done on epoxidations of olefins (usually ethylene) by performic acid and simple derivatives. However, asymmetric epoxidation is presently receiving theoretical treatment in the the research groups of Professors R. D. Bach (Wayne State University) and K. W. Houk (University of Pittsburgh).

It seems to be generally accepted that the initial orbital interaction of olefin and peroxide involves the olefin π orbital (HOMO) and the peroxide bond σ^* orbital (LUMO).[27,53,17] The geometry of this interaction is subject to some debate.

A secondary deuterium isotope study by Hanzlik and Shearer found evidence for unsymmetrical formation of C-O bonds in the transition state of the epoxidation of styrene with peroxy acids, the formation of the bond to the β-carbon ($=CH_2$) of styrene showing a greater secondary deuterium isotope effect than formation of the bond to the α-carbon.[53a] Hanzlik's proposal has been both supported[27a] and rejected (or ignored)[27d,17a,b] by subsequent theoretical studies, the latter studies proposing a symmetrical interaction of the reactive peroxy oxygen with the olefin C=C unit. As discussed in Section III.C., we have performed secondary deuterium isotope effect experiments that provide no evidence for unsymmetrical C-O bond formation.

Regardless of whether or not the epoxide C-O bonds are formed simultaneously, the interaction of the olefin with a planar peroxide system (i.e. a peroxy acid[27d,17b] or metal-alkylperoxo moiety) can occur in geometrically non-equivalent arrangements. The two simplest of these are the so-called "planar" and "spiro" orientations in which the planes defined by the olefin π orbital and the peroxide systems are coplanar or normal to each other, respectively (Figure 6).

Figure 6. Definitions of "planar" and "spiro" orientations of metal alkylperoxide and olefin in epoxidation reactions.

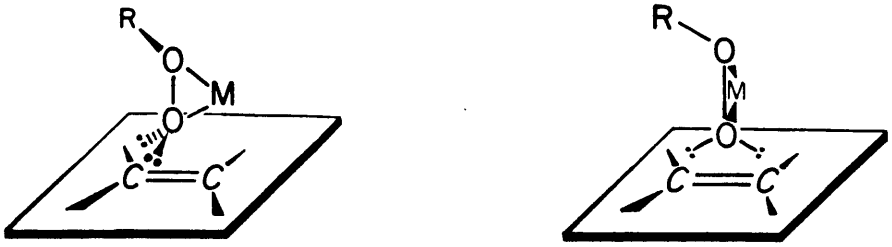

Note that the plane defined by the lone pairs of the reactive peroxy oxygen is coplanar with the olefin π orbital in the spiro arrangement and normal to the π orbital in the planar arrangement. One might expect the energies of these two states to be quite different. The planar avoids a seemingly

unfavorable four-electron interaction (lone pair - π) but also takes the lone pairs out of position to interact with the olefin π^* to facilitate C-O bond formation. The spiro transition state accomplishes the reverse; it brings the reactants into the orientation necessary to experience both the destabilizing four-electron repulsion and the stabilizing lone pair - π^* mixing.

The exact nature of lone pairs on oxygen in the transition state, an important question in the epoxidation mechanism discussion, has itself not been resolved. Photoelectron spectroscopy clearly shows the lone pairs on ground-state oxygen atoms to be non-equivalent (i.e. sp^2- and p-type).[54] However, chemists have for years successfully used arguments based on equivalent (sp^3) lone pairs in transition states to explain many stereochemical effects.[55] Studies of the geometries of hydrogen bonding and of lone pair electron densities by means of electron density difference mapping from x-ray diffraction data provide support for the sp^3 lone pair formalism, especially for peroxide oxygens.[56,52b] The only conclusion that can be drawn is that there is as yet no theoretical basis for expecting spiro and planar epoxidation transition states to be significantly different in energy.[27a,17]

A coherent theoretical picture for the epoxidation reaction developed by Professor R.D. Bach and coworkers was introduced in their study of the epoxidation of ethylene by ethylene oxide or oxaziridine.[17a] Starting with non-equivalent oxygen lone pairs, they proposed that the initial unavoidable four-electron interaction (sp^2-type lone pair with olefin π) drives the energies of the frontier orbitals together at the expense of an unoccupied antibonding orbital. Since the important interactions in their model involve orbitals of cylindrical or spherical symmetry, they see no reason to expect either the planar or spiro transition states to be favored.

Bach's subsequent treatment of metal-mediated epoxidations indicated the same independence of transition state energy with respect to spiro/planar orientations.[17c] More importantly, they identified a favorable molecular orbital pathway involving low-lying empty metal d-orbitals for the "migration" of a d^0 metal center from the distal to the proximal oxygen atom of a bound hydro-or alkylperoxide during reaction with an olefin. The model systems studied were the vanadium(V)-methyl hydro-

peroxide complex ($V\text{-}OOCH_3$) and the epoxidation of ethylene by lithium hydroperoxide (Li-OOH).

Two groups have developed epoxidation systems that appear able to distinguish between planar and spiro alignments, both favoring the former. Davis et al have asymetrically epoxidized prochiral olefins with chiral oxaziridines.[57] Reasoning that different enantiomers of epoxides would be produced from the two orientations, they obtained up to 40% enantiomeric excess at 60°C ($\Delta\Delta G^{\neq}$ = 0.56 kcal/mole) of the product corresponding to the planar transition state geometry. Rebek and coworkers have prepared conformationally constrained peroxy acids that show unprecedentedly high rates of epoxidation of cis alkenes relative to trans and 1,1-disubstituted alkenes,[58] rationalized on the basis of a restriction of transition state conformation to a planar arrangement. Neither case can be applied to epoxidation reactions in general, however. Rebek's work shows only that epoxidation can be made to occur through a planar arrangement if the steric conditions demand it, and Davis's conclusions certainly require further testing before we can consider them proof of a lower energy planar transition state pathway.

By emphasizing the importance of the overlap of an oxygen sp^3 lone pair with the olefin π^* orbital, we have proposed an intermediate orientation between spiro and planar[12f] that is also consistent with the experimental data: with backside attack of olefin on the O-O bond, one oxygen lone pair should be in the plane of the olefin π^* orbital. In peracid epoxidations of allylic alcohols, the other lone pair of the reactive oxygen participates in a hydrogen bond with the allylic hydroxyl group.[12f] In metal-catalyzed oxidations, the other lone pair is involved in a bond with the d^0 metal center. This orbital requirement restricts the allowed transition state orientations to two possibilities, namely, alignment of the olefin with each of the two available oxygen lone pairs,[3e] conformations in between spiro and planar as defined above.

C. Asymmetric Epoxidations

We present here a brief review of abiotic asymmetric epoxidations reported in the literature. Those that contribute little to the understanding of epoxidation mechanisms (especially the early examples) will

simply be referenced and not discussed.

The first reported asymmetric epoxidation was performed, appropriately, by Henbest in 1965.[59] He used (+)-peroxycamphoric acid and isolated olefins (e.g. styrene) to obtain enantiomeric excesses (ee) of less than 5%. The remaining early attempts using chiral peroxy acids never achieved higher than 10% ee.[60] In 1977, Pirkle re-investigated this method and found that the peroxycamphoric acids used by earlier investigators were not pure.[61] With purified oxidants, he achieved up to twice the level of asymmetric induction of that previously reported for isolated olefins and up to 60% e.e. for the oxidation of an imine to an oxaziridine. Presumably the chiral functionality is too far from the site of reaction to effect much enantioselectivity in most of these cases.

Greater success has been achieved in the base-catalyzed epoxidation of α,β-unsaturated ketones by H_2O_2, mediated by chiral quinine derivatives as phase-transfer agents.[62] The best e.e. observed was 55%.[62b] By far the most effective phase transfer catalyst has been the "synthetic enzyme" poly-(S)-alanine, giving up to 96% e.e. in the epoxidation of trans-chalcone.[63] Quinine salts mediate asymmetric induction in epoxidations by molecular oxygen[64] and by hypochlorite.[65a,b] They also function as chiral auxiliaries in epoxide formation by Darzens condensation, ring closure of halohydrins, and addition of cyanide to α-haloketones, all to less than 10% e.e.[65a,b] Catalytic amounts of cyclodextrins have been used as phase transfer agents for the asymmetric epoxidation of trans-chalcone to 11% e.e. in the best case.[65c]

The epoxidation of olefins by various chiral α-substituted hydroperoxy ketals gives disappointingly low levels of asymmetric induction (<5%).[43] It had been hoped that the levels of asymmetric induction would be improved with these hydroperoxy ketals, since the chiral group is closer to the peroxy oxygen than in the case of chiral peracids. The most recent non-metal-mediated asymmetric epoxidation is Davis' aforementioned oxidation of olefins by chiral oxaziridines to a maximum of 40% ee.[48]

Insofar as the achievement of high levels of enantiomeric induction implies the attainment of a transition state with restricted degrees of freedom, it is not surprising that the first reported cases of metal-catalyzed asymmetric epoxidation involved allylic alcohols and a high-

valent metal. In 1977, Yamada et al reported the use of cumene hydroperoxide with a dioxomolybdenum complex of N-ethylephedrine (complex 3),[66] while Sharpless' group employed TBHP and vanadium with chiral hydroxamic acid ligand 4.[67] The former gave up to 33% ee, the latter up to 50% ee. The need to maintain the association of the chiral ligand with the metal was emphasized by Sharpless' report that a 3-fold excess of 4 is necessary to obtain high enantiomeric excess. An industrial group later reported the same phenomenon in the epoxidation of an allylic alcohol with cumene hydroperoxide and a dioxomolybdenum L-N-methylprolinol complex 5.[68]

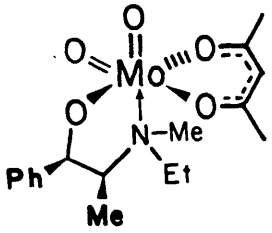

3

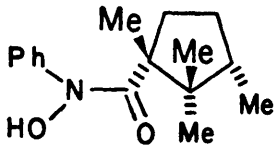

4

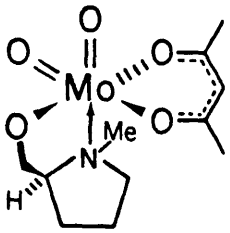

5

These discoveries were followed by the report of Kagan, Mimoun, and colleagues that the peroxomolybdenum complex 6 functions as a stoichiometric oxidant for isolated olefins in up to 33% e.e.[69] Otsuka reported the epoxidation of isolated olefins by TBHP and $MoO_2(acac)_2$ in the presence of optically active diols (sugar derivatives and tartrate esters) to a maximum of 14% e.e.[70] The highest level of asymmetric induction in the epoxidation of unfunctionalized alkenes (51% e.e. in the best case) has been achieved by Groves and Myers using a chiral iron porphyrin complex and iodosylmesitylene.[41] A French group has recently epoxidized p-chlorostyrene with a chiral ("basket handle") iron porphyrin and iodosylbenzene to 50% ee.[71]

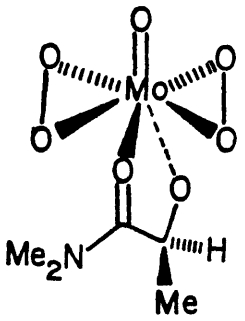

6

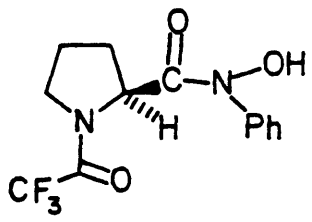

7

Sharpless and Oshima improved the vanadium-catalyzed epoxidation of allylic alcohols by using a different hydroxamate ligand, **7**, to give 80% ee for the epoxidation of (E)- -phenylcinnamyl alcohol,[12f] the best result prior to the titanium-tartrate catalyzed asymmetric epoxidation. Oshima later reported the use of the same chiral hydroxamate with an aluminum alkoxide to epoxidize allylic alcohols in 30-40% ee.[41]

D. Asymmetric Epoxidation Mediated by Titanium-Tartrate

Asymmetric epoxidation of allylic alcohols by titanium-tartrates was discovered in 1980,[3a] after several man-years of effort in designing and testing chiral ligands to modify va.adium- and titanium-catalyzed epoxidations.[3h] It involves the use of complexes formed by mixing titanium tetraalkoxides with dialkyl esters of tartaric acid, and an alkyl hydroperoxide (usually TBHP) as the oxidant in a non-polar organic solvent (usually methylene chloride). The recommended procedures for performing the reaction have been summarized elsewhere.[3d,f,i] It should be noted that, until recently, titanium-tartrates, which in principle are true catalysts of asymmetric epoxidation, have not been employed in catalytic concentrations. When used at below approximately 50 mole% concentration with respect to substrate under the first published conditions for the reaction, the enantiomeric excess is usually diminished and the reaction often does not go to completion. This important limitation to the application of asymmetric epoxidation has now largely been overcome.[73]

In addition to being able to asymmetrically oxidize prochiral substrates to a product of predictable absolute configuration (see Figure 1) the reaction is extremely sensitive to pre-existing chirality in selected positions of the allylic alcohol.[3c] For example, the epoxidation of a racemic mixture of a 1-alkyl-substituted allylic alcohol with half an equivalent of hydroperoxide per equivalent of substrate produces an epoxy alcohol product of high diastereomeric and enantiomeric purity plus unreacted allylic alcohol that is greatly enriched in one enantiomer. This process of kinetic resolution is depicted below in Figure 7. Examples of secondary allylic alcohols that undergo efficient kinetic resolution are presented in Table 2.

Table 2. Allylic alcohols undergoing kinetic resolution with relative rates greater than 15 at -20°C.

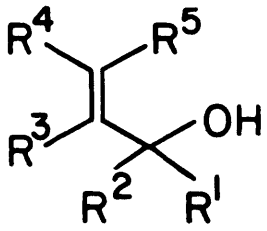

Entry	Substituents[a]	k_{rel}	erythro/threo ratio from faster-reacting enantiomer	Reference
1	R^1 = n-C_6H_{13}	83	99/1	b
2	R^1 = CH_2CH_2Ph	>15		c
3	R^1 = 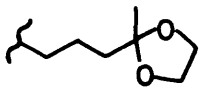	>15		c
4	R^1 = cyclohexyl	>15	98/2	d
5	R^1 = 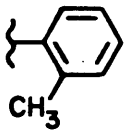	>15		e
6	R^1=n-C_4H_9, R^3=Me	138	98/2	b
7	R^1=cyclohexyl, R^3=Me	>15		e
8	R^1=n-C_4H_9, R^4=Et	>15	90/10	d
9	R^1=n-C_4H_9, R^4=Me	>15		e
10	R^1=cyclohexyl, R^4=Me	104	97/3	b
11	R^1=Et, R^4=Ph	>15		c
12	R^1=$CH_2CH(CH_3)_2$, R^4=Me	>15	90/10	d
13	R^1 = R^5 = Me	ca. 20	81/19	b
14	R^1=Et, R^5=n-C_6H_{13}	16	40/60	b

Table 2. Continued.

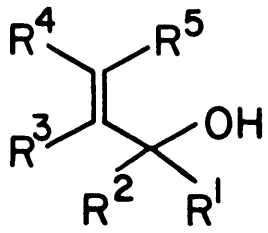

Entry	Substituents[a]	k_{rel}	erythro/threo ratio from faster-reacting enantiomer	Reference
15	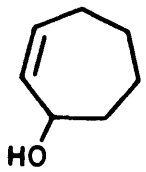	ca. 16		b
16	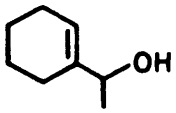	83	98/2	b
17	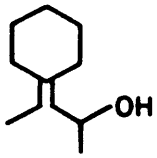	≥15	ca. 35/65 or 65/35	e,f

a) R^n = H, unless otherwise indicated
b) Reference 3c.
c) Reference 3d.
d) Martin, V.S.; Sharpless, K.B., unpublished results. Reaction performed with (+)-DIPT at -20°C in CH_2Cl_2.
e) Reference 3g.
f) The structures of the two diastereomeric epoxy alcohol products were not assigned.

Figure 7. Epoxidation of each enantiomer of cyclohexyl propenyl carbinol by TBHP, $Ti(O\underline{i}Pr)_4$, and (+)-DIPT.

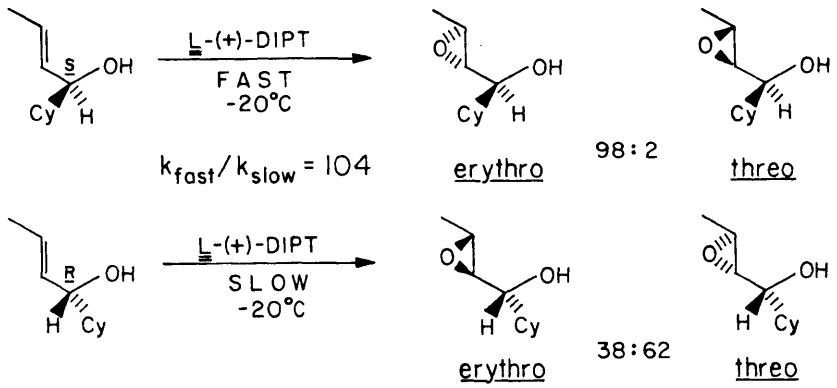

It is also instructive to note the allylic alcohol cases that are not successfully resolved by Ti-tartrate epoxidation, some of which are presented in Table 3. They constitute two separate classes, representing different limitations to the scope of asymmetric epoxidation. The first is those substrates that react slowly and give poor enantiomeric excess, e.g. some (Z)-allylic alcohols and a few severely hindered molecules of other substitution types. In these cases, oxidation to the α,β-unsaturated carbonyl compound is sometimes a major side reaction.[36a,74] The second class of poor substrates is those that are epoxidized at a rapid rate and with high selectivity but yield epoxy alcohols that are unstable to the reaction conditions. The opening of epoxy alcohols by alcohols in solution to give diol ethers is accelerated by Lewis acids, including Ti(IV),[75] as depicted below.

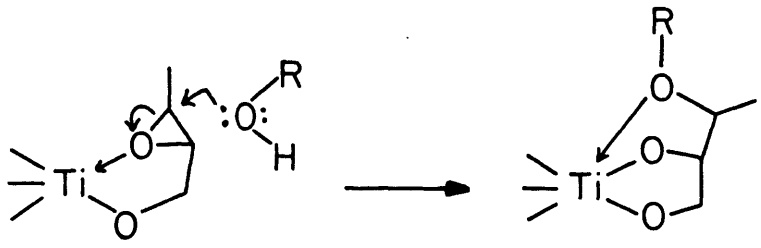

It is this process of epoxy alcohol opening that was originally assumed to be responsible for the inability of Ti-tartrates to act effectively in catalytic amounts. Diols can be expected to bind well to titanium and thus reduce the catalyst activity by competing for ligand sites that allylic alcohol and hydroperoxide must occupy for epoxidation to take

Table 3. Poor substrates for titanium-tartrate catalyzed asymmetric epoxidation or kinetic resolution.

Entry	Substrate	Result	Reference
1	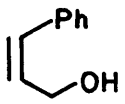	Slow epoxidation, 65% e.e.	a
2	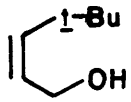	Slow epoxidation, 25% e.e.	b
3	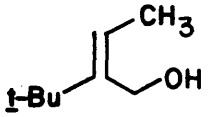	Slow epoxidation, 60% e.e.	b
4	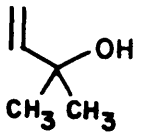	Slow epoxidation, no epoxy alcohol isolated	n
5	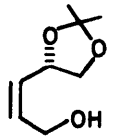	Slow epoxidation using (-)-tartrate, 23% e.e. (2R diastereomer)	d,e
6	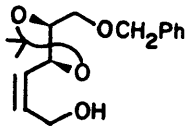	No reaction using (-)-tartrate	c,f
7	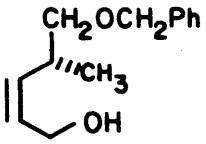	Slow epoxidation 67% e.e. using (+)-tartrate ca. 0% e.e. using (-)-tartrate	d
8	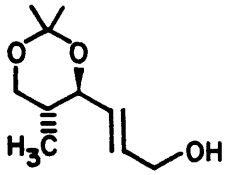	No reaction using (+)-DET	g
9	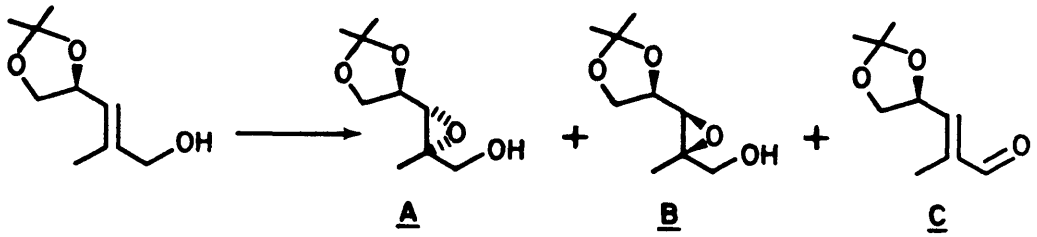	Use of (+)-DET affords 4:1 A:B in 75% yield. Use of (-)-DET affords 50% yield of B plus ca. 20% of the α,β-unsaturated aldehyde C.	h

Table 3. Continued.

Entry	Substrate	Result	Reference
10	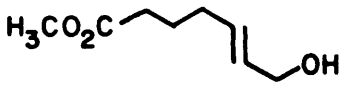	95% e.e., 58% yield. Difficult to reproduce due to lactone diol formation.	i
11	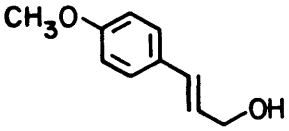	Product epoxy alcohol unstable to reaction conditions; either no product or only very low yields obtained under standard conditions.	j
12	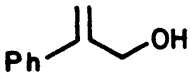		j
13			j

Kinetic Resolutions

14	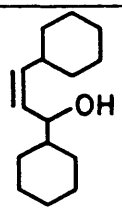	Very slow reaction, ca. 10% e.e. at 60% completion (k_{rel} = ca. 1.2)	k
15		30% e.e. at 60% completion (k_{rel} = ca. 1.9)	k
16	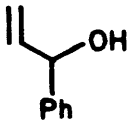	Slow epoxidation, k_{rel} = 4-10.	l
17	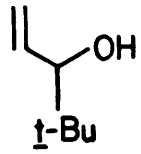	Very little kinetic resolution	See Table 45
18	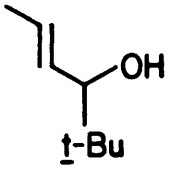	Very little kinetic resolution	See Table 45
19	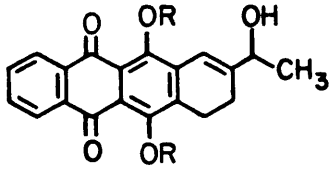	R=COC$(CH_3)_3$ No reaction. R=$COCH_3$ Successful kinetic resolution to unreported k_{rel}	m

Table 3. Continued.

a) Tuddenham, D.; Martin, V.S.; Sharpless, K.B., unpublished results.
b) Reference 3j.
c) Reference 6a.
d) Nagaoka, H.; Kishi, Y. Tetrahedron 1981, 37, 3873-3888. A Ti:tartrate ratio of 1.0:1.0 was used; it is possible that the diastereofacial selection observed is at least partly the product of epoxidation by a small amount of $Ti_2(tartrate)(OR)_6$ or $Ti(OR)_4$ present in solution. For entry 5, see also: Minami, N.; Ko, S.S.; Kishi, Y. J. Am. Chem. Soc. 1982, 104, 1109-1111.
e) This substrate is epoxidized slowly with the $Ti(O\underline{i}Pr)_4$:(+)-DET catalyst to high enantiomeric excess. See Table 1.
f) Epoxidation using (+)-tartrate was not attempted.
g) Ito, Y.; Ma, P.; Masamune, S., unpublished results. Epoxidation with Ti:(-)-DIPT was not attempted.
h) Viti, S.M.; Sharpless, K.B., unpublished results.
i) Reference 3b.
j) Martin, V.S.; Katsuki, T.; Woodard, S.S.; Tuddenham, D.; Sharpless, K.B., unpublished results.
k) Reference 3c.
l) Martin, V.S.; Sharpless, K.B., unpublished results.
m) Dominguez, D.; Cava, M.P. J. Org. Chem. 1983, 48, 2820-2825.
n) Katsuki, T.; Sharpless, K.B., unpublished results.

place.

An important observation made by Dr. Robert Hanson in the Sharpless laboratory has proved these suppositions to be incorrect: the inclusion of molecular sieves in the asymmetric epoxidation reaction mixture serves to prolong the life of catalytic Ti-tartrate to an astonishing degree.[73] For example, the epoxidation of many simple allylic alcohols (such as 2-hexenol, cinnamyl alcohol, and 2,4-pentadienol) in the presence of 5 mol% Ti-tartrate (meaning 5% $Ti(O\underline{i}Pr)_4$ and 6% tartrate with respect to substrate) proceed to only partial completion (about 5-50%) in the absence of sieves, but in the presence of 3- or 4-A sieves the reactions go rapidly to completion. Even allyl alcohol, one of the least reactive substrates we have encountered, is completely epoxidized in 5 h at $0^{\circ}C$ using the sieve modification with 5% catalyst (Ti-DIPT) and cumyl hydroperoxide in place of TBHP.[76] The %ee is generally (85-95%) using this new catalytic modification, but workup and purification of the product is much easier and the yields are higher.

While we have not measured the equilibrium constant for binding of tartrate to $Ti(O\underline{i}Pr)_4$ (equation (1), below), we suggest that the slight reduction in %ee is due to the displacement of a small amount of tartrate from the metal under 5 mol% conditions. As the catalyst level is dropped further, the %ee declines even more, as one would expect from the liberation of more tartrate by alcohol mass action.[77]

The beneficent effect of molecular sieves suggests that adventitious water in the reaction mixture is the major source of Ti-tartrate poisoning under catalytic conditions. That diols may not be such potent inhibitors as first thought is suggested by Hanson's observation that the use of a greater than twofold excess of tartrate per titanium atom under 5 mol% titanium conditions results in an active asymmetric epoxidation system even though such a mixture under pseudo-first order conditions is inactive. The recommended amounts of titanium and tartrate for catalytic epoxidation are now 5 mol% Ti and 6 mol% tartrate with respect to 100 mol% allylic alcohol. Section II.B.3. presents data relating to the kinetic behavior of the asymmetric epoxidation in the presence of molecular sieves.

1. Equilibria and Kinetics

The work of Dr. Scott Woodard[78] provides much of what is known about

the equilibria and kinetics of Ti-tartrate; his findings are summarized here as an introduction to subsequent experiments.

When 1 equivalent of dialkyl tartrate is mixed with 1 equivalent of titanium tetraalkoxide, 2 equivalents of alcohol are released into solution, in accordance with Eq. (1).

$$Ti(OR)_4 + \text{tartrate} \rightleftharpoons Ti(\text{tartrate})(OR)_2 + 2ROH \quad (1)$$

This has been demonstrated by the use of NMR spectroscopy and vapor-phase gas chromatography and is supported by the kinetic measurements described below. The released alcohol can then be removed in vacuo or by molecular sieves to give a complex that is identical spectroscopically and in reactivity to the initial product, as shown in section II.C.

The exchange of alkoxides on d^0 metal alkoxide complexes is rapid,[79] so in most cases Eq. (1) proceeds quickly. However, when the steric demand of the alkoxide or tartrate is great, the product complex may require a significant amount of time to form. For example, a solution containing $Ti(O\underline{t}Bu)_4$ and (+)-DIPT requires about 20 minutes at 0°C to give a complex that is effective in asymmetric epoxidation. If less time is allowed, the %ee of the product epoxy alcohol can be substantially reduced.

It is important to note that titanium alkoxides are effective catalysts for transesterification reactions of carboxylic esters[80] as shown in Eq. (2).

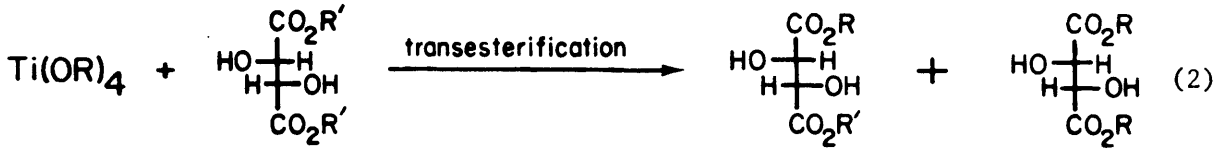

(2)

In virtually all cases, the rates of transesterification of tartrate esters are far slower than those of epoxidation, especially at the temperatures usually employed (about -20°C). This stands in contrast to Ti-catalyzed transesterifications of other α-hydroxy esters, which are quite rapid.[81] However, when Ti-tartrates are allowed to stand for long periods of time at room temperature or warmer, transesterification is likely to occur to some extent.

The dependence of the rate of epoxidation on the concentration of each of the components of the system has been measured by monitoring the disap-

pearance of allylic alcohol under pseudo-first order conditions.[78] In these experiments, the concentrations of catalyst and hydroperoxide are at least 15 times greater than that of the substrate to mandate a first order rate dependence on allylic alcohol.

With the advent of the 5 mol% catalytic reaction in the presence of molecular sieves, it may be possible to perform saturation kinetics experiments, which would be even more informative than pseudo-first order measurements. Preliminary results indicate that the observed rates under such conditions are reproducible, though we do not yet have evidence that the catalyst is saturated. As discussed above, if the catalyst level is reduced to the range normally used for saturation rate measurements (<2 mol% of Ti-tartrate per mole of substrate), the enantiomeric excess drops sharply.

The pseudo-first order kinetics experiments have demonstrated a first order dependence on both the catalyst [in the form Ti(tartrate)$(OR)_2$] and the hydroperoxide, just as was reported for molybdenum and vanadium systems. In the Ti-tartrate measurements, a large excess of nonreactive alcohol (e.g. isopropanol) had to be added to slow the reaction rate to an easily measured range. The rate dependence on added alcohol was found to be inverse second order. These results are summarized by the observed rate law given in Eq. (3). Similar kinetic measurements, including those of the asymmetric epoxidation reaction in other solvents, are reported in Section II-B.

$$-\frac{d[\text{allylic alcohol}]}{dt} = \frac{k\,[\text{allylic alcohol}]^{1}\,[\text{TBHP}]^{0.99}\,[\text{Ti(DRT)(OR)}_2]^{1.01}}{[\text{inhibitor alcohol}]^{2.03}} \qquad (3)$$

Consistent with this expression is the exchange pathway outlined in Fig. 8. After the formation of the Ti-tartrate complex **8**, the two remaining alkoxide ligands are replaced in reversible exchange reactions with TBHP and the allylic alcohol to give the "loaded" complex **9**. The reaction is independent of which of the two possible pathways is used to reach complex **9**. Oxygen transfer can then occur in the loaded complex **9** to give the coordinated epoxy alkoxide and t-butoxide in complex **10**. These product alkoxides are replaced by more allylic alcohol and TBHP to regenerate the loaded complex

9 and complete the catalytic cycle. The inverse squared dependence on nonreactive alcohol is due to the necessary replacement of the two alkoxide ligands in 8 with hydroperoxide and the allylic alcohol.

Figure 8. Ligand exchange pathway in the asymmetric epoxidation catalytic cycle.

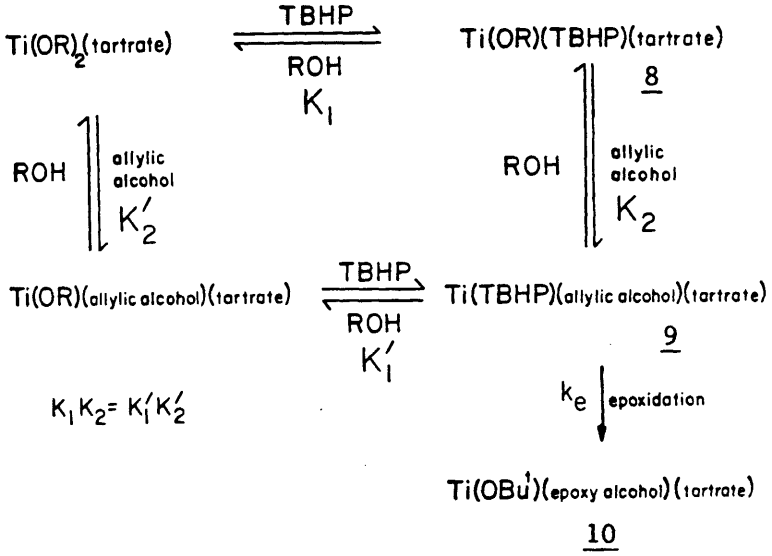

Note that the observed rate constant k in Eq. 3 is actually the product of the rate of epoxidation k_e and the equilibrium constants K_1 and K_2 (or K_1' and K_2'). It is assumed that the equilibrium constant for the replacement of isopropoxide by secondary allylic alcohol is approximately 1, since their steric and electronic properties are roughly equivalent. The equilibrium constant for the replacement of isopropanol with hydroperoxide on Ti-DIPT (K_1) was measured by Woodard as 1.15, but has been revised to 0.7 ± 0.2 by a later experiment (see Section II.A.). To the extent that $K_1K_2=1$, then, the observed reaction rate is approximately equal to the rate of oxygen transfer k_e.

Of course, the dependence on nonreactive alcohol is so simple in Eq. (3) only because it is derived from experiments in which one nonreactive alcohol (i.e. isopropanol) is present in great excess over all others. Under normal epoxidation conditions, the rate law is more complicated because potential inhibitors include the epoxy alcohol, liberated alcohol from the Ti tetraalkoxide, and even allylic alcohol and hydroperoxide themselves [since Ti(tartrate)(allylic alcohol)$_2$ and Ti(tartrate)(hydroperoxide)$_2$ are also unreactive]. Interestingly, the aforementioned use of molecular sieves with catalytic concentrations of Ti-

tartrate gives an epoxidation system that is extremely reactive. One reason for the speed of reaction under these conditions is that the smaller amount of $Ti(OR)_4$ gives rise to lower concentrations of inhibitor alcohol (ROH) at the start of the reaction.

With the rate law in hand, observed rates of epoxidation were compared for different substrates.[78] As expected, the nucleophilic nature of the olefin was indicated by the behavior of para-substituted cinnamyl alcohols. Electron-withdrawing groups, such as nitro, decreased the rate of epoxidation while electron-donating groups increased the rate. The expected dependence of rate on alkene substitution was also observed - the more highly substituted the double bond, the greater the epoxidation rate.

In an important series of experiments, Woodard found that, under pseudo-first order conditions, addition of more than 1 equivalent of tartrate to titanium caused a rate decrease consistent with the formation of a species of stoichiometry $Ti(tartrate)_2$ that is catalytically inactive. Use of less than 1 equivalent of tartrate per Ti usually results in some loss of enantioselectivity. For this reason, the recommended ratio of Ti to tartrate for a normal asymmetric epoxidation reaction is 1:1.2. Formation of species with <1 equivalent of tartrate to Ti is thus diminished, and the excess ligand merely decreases the rate slightly.

2. Kinetic Resolution

The kinetic resolution of racemic secondary allylic alcohols by Ti-tartrate-TBHP was first reported in 1981.[3c,82] The parameter of interest is the ratio of the rates of epoxidation of the two enantiomers k_{fast}/k_{slow}, termed the "relative rate" (k_{rel}). By measuring the rates of epoxidation of both enantiomers of five secondary allylic alcohols with different Ti-tartrates, Woodard concluded that the relative rate values increase markedly with the size of the tartrate ester group, DIPT > DET > DMT.

The activation parameters have been determined for the epoxidation of both enantiomers of cyclohexenyl methyl carbinol and are given below.[78] Keep in mind that the values of $\Delta S^{\ddagger}$ and $\Delta H^{\ddagger}$ include contributions from the equilibrium constants as well as the epoxidation step. Nevertheless, the sizeable negative value of $\Delta S^{\ddagger}$ supports the notion of a highly ordered transition state.

Table 4. Activation parameters for epoxidation of cyclohexyl methyl carbinol with Ti-DIPT.

	$\Delta H^{\neq}$ (kcal/mole)	$\Delta S^{\neq}$ (e.u.)
faster-reacting enantiomer	10.6	-13
slower-reacting enantiomer	12.4	-14

The relative rates for epoxidation of cyclohexylpropenyl carbinol in the presence of isopropanol and n-butanol have also been measured by Woodard. While the epoxidation rates are slower by a factor of about 7 in the presence of n-butanol, the relative rates are identical for the two cases. This suggests that no spectator alcohol molecule is present in the transition state. This important conclusion is supported by the fact that protic sources can be removed from the reaction system with no loss in the rate of vanadium-catalyzed epoxidations; in fact, the rate increases slightly.[83] In addition, alcohol-free preparations of the Ti-tartrate-substrate-TBHP system have been observed to epoxidize allylic alcohols with the same enantioselectivity and at similar rates to those realized with Ti-tartrate preparations that were freshly prepared in situ and thus contain free alcohol molecules. And, as discussed later, we observed no solvent deuterium isotope effect when pseudo-first order kinetics were done in the presence of iPrO-D instead of iPrO-H.

Kinetic resolution has also been observed when the chiral center resides at other sites in the allylic alcohol.[3d] Kinetic resolution at the trans C-3 position of an acyclic allylic alcohol is ineffective. However, resolution at the C-2 and cis C-3 positions can be much more efficient. Section III.B. presents another example of an unusual kinetic resolution.

3. Other Titanium-Tartrate Systems

While the catalyst for asymmetric epoxidation is apparently a species in which titanium and tartrate are present in a 1:1 ratio, it has been found that Ti-tartrate systems of other compositions exhibit different catalytic activity. Three of these catalysts differ from the parent system in that a 2:1, rather than a 1:1, ratio of titanium alkoxide to tartrate ligand is involved. The first new system discovered utilizes tartrate

diamides instead of diesters to achieve the striking ratio-dependent behavior shown below for the epoxidation of (E)-α-phenylcinnamyl alcohol.[84]

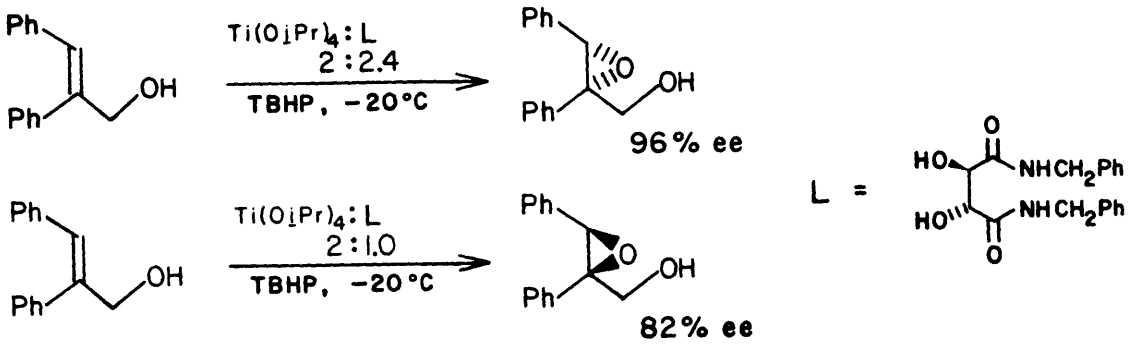

Note that the use of a 2:2 ratio of titanium:tartramide results in epoxidation in the "normal" (2S) direction to high enantiomeric excess. Simply by changing the ratio to 2:1, the enantioselectivity reverses to give 2R epoxy alcohol in 82% ee and high yield. The most successful tartramide ligand is shown in the figure above, the di-N-benzyl derivative, abbreviated DNBnT.

The second 2:1 system discovered consists of two parts $TiCl_2(OiPr)_2$ and one or two parts dialkyl tartrate.[84] This catalyst system exploits the ability of chlorotitanium alkoxides (which are much more Lewis acidic than titanium tetraalkoxides) to effect the opening of epoxides to chlorohydrins. The observed products from the rapid opening of 2,3-epoxy alcohols (which cannot be isolated from the reaction mixture) are 3-chloro-1,2-diols. Treatment of the isolated chlorodiols with hydroxide provides epoxy alcohols of opposite configuration to those produced using the parent epoxidation system.

The use of a 2:1 ratio of $Ti(OR)_4$ to tartrate diester results in epoxidation of the "normal" olefin face (i.e., affording the 2S product) to 80% ee in the case of (E)-α-phenylcinnamyl alcohol. As presented in Appendix 1, the addition of electron withdrawing ligands to this 2:1 Ti:tartrate system also results in a reversal of enantioselectivity in epoxidation of allylic alcohols.

The 2:1 Ti:tartrate mixture has also been shown to be very effective for the kinetic resolution of racemic β-hydroxy amines by oxidation with TBHP.[85] As with allylic alcohols, the absolute configuration of fast- and slow-reacting enantiomers is highly predictable. Since amino alcohols and

especially the product N-oxides are better ligands than allylic alcohols and epoxy alcohols,[86] the catalyst system in the β-hydroxy amine oxidation reaction is likely to be more complicated than the asymmetric epoxidation system.

Finally, titanium tartrate has been found by Kagan and Pitchen to be an excellent catalyst for the asymmetric oxidation of sulfides to sulfoxides.[87] Three different catalyst preparations are useful: a 1:2 mixture of titanium to tartrate, and mixtures of $Ti(O\underline{i}Pr)_4$, tartrate, and water in ratios of 1:1:1 and 1:2:1. All mediate the asymmetric oxidation of sulfides in the same enantioselective sense; the best %ee is achieved with the last system. With TBHP and (+)-DET, the oxidation of methyl p-tolyl sulfide produces the R sulfoxide in 95% yield and 93% ee. The most remarkable aspect of this reaction is that the substrate has no obvious handle for prior coordination to the catalyst. Kagan's work inspired us to explore the effect of added water on the asymmetric epoxidation of allylic alcohols, since trace moisture is a likely contaminant of these reactions. These results are summarized in Appendix 1.

The titanium tartrate systems other than the parent asymmetric epoxidation catalyst to have appeared in the literature to date are therefore:

- 2:1 Ti:tartramide (asymmetric epoxidation)
- 2:1 $TiCl_2(OR)_2$:tartrate (asymmetric chlorohydroxylation)
- 2:1 Ti:tartrate (kinetic resolution of β-hydroxy amines)
- 1:2 Ti:tartrate, 1:1:1 Ti:tartrate:H_2O, and 1:2:1 Ti:tartrate:H_2O (asymmetric oxidation of sulfides)

Section II

Results and Discussion

A. Equilibrium Constants

It is the ability of Ti(IV) alkoxides to rapidly exchange ligands that enables the asymmetric epoxidation (and, indeed, achiral epoxidations of allylic alcohols on d^0 metal alkoxides) to occur. By the same token, this pervasive exchange behavior makes the asymmetric epoxidation reaction mixture difficult to characterize. Because diols such as tartrate exhibit much higher binding constants than monodentate alcohols, we consider their equilibrium phenomena separately from that of monodentate alcohols.

Exchange of bound monodentate alkoxide (including allylic alcohol and "spectator" alcohols such as iPrOH) for free alcohol or exchange among different alkoxide species is rapid in most cases.[39] Therefore, a statistical mixture of all possible Ti species involving monodentate alkoxides is expected to be present, subject only to thermodynamic factors (equilibrium constants). Hydroperoxides and epoxy alcohols, potential bidentate ligands, are also included in this category since their exchange reactions are fast compared with those of tartrate. We have determined the equilibrium constants for binding of tert-butyl hydroperoxide and triphenylmethyl (trityl) hydroperoxide to several different titanium species, with the desire to gain some insight into the manner of alkylperoxide binding to titanium.

The experimental procedure was that of Woodard,[78] relying on the difference in O-H stretching frequency of alcohols and hydroperoxides of approximately 100 cm^{-1} under dilute conditions in methylene chloride. By monitoring the absolute intensities of the two bands as known quantities of hydroperoxide are added to a solution of titanium alkoxide, the concentration of free and bound hydroperoxide can be calculated at every point. In principle, the equilibrium constant for the replacement of each of the four alkoxides of a titanium tetraalkoxide (K_1 - K_4 below) or for each of the

$$Ti(OR)_4 \underset{ROH}{\overset{R'OOH}{\rightleftharpoons}} Ti(OR)_3(OOR') \underset{ROH}{\overset{R'OOH}{\rightleftharpoons}} Ti(OR)_2(OOR')_2 \underset{ROH}{\overset{R'OOH}{\rightleftharpoons}} \cdots$$

K_1 K_2 K_3

two monodentate alkoxides of a Ti(tartrate)$(OR)_2$ unit can be determined by this method.

In practice, however, the decomposition of hydroperoxides at room temperature in the presence of titanium proved to be a limiting factor. In the presence of isopropoxide ligands, oxidation to acetone was observed; in the presence of t-butoxide ligands an unidentified decomposition process was found to turn the solutions yellow. Both of these reactions took place at a slow rate when less than one equivalent of hydroperoxide per titanium was added, but the rates increased with greater concentration of oxidant. Therefore, only the data for small amounts of added hydroperoxide were used, and the contribution of binding of more than one hydroperoxide per titanium was neglected. As detailed in the Experimental section, the data was treated as though only one exchangeable alkoxide was available per titanium center, except for Ti(OiPr)$_4$. The results reported in Table 5 therefore represent an upper bound to the first equilibrium constant since any contributions from the coordination of a second or third equivalent of hydroperoxide are included.

Table 5. Equilibrium constants for the exchange of hydroperoxide for alkoxide: $Ti(X)_3(OR) + R'OOH \rightleftharpoons Ti(X)_3(OOR') + ROH$.

$K_{eq} = [Ti(X)_3(OOR')][ROH]/[Ti(X)_3(OR)][R'OOH]$

entry	$Ti(X)_3(OR)$	R'OOH	K_{eq}
1	Ti(OiPr)$_4$	$(Me)_3COOH$	$K_1 = K_2 = 3.5 \pm 1$
2	Ti(DIPT)(OiPr)$_2$	$(Me)_3COOH$	0.7 ± 0.2
3	Ti(DIPT)(OtBu)$_2$	$(Me)_3COOH$	0.34 ± 0.1
4	Ti(OiPr)$_4$	$(Ph)_3COOH$	0.2 ± 0.1
5	Ti(DIPT)(OiPr)$_2$	$(Ph)_3COOH$	ca. 0.01

These figures must be considered in the light of recent measurements of the thermochemistry of ligand substitution reactions of titanium tetraalkoxides, undertaken by Professor Carl Hoff and coworkers at the University of Florida.[88] They have found that Ti(OiPr)$_4$ is 10-12 kcal/mole(monomer) higher in energy than Ti(OEt)$_4$, presumably because the former is largely a monomer and cannot form the stabilizing bridging al-

koxide linkages that trimeric $Ti(OEt)_4$ does. On the other hand, $Ti(DIPT)(O\underline{i}Pr)_2$ was found to be only ca. 4 kcal/mole higher in energy than $Ti(DIPT)(OEt)_2$, indicating that these two Ti-DIPT complexes have the same degree of association, differing in the steric environment of the alkoxide ligands.

Observed binding constants can therefore be the result of changes in molecularity or changes in the stability of a complex of constant molecularity. The stability of the product complex can be affected by both steric and electronic factors. That is, the exchange of one ligand for another may be favored by virtue of a more relaxed steric environment in the product or a more stable metal-ligand interaction in the product, regardless of steric factors. It thus becomes a complicated matter to attempt to assign reasons for the binding constant values of Table 5; the degrees of aggregation of the product complexes must first be determined. Nevertheless, a few simple conclusions may be drawn.

First, note that K_{eq} values for the Ti-tartrate complexes are much smaller than for $Ti(O\underline{i}Pr)_4$ alone. The binding of TBHP to $Ti(O\underline{i}Pr)_4$ is probably driven to some extent by a change in aggregation in going from $Ti(O\underline{i}Pr)_4$ to $Ti(O\underline{i}Pr)_3(O\underline{t}Bu)$ and $Ti(O\underline{i}Pr)_2(O\underline{t}Bu)_2$.[89] Such a change apparently does not occur with trityl hydroperoxide, since K_{eq} is less than 1.0. Ignoring for the moment possible electronic influences, from the lower K_{eq} for trityl hydroperoxide we can infer that the metal environment in Ti-tartrates is more sterically congested than in $Ti(O\underline{i}Pr)_4$.

Secondly, note that the K_{eq} value for Ti-tartrate plus trityl hydroperoxide (entry 5) is much smaller than for TBHP (entry 2), as expected given the much greater size of the triphenylmethyl group relative to the tert-butyl moiety. The magnitude of the difference suggests that the alkylperoxide ligand is bound in a bidentate fashion, bringing the alkyl group close to the metal center.

The proposition of bidentate coordination of the alkylperoxide is also supported by the observation that K_{eq} for TBHP is less than 1.0 with both $Ti(DIPT)(O\underline{i}Pr)_2$ and $Ti(DIPT)(O\underline{t}Bu)_2$. Assuming that no change in molecularity takes place, this implies that coordinated alkylperoxide is more sterically demanding than isopropoxide or t-butoxide; unlikely unless bidentate coordination of the alkylperoxide were important.

Finally, it is interesting to note that despite the very small value

of K_{eq} in entry 5, asymmetric epoxidation using trityl hydroperoxide proceeds at a rapid rate - one third of that with TBHP under pseudo-first order conditions (Appendix 1).[91] In the determination of K_{eq} values equilibrium was always achieved within one minute (the fastest possible observation time) after mixing the hydroperoxide with titanium alkoxide solution. These observations support the contention that ligand exchange reactions are rapid in titanium tartrate systems.

B. Kinetics

Employing the pseudo-first order kinetics technique of Woodard, we have attempted to answer the following questions:

(1) How far can the range of concentration of Ti-tartrate be extended before the first order dependence of rate on titanium concentration breaks down?

(2) Do molecular sieves affect the rates of epoxidation under pseudo-first order conditions?

(3) What is the effect of performing asymmetric epoxidation in solvents other than methylene chloride?

(4) What are the relative rates of epoxidation mediated by several Ti-tartrate systems of interest?

(5) Does asymmetric epoxidation exhibit a primary solvent deuterium isotope effect?

To avoid confusion in the comparison of different epoxidation systems, the concentration of catalytically active titanium, $[Ti]_{active}$, refers to the concentration of Ti atoms that are not tied up in $Ti(tartrate)_2$ or $Ti(tartramide)_2$ complexes, regardless of the actual aggregation state of any titanium complex. So while we will often write "$Ti(DIPT)(O\underline{i}Pr)_2$", we are not implying that the complex is a monomer.

The experiment by Woodard that allows us to make the above definition of $[Ti]_{active}$ is an important one to emphasize. While keeping the concentrations of $Ti(O\underline{i}Pr)_4$ and TBHP constant, he varied the concentration of DET from 1.0 to 2.0 equivalents with respect to $Ti(O\underline{i}Pr)_4$. The rate of epoxidation of (E)-α-phenylcinnamyl alcohol was observed to decrease linearly to a value very close to zero at 2.0 equivalents of DET. This suggests that, under pseudo-first order conditions, excess tartrate binds strongly

to Ti(DIPT)(O$\underline{i}$Pr)$_2$, giving catalytically inactive [Ti(tartrate)$_2$]$_x$.

Recall also that Hanson has observed that under catalytic conditions (5 mol% Ti with respect to substrate) the use of greater than a two-fold excess of tartrate to titanium still gives an active epoxidation system. This must mean that the second equivalent of tartrate per Ti has a lower binding constant than the first equivalent of ligand:

$$Ti(OR)_4 \underset{}{\overset{}{\rightleftharpoons}} Ti(OR)_2(tartrate) \underset{}{\overset{}{\rightleftharpoons}} Ti(tartrate)_2$$

$$K_b \qquad\qquad K_b'$$

$$K_b > K_b'$$

1. Rate order in $\underline{i}$PrOH; Rate of 1.0:1.0 Ti:tartrate.

We first present verification of Woodard's determination of the rate order in inhibitor alcohol, isopropanol, in CH_2Cl_2 solvent. Table 6 and Figure 9 summarize the experiments for the epoxidation of (E)-2-decen-1-ol by TBHP and Ti(DIPT)(O$\underline{i}$Pr)$_2$. With titanium concentrations close to 0.0145 M, [$\underline{i}$PrOH] was varied from 0.150 M to 0.412 M, including the isopropanol released in the binding of tartrate to Ti(O$\underline{i}$Pr)$_4$. Assuming, (as is confirmed by Table 7) that the rate is first order in [Ti]$_{active}$, we multiplied each of the observed rates by a small factor (0.0145/[Ti]$_{active}$) to normalize all values with respect to [Ti]$_{active}$. Plotting ln([$\underline{i}$PrOH]) vs. ln(Rate$_{corr}$) produces a line of slope = -1.91, the pseudo-first order rate dependence on [$\underline{i}$PrOH]. This compares well with the value of -2.03 found by Woodard for the epoxidation of (E)-2,7-octadien-1-ol. In Table 7 and Figure 10 are found another determination of the rate order in isopropanol; for (E)-2-hexenol and Ti(DIPT)(O$\underline{i}$Pr)$_2$ it was also found to be -1.91 (though with a larger error margin, since only three data points were obtained).

Woodard also observed that use of a 1.0:1.0 ratio of Ti:tartrate resulted in decreased enantioselectivities and poor reproducibility in the rates of epoxidation of slower reacting substrates. We took advantage of the synthesis of the analytically pure compound Ti(DIPT)(O$\underline{i}$Pr)Br, **13d**, by Dr. Steven Pedersen[96b] as a source of Ti(DIPT)(O$\underline{i}$Pr)$_2$ of exactly equimolar Ti:tartrate composition, to demonstrate this phenomenon in the epoxidation of (E)-2-decen-1-ol.

Table 6. Pseudo-first order kinetics; rate order in isopropanol (inhibitor).
Substrate = trans-2-decenol. Catalyst = Ti(DIPT)(O$\underline{i}$Pr)$_2$.
Solvent = CH_2Cl_2 (distilled from CaH_2, unless otherwise noted). Oxidant = TBHP in toluene.

Entry	(M) $[Ti]_{active}$[a]	(M) $[\underline{i}PrOH]$[b]	(M) [TBHP]	(10^{-4} sec^{-1}) $Rate_{obs}$	Sieves	(10^{-4} sec^{-1}) $Rate_{corr}$[c]	(10^{-4} M^2 sec^{-1}) $Rate_{obs} \times [\underline{i}PrOH]^2$	Notes
1	0.0146	0.412	0.0150	7.07	4A	7.02	1.20	
2	0.0141	0.408	''	7.32	3A	7.50	1.22	
3	0.0148	0.299	''	12.3	none	12.1	1.10	
4	0.0142	0.301	''	13.4	none	13.7	1.22	Solvent dist'd, then treated with 3A sieves
5	0.0143	0.305	''	13.0	4A	13.2	1.21	
6	0.0145	0.303	''	13.4	3A	13.4	1.23	
7	0.0143	0.301	''	13.6	4A	13.8	1.23	
8	0.0145	0.301	''	13.8	3A	13.8	1.25	TBHP in CH_2Cl_2
9	0.0153	0.211	''	27.2	none	26.3	1.21	Reag. grade solvent (not distilled), dried over 3A sieves
10	0.0145	0.202	''	28.2	4A	28.2	1.15	
11	0.0145	0.194	''	31.2	3A	31.2	1.17	
12	0.0145	0.151	''	50.5	3A	50.5	1.15	
13	0.0142	0.150	''	48.2	none	49.2	1.08	

a. $[Ti]_{active} = 2[Ti(O\underline{i}Pr)_4] - [DIPT]$
b. $[\underline{i}PrOH] = [\underline{i}PrOH]_{added} + 2[DIPT]$
c. $Rate_{corr}$ = Rate corrected for $[Ti]_{active} \neq 0.0145$;
$= Rate_{obs} \times (0.0145/[Ti]_{active})$

Omitting entry 3, a plot of $\ln([\underline{i}PrOH])$ vs. $\ln(Rate_{corr})$ gives a straight line.
$R^2 = 0.999$, slope = -1.91.

Table 7. Pseudo-first order kinetics; rate order in isopropanol (inhibitor).
Substrate = trans-2-hexenol. Catalyst = Ti(DIPT)(O$\underline{i}$Pr)$_2$.
Solvent = CH_2Cl_2 (distilled from CaH_2). Oxidant = TBHP in toluene.

Entry	(M) $[Ti]_{active}$[a]	(M) $[\underline{i}PrOH]$[b]	(M) [TBHP]	(10^{-4} sec^{-1}) $Rate_{obs}$	Sieves	(10^{-4} sec^{-1}) $Rate_{corr}$[c]	(10^{-4} M^2 sec^{-1}) $Rate_{corr} \times [\underline{i}PrOH]^2$	Notes
53	0.0130	0.103	0.0150	72	none	71		too fast to measure
54	0.0129	0.200	''	22.3	''	22.5	0.900	
55	0.0129	0.299	''	11.5	''	11.6	1.04	
56	0.0133	0.462	''	4.65	''	4.55	0.971	

a. $[Ti]_{active} = 2[Ti(O\underline{i}Pr)_4] - [DIPT]$
b. $[\underline{i}PrOH] = [\underline{i}PrOH]_{added} + 2[DIPT]$
c. $Rate_{corr}$ = Rate corrected for $[Ti]_{active} \neq 0.0130$;
$= Rate_{obs} \times (0.0130/[Ti]_{active})$

For entries 54-56, a plot of $\ln([\underline{i}PrOH])$ vs. $\ln(R_{corr})$ gives a straight line;
$R^2 = 0.994$, slope = -1.91.

Figure 9. Rate order in iPrOH; (E)-2-decenol in CH_2Cl_2 (Table 6).

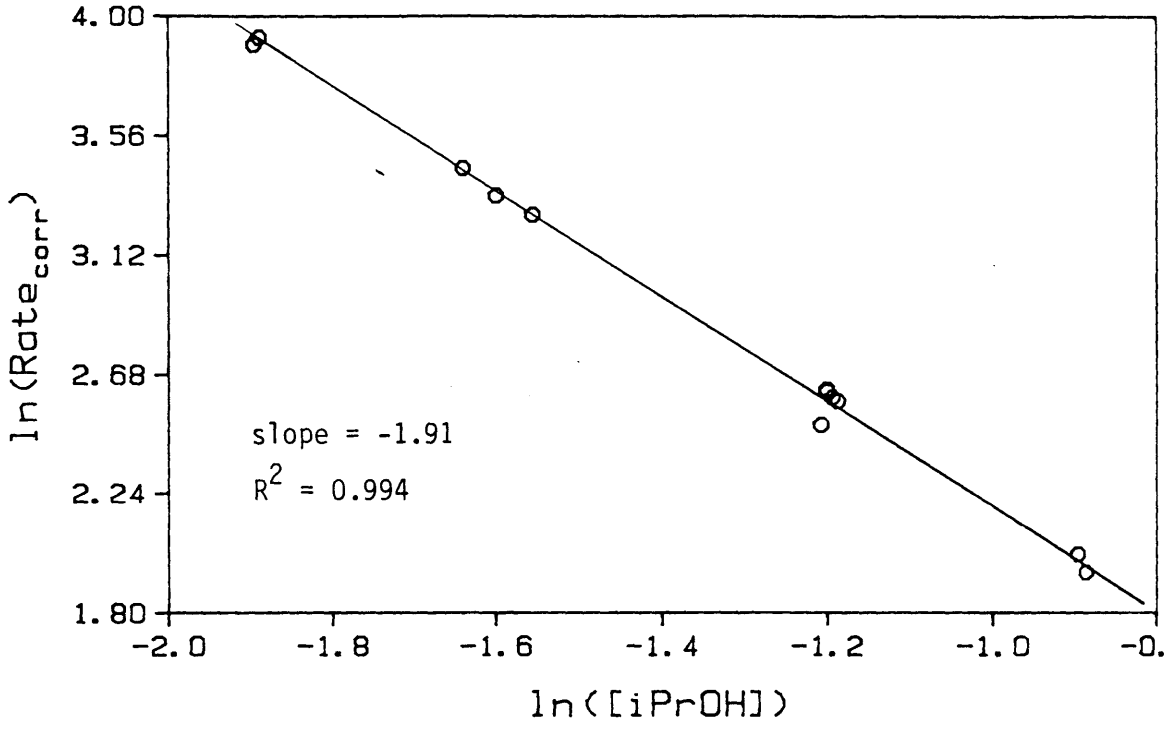

Figure 10. Rate order in iPrOH; (E)-2-hexenol in CH_2Cl_2 (Table 7).

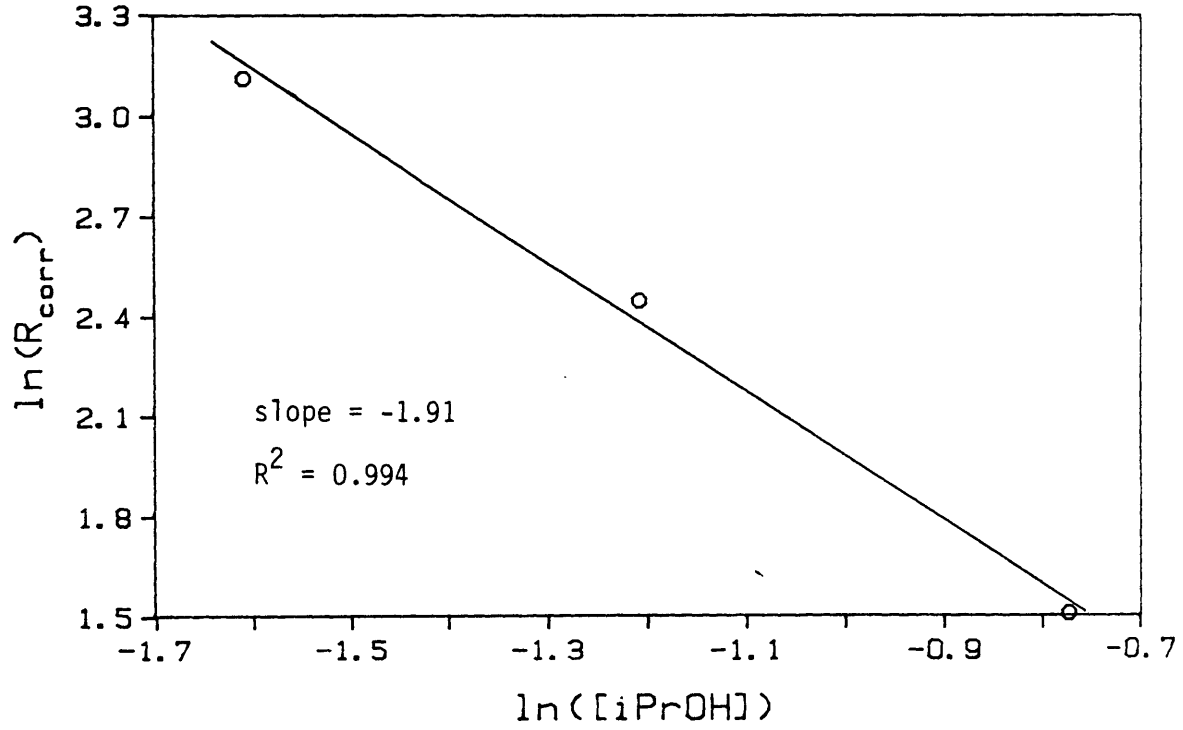

Reactions 26 and 27 of Table 8 show that the rate of epoxidation using Ti(DIPT)(O$\underline{i}$Pr)$_2$ generated from **13d** is significantly slower than when DIPT is present in excess. In fact, when DIPT is added to Ti(DIPT)(O$\underline{i}$Pr)$_2$ prepared from **13d** (entry 28), epoxidation returns to exactly the same rate as is observed with catalysts prepared from Ti(O$\underline{i}$Pr)$_4$ plus excess DIPT.

The poor behavior of 1.0:1.0 Ti:tartrate arises from the presence of small amounts Ti:tartrate complexes of different composition (2:1, 2:3, 3:2, etc.). Complexes with more tartrate than Ti per molecule (such as Ti(tartrate)$_2$) are likely to be catalytically inactive. It is the species that contain more Ti than tartrate that are active; the result above suggests that they are less enantioselective and slower. At a greater than 1:1 ratio of tartrate:Ti, the concentration of the these "harmful" complexes is reduced at the expense of increased amounts of catalytically inactive species. We have obtained nmr evidence to support these conclusions, discussed later in Sections II.C.4 and II.C.7.

2. Rate order in $[Ti]_{active}$

As mentioned in the introduction, Woodard observed that the dependence of rate on concentration of Ti(DIPT)(O$\underline{i}$Pr)$_2$ was first order in the range of concentrations from 0.012-0.035 M for (E)-2,7-octadien-1-ol, and first order for Ti(DET)(O$\underline{i}$Pr)$_2$ and (E)- α-phenylcinnamyl alcohol. A strictly first order rate dependence supports the suggestion that the catalytically active species is not a minor component of different aggregation state than the major species in solution. For example, if a small amount of monomeric titanium tartrate were the active agent (in the presence of a larger amount of inactive dimeric material), or if monomeric and dimeric species were active to significantly different degrees, we would expect the rate order in Ti-tartrate to change with concentration, as the relative concentrations of monomeric and dimeric species changes. The observation that the rate dependence is strictly first order is therefore important, and we decided to extend the measurements over a greater range of Ti-tartrate concentration.

The rates of pseudo-first order epoxidation of trans-2-decenol with varying amounts of Ti-tartrate are given below in Table 9. A plot of $\ln(R_{obs} \times [\underline{i}PrOH]^2)$ vs. $\ln([Ti]_{active})$ (Figure 11) reveals a first order

Table 8. Pseudo-first order kinetics; Control reactions with sieves;
Catalyst preparations from Ti(DIPT)(O*i*Pr)Br.
Substrate = *trans*-2-decenol. Catalyst = $Ti(DIPT)(O\underline{i}Pr)_2$.
Solvent = CH_2Cl_2 (distilled from CaH_2). Oxidant = TBHP in toluene.

Entry	(M) $[Ti]_{active}$[a]	(M) $[\underline{i}PrOH]$[b]	(M) [TBHP]	(10^{-4} sec^{-1}) $Rate_{obs}$	Sieves	(10^{-4} sec^{-1}) $Rate_{corr}$[c]	(10^{-4} M^2 sec^{-1}) $Rate_{corr} \times [\underline{i}PrOH]^2$	Notes
24	none	none	0.0150	0.086	4A	.....	.....	0.600 g sieves used
25	none	none	''	0.042	4A	.....	.....	Rxn flask acid washed
26	0.0143	0.297	0.0150	9.30	none	9.43	0.832	Ti(DIPT)(O*i*Pr)Br + *i*PrOH exactly 1:1 Ti:DIPT
27	0.0146	0.303	''	9.62	4A	9.55	0.877	Ti(DIPT)(O*i*Pr)Br + *i*PrOH exactly 1:1 Ti:DIPT
28	0.0145	0.300	''	13.20	4A	13.20	1.19	DIPT added, Ti:DIPT = 1.0:1.17

a. $[Ti]_{active} = 2[Ti(O\underline{i}Pr)_4] - [DIPT]$
b. $[\underline{i}PrOH] = [\underline{i}PrOH]_{added} + 2[DIPT]$
c. $Rate_{corr}$ = Rate corrected for $[Ti]_{active} \neq 0.0145$;
$= Rate_{obs} \times (0.0145/[Ti]_{active})$

Table 9. Pseudo-first order kinetics; rate order in $Ti(DIPT)(O\underline{i}Pr)_2$.
Substrate = trans-2-decenol. Catalyst = $Ti(DIPT)(O\underline{i}Pr)_2$.
Solvent = CH_2Cl_2 (distilled from CaH_2). Oxidant = TBHP in toluene.

Entry	(M) $[Ti]_{active}$[a]	(M) $[\underline{i}PrOH]$[b]	(M) [TBHP]	(10^{-4} sec^{-1}) $Rate_{obs}$	Sieves	(10^{-4} M^2 sec^{-1}) $Rate_{obs} x [\underline{i}PrOH]^2$	Notes
14	0.00620	0.152	0.0150	22.2	3A	0.512	
15	0.00810	0.301	''	7.58	4A	0.687	
	0.0145	varies	''	varies		1.19	Average of entries 1-13
16	0.0251	0.312	''	20.2	3A	1.97	
17	0.0251	0.304	''	23.2	4A	2.13	
18	0.0334	0.313	''	28.0	4A	2.75	
19	0.0428	0.498	''	14.8	4A	3.67	
20	0.0436	0.301	''	38.0	4A	3.45	
21	0.0622	0.201	0.0075	62.3	3A	5.03	Rate corrected for [TBHP] by multiplying by 2.0.
22	0.0790	0.315	0.0150	63.3	3A	6.28	
23	0.0776	0.661	''	11.1	3A	4.85	

a. $[Ti]_{active} = 2[Ti(O\underline{i}Pr)_4] - [DIPT]$
b. $[\underline{i}PrOH] = [\underline{i}PrOH]_{added} + 2[DIPT]$

For entries 14-21, a plot of $\ln([Ti]_{active})$ vs. $\ln(R_{obs} x [\underline{i}PrOH]^2)$ gives a straight line.
$R^2 = 0.9985$, slope = 0.99.

Fig. 11. Rate order in Ti(DIPT)(O$\underline{i}$Pr)$_2$; ($\underline{E}$)-2-decenol in CH_2Cl_2 (Table 7).

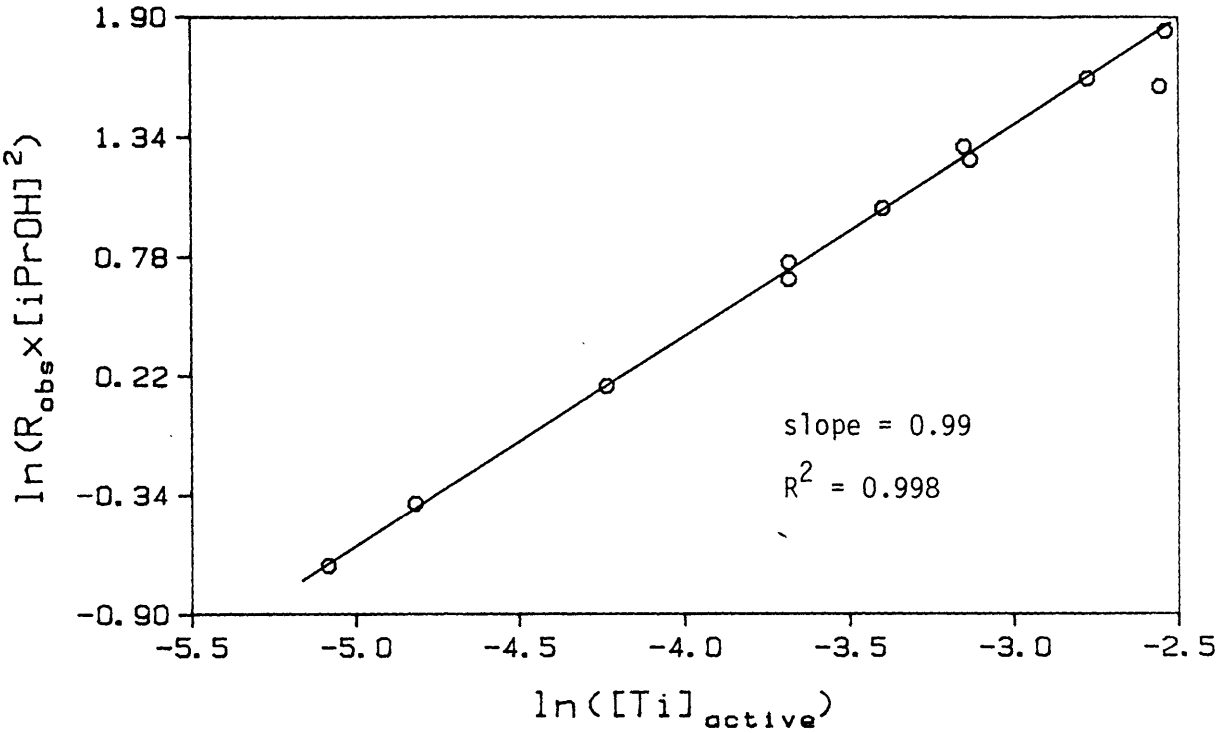

dependence from 0.0062 M to 0.0622 M (slope = 0.99). At 0.0790 M (entry 22), the rate falls below that expected by a first order relationship. At this concentration, however, the overall polarity of the reaction mixture has been significantly increased. We can expect that a more coordinatively polar medium slows the reaction rate. This is highlighted by entry 23, in which the concentration of isopropanol is doubled and the corrected rate drops further from first order behavior.

It was possible to extend the observation of first order dependence on $[Ti]_{active}$ beyond 0.044 M only by lowering the TBHP concentration. In entry 21, [TBHP] was reduced to half the value of the other experiments. Woodard found the rate dependence on [TBHP] to be first order; therefore the rate was correspondingly reduced so that less isopropanol could be used, thus lowering the polarity of the reaction mixture. By the same token, it should be possible to obtain measurements at well below 0.006 M $[Ti]_{active}$ by increasing [TBHP] and lowering [$\underline{i}$PrOH], keeping in mind the requirement that the concentration of allylic alcohol be at least 20 fold less than each of the other reactants.

For epoxidation in CH_2Cl_2, then, the experimental rate law found here

matches that found previously. Also, the suggestion that the asymmetric epoxidation catalyst is of a single aggregation state is strengthened by the observation of first order rate dependence on $[Ti]_{active}$ over a 10-fold concentration range.

3. Molecular sieves

As mentioned in the introduction, Dr. Robert Hanson has discovered that powdered molecular sieves dramatically increase both the activity and longevity of catalytic (5 mol% relative to substrate) quantities of Ti-tartrate, presumably by removing adventitious water from the reaction mixture. We tested this hypothesis by examining the effect of including molecular sieves in pseudo-first order reactions.

In Table 6, we see that the rate of epoxidation in the presence of molecular sieves (entries 5-8) is the same as in their absence (entry 4). The difference between entry 4 and entry 3 is interesting. Entry 3 was run under the previously standard pseudo-first order conditions, in which CH_2Cl_2 was freshly distilled from CaH_2. In entry 4, that distilled solvent was allowed to stand over activated 3A sieve beads for 1 h, and then was transferred to the reaction flask. We see that distillation is not foolproof, since the rate in entry 3 is significantly less than entry 4. (Compare the values of $rate_{obs} x [\underline{i}PrOH]_2$.) Distillation alone also works adequately sometimes, as seen by comparing entry 13 with entry 12.

From entry 9, it also appears that distillation itself is unnecessary. In that reaction, a freshly opened gallon bottle of reagent grade CH_2Cl_2 was treated with approximately 500 g of activated 3A molecular sieve beads for 2 h at room temperature before use. The epoxidation rate was the same as reactions containing distilled solvent and 3A or 4A sieve powder (entries 10 and 11).

Reaction 26 (Table 8), using CH_2Cl_2 distilled and dried over sieves but without sieves in the reaction mixture, shows the same rate as reaction 27, done in the presence of 4A sieves. For epoxidations in ether, Table 10 provides four examples of cases in which reactions in dry solvent alone and solvent+sieves proceeded at the same rate (entry 31 vs. 29-30, 35 vs. 32-34, 37 vs. 36, and 39 vs. 38). In Table 13 (reactions in pentane), entry 47 (no sieves) fits in perfectly with the other data points, all obtained in the presence of sieves.

Therefore, when care is taken to dry solvents by other means, there is no measurable rate difference between reactions run under pseudo-first order conditions in dry solvent alone or in a medium containing activated molecular sieves. When the solvent is not dry, it appears that sieves are quite effective at removing trace amounts of water. Control reactions (Table 8, entries 24-25) show that in the absence of Ti, sieves alone mediate the disappearance of allylic alcohol to a negligible extent.

This suggests that in cases when adventitious water is a problem, it is the solvent that should be checked first when routine precautions have been taken with tartrate, substrate, and hydroperoxide. The inclusion of sieves can therefore make the handling of solvents and reagents much easier, as demonstrated by the successful use of reagent grade CH_2Cl_2. As long as one starts with reasonably dry solvent, the use of sieves should insure an acceptably dry environment for asymmetric epoxidation.[92]

We must point out some disagreement between the rate determinations in CH_2Cl_2 in this work and Woodard's. For the purposes of comparing reactions of differing catalyst, oxidant, and inhibitor concentrations, the absolute rate constant from the full rate expression is used:

$$k_{abs} = Rate_{obs} x [\underline{i}PrOH]_2 / ([TBHP][Ti]_{active}).$$

For Woodard's epoxidations of (E)-2,7-octadien-1-ol, $k_{abs} = 0.32\ sec^{-1}$. For the structurally similar (E)-2-decen-1-ol (Tables 6, 9), we find $k_{abs} = 0.55\ sec^{-1}$. For (E)-2-hexen-1-ol (Table 7), $k_{abs} = 0.50\ sec^{-1}$.

It is possible, though not likely, that the slower rate of epoxidation of octadienol is real. Since the same rate dependence on $[Ti]_{active}$ and [$\underline{i}$PrOH] were found, it appears more likely that a systematic error afflicts one or the other set of data. We have found that unless great care is taken in the maintainance of a CaH_2 still, a volatile solid coats the walls of the still, possibly contaminating the distilled solvent. We now recommend that CH_2Cl_2 not be distilled from CaH_2, but rather be dried over 3A molecular sieves.

4. Other Solvents

It has been observed for Mo(VI)-catalyzed epoxidations that reaction rate follows a small and roughly inverse dependence on solvent polarity for

aprotic solvents.[31] The response of asymmetric epoxidation to solvent polarity was determined by pseudo-first order kinetics in ether and pentane.

a. Ether

Epoxidations of (E)-2-decen-1-ol in ether are summarized in Table 10 and Figure 12; the results for (E)-2-hexen-1-ol comprise Table 11 and Figure 13.

For (E)-2-decen-1-ol, the rate order in isopropanol was found to be -1.83 for isopropanol concentrations from 0.101 M to 0.301 M, fairly close to the expected value of -2.0. The pseudo-first order rate of epoxidation in ether, k_{abs}, is 0.056 sec^{-1}; 9.8 times slower than in CH_2Cl_2.

Entries 38 and 39 of Table 10 lie well off the ln([iPrOH]) vs. $ln(Rate_{corr})$ line. No isopropanol was added to these reactions; free isopropanol is only generated by coordination of DIPT to $Ti(OiPr)_4$. We cannot explain these results, except to note that these are very rapid reactions and may not be accurately measured by our technique.

For (E)-2-hexen-1-ol, the rate order in isopropanol is -1.89 (Table 11 entries 40-42); k_{abs} = 0.050 sec^{-1}, 10 times slower than in CH_2Cl_2. As with (E)-2-decen-1-ol, epoxidations done in the presence of very little inhibitor alcohol ([iPrOH] = 0.0315) are reproducible and are slower than expected for an inverse second order dependence on isopropanol concentration.

b. Pentane

Asymmetric epoxidations in pentane appear in Table 12 and Figure 14. Variation of [iPrOH] while holding other variables constant (entries 46-49) yields a rate dependence on isopropanol of -1.50. Using this value, the rate order in $[Ti]_{active}$ was found to be approximately 0.49 (entries 50-52).

The kinetic behavior in pentane, then, is much different from the more polar CH_2Cl_2 and ether, and strongly signals a change in mechanism or a change in the structural behavior of Ti-tartrate, or both. In fact, Signer molecular weight determinations in pentane (section II.C.1) provide

Table 10. Pseudo-first order kinetics; rate order in isopropanol (inhibitor).
Substrate = trans-2-decenol. Catalyst = Ti(DIPT)(O$\underline{i}$Pr)$_2$.
Solvent = Ether (distilled from Na/benzophenone). Oxidant = TBHP in toluene.

Entry	(M) $[Ti]_{active}$[a]	(M) $[\underline{i}PrOH]$[b]	(M) [TBHP]	(10^{-4} sec^{-1}) $Rate_{obs}$	Sieves	(10^{-4} sec^{-1}) $Rate_{corr}$[c]	(10^{-4} M^2 sec^{-1}) $Rate_{corr} x [\underline{i}PrOH]^2$
29	0.0148	0.301	0.0150	1.44	none	1.41	0.128
30	0.0145	0.301	''	1.43	none	1.43	0.130
31	0.0143	0.299	''	1.48	4A	1.50	0.134
32	0.0144	0.199	''	3.00	none	3.17	0.126
33	0.0141	0.202	''	3.02	none	3.10	0.126
34	0.0140	0.201	''	2.87	none	2.97	0.120
35	0.0151	0.202	''	3.05	4A	2.93	0.119
36	0.0149	0.102	''	10.2	none	10.4	0.108
37	0.0149	0.101	''	10.9	4A	10.6	0.108
38	0.0140	0.0425	''	32.4	none	33.6	0.060
39	0.0144	0.0431	''	33.3	4A	33.5	0.062

a. $[Ti]_{active} = 2[Ti(O\underline{i}Pr)_4] - [DIPT]$
b. $[\underline{i}PrOH] = [\underline{i}PrOH]_{added} + 2[DIPT]$
c. $Rate_{corr}$ = Rate corrected for $[Ti]_{active} \neq 0.0145$;
$= Rate_{obs} \times (0.0145/[Ti]_{active})$

For entries 29-37, a plot of $\ln([\underline{i}PrOH])$ vs. $\ln(R_{corr})$ gives a straight line;
$R^2 = 0.9991$, slope = -1.83.
For entries 29-39, $R^2 = 0.994$, slope = -1.63.

Table 11. Pseudo-first order kinetics; rate order in isopropanol (inhibitor).
Substrate = trans-2-hexenol. Catalyst = Ti(DIPT)(O$\underline{i}$Pr)$_2$.
Solvent = Ether (distilled from Na/benzophenone). Oxidant = TBHP in toluene.

Entry	(M) $[Ti]_{active}$[a]	(M) $[\underline{i}PrOH]$[b]	(M) [TBHP]	(10^{-4} sec^{-1}) $Rate_{obs}$	Sieves	(10^{-4} sec^{-1}) $Rate_{corr}$[c]	(10^{-4} M^2 sec^{-1}) $Rate_{corr} \times [\underline{i}PrOH]^2$
40	0.0122	0.286	0.0150	1.14	none	1.31	0.107
41	0.0142	0.200	''	2.65	''	2.62	0.105
42	0.0133	0.152	''	4.12	''	4.33	0.100
43	0.0140	0.0317	''	31.2	''	31.2	0.031
44	0.0136	0.0312	''	30.8	''	31.7	0.031
45	0.0136	0.0318	''	29.8	''	30.7	0.031

a. $[Ti]_{active} = 2[Ti(O\underline{i}Pr)_4] - [DIPT]$
b. $[\underline{i}PrOH] = [\underline{i}PrOH]_{added} + 2[DIPT]$
c. $Rate_{corr}$ = Rate corrected for $[Ti]_{active} \neq 0.0140$;
$= Rate_{obs} \times (0.0140/[Ti]_{active})$

For entries 40-42, a plot of $\ln([\underline{i}PrOH])$ vs. $\ln(R_{corr})$ gives a straight line;
$R^2 = 0.9997$, slope = -1.89.

Figure 12. Rate order in iPrOH; (E)-2-decenol in ether (Table 10).

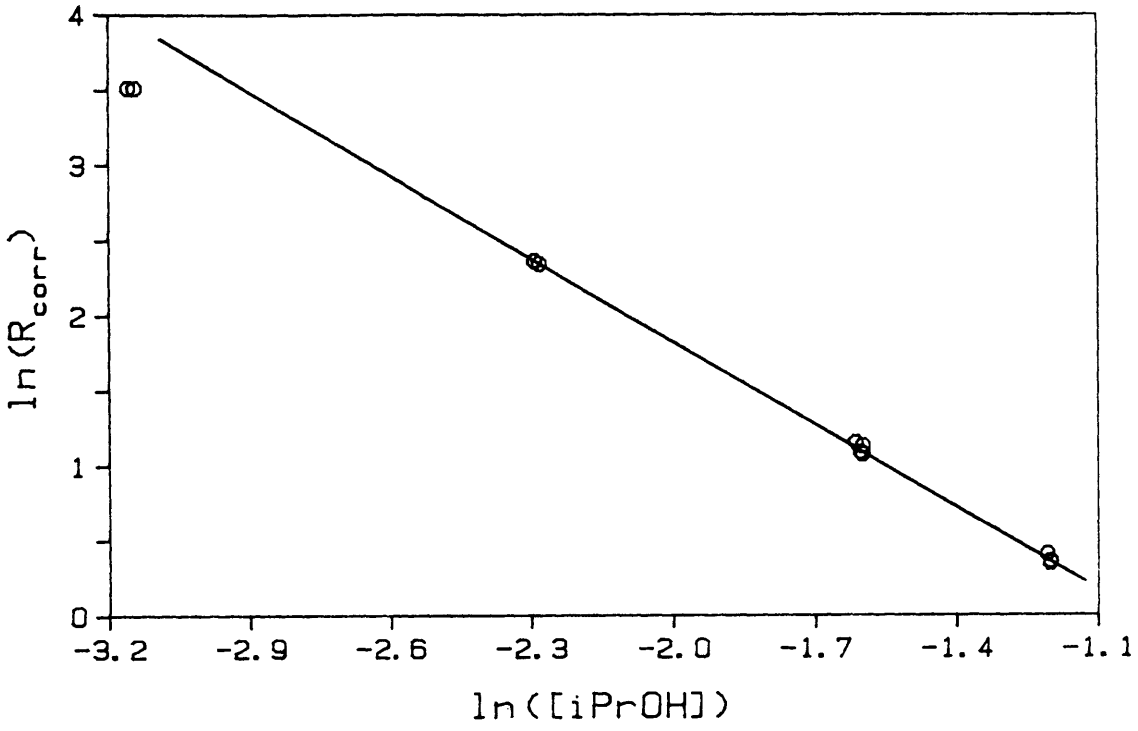

Figure 13. Rate order in iPrOH; (E)-2-hexenol in ether (Table 11).

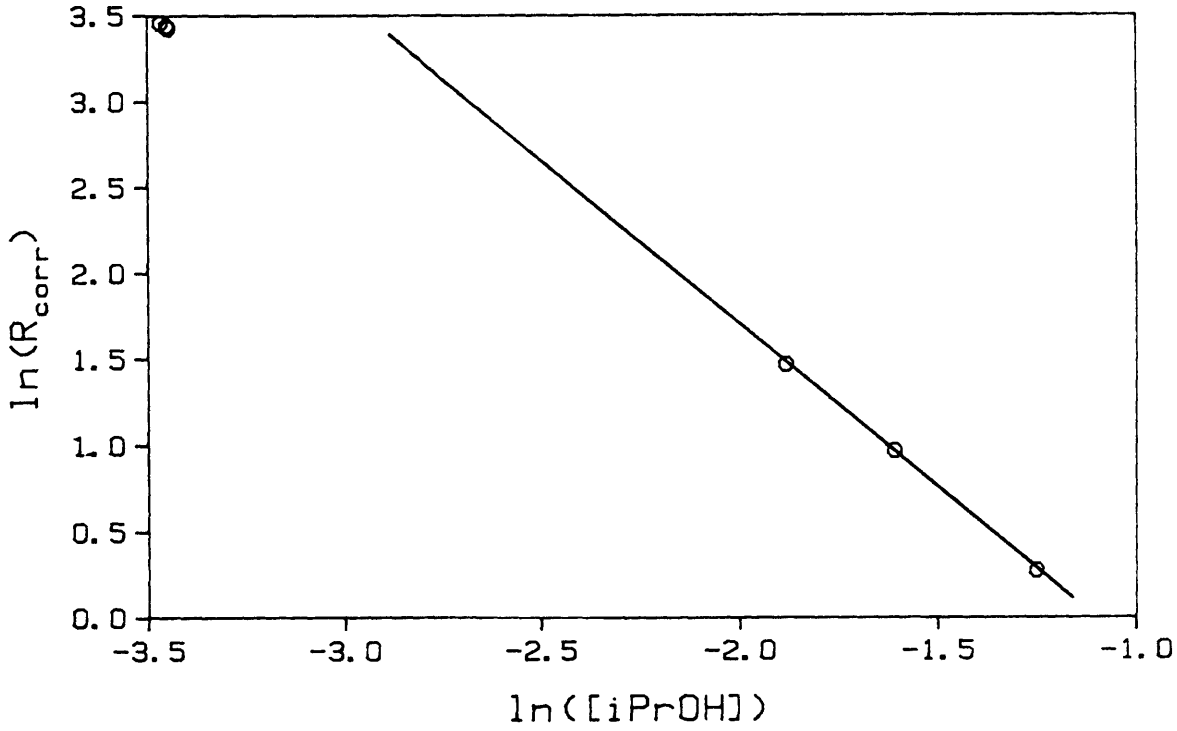

evidence that Ti(DIPT)(O$\underline{i}$Pr)$_2$ is largely a trimer. The epoxidation of ($\underline{E}$)-α-phenylcinnamyl alcohol suffers as well; the epoxy alcohol was isolated in 90% yield but only 94% ee.

Since the rate law is not the same as for CH_2Cl_2 and ether, for the purposes of rate comparison we select one set of conditions to compare the solvents: [Ti]active = 0.0145 M, [$\underline{i}$PrOH] = 0.300 M, and [TBHP] = 0.0150 M.

CH_2Cl_2: $Rate_{obs} = 13.8 \times 10^{-4}$ sec^{-1} $R_{rel} = 1.0$

Ether: $Rate_{obs} = 1.45 \times 10^{-4}$ sec^{-1} $R_{rel} = 0.10$

Pentane: $Rate_{obs} = 4.35 \times 10^{-4}$ sec^{-1} $R_{rel} = 0.32$

From a practical standpoint, we see that the asymmetric epoxidation may be performed in any of these solvents without a great decrease in rate, though with decreasing inhibitor alcohol concentration, the rates of reaction in pentane will diverge from that in CH_2Cl_2 and ether.

Figure 14. Rate order in $\underline{i}$PrOH and Ti(DIPT)(O$\underline{i}$Pr)$_2$; ($\underline{E}$)-2-decenol in pentane (Table 12).

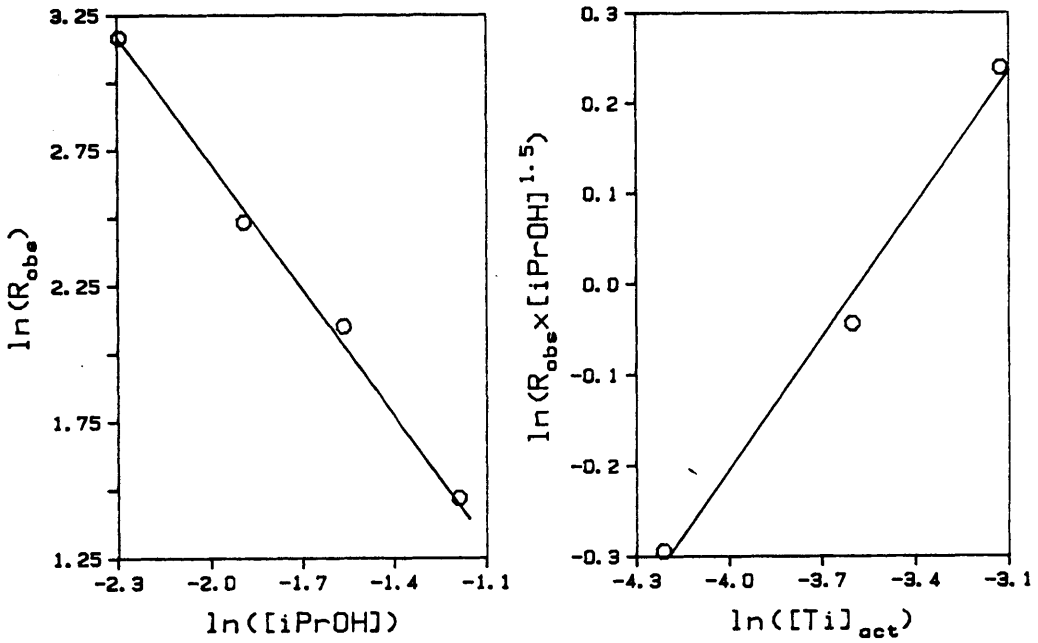

Table 12. Pseudo-first order kinetics; rate order in isopropanol, Ti(DIPT)(O$\underline{i}$Pr)$_2$.
Substrate = trans-2-decenol. Catalyst = Ti(DIPT)(O$\underline{i}$Pr)$_2$.
Solvent = Pentane (distilled from Na/benzophenone). Oxidant = TBHP in toluene.

Entry	(M) $[Ti]_{active}$[a]	(M) [$\underline{i}$PrOH][b]	(M) [TBHP]	(10^{-4} sec^{-1}) $Rate_{obs}$	Sieves	(10^{-4} M^2 sec^{-1}) $Rate_{obs} \times [\underline{i}PrOH]^{1.50}$	Notes
46	0.0147	0.101	0.0150	23.7	4A	0.761	
47	0.0148	0.151	''	12.0	none	0.703	
48	0.0149	0.209	''	8.17	4A	0.781	
49	0.0148	0.305	''	4.35	4A	0.733	
50	0.0273	0.308	''	5.60	3A	0.957	
51	0.0439	0.420	''	4.65	3A	1.27	
52	0.0148	varies	''	varies		0.745	Average of entries 46-49

a. $[Ti]_{active} = 2[Ti(O\underline{i}Pr)_4] - [DIPT]$
b. $[\underline{i}PrOH] = [\underline{i}PrOH]_{added} + 2[DIPT]$

For entries 46-49, a plot of $\ln([\underline{i}PrOH])$ vs. $\ln(R_{obs})$ gives a straight line;
$R^2 = 0.996$, slope = -1.50.

For entries 50-52, a plot of $\ln([Ti]_{active})$ vs. $\ln(R_{obs} \times [\underline{i}PrOH]^{1.5})$ gives a straight line;
$R^2 = 0.988$, slope = 0.49.

The enantiomeric excess of epoxidation of (E)-α-phenylcinnamyl alcohol by stoichiometric Ti(DIPT)(OiPr)$_2$ at -20°C is also solvent dependent. Table 13 summarizes the results:

Table 13. Asymmetric epoxidation of (E)-α-phenylcinnamyl alcohol.

Solvent	% ee (Configuration)	% Yield
CH_2Cl_2	>98 (2S)	90
Ether	98 (2S)	89
Pentane	94 (2S)	90
Cyclohexane	95 (2S)	88

The level of asymmetric induction parallels the kinetic behavior: epoxidations in CH_2Cl_2 and ether obey the same pseudo-first order rate law and proceed in high ee; in pentane the kinetics differ and enantiomeric excess is reduced. In energetic terms, the difference between CH_2Cl_2 and pentane is significant: a decrease in ee from 98% to 94% represents a difference of 0.6 kcal/mole in $\Delta\Delta G^{\neq}$ for epoxidation, and a decrease from 99.1% to 94% indicates a difference of fully 1.0 kcal/mole.

5. Other Titanium Tartrate Systems

Pseudo-first order rate measurements were also made in CH_2Cl_2 to compare the epoxidation activity of Ti(OiPr)$_4$ in the presence of varying amounts of tartrate. As we have seen, a 1:1 mixture of Ti:tartrate may contain species of several different stoichiometries. The success of the asymmetric epoxidation reaction can be due to one of three situations: (1) only one Ti:tartrate species is present in the 1:1 mixture, and this species is the enantioselective catalyst, (2) more than one Ti:tartrate species is present, but only one is catalytically active (that the active species need not be the major component of the catalyst mixture is demonstrated by the asymmetric hydrogenation reaction[90]), or (3) more than one Ti:tartrate species is present and more than one is active, but each mediates epoxidation with high enantioselectivity.

Structural studies discussed in Section II.C. indicate that there is one major Ti:tartrate species present in a 1:1 solution and that it is the dominant asymmetric epoxidation catalyst. However, it is interesting to

Table 14. Pseudo-first order kinetics; rate order in isopropanol (inhibitor).
Substrate = trans-2-hexenol. Catalyst = $Ti_2(DIPT)(O\underline{i}Pr)_6$ (2:1 Ti:DIPT).
Solvent = CH_2Cl_2 (distilled from CaH_2). Oxidant = TBHP in toluene.

Entry	(M) $[Ti(O\underline{i}Pr)_4]^a$	(M) [DIPT]	(M) $[\underline{i}PrOH]^b$	(M) [TBHP]	(10^{-4} sec^{-1}) $Rate_{obs}$	Sieves
57	0.0134	0.00654	0.103	0.0150	14.1	none
58	0.0137	0.00681	0.213	''	5.72	''
59	0.0130	0.00650	0.300	''	3.18	''

a. In this case, $[Ti]_{active} = [Ti(O\underline{i}Pr)_4]$ used to prepare the 2:1 complex.
b. $[\underline{i}PrOH] = [\underline{i}PrOH]_{added} + 2[DIPT]$

A plot of $\ln([\underline{i}PrOH])$ vs. $\ln(R_{obs})$ gives a straight line; $R^2 = 0.993$, slope = -1.37.

Table 15. Pseudo-first order kinetics; rate order in isopropanol (inhibitor).
Substrate = trans-2-hexenol. Catalyst = $Ti(O\underline{i}Pr)_4$
Solvent = CH_2Cl_2 (distilled from CaH_2). Oxidant = TBHP in toluene.

Entry	(M) $[Ti(O\underline{i}Pr)_4]$	(M) $[\underline{i}PrOH]$	(M) [TBHP]	(10^{-4} sec^{-1}) $Rate_{obs}$	Sieves
60	0.0134	0.106	0.0150	12.1	none
61	0.0130	0.200	''	7.38	''
62	0.0130	0.300	''	4.37	''

A plot of $\ln([\underline{i}PrOH])$ vs. $\ln(R_{obs})$ gives a straight line; $R^2 = 0.98$, slope = -0.96.

Table 16. Pseudo-first order kinetics.
Substrate = trans-2-hexenol. Catalyst = Ti:DNBnT Complexes.
Solvent = CH_2Cl_2 (distilled from CaH_2). Oxidant = TBHP in toluene.

Entry	Catalyst	(M) $[Ti]_{active}$[a]	(M) $[iPrOH]$[b]	(M) [TBHP]	(10^{-4} sec^{-1}) $Rate_{obs}$	Sieves	Notes
63	$Ti(DNBnT)(OiPr)_2$	0.0132	0.101	0.0150	1.52	none	
64	''	0.0130	0.300	''	0.338	''	
65	$Ti_2(DNBnT)(OiPr)_6$	0.0130	0.300	''	1.32	''	[DNBnT] = 0.0065

a. For entries 63 and 64, $[Ti]_{active} = 2[Ti(OiPr)_4] - [DNBnT]$. Ti:DNBnT = 1.0:1.1.
For entry 65, $[Ti]_{active} = [Ti(OiPr)_4]$ used to prepare the 2:1 complex.
b. $[iPrOH] = [iPrOH]_{added} + 2[DNBnT]$

A line drawn through the points of entries 63 and 64 has slope = -1.38.

compare the pseudo-first order rates for other possible components of the asymmetric epoxidation reaction mixture. Tables 14, 15, and 16 list the observed rates for epoxidation of (E)-2-hexen-1-ol by TBHP and four catayst preparations: 2:1 Ti:DIPT, $Ti(OiPr)_4$, 2:1 Ti:DNBnT and 2:2 Ti:DNBnT.

The data was found to fit a pseudo-first order treatment, with rate dependence on [iPrOH] of approximately -1.37 for $Ti_2(DIPT)(OiPr)_6$, and -0.96 for $Ti(OiPr)_4$.

An inverse first order dependence in isopropanol for $Ti(OiPr)_4$ makes sense in terms of the high affinity of primary alcohols for $Ti(OiPr)_4$ (recall Hoff's determination of a 10-12 kcal/mole driving force for the exchange of four isopropoxides for ethoxides). Because coordination of a primary alkoxide allows the complex to form a more stable bridged dimer, the loading of allylic alcohol, one of the two epoxidation reactants, occurs with a very large equilibrium constant. The observed rate law reflects the fact that isopropanol can only compete effectively with hydroperoxide for coordination to titanium.[89] Figure 15 depicts a possible exchange pathway for the $Ti(OiPr)_4$ system.

Figure 15. Possible ligand exchange pathway in epoxidation by TBHPand $Ti(OiPr)_4$.

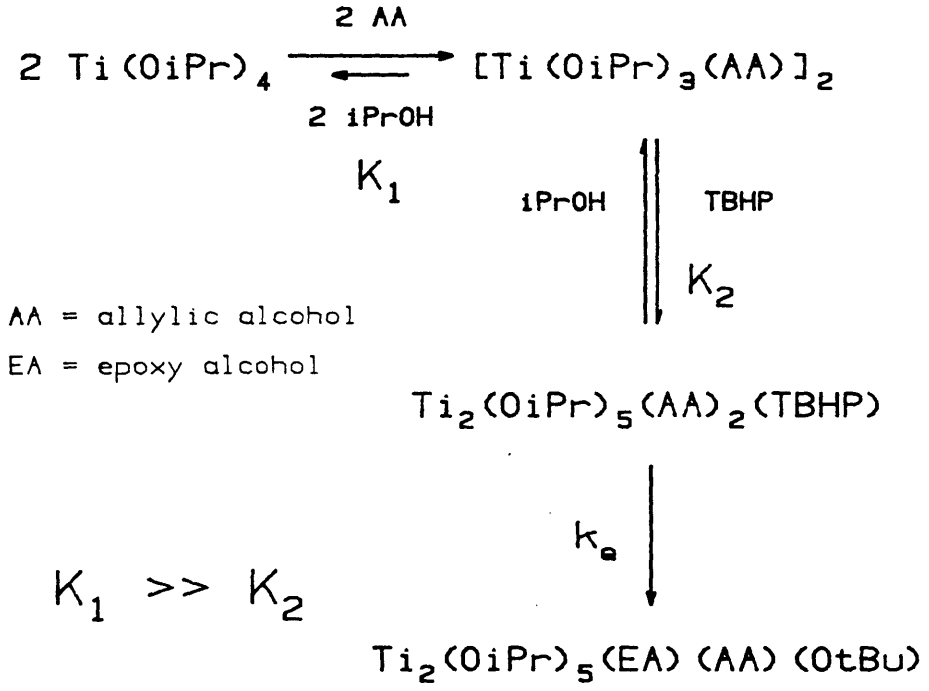

Again, since the epoxidation rate laws for these catalysts are not the same, a standard set of conditions must be chosen at which to compare rates: $[Ti]_{active}$ = 0.0130, [iPrOH] = 0.300, and [TBHP] = 0.0150.

Table 17. Pseudo-first order rate constants for epoxidation of (E)-2-hexen-1-ol in CH_2Cl_2 under standard conditions.

Entry	Catalyst	$Rate_{observed}$ (10^{-4} sec^{-1})	R_{rel}
55	Ti(DIPT)(OiPr)$_2$	11.5	1.00
59	Ti_2(DIPT)(OiPr)$_6$	3.18	0.276
62	Ti(OiPr)$_4$	4.37	0.380
64	Ti(DNBnT)(OiPr)$_2$	0.338	0.029
65	Ti_2(DNBnT)(OiPr)$_6$	1.32	0.115

Interestingly, the 2:2 Ti:DIPT reaction is the fastest and the 2:1 Ti:DIPT reaction slowest of the first three entries; the magnitude of the rate differences is probably larger than indicated in the Table. For example, we have shown that Ti(OiPr)$_4$ is subject to a milder inhibition effect from spectator alcohol molecules. The difference in oxygen transfer rate (the rate of intramolecular epoxidation of bound allylic alkoxide by bound alkylperoxide) beteween the Ti:DIPT and Ti(OiPr)$_4$ reactions is therefore much greater than that indicated by the observed rates of epoxidation after making the statistical correction for sites available.

Table 17 also supplies a lower limit for the rate difference between 2:2 Ti:tartrate and 2:1 Ti:tartrate. The 2:1 Ti(OiPr)$_4$:DIPT mixture actually contains a significant amount (10-20%) of Ti(DIPT)(OiPr)$_2$, plus an equal amount of Ti(OiPr)$_4$ (section II.C.4-5). Both contaminants are more active epoxidation catalysts than Ti_2(DIPT)(OiPr)$_6$ itself, so epoxidation mediated by 2:1 Ti:tartrate must be sluggish indeed.

Consider, too, that Ti(OiPr)$_4$ has four labile ligand sites per metal center, Ti_2(DIPT)(OiPr)$_6$ three (assuming that tartrate is bound strongly), and Ti(DIPT)(OiPr)$_2$ only two. From a purely statistical viewpoint, Ti(OiPr)$_4$ provides more opportunities for the reactants to get together than Ti(DIPT)(OiPr)$_2$, and yet Ti(OiPr)$_4$ is a less active epoxidation catalyst. It makes sense, then, to speak of reactivity per available

ligand site, and to note that the 2:2 system is by far the most potent oxygen transfer system.

The fact that 2:2 Ti:tartrate is the most active among the species listed in Table 17 is extremely fortunate (and probably necessary) for the successful operation of the asymmetric epoxidation reaction. It should first be appreciated that an increase in rate upon addition of a chelating ligand in a reaction such as this is rare. It is usually assumed that a ligand that restricts the course of a reaction to an enantio- or diastereoselective path does so at the expense of reaction rate. We discuss some reasons for this rate increase in a section III.E., and consider here what this result implies for the distribution and activity of possible complexes in solution.

If the 2:2 system contains species of other stoichiometry, they must be comprised of Ti:tartrate ratios both more and less than 2:2 (the result of a disproportionation process). That is, there would likely be 2:1 Ti:tartrate or free $Ti(OR)_4$ ("2:0") present as well as species such as 2:3 or 1:2 Ti:tartrate. If, for example, free $Ti(O\underline{i}Pr)_4$ were a much more active catalyst than Ti:tartrate, then even a small amount of it would seriously reduce the enantioselectivity of the reaction, since $Ti(O\underline{i}Pr)_4$ cannot produce enantiomerically enriched epoxide. The relatively high activity of the 2:2 system guards against the deleterious effects of any 2:1 or free Ti that might be present.

Of course, the recommended Ti:tartrate ratio for routine asymmetric epoxidation is 1:1.2, to further insure that only 2:2 Ti:tartrate is available for epoxidation. If the 2:2 catalyst was not more active than the 2:1 system or free $Ti(OR)_4$, much more tartrate relative to titanium would be required to obtain high ee, and the rate would suffer. This is exactly the situation observed with vanadium and the hydroxamic acid ligand 4.

In considering the nature of the actual asymmetric epoxidation catalyst, we know from Table 17 that the dominant catalyst cannot be of a 2:1 stoichiometry, and is probably not composed of any complex that has fewer equivalents of tartrate than titanium. If it were, the rate for the 2:1 case would be greater than the 2:2 reaction, and the enantiomeric excess would be high (when in fact it is only 80% for (E)-α-phenylcinnamyl

alcohol).

That the 2:1 system is the slowest of the three is significant in that it indicates that the 2:1 mixture does not disproportionate (to give 2:2 Ti:tartrate and free titanium tetraalkoxide) to a great extent. If disproportionation were complete, the rate of the 2:1 system would be an average of the 2:2 and $Ti(O\underline{i}Pr)_4$ results. Therefore, there must be one or more discrete 2:1 complexes that are sluggish epoxidation catalysts (a deduction supported by nmr studies of the 2:1 system).

Since the rate for the 2:2 system is about three times that of free $Ti(O\underline{i}Pr)_4$, it is interesting to note that the value of 80% ee for epoxidation of α-phenylcinnamyl alcohol by 2:1 Ti:tartrate is close to that obtained by multiplying the relative rates of the 2:2 and 2:0 tartrate systems by their enantioselectivities:

$$\% \text{ ee} = [(3\text{x}100 + 1\text{x}0)] \; / \; 4 = 75\% \text{ ee.}$$

Assuming that the relative rates of 2:2 and 2:0 systems are approximately the same under standard reaction conditions as under pseudo-first order conditions, then, we can say that the 2:1 Ti:tartrate species displays one of two properties: either it is completely inactive as an epoxidation catalyst (and so the 2:1 behavior arises solely from the 2:2 and 2:0 disproportionation products), or the 2:1 Ti:tartrate species itself mediates the epoxidation of (E)-α-phenylcinnamyl alcohol to approximately 80% ee at a slow but significant rate. The second scenario is much more reasonable, as it is difficult to conceive of structural features in a 2:1 complex that would render it completely inactive.

Note that the rates of pseudo-first order epoxidations involving the tartramide ligand (Table 17, entries 64 and 65) are in keeping with the conventional expectation that increasing amounts of chelating ligand decrease the rate: free $Ti(O\underline{i}Pr)_4$ is fastest, followed by 2:1 Ti:D<u>N</u>BnT and then by 2:2 Ti:D<u>N</u>BnT. Coupling this result with the observation that the 2:1 and 2:2 Ti:tartramide systems provide <u>opposite</u> senses of asymmetric induction, it is not surprising that the enantiomeric excess of epoxidations using tartramide catalysts are very sensitive to substrate structure. We belive that it is the 2:1 Ti:tartramide reagent that is unique; the 2:2 Ti:tartrate and Ti:tartramide systems are quite similar in structure if not in activity.

6. Solvent Deuterium Isotope Effect

After finding that the relative rate for kinetic resolution of a secondary allylic alcohol was the same regardless of whether isopropanol or n-butanol was used as the inhibitor, Woodard concluded that no molecules of alcohol were involved in the epoxidation transition state.[78] Since this is an important point, we decided to see if the rate of pseudo-first order epoxidation was different in the presence of iPrO-D as inhibitor relative to iPrO-H. If a proton transfer is a part of the transition state, one would expect a normal primary isotope effect, $k_H/k_D > 1.0$. If a dative coordination of alcohol to titanium (without proton transfer) is present, an inverse isotope effect should be observed, $k_H/k_D < 1.0$.[93] The magnitudes of these rate differences would be smaller than normal, since protons would not be the only species undergoing bond changes in the transition state. Table 18 below shows that the epoxidation rate ($R_{corr}x[\text{inhibitor}]^2$) was found to be exactly the same for both reactions. Admittedly such negative evidence is inconclusive, but it is consistent with our proposed mechanism.

Table 18. Pseudo-first order kinetics, in the presence of iPrOH vs. iPrOD.
Substrate = trans-2-decenol. Catalyst = Ti(DIPT)(OiPr)$_2$.
Solvent = CH_2Cl_2 (distilled from CaH_2). Oxidant = TBHP in toluene.

Entry	(M) $[Ti]_{active}$[a]	(M) [iPrOH][b]	(M) [iPrOD][b]	(M) [TBHP]	(10^{-4} sec^{-1}) $Rate_{obs}$	Sieves	(10^{-4} sec^{-1}) $Rate_{corr}$[c]	(10^{-4} M^2 sec^{-1}) $Rate_{corr}$x[inhibitor]^2
69	0.0141	0.194	-----	0.0150	26.1	3A	26.8	1.01
70	0.0144	-----	0.201	''	24.8	3A	25.0	1.01

a. $[Ti]_{active} = 2[Ti(OiPr)_4] - [DIPT]$
b. $[iPrOH] = [iPrOH]_{added}$. Isopropanol released from $Ti(OiPr)_4$ on addition of DIPT was removed *in vacuo*.
c. $Rate_{corr}$ = Rate corrected for $[Ti]_{active} \neq 0.0145$;
$= Rate_{obs} \times (0.0145/[Ti]_{active})$

$$k_D/k_H = 1.01/1.01 = 1.00$$

C. Catalyst Structure

It must be emphasized at the outset that most of our work concerned with establishing the structure of the asymmetric epoxidation catalyst in solution has focused on the product of mixing of titanium tetraalkoxide and dialkyl tartrate. For the purposes of structural characterization, allylic alcohols behave like other simple alcohols; the olefinic unit does not interact with titanium. For this reason, inclusion of hydroperoxides in the mixtures under study is much more important. However, solutions of hydroperoxides in the presence of titanium alkoxides decompose at a slow but significant rate, sometimes rapidly at room temperature, making characterization of alkylperoxide complexes difficult. Other than a few NMR and IR experiments reported here, exploration of Ti-tartrate-alkylperoxide compounds has awaited the recent preparation of 1-adamantyl hydroperoxide by P.T. Ho of the Sharpless group; its complexes with titanium and zirconium alkoxides are currently being examined.

The structure of Ti-tartrate has been explored in a number of ways; they shall be discussed in the following order:

(1) Molecular weight measurements
(2) Mass spectroscopy
(3) X-ray crystallography
(4) ^{1}H and ^{13}C NMR in solution
(5) IR in solution
(6) ^{17}O NMR
(7) Difference FTIR of deuterium-labeled alkoxides

1. Molecular Weight

The first clue to the aggregation state of titanium tartrates in solution came, not from a molecular weight measurement, but from diastereoselective epoxidations of secondary allylic alcohols in the presence of (dl)-tartrates. Recall that kinetic resolution of secondary allylic alcohols produces epoxy alcohol products highly enriched in the erythro isomer. If Ti-tartrate were a monomer, we would expect the epoxidation in the presence of (dl)-tartrate to give exactly the same erythro/threo ratio of racemic epoxy alcohols. Woodard was the first to find that erythro/threo ratios change when (dl)-tartrate is used; below we summarize the later

experiments that confirmed his observation.

In Table 19 are compared the results of diastereoselective epoxidations using homochiral and racemic tartrates.

Table 19. Diastereoselective epoxidations of 1-nonen-3-ol (**11**) and (E)-1-cyclohexyl-2-buten-1-ol (**12**) with (dl)-tartrates.

Rxn.	Substrate	Tartrate	Ti:Tartrate	% Completion	erythro:threo
1	Nonenol	(+)-DET	1:1.20	52	98:2
2	''	(-)-DET	1:1.22	52	98:2
3	''	(dl)-DET	1:1.20	56	82:18
4a	''	''	1:1.00	60, 71	84:16, 86:14
4b	''	''	''	70, 75	80:20, 80:20
5a	''	''	1:1.30	53, 68	83:17, 82:18
5b	''	''	''	57, 65	79:21, 78:22
6a	''	(dl)-DIPT	1:1.00	90	81:19
6b	''	''	''	80, 85	81:19, 82:18
7a	''	''	1:1.30	90	80:20
7b	''	''	''	62, 69	79:21, 80:20
8	**12**	(+)-DIPT	1:1.30	70, 100	87:13, 76:24
9	''	(-)-DIPT	''	25	96:4
10	''	(dl)-DIPT	''	70, 100	82:18, 83:17
11	''	''	''	25	85:15

Note that the erythro/threo ratio is high for epoxidation using homochiral tartrate in the first half of the reaction (entries 1, 2, and 9), but it declines as epoxidation is carried further, since the slower reacting enantiomer is epoxidized in a slightly threo-selective fashion (entry 8). In contrast, the diastereomer ratio from the (dl)-tartrate reactions is constant no matter the extent of reaction (entries 11 vs. 10, entries 3-7b), and it is different from the value obtained with enantiomerically pure tartrate. These results indicate the presence of at least some active catalyst with more than one tartrate ligand per molecule. In fact, nmr spectra of the Ti:(dl)-tartrate system show bands from a (dl)-tartrate complex in addition to those found for the homochiral complex (see Appendix 2).

The molecular weight of Ti(DIPT)(O$\underline{i}$Pr)$_2$ in CH_2Cl_2 solution was first measured by vapor phase osmometry. Two determinations were made, showing molecular weights of 752 and 796, compared to a dimer molecular weight of 797.

Not discussed here are molecular weight measurements made by Rayleigh light scattering (in collaboration with Professor Wilfred Nelson of the University of Rhode Island) on solutions of Ti(DIPT)(O$\underline{i}$Pr)$_2$ in cyclohexane, showing the complex to be a dimer at 0.05 - 0.4 M.

We then turned to the isopiestic Signer method,[94] a technique closely related to vapor phase osmometry. Table 20 below lists the results for titanium tartrates and tartramides.

Table 20. Molecular weight determinations by the Signer method.

Entry	Sample	Solvent	Conc.[a]	MW_{obs}	N[b]	MW_{calc}[c]
Titanium Tetraalkoxides						
1.	Tetrabutyl tin	CH_2Cl_2	0.25	346	1.00	347
	Standard = Azobenzene					
2.	Ti(O$\underline{i}$Pr)$_4$	CH_2Cl_2	0.22	275	0.97	284
3.	Ti(OEt)$_4$	CH_2Cl_2	0.23	623	2.73	684
4.	''	CH_2Cl_2	0.35	658	2.88	684
5.	''	CH_2Cl_2	0.50	844	3.70	684
6.	Ti(OBn)$_4$	CH_2Cl_2	0.27	840	1.76	953
1:1 Ti:Tartrate						
7.	Ti(DIPT)(O$\underline{i}$Pr)$_2$	CH_2Cl_2	0.17	864	2.17	797
8.	''	CH_2Cl_2	0.20	798	2.00	797
9.	''	CH_2Cl_2	0.69	1119	2.81	1195
10.	Ti(DET)(OEt)2	CH_2Cl_2	0.44	628	1.84	684
11.	''	CH_2Cl_2	0.28	703	2.06	684
12.	Ti(DET)(O$\underline{i}$Pr)$_2$	CH_2Cl_2	0.42	620	1.68	740
13.	''	CH_2Cl_2	0.25	700	1.89	740
14.	Ti(O$\underline{n}$C$_{12}$H$_{25}$)$_2$(DC$_{12}$T) + 2 $\underline{n}$-C$_{12}$OH	CH_2Cl_2	0.10	495	1.73	509[d]
15.	''	CH_2Cl_2	0.18	504	1.88	509[d]

Sovents other than CH_2Cl_2

Entry	Sample	Solvent	Conc.[a]	MW_{obs}	N[b]	MW_{calc}[c]
16.	Ti(DIPT)(O<u>i</u>Pr)$_2$	pentane	0.36	1082	2.70	1194
17.	''	pentane	0.51	1107	2.78	1194
18.	''	pentane	0.32	1195	3.00	1194
19.	Ti(DIPT)(O<u>t</u>Bu)$_2$	pentane	0.34	919	2.16	853
20.	''	pentane	0.38	868	2.04	853
21.	Ti(DET)(O<u>i</u>Pr)$_2$	pentane	0.38	1245	3.36	1111
22.	Ti(O<u>n</u>C$_{12}$H$_{25}$)$_2$(DC$_{12}$T) + 2 <u>n</u>-C$_{12}$H$_{25}$OH	pentane	0.14	892	???	d
23.	''	pentane	0.09	893	???	d
24.	Ti(DIPT)(O<u>i</u>Pr)$_2$	cyclopentane	0.27	747	1.88	797
25.	''	cyclopentane	0.27	964	2.42	797
26.	''	cyclopentane	0.54	1021	2.57	797
27.	Ti(DIPT)(O<u>i</u>Pr)$_2$	ether	0.31	744	1.87	797
28.	''	ether	0.24	787	1.95	797
Ti:D<u>N</u>BnT, 2:1 Ti:DIPT						
29.	1:1 Ti(O<u>i</u>Pr)$_4$:D<u>N</u>BnT	CH_2Cl_2	0.29	1003	2.04	985
30.	''	CH_2Cl_2	0.25	979	1.99	985
31.	2:1 Ti(O<u>i</u>Pr)$_4$:D<u>N</u>BnT	CH_2Cl_2	0.37	834	1.07	777
32.	''	CH_2Cl_2	0.23	794	1.02	777
33.	2:1 Ti(O<u>i</u>Pr)$_4$:DIPT	CH_2Cl_2	0.52	657	0.96	683
34.	''	CH_2Cl_2	0.50	636	0.93	683

[a] Concentration of titanium at equilibrium.

[b] N = Degree of association.

[c] MW_{calc} = Molecular weight of oligomer nearest to the observed MW.

[d] See discussion in text.

In entry 2, $Ti(O\underline{i}Pr)_4$ was found to be a monomer, consistent with other molecular weight determinations in the literature.[79] The molecularity of $Ti(OEt)_4$ has been subject to some debate; most measurements placing it as a trimer or a tetramer, depending on the age of the sample, concentration, and temperature. Our determinations by the Signer method (entries 3-5) indicate a trimeric aggregation state, with possibly increasing amounts of tetramer present at higher concentrations (though entry 5 should be repeated to confirm this).

In CH_2Cl_2, $Ti(DIPT)(O\underline{i}Pr)_2$ (entries 7-8), $Ti(DET)(OEt)_2$ (10-11), and $Ti(DET)(O\underline{i}Pr)_2$ (12-13), were found to be dimeric. Note that in the time required for the experiment (about 10 days), $Ti(DET)(O\underline{i}Pr)_2$ undergoes transesterification to a statistical mixture of complexes involving DET, DIPT, and the mixed diester. Entry 9 indicates that at high concentration (0.69 M Ti), larger oligomers or intermolecular interactions between dimers may be present for $Ti(DIPT)(O\underline{i}Pr)_2$, though at a concentration of 0.44 M, $Ti(DET)(OEt)_2$ showed no tendency to form higher molecular weight species (entry 10).

Because the Signer method measures the total amount of solute in solution, most of these experiments were performed with alcohol-free samples. Two experiments were performed using equimolar mixtures of di-$\underline{n}$-dodecyl tartrate ($DC_{12}T$) and titanium tetra-$\underline{n}$-dodecyloxide (entries 14 and 15). The two equivalents of dodecyl alcohol released per equivalent of tartrate were allowed to remain in solution; dodecyl alcohol was chosen because of its low volatility. Thus, the solute was comprised of two equivalents of nonvolatile alcohol (MW = 186.3) plus the Ti-tartrate complex (MW = 903.3 per monomeric unit); the observed molecular weight represents an average of these species. For example, if 1.0 mmol each of tartrate and tetraalkoxide were used, the total amount of solute would be 3.0 mmol if the Ti-tartrate complex were a monomer, 2.5 mmol if it were a dimer, and 2.33 mmol if it were a trimer. The average molecular weights would then be 425 for monomeric Ti-tartrate, 510 for a dimer, and 547 for a trimer. This allows for a much smaller error range in the molecular weight measurement. The molecularity (N) was calculated from the observed molecular weight by the following formula:

$$MW_{obs} = [(2x186.3) + 903.4] / (2 + 1/N)$$

Entries 14 and 15 provide clear evidence that the Ti-tartrate complex is a

dimer in the presence, as well as in the absence, of free alcohol.

Because of the differences in kinetic behavior of asymmetric epoxidation in pentane and ether solvents (as compared to CH_2Cl_2), the molecular weights of several complexes were determined in these solvents. The results in pentane and cyclopentane are surprising. Entries 16, 17, 18, and 21 show that Ti(DIPT)(O$\underline{i}$Pr)$_2$ and Ti(DET)(O$\underline{i}$Pr)$_2$ are largely trimeric in pentane. The more sterically hindered Ti(DIPT)(O$\underline{t}$Bu)$_2$, on the other hand, is a dimer in pentane (entries 19-20). Curiously, the molecular weight determinations of Ti(DIPT)(O$\underline{i}$Pr)$_2$ in cyclopentane seem to indicate a large proportion of dimeric material at lower concentration (0.27 M, entries 24-25), with increasing amounts of larger oligomers at higher concentration (0.54 M, entry 26). Cyclopentane is slightly more polar than pentane (dielectric constants of 1.97 and 1.84, respectively), but it is difficult to imagine that so small a polarity difference can be responsible for a change in average aggregation state.

Even more interesting are the results in pentane with Ti(DC$_{12}$T)(O$\underline{n}$C$_{12}$H$_{25}$)$_2$ in the presence of two equivalents of dodecyl alcohol (entries 22-23). The analysis given above for this experiment in CH_2Cl_2 predicts that the highest MW_{obs} possible would be 638 (if N is very large). This analysis must therefore be incorrect for pentane, since the observed molecular weight is 893. We assumed that free alcohol and Ti-tartrate could be treated as independent, non-interacting molecules; the total number of moles of solute would then be simply the sum of the number of moles of alcohol and titanium complex. Apparently, this assumption is not true in pentane. It is not unreasonable to postulate intermolecular associations among the polar solute molecules in the nonpolar solvent. For some reason, these interactions seem to be more frequent in pentane than cyclopentane, but increasing the concentration of Ti-tartrate in cyclopentane causes the apparent molecular weight to increase, as would be expected. Ti(DIPT)(O$\underline{t}$Bu)$_2$, which is probably quite a bit less able to associate than Ti(DIPT)(O$\underline{i}$Pr)$_2$, was found to be dimeric presumably because it does not suffer from the same sort of intermolecular associations. Finally, molecular weight measurements in ether show exactly dimeric behavior for Ti(DIPT)(O$\underline{i}$Pr)$_2$ (entries 27-28), consistent with the idea that a more polar solvent prevents association between solute molecules.

Because of the unusual results in pentane, we verified that mixing of

equimolar amounts of tartrate and titanium tetraalkoxide in pentane does result in displacement of two equivalents of alcohol, as Woodard observed in CH_2Cl_2. The vapor phase gc experiments, performed for $Ti(O\underline{i}Pr)_4$ + DIPT, and $Ti(OEt)_4$ + DET, found that exactly two equivalents of alcohol are released into solution.

Signer measurements were also performed in CH_2Cl_2 for complexes of $Ti(O\underline{i}Pr)_4$ and (2R,3R)-N,N'-dibenzyltartramide (DNBnT). The 1:1 complex is a dimer (entries 29-30) and the 2:1 complex has two Ti atoms and one ligand per complex (entries 31-32). The 2:1 Ti:DIPT complex also has two Ti atoms and one ligand per molecule (entries 33-34).

2. Mass Spectroscopy

The assignment of titanium tartrates as dimeric species is supported by low resolution electron impact mass spectra. Parent ions were never observed; the highest molecular weight ion was usually parent minus coordinated alkoxide. Spectra are reproduced in Figure 16 for the following solutions in CH_2Cl_2: $Ti(O\underline{t}Bu)_4$ + DIPT; $Ti(O\underline{t}Bu)_4$ + DET; $Ti(O\underline{i}Pr)_4$ + DIPT; $Ti(DIPT)(O\underline{i}Pr)_2$ (alcohol-free); $Ti(O\underline{i}Pr)_4$ + DET; and $Ti(O\underline{t}Bu)_4$ alone. Table 21 below lists the high molecular weight peaks and possible assignments for each sample.

Peaks of greater than dimer m/e values were observed only for the mixture of $Ti(O\underline{i}Pr)_4$ and DIPT, with heating of the sample holder (about 150°C). Corresponding roughly to a trimer, these peaks were weak in intensity. When free isopropanol was removed from the mixture, volatilization of the sample by heating did not yield these high m/e peaks. The rest of the samples required gentle probe heating (approximately 70°C). For all samples, the pattern of high m/e bands corresponds to cleavage of alkoxide ligands and methyl, isopropyl, and t-butyl groups. The spectrum of $Ti(O\underline{i}Pr)_4$ + DET is more complicated because of transesterification of the tartrate ester.

The spectrum of $Ti(O\underline{t}Bu)_4$ also lacks a parent m/e peak. An intense band due to loss of a methyl group was the highest m/e signal found. Despite being a trimer in solution, the spectrum of $Ti(OEt)_4$ showed peaks only between monomer and dimer m/e values.

Figure 16. Electron impact mass spectroscopy.

$Ti(O\underline{t}Bu)_4$ + DIPT

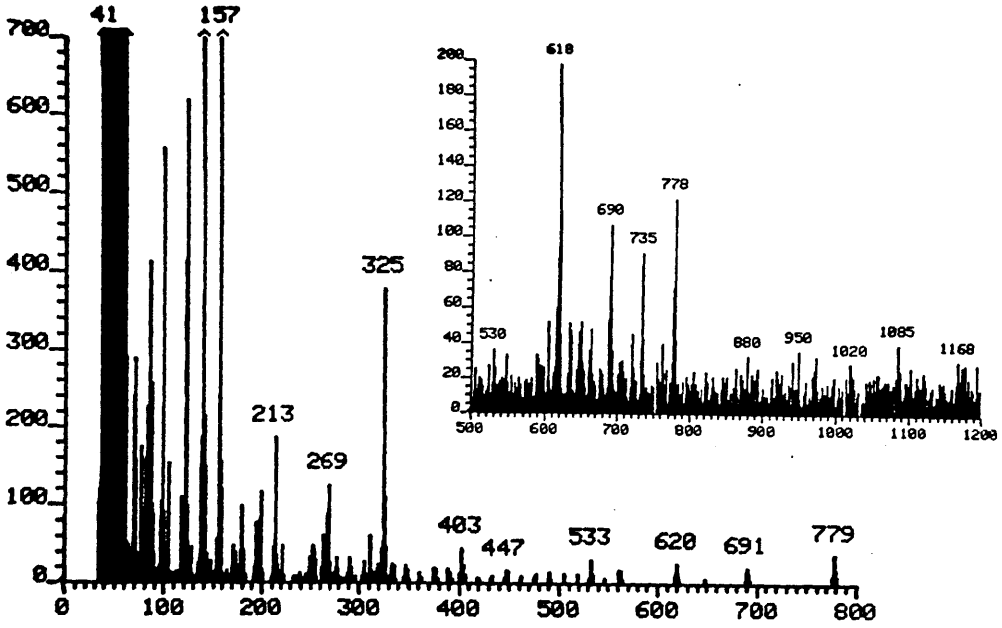

$Ti(O\underline{t}Bu)_4$ + DET (Inset = higher temperature probe)

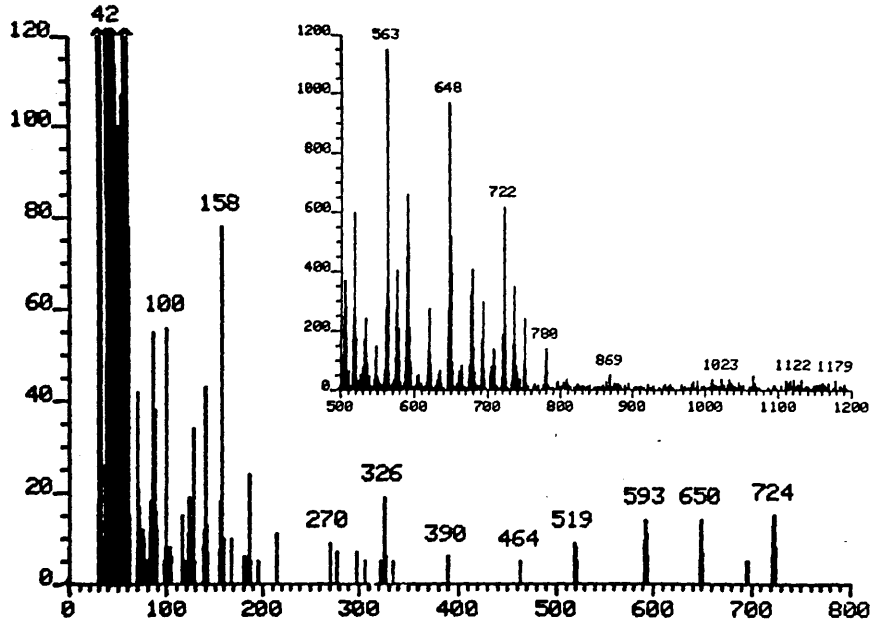

Figure 16, continued.

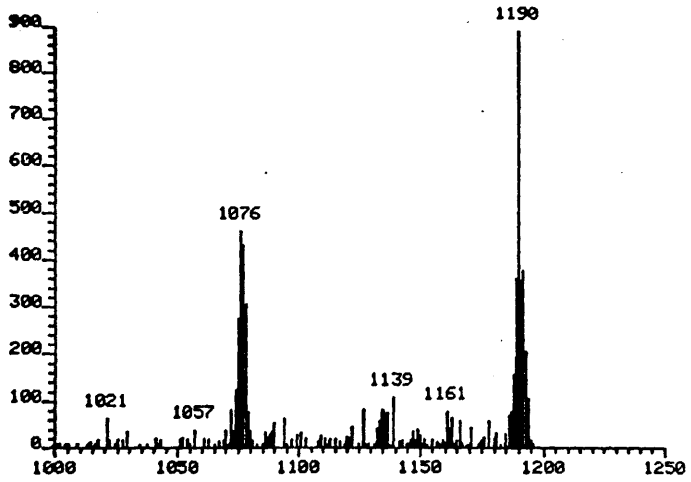

$Ti(O\underline{i}Pr)_4$ + DIPT

high temperature

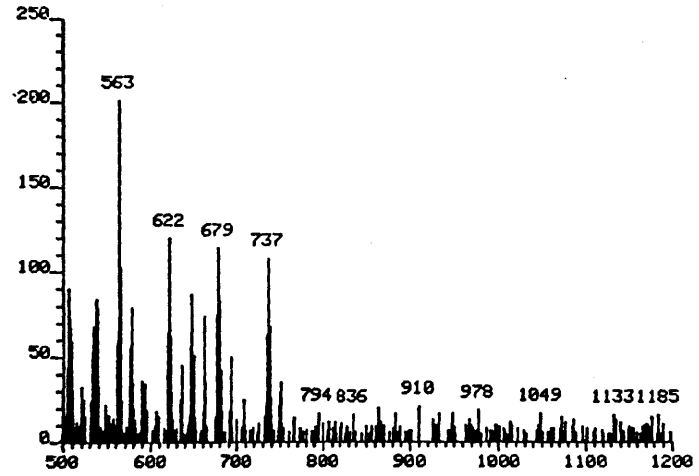

$Ti(DIPT)(O\underline{i}Pr)_2$

low temperature

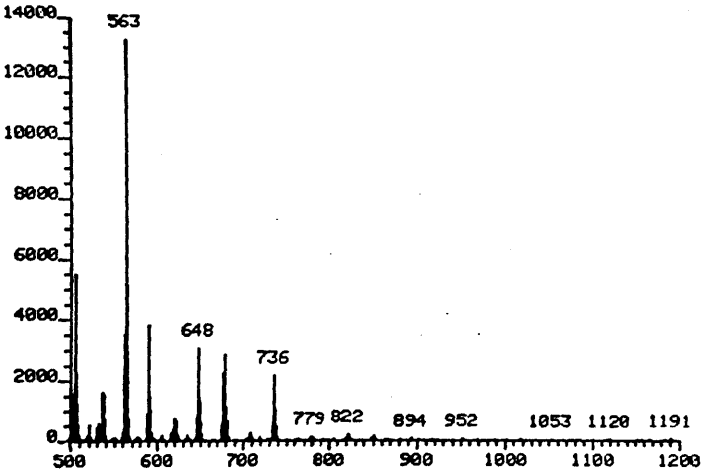

$Ti(DIPT)(O\underline{i}Pr)_2$

high temperature

Figure 16, continued.

$Ti(O\underline{i}Pr)_4$ + DET

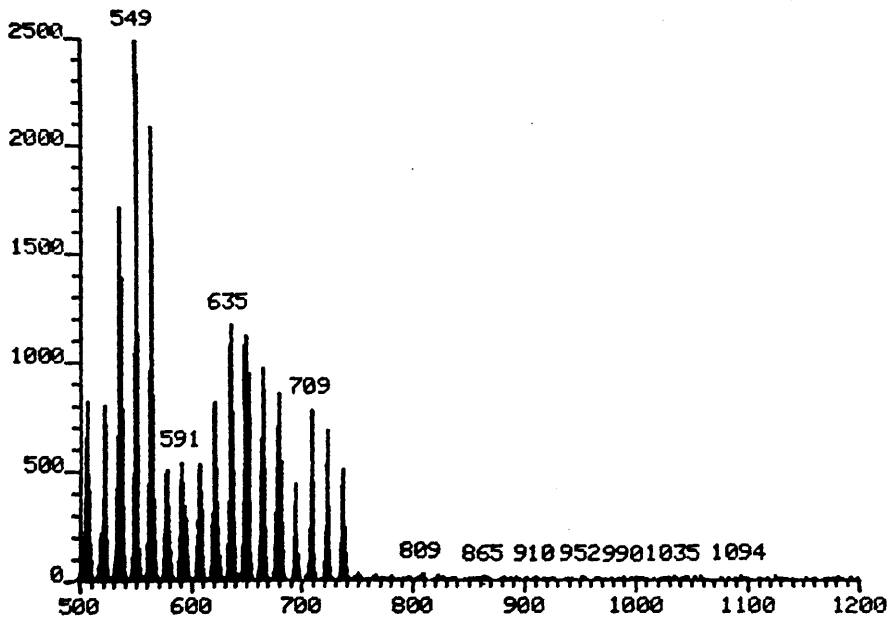

$Ti(O\underline{t}Bu)_4$

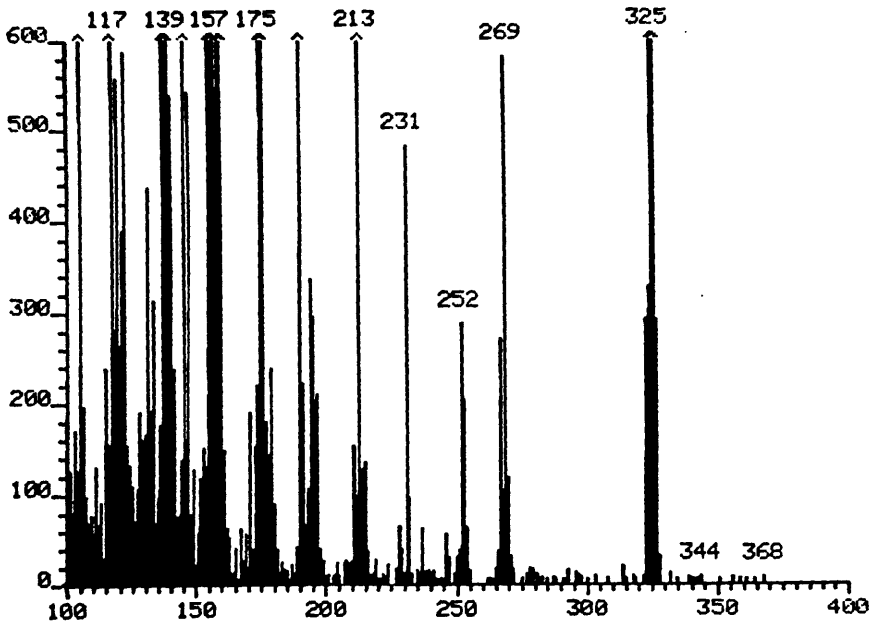

Table 21. Mass spectra assignments.

Sample	Peak	I_{rel}	Assignment	Notes
$Ti(O\underline{t}Bu)_4$ + DIPT	779	10	$M^+ - O\underline{t}Bu$	dimer, $M^+ = 852$
	691	4	$M^+ - (-O\underline{t}Bu)_2 - CH_3$	
	620	7	$M^+ - (-O\underline{t}Bu)_3 - CH_3$	
	561	4	$M^+ - (-O\underline{t}Bu)_4$	
	533	8	$M^+ - (-O\underline{t}Bu)_3 - \underline{t}Bu - \underline{i}Pr$	
	325	100		
$Ti(O\underline{t}Bu)_4$ + DET	780	17	$M^+ - CH_3$	dimer, $M^+ = 796$
	751	20	$M^+ - (CH_3)_3$	
	736	29	$M^+ - (CH_3)_4$	
	723	80	$M^+ - O\underline{t}Bu$	
	650	75	$M^+ - (-O\underline{t}Bu)_2$	
	593	75	$M^+ - (-O\underline{t}Bu)_2 - \underline{t}Bu$	
	519	50	$M^+ - (-O\underline{t}Bu)_3 - \underline{t}Bu$	
	326	100		
$Ti(O\underline{i}Pr)_4$ + DIPT	1190	3	trimer (m/e = 1195)	high probe heat
	1076	2	trimer - $O\underline{t}Bu$ - $\underline{t}Bu$	
	lower MW peaks as below			
	563	100		
$Ti(DIPT)(O\underline{i}Pr)_2$	737	44	$M^+ - O\underline{i}Pr$	dimer, $M^+ = 796$
	679	46	$M^+ - (-O\underline{i}Pr)_2$	alcohol free,
	648	36	$M^+ - (-O\underline{i}Pr)_2 - (CH_3)_2$	low probe heat
	622	48	$M^+ - (-O\underline{i}Pr)_3$	
	563	100	$M^+ - (-O\underline{i}Pr)_4$	
$Ti(O\underline{i}Pr)_4$ + DET	737	20		dimer, $M^+ = 740$
	723	28		
	709	32		
	695	18	$M^+ - OEt$	
	680	34	$M^+ - O\underline{i}Pr$	
	665	40		
	649	46	$M^+ - (OEt)_2$	
	635	48	$M^+ - O\underline{i}Pr - OEt$	
	621	32	$M^+ - (O\underline{i}Pr)_2$	
	607	22		
	591	22		
	563	84	$M^+ - (O\underline{i}Pr)_3$	
	549	100	$M^+ - (OEt)_3 - O\underline{i}Pr$	
$Ti(O\underline{t}Bu)_4$	325		$M^+ - CH_3$	$M^+ = 340$

3. X-ray Crystallography

Bridging alkoxides are a ubiquitous feature of Ti(IV) chemistry. Titanium(IV), when bound to just four alkoxide ligands, remains an electron deficient Lewis acid center. Where sterically possible, titanium tetraalkoxides complexes are usually found in six-coordinate, octahedral configurations.

Having established that Ti-tartrate is a dimer, it was perhaps foolish, then, for our first proposal of the Ti-tartrate structure to feature no bridging alkoxide bonds.[3e] At that time, the only tartrate structures of early transition metals in the literature were the seductively symmetric dimeric complexes of tartaric acid with V(IV), Sb(III), As(III), Cu(II), and Cr(III), found by Tapscott and coworkers.[95] These structures featured a ten-membered $M_2(tartrate)_2$ ring with both carboxylate groups of each tartrate bound. We based our Ti-tartrate structural proposal on these symmetric models, suggesting a complex of C_2 symmetry and pentacoordinate titanium atoms, as shown below in Figure 17.

Figure 17. Ten-membered ring structure of Ti-tartrate analogous to tartaric acid complexes.

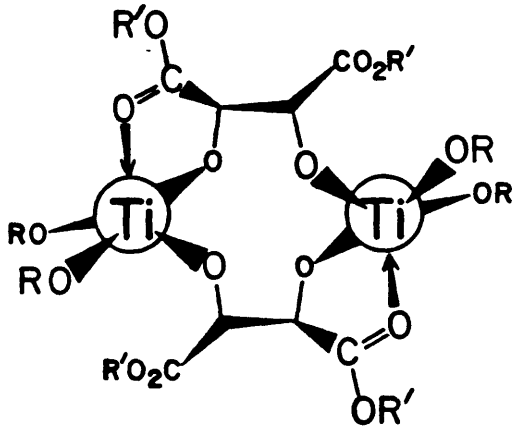

Figure 17 is included largely for historical and nostalgic interest, since the ten-membered ring configuration has been excluded for Ti-tartrate by spectroscopic and crystallographic evidence presented below.

Reproduced below in Figure 18 are drawings of the x-ray crystal structures of five titanium tartrate derivatives, all obtained by Dr. Steven F.

Pedersen in the Sharpless group.[96] The most significant feature of these structures is the ubiquitous presence of bridging tartrate alkoxide groups; that is, titanium centers are invariably linked by bridging tartrate alkoxide oxygen atoms, never by bridging isopropoxides or ethoxides. Since these structures are consistent with NMR and IR spectra taken in solution, they represent the best evidence available concerning the structure of the asymmetric epoxidation catalyst. Two structures, designated **13a** and **13b** (Figure 18), are of complexes very similar to the parent Ti-tartrate system and form the basis for our mechanistic proposals. The otcomplexes very similar to the parent Ti-tartrate system and form the basis for our mechanistic proposals. The other three structures are of complexes containing hydroxylamine or bromide ligands and show an impressive variety of tartrate coordination geometries.

Structure **13a** is of the dimeric complex $[Ti(DET)(L)(OEt)]_2$, where L is the N-phenylhydroxamate ligand ON(Ph)C(Ph)O. In structure **13b**, the tartrate diester has been replaced by the benzyl diamide of (+)-tartrate (DNBnT). It is important to note that this 1:1 Ti:tartramide complex does mediate epoxidation to high enantiomeric excess for some substrates, as mentioned in the introduction. Structures **13a** and **13b** are quite similar, both having C_2 symmetry with the C_2 rotation axis perpendicular to the planar four-membered Ti_2O_2 core. In **13a**, none of the tartrate carbonyls is associated with the metal, presumably because the titanium centers are six-coordinate by virtue of the monobasic, bidentate nature of the hydroxamate ligands. However, **13b** demonstrates the spectroscopically required dative association of one carbonyl per tartrate with the titanium center (see Section II.4,5).

Two other features of **13a** and **13b** are important to notice. The Ti-O-C bond angles of the ethoxide and isopropoxide ligands are approximately 155-160°, indicating π-type overlap of oxygen lone pairs with empty d-orbitals on titanium. This is a common feature of d^0 metal alkoxide systems, and we assume that allylic alkoxide ligands adopt the same Ti-O-C bond angles in the ground state. Also note that the central Ti_2O_2 core is planar and that the bridging tartrate alkoxide oxygens are sp^2-like in that the carbon atom to which each is attached also lies very close to the Ti_2O_2 plane. In the following discussion we designate the Ti_2O_2 plane as the equatorial plane of the roughly octahedral titanium coordination geometry.

Figure 18. X-ray crystal structures of Ti-tartrate derivatives.

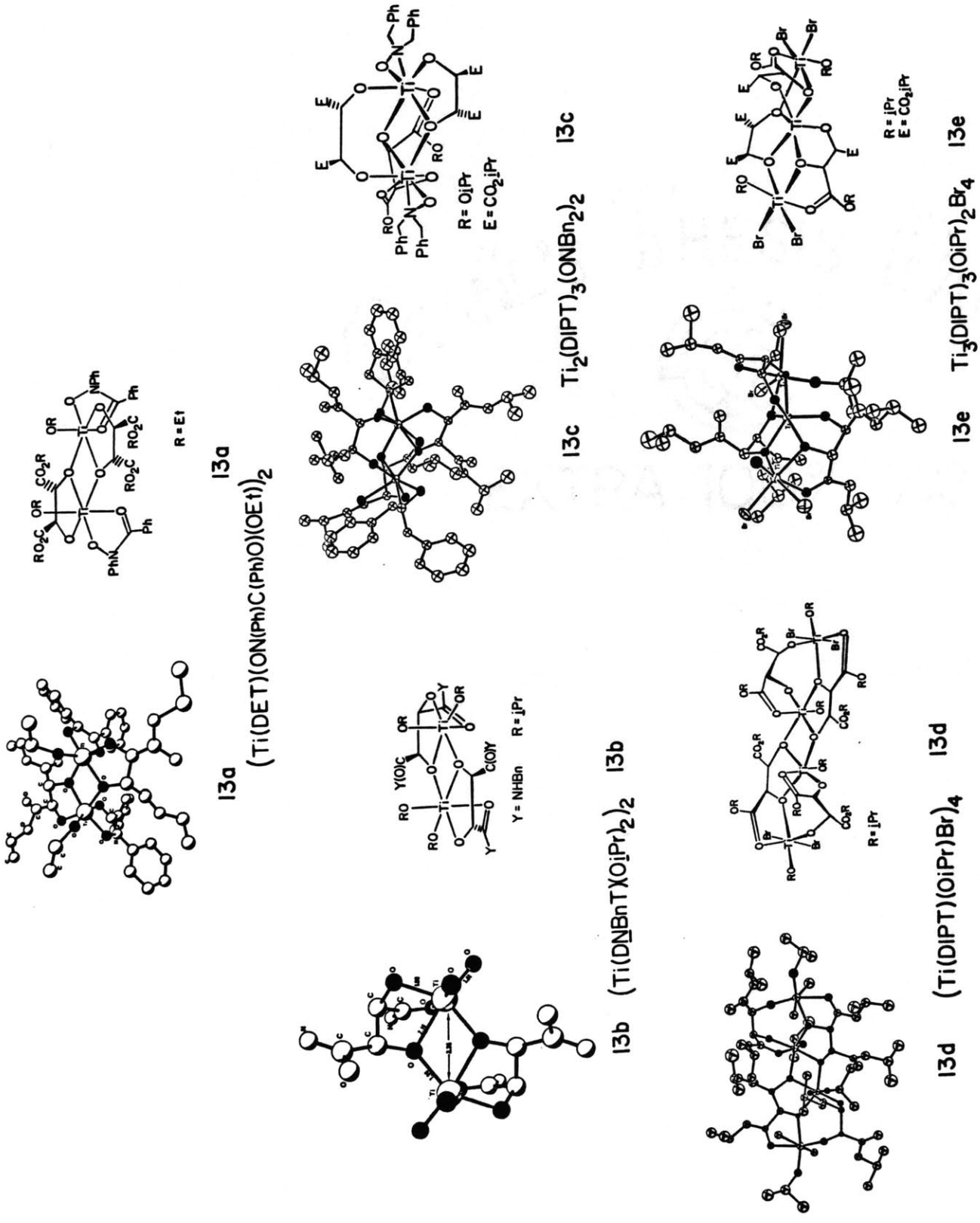

The other three structures provide examples of several additional modes of tartrate binding, though tartrates provide the bridging oxygen atoms in all cases. Structure **13c** features a pentagonal bipyramidal titanium coordination geometry. In this case, the dibenzylhydroxylamine ligand is intended to model alkylperoxide and is found in the equatorial plane of the pentagonal bipyramid, as in Mimoun's vanadium-TBHP complex **1**.[40a] This is accompanied by a change in the style of tartrate coordination. One terminal (nonbridging) tartrate alkoxide oxygen is found in an axial position and a bound carbonyl in an equatorial site, resulting in the first observed tetradentate tartrate diester ligand in which both hydroxyls and both carbonyls are used in binding. Note the presence of a third tartrate molecule that replaces the two *syn* axial alkoxides of **13a** and **13b**. This was our first example of a tartrate ligand in which neither alkoxide oxygen is used in a bridging manner.

Structures **13d** and **13e** possess bromide ligands and are thus far removed from the asymmetric epoxidation system. $[Ti(DIPT)(O\underline{i}Pr)Br]_4$, **13d** is important to mechanistic studies as a source of $Ti(DIPT)(O\underline{i}Pr)_2$ of exactly 1.0:1.0 Ti:DIPT stoichiometry. Reaction of **13d** with isopropanol in the presence of an equivalent of Et_3N in ether provides quantitative yields of $[Ti(DIPT)(O\underline{i}Pr)_2]_2$ and insoluble $Et_3NH^+Br^-$.

Structure **13d** features an extended array of four titanium atoms; complex **13e** holds three titanium atoms in a tartrate framework. Two bromide ligands are found on each of the outer Ti atoms of both structures; in **13d** they are *trans* to each other while in **13e** they are *cis*. In both structures the ubiquitous Ti_2O_2 ring is found, with bridging oxygens that display planar sp^2-like geometry, but in both structures there are also bridging oxygen units that are not planar. Note the presence in **13d** and **13e** of tartrates in which both alkoxide oxygens are used in a bridging manner. Two tartrate ligands in which no alkoxide oxygens are bridging can also be found on each end of structure **13d**. These are remarkable in that the Ti-O-C(tartrate) bonds to the outer Ti atoms are nearly linear, the largest bond angle being 173°.

A Ti-tartrate structure analogous to that of **13b**, with tartrate diamides replaced by tartrate diesters, is strongly suggested by the x-ray evidence. Since the conformation in solution does not have to be the same as in the solid phase, three general types of 2:2 structures (each in

accord with the basic NMR and IR evidence discussed below) must be considered. The possibilities, depicted in Figure 19, include an alkoxide-bridged, tartrate-capped dimer, 20, a ten-membered ring form, 21, and the tartrate-bridged structure suggested by the crystal structures, 22. One characteristic that sets 22 apart from the others is the presence of bridging tartrate oxygen atoms. The spectroscopic studies reported below will be discussed largely in terms of "bridging" vs. "terminal" (non-bridging) oxygens.

Figure 19

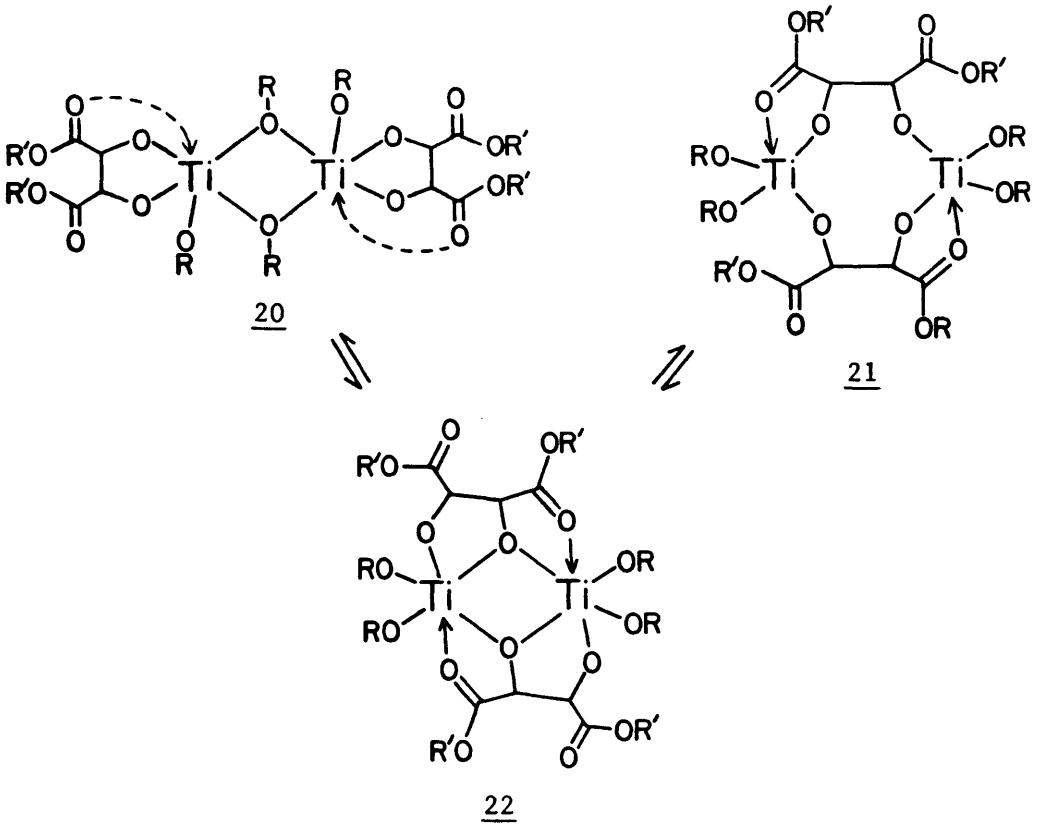

4. ^{1}H and ^{13}C NMR in $CDCl_3$

a. Introduction

The ^{1}H (Figure 20) and ^{13}C (Figure 21) spectra of Ti(DIPT)(O$\underline{i}$Pr)$_2$, from which free isopropanol has been removed *in vacuo*, are quite simple. A single set of resonances appears for tartrate and bound isopropoxide (Ti-O$\underline{i}$Pr), consistent with a single type of symmetrically-bound tartrate ligand. As demonstrated in Figure 22, the mixing of Ti(O$\underline{i}$Pr)$_4$ and DIPT releases two equivalents of isopropanol into solution per Ti atom; this spectrum at lower concentration is identical to the first but for the presence of the free alcohol resonances. Table 22 lists the peak assignments for the Ti(DIPT)(O$\underline{i}$Pr)$_2$ NMR spectra, as well as for the free ligands. Note the downfield shifts that accompany binding to the Lewis acidic metal. One carbonyl resonance (172.4 ppm) in the ^{13}C nmr is close to that of DIPT alone, and presumably represents a free (uncoordinated) ester group. The other carbonyl is shifted downfield, and is therefore assigned to an ester group datively bound to titanium through the carbonyl oxygen.

Table 22. Peak positions and assignments for Ti(DIPT)(O$\underline{i}$Pr)$_2$.

Sample	Tartrate Methine	-CO$_2\underline{i}$Pr Methine	Ti-O$\underline{i}$Pr Methine	HO$\underline{i}$Pr Methine	-CO$_2\underline{i}$Pr Methyl	Ti-O$\underline{i}$Pr Methyl
Ti(DIPT)(O$\underline{i}$Pr)$_2$	5.08	5.02	4.69		1.2	1.2
^{13}C	85.7	70.3,68.8	78.8		21.6	25.2
	(175.7, 172.4 = C=O)					
Ti(O$\underline{i}$Pr)$_4$			3.98			1.21
^{13}C			76.1			26.4
DIPT	4.32	5.01			1.20	
^{13}C	72.1	70.1			21.5	
	(171.0 = C=O)					
Isopropanol				3.98		1.15
				63.8		25.0

b. Alkoxide-Alcohol Exchange

The ability of Ti(IV) to exchange bound alkoxide for alcohol in solution is essential to the successful operation of asymmetric epoxidation in a catalytic and convenient stoichiometric sense. The nmr spectra are also affected by ligand exchange, the rate of which varies from fast to slow with respect to the timescale of nmr observation.

Figure 20. ^{1}H NMR of Ti(DIPT)(O$\underline{i}$Pr)$_2$ in $CDCl_3$ at 295°K.

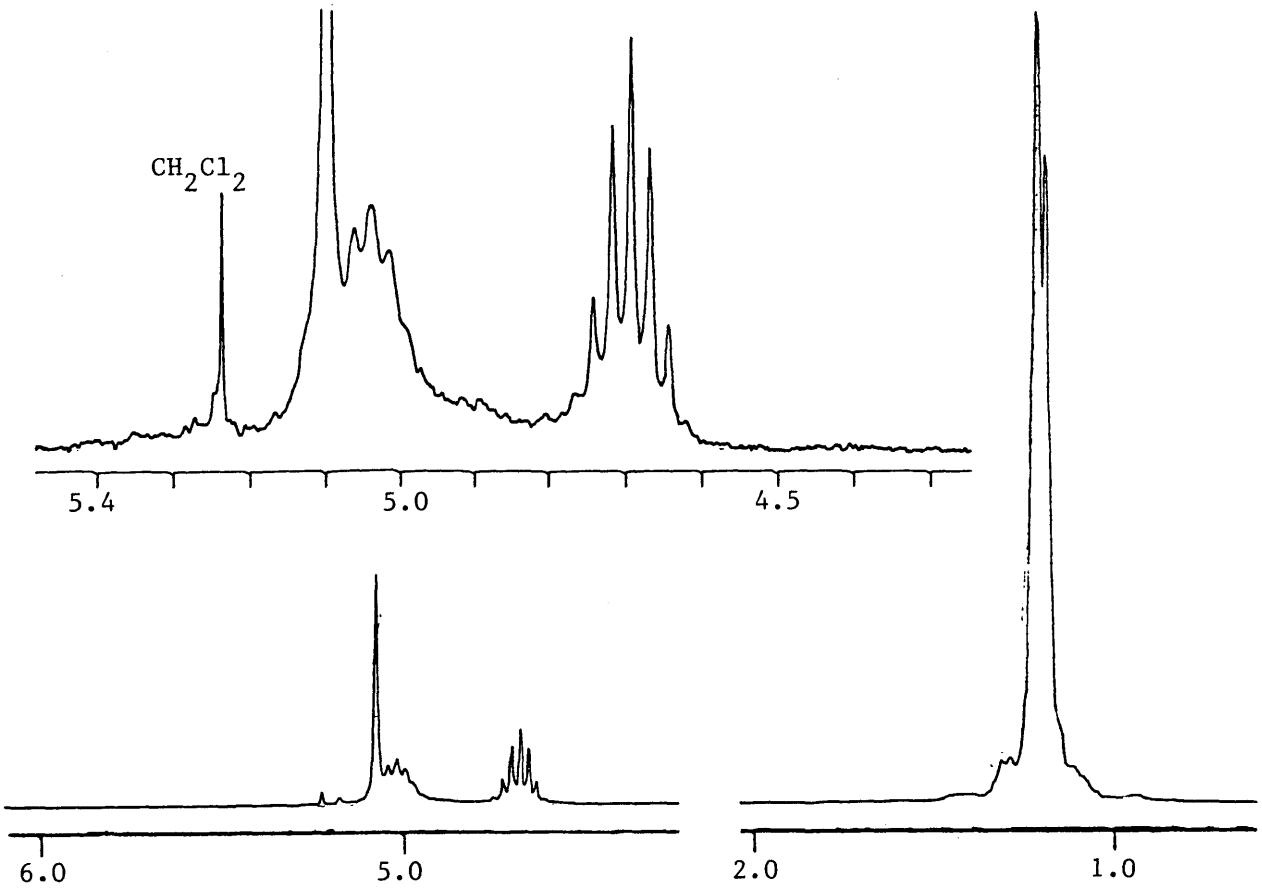

Figure 21. ^{13}C NMR of Ti(DIPT)(O$\underline{i}$Pr)$_2$ in $CDCl_3$ at 295°K

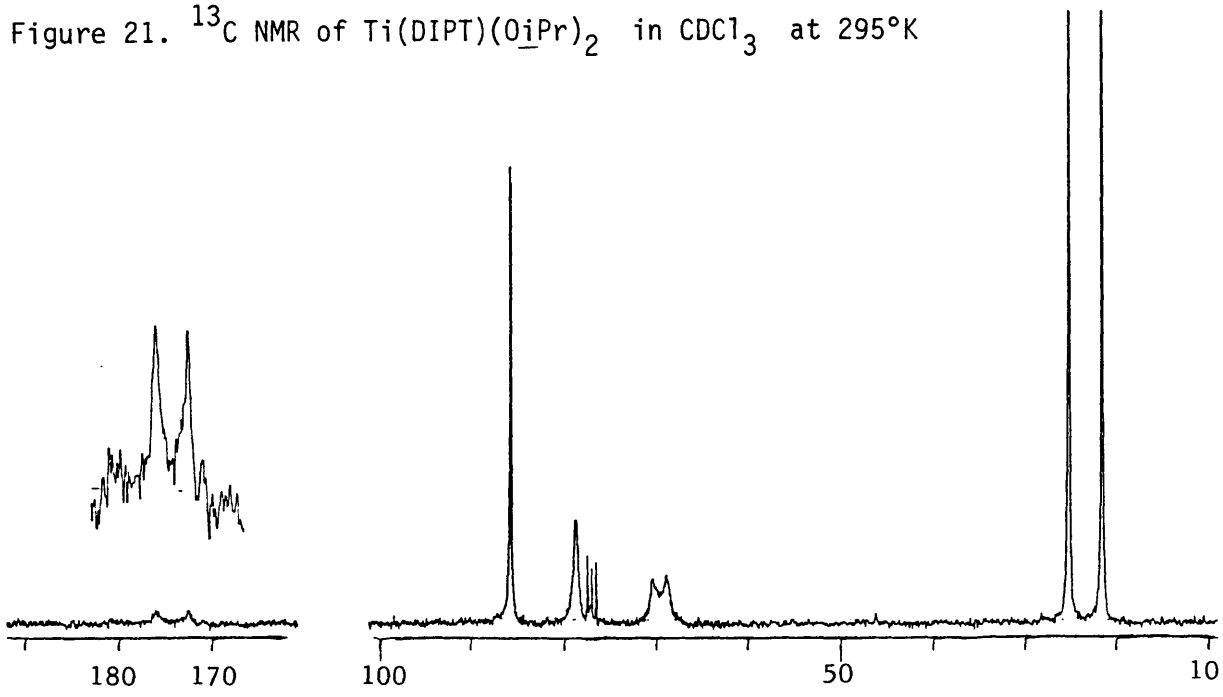

A striking example is presented in Figure 22, which shows an equimolar mixture of $Ti(O\underline{i}Pr)_4$ and DIPT at 0.35 M Ti, 0.17 M, and 0.07 M, respectively. Under dilute conditions, free isopropanol (3.98 ppm) and bound isopropoxide (4.70 ppm) are sharp heptet signals of equal intensity. At 0.07 M, these signals begin to broaden, and at 0.17 M an intermediate resonance appears. By 0.35 M, all traces of a distinct isopropanol methine resonance have disappeared, to be replaced by a broad lump stretching from 4.8 to 3.9 ppm. Note, however, the narrower (but still broadened) resonance that remains at 4.7 ppm, superimposed on the lump. Its integral intensity is perhaps slightly less than half that of the 4.7 ppm band in the 0.07 M spectrum; that is, it represents one of the two possible bound isopropoxide ligands. The 4.8-3.9 band, then, is due to the exchange of two equivalents of isopropanol with bound isopropoxide, one isopropoxide undergoing exchange with isopropanol at a faster rate than the other. One isopropoxide signal remains relatively unaffected and the other merges with the isopropanol signal.

Thus, we have discovered that the solution phase structure of $Ti(DIPT)(O\underline{i}Pr)_2$ features two chemically different isopropoxide ligands, which are exchanged with each other rapidly on the nmr timescale.

The nonequivalence of isopropoxides is also demonstrated by the Figure 23, showing the downfield resonances of $Ti(DIPT)(O\underline{i}Pr)_2$ at 0.17 M on the bottom, and the same region with the upfield methyl bands (1.3-1.1 ppm) irradiated, on top. The isopropyl ester methine signal collapses to a singlet at 5.05 ppm. Note the change in the bound isopropoxide signal at 4.7 ppm: decoupling reveals a sharpened resonance superimposed on a broader one. The free $\underline{i}$PrOH signal at 3.98 ppm is also not sharpened very much. Therefore, one isopropoxide is broadened by chemical exchange with free $\underline{i}$PrOH and the other is not.

Figure 24 shows the ^1H nmr spectrum of $Ti(DIPT)(O\underline{i}Pr)_2$ in isopropanol-d_8. Here, alkoxide exchange manifests itself in the disappearance of Ti-O$\underline{i}$Pr signal, as a consequence of exchange with the bulk perdeuterated solvent.

If we regard the top spectrum of Figure 22 as one of coalescence between free isopropanol and one bound isopropoxide, a very rough approximation of the rate of exchange can be determined, treating each titanium

Figure 22.

^1H NMR ($CDCl_3$) of Ti(DIPT)(O$\underline{i}$Pr)$_2$ + 2 $\underline{i}$PrOH

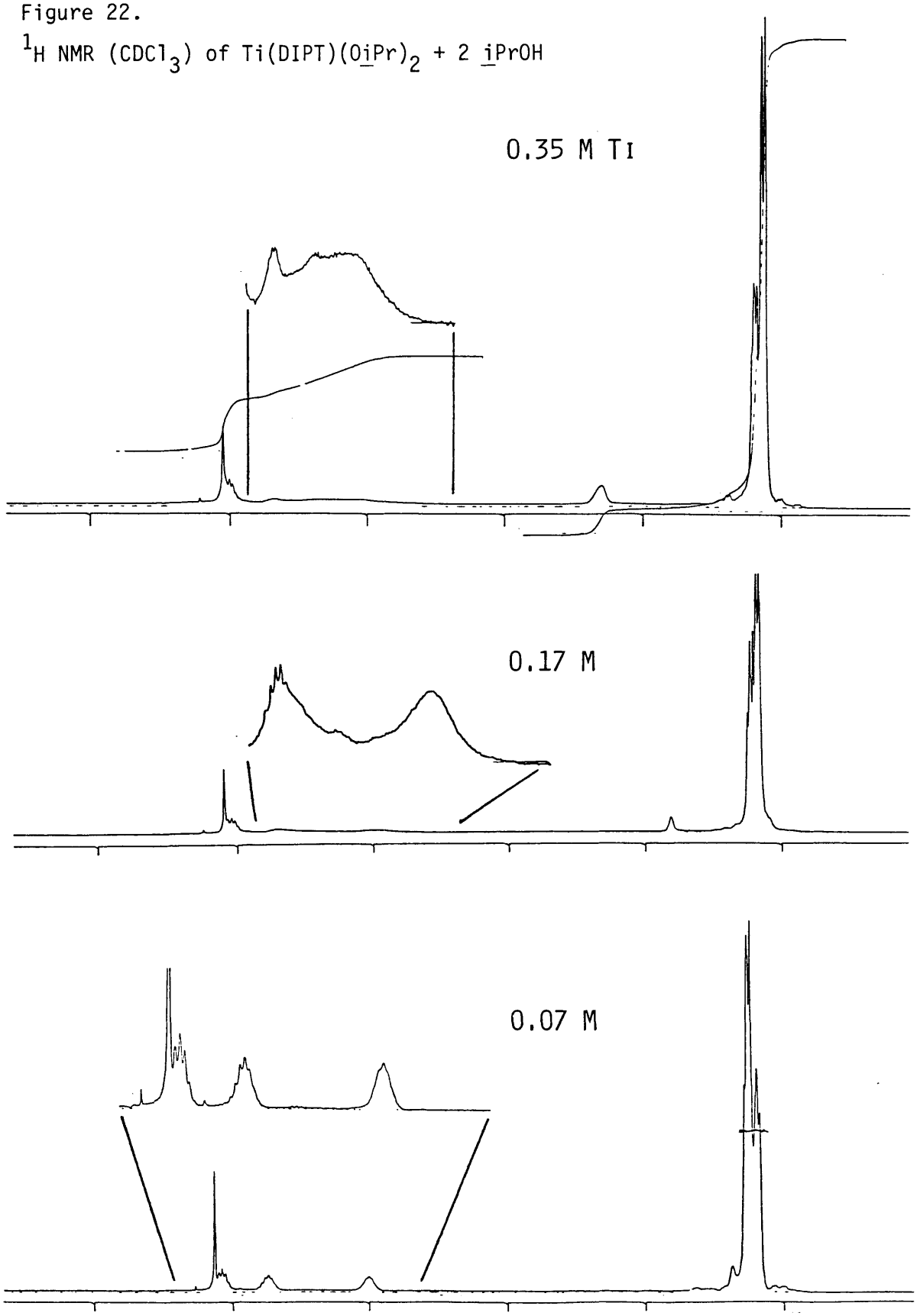

Figure 23. ^1H NMR ($CDCl_3$) of Ti(DIPT)(O$\underline{i}$Pr)$_2$ + 2 $\underline{i}$PrOH , 0.18 M in Ti

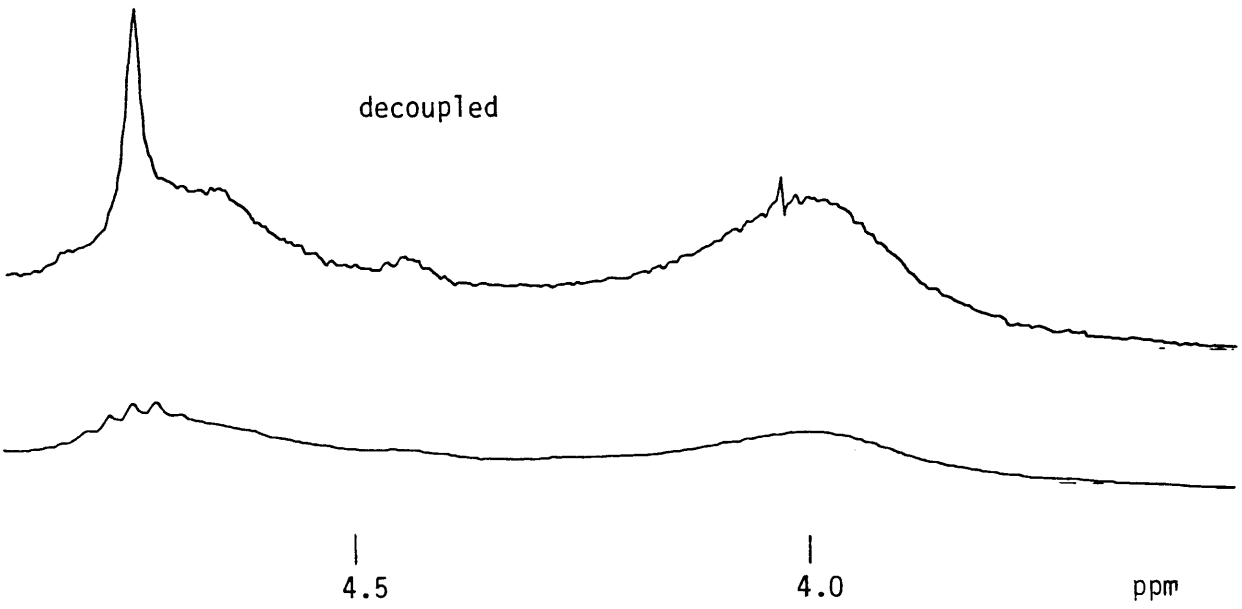

Figure 24. ^1H NMR of Ti(DIPT)(O$\underline{i}$Pr)$_2$ in isopropanol-d_8.

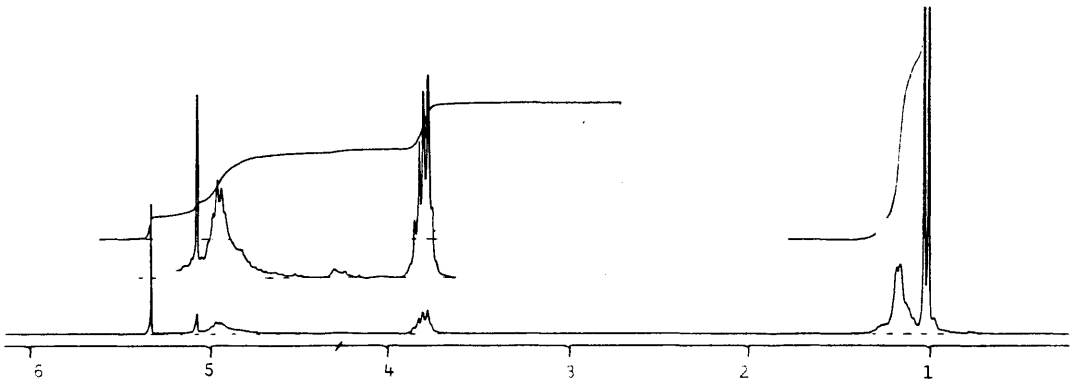

center of the Ti-DIPT dimer as an independent unit, and considering only the contribution of exchange with the more labile isopropoxide to coalescence. Employing the analysis related by Sandstrom,[97] with $p_{\underline{i}PrOH}$ = 0.67 and $p_{Ti\text{-}O\underline{i}Pr}$ = 0.33 as the populations of exchanging sites, at

coalescence,

$2\pi\tau_c(\delta\nu) = 2.0961$ (from Table 6.1 of reference 97, using $\Delta p = 0.34$)

$\delta\nu = 4.70 \text{ ppm} - 3.98 \text{ ppm} = 180 \text{ Hz}$

$\tau_c = 1.9 \times 10^{-3} = 0.33/\text{rate}_{\underline{i}\text{PrOH}} = 0.67/\text{rate}_{\text{Ti-O}\underline{i}\text{Pr}}$

So, $\text{rate}_{\underline{i}\text{PrOH}} = 174 \text{ sec}^{-1}$ $\text{rate}_{\text{Ti-O}\underline{i}\text{Pr}} = 353 \text{ sec}^{-1}$

The second order rate constant is therefore:

$k = \text{Rate}_{\underline{i}\text{PrOH}}/[\text{Ti-O}\underline{i}\text{Pr}] = \text{Rate}_{\text{Ti-O}\underline{i}\text{Pr}}/[\underline{i}\text{PrOH}]$

$k = (174 \text{ sec}^{-1})/(0.35 \text{ M}) \cong (353 \text{ sec}^{-1})/(0.70 \text{ M}) \cong \underline{500 \text{ L}^1\text{mol}^{-1}\text{sec}^{-1}}$,

giving a $\Delta G^{\neq}$ of approximately 14 kcal/mole for exchange of the more labile isopropoxide with isopropanol in solution.

^{13}C NMR spectra of $Ti(DIPT)(O\underline{i}Pr)_2$ also exhibit concentration-dependent exchange behavior. Figure 25 shows the complete ^{13}C nmr spectra for $Ti(DIPT)(O\underline{i}Pr)_2$ at 0.35 M and 0.07 M in $CDCl_3$, Figure 26 the 95-60 ppm region for each. Note the broadening of bands at 66 ppm ($\underline{i}$PrOH) and 79 ppm (Ti-O$\underline{i}$Pr) in the more concentrated sample. The lineshapes of the tartrate resonances (70.2 and 71.8 ppm for tartrate carbinol carbons, and 87 ppm for the isopropyl ester methines) do not change with concentration.

c. Variable Temperature ^1H NMR

The ^{13}C nmr spectra of Figures 25 and 26 feature two resonances each for the carbonyl and carbinol centers of tartrate. Yet the ^1H nmr of $Ti(DIPT)(O\underline{i}Pr)_2$ show only a single type of tartrate ligand. A fluxional exchange process that renders the two halves of unsymmetrically bound tartrate equivalent on the proton nmr timescale at room temperature is therefore indicated. As first demonstrated by Woodard, variable temperature ^1H nmr of titanium tartrates reveals the nonequivalent nature of the ester groups and carbinol centers of bound tartrate. We have determined the thermochemical parameters for the fluxional exchange process by coalescence temperature measurements and by bandshape analysis.

In order to avoid transesterification of the tartrate esters during the experiments, combinations in which transesterification is very slow (i.e., with $Ti(O\underline{t}Bu)_4$) or degenerate were used. In order to avoid the contribution of alcohol-alkoxide exchange to the line broadening of the nmr spectra, alcohol-free samples of $Ti(DIPT)(O\underline{i}Pr)_2$ and $Ti(DET)(OEt)_2$ were employed.

Figure 25. ^{13}C NMR ($CDCl_3$) of Ti(DIPT)(O$\underline{i}$Pr)$_2$ + 2 $\underline{i}$PrOH

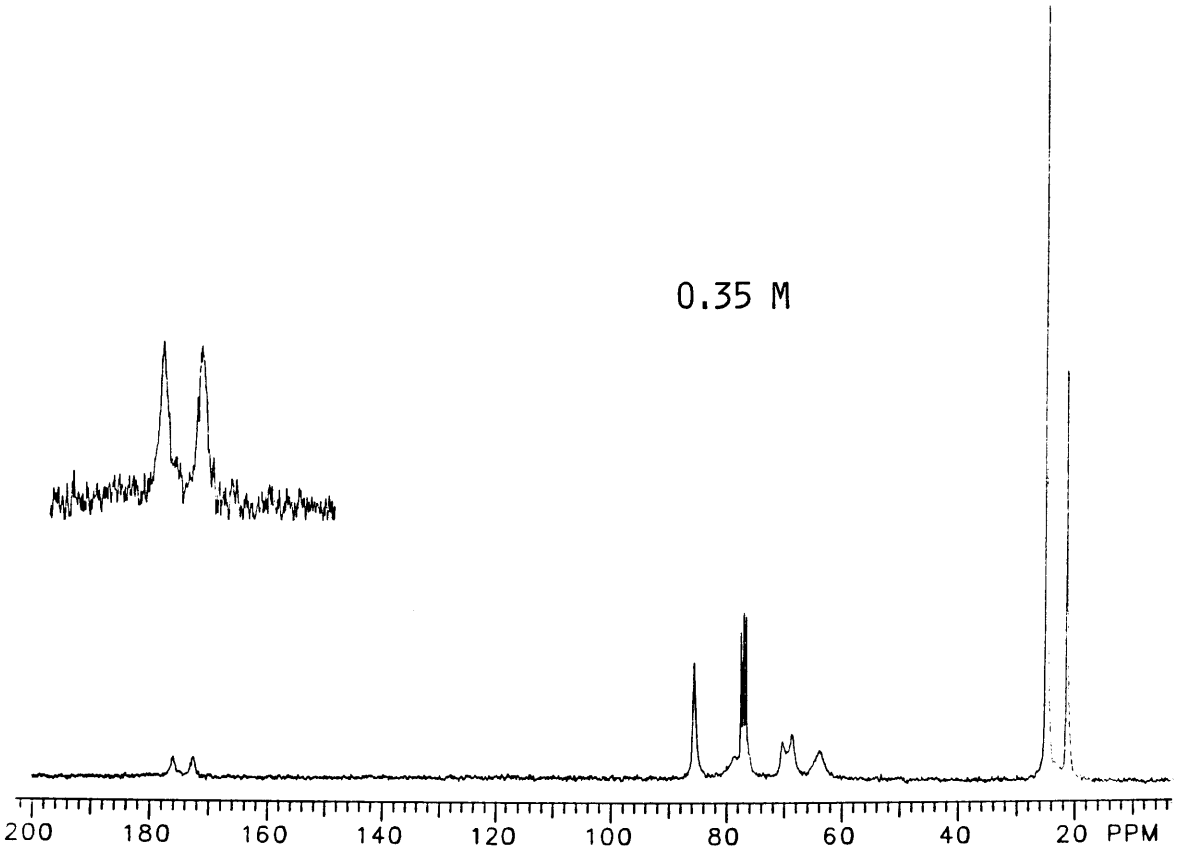

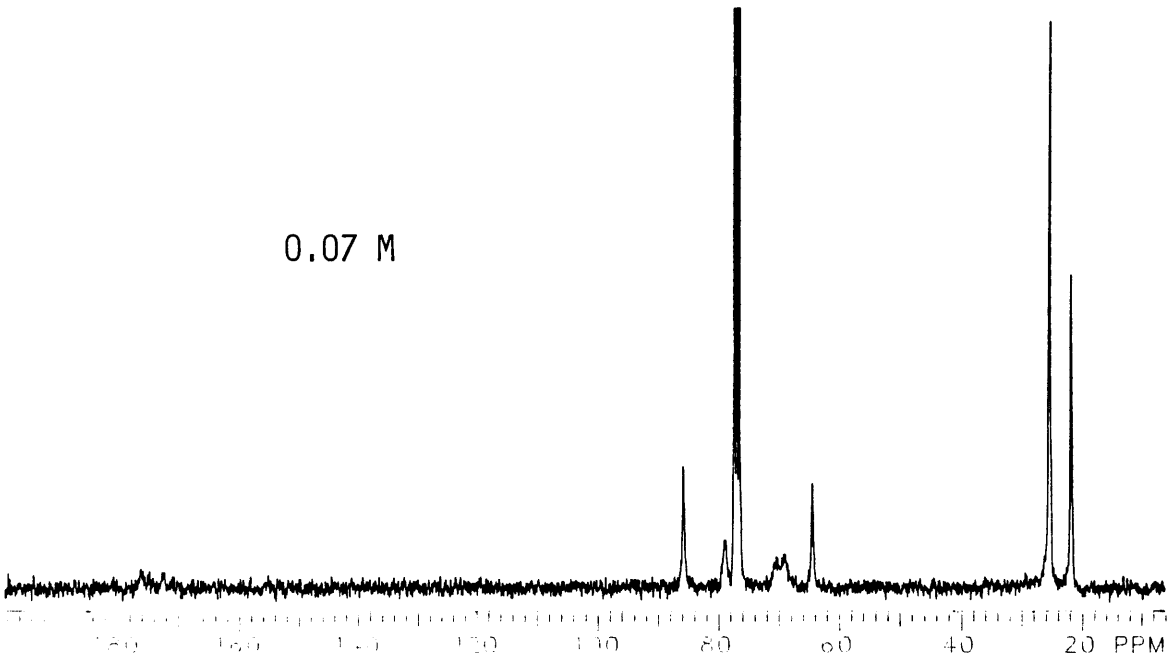

Figure 26.
^{13}C NMR ($CDCl_3$) of Ti(DIPT)(O$\underline{i}$Pr)$_2$ + 2 $\underline{i}$PrOH

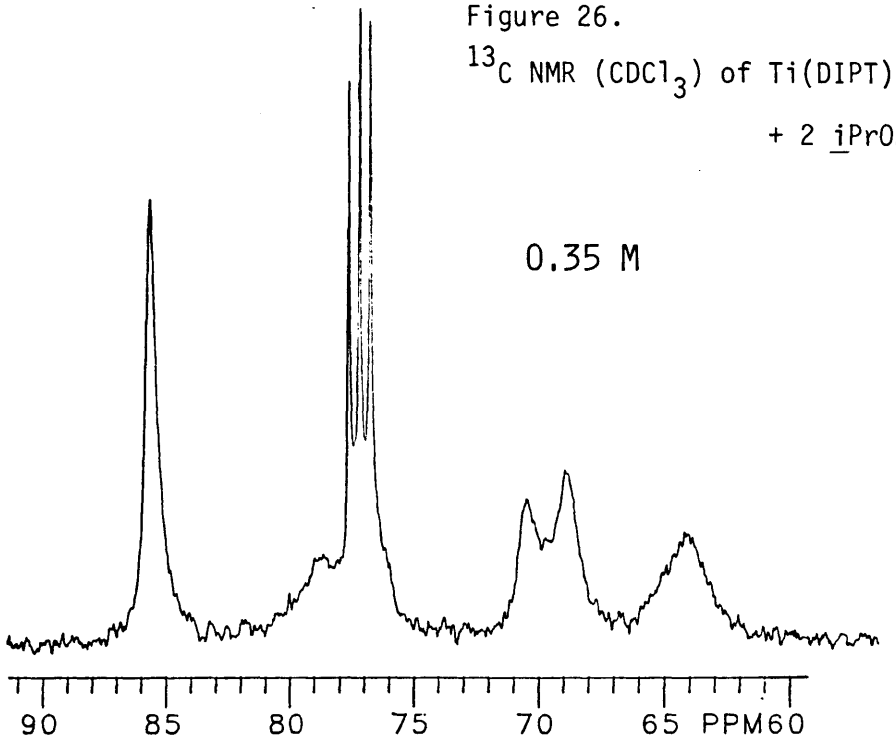

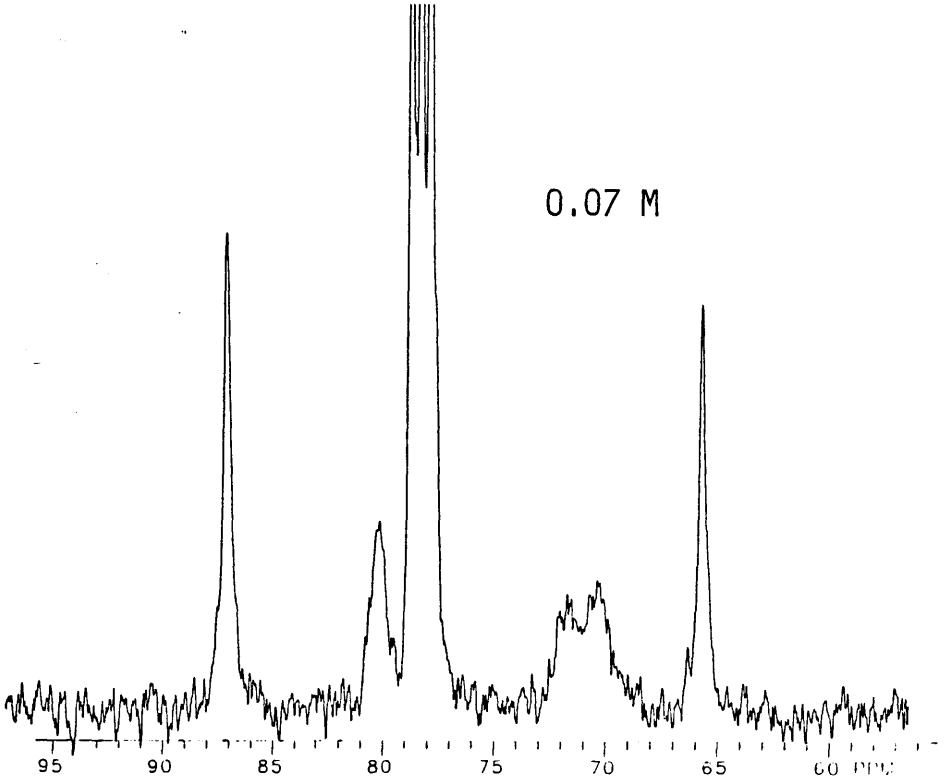

In the variable temperature nmr spectra of Ti-tartrates, every set of resonances displayed exchange behavior: the tartrate methine protons (H^a and H^b below), the titanium alkoxide resonances, and the tartrate ester groups.

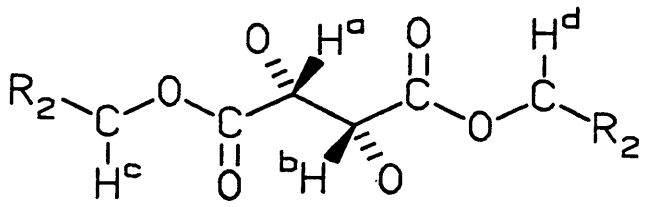

Since we required cleanly resolvable signals for bandshape analysis or coalescence temperature measurements, the upfield signals of isopropyl or ethyl groups were not useful. Therefore, of the Ti-OR signals only the t-butoxides and the methine protons of the isopropoxides were employed. Of the tartrate ester groups, only the isopropyl methine protons of DIPT were used.

Coalescence temperatures (T_c) were measured first; the results are listed below in Table 23. In order to calculate a free energy barrier to equilibration ($\Delta G^{\neq}$), the separation of peak positions at the slow-exchange limit (that is, when the signals are fully resolved, $\delta\nu_{k=0}$) was also obtained by cooling the samples to 230-235°K. Cooling to 220°K produced no further change in the nmr spectra, except for some resolution problems caused by increased sample viscosity. The rate constants at coalescence (k_c) were estimated with the simple equation (1). $\Delta G^{\neq}$ was calculated from equation (2).

$$k_c = \pi\delta\nu_{k=0} / \sqrt{2} \qquad (1)$$

$$\Delta G^{\neq} \text{ (kcal/mol)} = (1.987 \times 10^{-3})(T)[23.76 + \ln(T/k)] \qquad (2)$$

In order to obtain $\Delta G^{\neq}$ at different temperatures for a determination of $\Delta H^{\neq}$ and $\Delta S^{\neq}$, nmr bandshape analysis was performed using the DNMR4 program of Bushweller, et al (Quantum Chemistry Program Exchange No. 466). Since the program is incapable of handling more than five nuclei at a time, it was impossible to model the heptet signals due to isopropyl methine groups. Therefore, those spectra having isopropyl methine signals of

Table 23. Coalescence temperature measurements for the fluxional equilibration of Ti-tartrates in $CDCl_3$.

Complex	Peak Position (ppm)	Assignment	$\delta\nu_{k=0}$ (Hz)	T_c (^oK)	k_c (sec^{-1})	$\Delta G^{\neq}$ (kcal/m)
Ti(DMT)(O<u>t</u>Bu)$_2$	1.31	Ti-O<u>t</u>Bu	2.5	271	5.6	14.9
	5.11	H^a,H^b	91	314	202	15.1
	4.97, 5.34	H^a,H^b	1.6	265	3.6	14.8
Ti(DET)(O<u>t</u>Bu)$_2$	1.29	Ti-O<u>t</u>Bu	5.6	283	12.4	15.1
	5.13	H^a,H^b	65	310	144	15.1
	5.00, 5.26	H^a,H^b	3.1	279	6.9	15.2
Ti(DET)(OEt)$_2$	5.22	H^a,H^b	28.5	250	63.3	12.8

interest were also recorded with decoupling of the upfield methyl bands (decoupling power = 3L), reducing the methine resonances to singlets. Details of the bandshape analysis procedure are given in the experimental section. The results for each complex are presented and discussed below.

Ti(DET)(O<u>t</u>Bu)$_2$

Resonance	Peak Pos. at k=0 (Hz)
Tartrate methines (H^a, H^b)	1296.4, 1231.7 (J = 2.9)
Ti-O-<u>t</u>Bu	324.2, 318.7

The figures below show observed and calculated spectra for a range of temperatures in the range of 5.5-4.7 ppm (Fig. 27) and 1.7-0.7 ppm (Fig. 28). The former shows a singlet at 5.32 ppm for CH_2Cl_2 and a singlet due to an impurity at 5.0, as well as the tartrate methine resonances. In Figure 28, the methyl resonances from Ti-O<u>t</u>Bu are calculated, and compared to the observed spectra that also show methyl resonances from DET and <u>tert</u>-butanol.

Notice that the values of $\Delta G^{\neq}$ derived from $H^{a,b}$ and the <u>t</u>Bu resonances are the same within the error of measurement, indicating that one chemical process of $\Delta H^{\neq}$ = 15.0 ± 0.1 kcal/mole and $\Delta S^{\neq}$ = 0 e.u. is responsible for the nmr exchange behavior.

Figure 27. Dynamic NMR Bandshape Analysis of $Ti(DET)(O\underline{t}Bu)_2$ 5.5-4.7 ppm

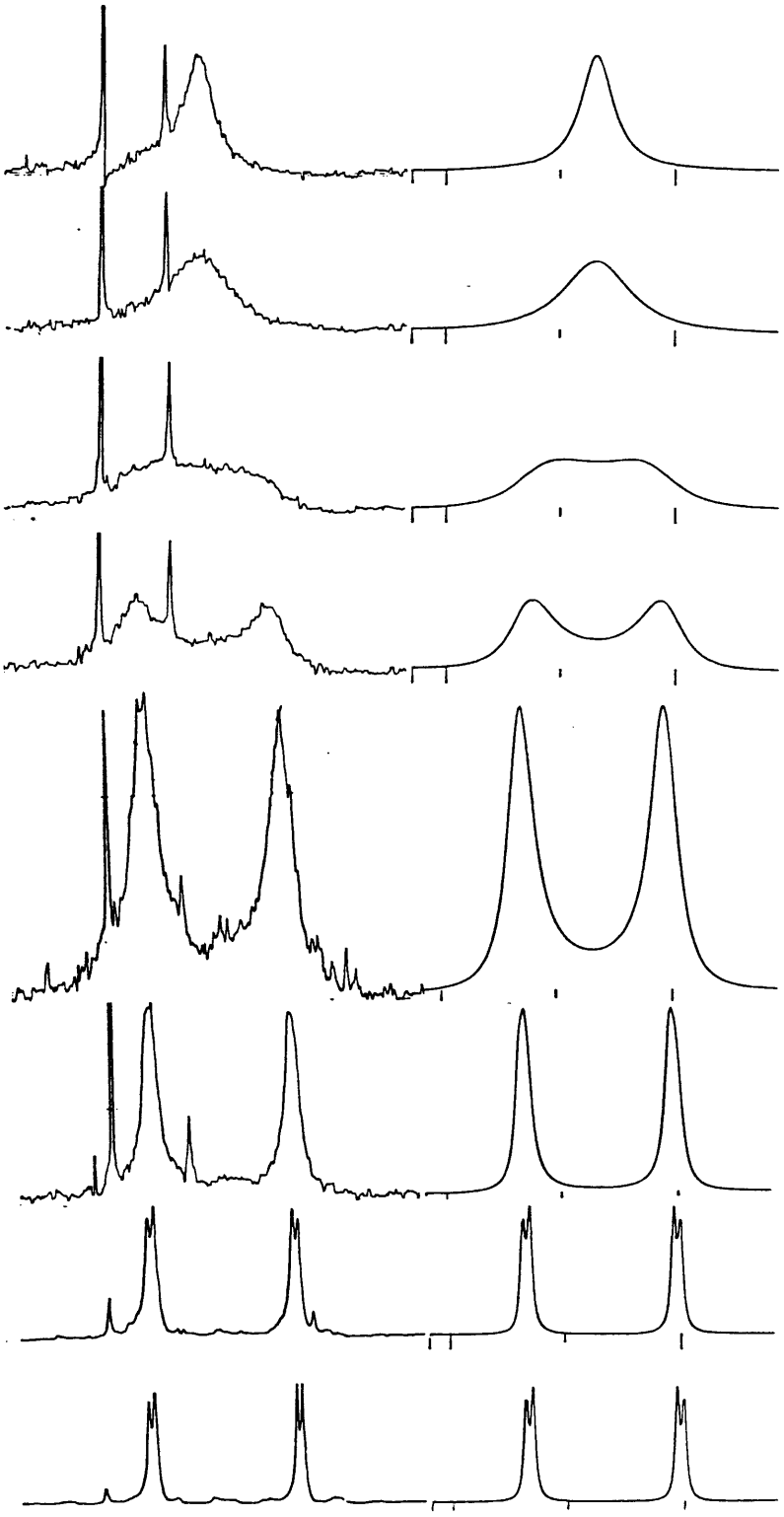

Temp.(°K)	k_{exch}
322.6	420 ± 20
314.1	235 ± 10
304.9	125 ± 10
297.4	70 ± 5
291.7	35 ± 6
283.7	12 ± 3
271.0	3.0 ± 1.0
252.7	ca. 0.0

Figure 28. Dynamic NMR bandshape analysis of $[Ti(DET)(O\underline{t}Bu)_2]_2$ 1.5-0.6 ppm; tert-Butyl signals are calculated; underlying OEt methyl resonances are ignored.

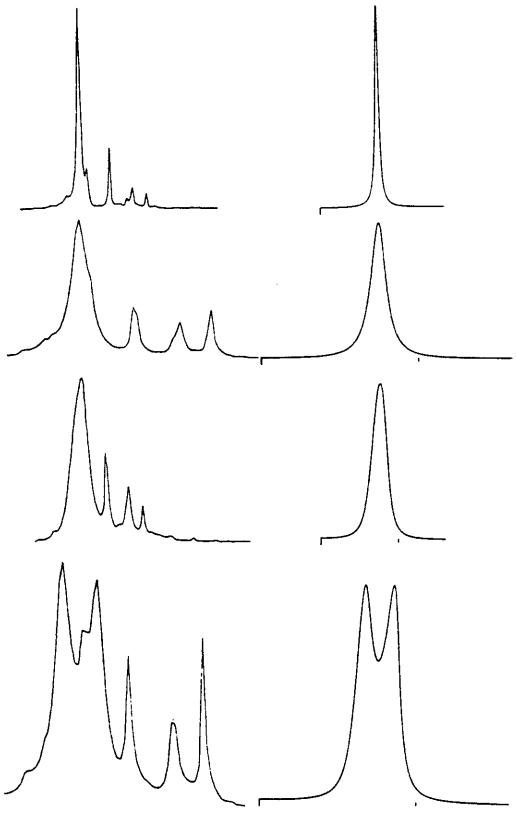

Temp. (^{o}K)	k_{exch}
304.9	130 ± 15
291.7	30 ± 5
283.7	14 ± 2
271.0	6 ± 2

Table 24. Dynamic NMR bandshape analysis of $Ti(DET)(O\underline{t}Bu)_2$ in $CDCl_3$.

Resonance	Temp. (°K)	T2 (sec)	Rate Constant (Hz)	$\Delta G^{\neq}$ (kcal/mole)
$H^{a,b}$	271.0	0.16	3.0 ± 1.0	15.2 ± 0.3
t-Bu	271.0	0.33	6.0 ± 2.0	14.8 ± 0.3
$H^{a,b}$	283.7	0.22	12 ± 3	15.2 ± 0.2
t-Bu	283.7	0.25	14 ± 2	15.1 ± 0.1
$H^{a,b}$	291.7	0.20	35 ± 5	15.0 ± 0.1
t-Bu	291.7	0.29	30 ± 5	15.1 ± 0.1
$H^{a,b}$	297.2	0.23	62 ± 3	15.0 ± 0.1
t-Bu	297.2	0.23	50 ± 10	15.1 ± 0.2
$H^{a,b}$	297.4	0.39	70 ± 5	14.9 ± 0.1
t-Bu	297.4	0.35	75 ± 15	14.9 ± 0.2
$H^{a,b}$	304.9	0.24	125 ± 10	14.9 ± 0.1
t-Bu	304.9	0.35	130 ± 15	14.9 ± 0.1
$H^{a,b}$	314.1	0.25	235 ± 10	15.0 ± 0.1
$H^{a,b}$	322.6	0.39	420 ± 20	15.1 ± 0.1

$Ti(DIPT)(O\underline{t}Bu)_2$

The t-butyl resonances are separated by only 8 Hz at 235°K, and coalesce rapidly upon warming; DNMR4 modeling is therefore subject to a large error and so these resonances were not used.

Again, the values of $\Delta G^{\neq}$ derived from two different sets of resonances ($H^{a,b}$ and $H^{c,d}$) are the same, characteristic of a single dynamic exchange process: $\Delta H^{\neq}$ = 15.0 ± 0.2 kcal/mole and $\Delta S^{\neq}$ = 0 e.u.

$Ti(DMT)(O\underline{t}Bu)_2$

Figure 29 below displays examples of observed and calculated spectra for $Ti(DMT)(O\underline{t}Bu)_2$ in the 5.5-4.7 ppm range; the tartrate methine protons are shown.

From the values in Table 26, $\Delta H^{\neq}$ = 15.4 ± 0.2 kcal/mole and $\Delta S^{\neq}$ = 0 e.u.

Table 25. Bandshape analysis of Ti(DIPT)(O$\underline{t}$Bu)$_2$ in $CDCl_3$.

Resonance	Peak Pos. at k=0 (Hz)
Tartrate methines (H^a, H^b)	1284.7, 1245.8 (J = 4.7)
Isopropyl ester methines (H^c, H^d) (Methyls decoupled)	1272.0, 1262.2

Resonance*	Temp. (°K)	T2 (sec)	Rate Constant (Hz)	$\Delta G^{\neq}$ (kcal/mole)
$H^{a,b}$	255.4	0.13	0.75 ± 0.25	15.0 ± 0.2
$H^{c,d}$ - d	255.4	0.085	0.2 ± 0.15	15.7 ± 0.5
$H^{a,b}$	267.3	0.14	2.0 ± 1.0	15.2 ± 0.3
$H^{c,d}$ - d	267.3	0.21	4.0 ± 1.5	14.9 ± 0.2
$H^{a,b}$	271.0	0.21	6.5 ± 0.5	14.8 ± 0.1
$H^{a,b}$	274.4	0.23	6.0 ± 1.0	15.0 ± 0.1
$H^{c,d}$ - d	274.4	0.20	6.0 ± 1.0	15.0 ± 0.1
$H^{a,b}$	283.7	0.25	18 ± 2	14.9 ± 0.1
$H^{c,d}$ - d	283.7	0.23	18 ± 1	14.9 ± 0.1
$H^{c,d}$ - d	297.4	0.21	66 ± 3	14.9 ± 0.1

*A "d" indicates decoupling of upfield methyl groups.

Table 26. Bandshape analysis of Ti(DMT)(O$\underline{t}$Bu)$_2$ in $CDCl_3$.

Resonance	Peak Pos. at k=0 (Hz)
Tartrate methines (H^a, H^b)	1310.6, 1224.4 (J = 1.8)
Ti-O- $\underline{t}$ Bu	318.6, 316.1

Resonance	Temp. (°K)	T2 (sec)	Rate Constant (Hz)	$\Delta G^{\neq}$ (kcal/mole)
$\underline{t}$-Bu	252.7	0.19	0.5 ± 0.2	15.1 ± 0.2
$H^{a,b}$	271.0	0.31	2.5 ± 0.5	15.3 ± 0.1
$\underline{t}$-Bu	271.0	0.31	2.2 ± 0.3	15.4 ± 0.1
$H^{a,b}$	274.4	0.25	3.0 ± 0.5	15.4 ± 0.1
$\underline{t}$-Bu	274.4	0.25	2.3 ± 0.2	15.6 ± 0.1
$H^{a,b}$	283.7	0.33	6.5 ± 1.0	15.5 ± 0.1
$\underline{t}$-Bu	283.7	0.33	5.5 ± 0.5	15.6 ± 0.1
$H^{a,b}$	297.2	0.20	25 ± 5	15.5 ± 0.15
$\underline{t}$-Bu	297.2	0.20	20 ± 5	15.6 ± 0.2
$H^{a,b}$	297.4	0.27	30 ± 5	15.4 ± 0.1
$\underline{t}$-Bu	297.4	0.27	25 ± 10	15.5 ± 0.3
$H^{a,b}$	304.9	0.27	82 ± 6	15.2 ± 0.1
$H^{a,b}$	309.5	0.34	115 ± 10	15.2 ± 0.1
$H^{a,b}$	314.1	0.36	140 ± 10	15.3 ± 0.1
$H^{a,b}$	322.6	0.36	210 ± 10	15.5 ± 0.1

Figure 29. Dynamic NMR bandshape analysis of $[Ti(DMT)(O\underline{t}Bu)_2]_2$ 5.5-4.7 ppm; Low temperature range.

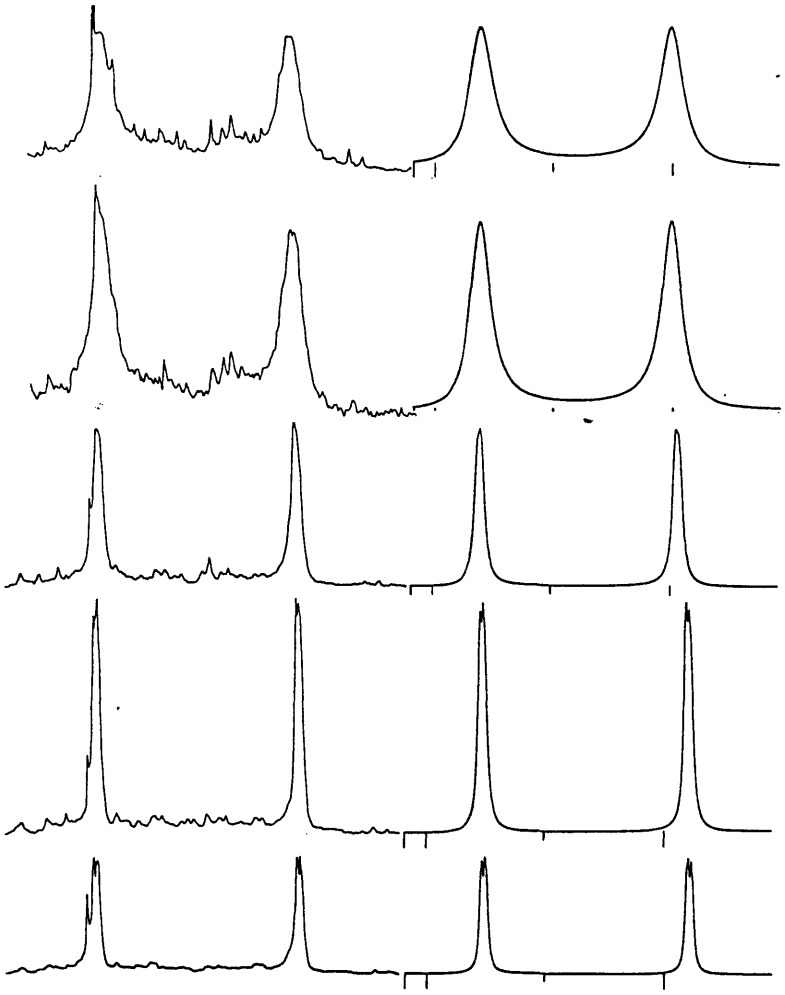

Temp. (^{o}K)	k_{exch}
297.4	30 ± 5
297.2	25 ± 5
283.7	6.5 ± 1.0
274.4	3.0 ± 0.5
271.0	2.5 ± 0.5

$Ti(DIPT)(O\underline{i}Pr)_2$

Figure 30 shows observed and calculated spectra for $Ti(DIPT)(O\underline{i}Pr)_2$ in the range from 5.5 to 4.3 ppm at 267^{o}K. On the bottom is the normal spectrum; the top shows the result of decoupling the upfield isopropyl methyl groups. Note the appearance of <u>three</u> sets of resonances for the isopropyl ester groups and the isopropoxide ligands.

Figure 30. ^{1}H NMR of Ti(DIPT)(O$\underline{i}$Pr)$_2$ ($CDCl_3$) at 267°K.
Top: $\underline{i}$Pr methyl groups decoupled; k_{calc} = 11.5, T2 = 0.23 sec^{-1}
Bottom: no decoupling; k_{calc} = 11.5, T2 = 0.32 sec^{-1}

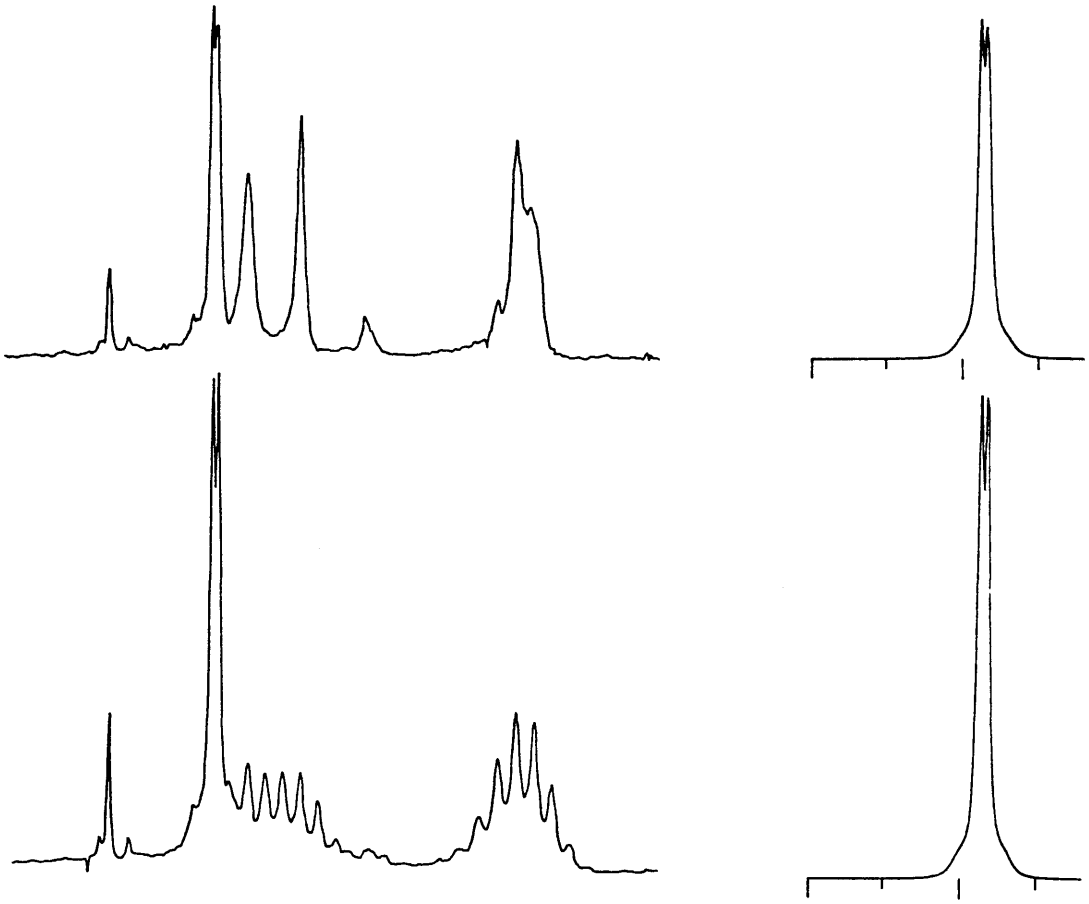

Observed Calculated

The peak positions and relative intensities for Figure 30 are tabulated below:

Table 27. Observed ^{1}H nmr bands for Ti(DIPT)(O$\underline{i}$Pr)$_2$ in $CDCl_3$ at 267°K.

Resonance	Peak Pos. at k=0 (Hz)
Tartrate methines (H^a, H^b)	1286.0, 1279.3 (J = 7.0)
Isopropyl ester methines (H^c, H^d) (Methyls decoupled)	1275.9 (Rel. Intens. = 0.43), 1257.5 (0.50), 1234.8 (0.07)
Ti-O$\underline{i}$Pr methines (H^e, H^f) (Methyls decoupled)	1191.0 (0.07), 1184.7 (0.50), 1178.1 (0.43)

The spectra of Fig. 30 are consistent with the presence of a second Ti-tartrate structure, which undergoes exchange with the major species in solution and thus does not appear at higher temperature. Three, and not four, bands appear for the two types of isopropyl groups in the decoupled spectra at low temperature because two bands overlap. The experimental spectrum was modeled effectively by assigning to the major species isopropyl ester methine resonances at 5.10 and 5.03 ppm, and to the minor species resonances at 5.03 and 4.94 ppm, giving rise to a pattern in which the central band is as intense as the sum of the outer bands. Thus, the assignment of resonances for bandshape analysis is as follows:

Table 28. Peak position assignments for bandshape analysis of $Ti(DIPT)(O\underline{i}Pr)_2$ in $CDCl_3$.

Resonance	Peak Pos. at k=0 (Hz)
Tartrate methines (H^a, H^b)	1286.0, 1279.3 (J = 7.0)
Isopropyl ester methines (H^c, H^d)	
(Methyls decoupled)	1275.9 (Rel. Intens. = 0.43), 1257.5 (0.50), 1234.8 (0.07)
Ti-O$\underline{i}$Pr methines (H^e, H^f)	
(Methyls decoupled)	1191.0 (0.07), 1184.7 (0.50), 1178.1 (0.43)

The DNMR4 program allows independent assignment of exchange rate constants. That is, each of the rate constants for exchange of sites within each complex and between complexes is designated separately by the user. In this case, three rate constants are required: exchange between the two sites of the major complex (k_{maj}), between the two sites of the minor component (k_{min}) and exchange between complexes (k_{exch}).

Displayed below on the left side of Figure 31 are a series of observed spectra for $Ti(DIPT)(O\underline{i}Pr)_2$ ("decoupled" denotes irradiation of upfield methyls). At 297.4°K, the three tartrate ester methines have coalesced to a single resonance, as have the isopropoxide ligand methines. At 283.7°K, the bands due to the minor species are still visible, whereas the Ti-O$\underline{i}$Pr bands of the major component have coalesced by 274.4°C, and the isopropyl ester resonances show significant line broadening.

On the right side of Fig. 31 is a series of calculated spectra with all the exchange rate constants equal to each other. The resonances due to

the minor component merge into those of the major species before coalescence of the major bands occurs. It is clear, therefore, that all the exchange rate constants cannot be equal. The fact that the minor species bands persist to higher temperatures means that the exchange rate between sites of the major species must be larger than that for the minor species and for exchange between structures.

In the middle of Figure 31 are displayed calculated spectra for which k_{maj} is the same as for the right hand column, but k_{min} and k_{exch} are 1/30 the value of k_{maj}. Note that the minor species bands are visible at higher values of k_{maj}, much like the observed spectra. The results below in Table 29 were obtained from calculated spectra in which $k_{maj} = 30 \times k_{min} = 30 \times k_{exch}$. While the error for the determination of $\Delta G^{\neq}$ of two-site exchange in the minor complex is larger than for the major one due to the small peak size, it is clear that the barrier to equilibration is much higher for the minor component; unfortunately, an evaluation of $\Delta H^{\neq}$ and $\Delta S^{\neq}$ cannot be made for the minor structure. Note, of course, that both the isopropyl ester methine and the isopropoxide methine signals of the major species are modeled at the same time by the same exchange rate constants, indicating that their DNMR behavior is the product of the same chemical process.

Table 29. Bandshape analysis of Ti(DIPT)(O<u>i</u>Pr)$_2$ in $CDCl_3$.

Resonance*	Temp. (°K)	T2 (sec)	Rate Constant (Hz)	$\Delta G^{\neq}$ (kcal/mole)
$H^{c,d,e,f}_{maj}$	260	0.15	2 ± 1	14.8 ± 0.3
$H^{c,d,e,f}_{min}$	260	0.15	ca. 0.07	ca. 16.5
$H^{c,d,e,f}_{maj}$	267.3	0.32	7 ± 1	14.6 ± 0.1
$H^{c,d,e,f}_{min}$	267.3	0.32	0.23 ± 0.1	16.4 ± 0.3
$H^{c,d,e,f}_{maj}$	274.4	0.20	14 ± 3	14.6 ± 0.2
$H^{c,d,e,f}_{min}$	274.4	0.20	≅ 0.3	≅16.7
$H^{c,d,e,f}_{maj}$	283.7	0.20	25 ± 6	14.8 ± 0.2
$H^{a,b}$	267.3	0.32	11.5 ± 0.5	14.3 ± 0.1
$H^{a,b}$ - d	267.3	0.23	11.5 ± 0.5	14.3 ± 0.1

*A "d" indicates decoupling of upfield methyl groups.

For the major species, $\Delta H^{\neq}$ = 14.5 ± 0.3 kcal/mole; $\Delta S^{\neq}$ = ca. 0 e.u. Note in the final two entries of Table 29 (which deal with the spectra in Figure

Figure 31. DNMR4 modeling of ^{1}H NMR spectra of Ti(DIPT)(O$\underline{i}$Pr)$_2$ in $CDCl_3$, including major (86%) and minor (14%) components.

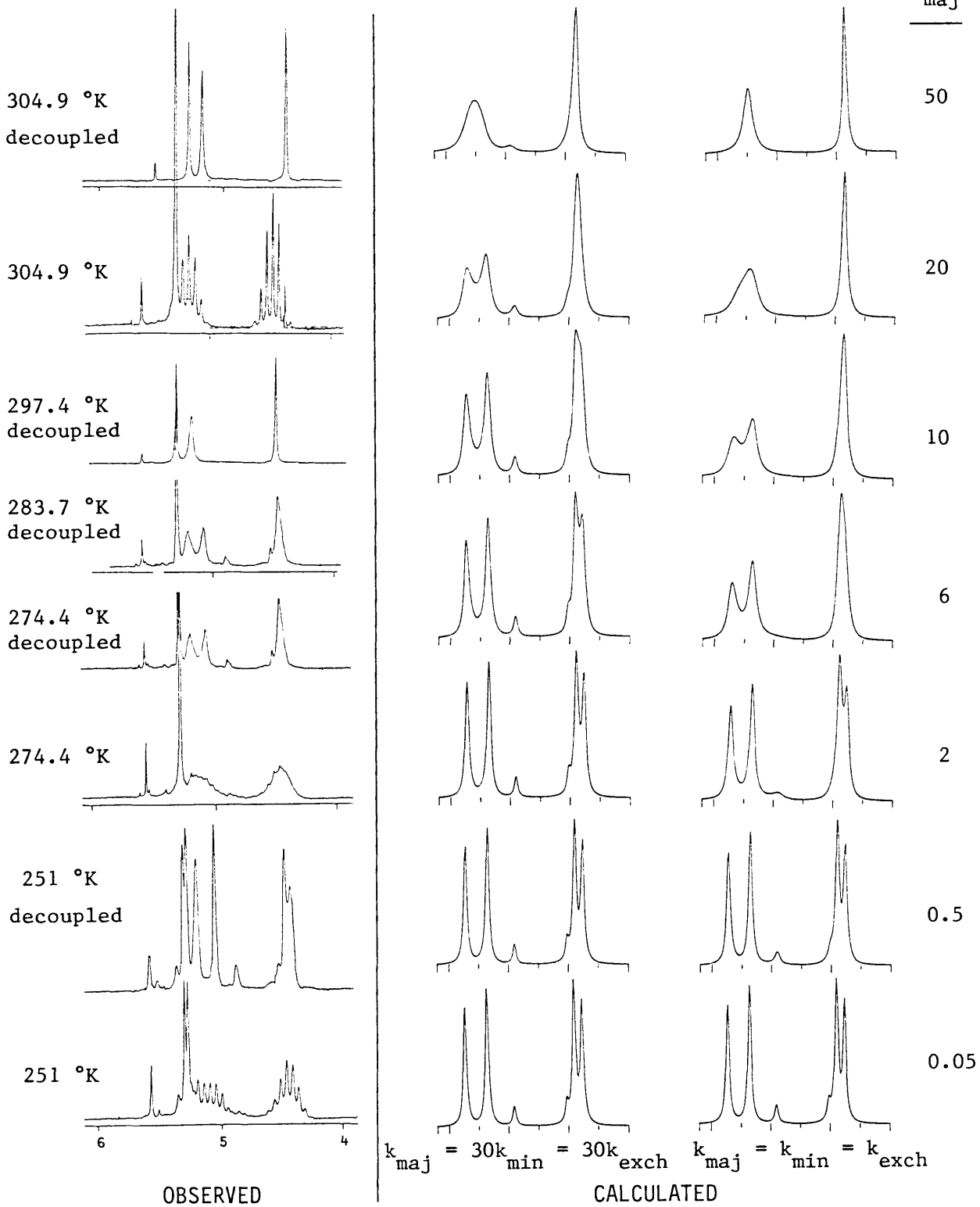

30) that the use of decoupling changes the spectral bandwidth (T2) but the calculated rate constant is the same.

$Ti(DET)(OEt)_2$

In this case, the calculated spectra include a singlet due to residual CH_2Cl_2 at 1322 Hz which overlaps the tartrate methine pattern.

Table 30. Bandshape analysis of $Ti(DET)(OEt)_2$ in $CDCl_3$.

Resonance	Peak Pos. at k=0 (Hz)
Tartrate methines (H^a, H^b)	1322.2, 1297.4

Resonance	Temp. (°K)	T2 (sec)	Rate Constant (Hz)	$\Delta G^{\neq}$ (kcal/mole)
$H^{a,b}$	246.0	0.25	29 ± 2	12.7 ± 0.1
$H^{a,b}$	252.7	0.19	32 ± 3	13.0 ± 0.1
$H^{a,b}$	262.0	0.14	43 ± 3	13.3 ± 0.1
$H^{a,b}$	271.0	0.17	70 ± 3	13.5 ± 0.1
$H^{a,b}$	283.7	0.21	110 ± 5	13.9 ± 0.1
$H^{a,b}$	295.1	0.22	160 ± 10	14.3 ± 0.1

In contrast to all the other cases, $\Delta G^{\neq}$ varies with temperature. A plot of temperature vs. $-\Delta G^{\neq}$ appears below; from this is calculated $\Delta H^{\neq}$ = +5.1 kcal/mole, $\Delta S^{\neq}$ = -31 cal/deg.

A summary of the thermochemical parameters is presented in Table 31.

Table 31. Results of dynamic nmr bandshape analysis.

Entry	Complex	$\Delta H^{\neq}$ (kcal/mole)	$\Delta S^{\neq}$ (e.u.)
1	$Ti(DIPT)(O\underline{t}Bu)_2$	15.0 ± 0.2	0.0
2	$Ti(DET)(O\underline{t}Bu)_2$	15.0 ± 0.1	0.0
3	$Ti(DMT)(O\underline{t}Bu)_2$	15.4 ± 0.2	0.0
4	$Ti(DIPT)(O\underline{i}Pr)_2$	14.5 ± 0.3	0.0
5	$Ti(DET)(OEt)_2$	5.1 ± 0.5	-31 ± 4

The enthalpy of activation varies with the size of the ligands: tert-butoxides have a higher barrier than isopropoxides (entry 1 vs. 4, and 2 vs. 5). On steric grounds alone, it is a little surprising that a DMT complex shows a higher activation energy for fluxional equilibration than the corresponding DET or DIPT complexes (entry 3 vs. entries 1 and 2). Most interesting of all, of course, are the unique values for

Figure 32. Plot of temperature vs. $\Delta G^{\neq}$ for the fluxional equilibration of $Ti(DET)(OEt)_2$.

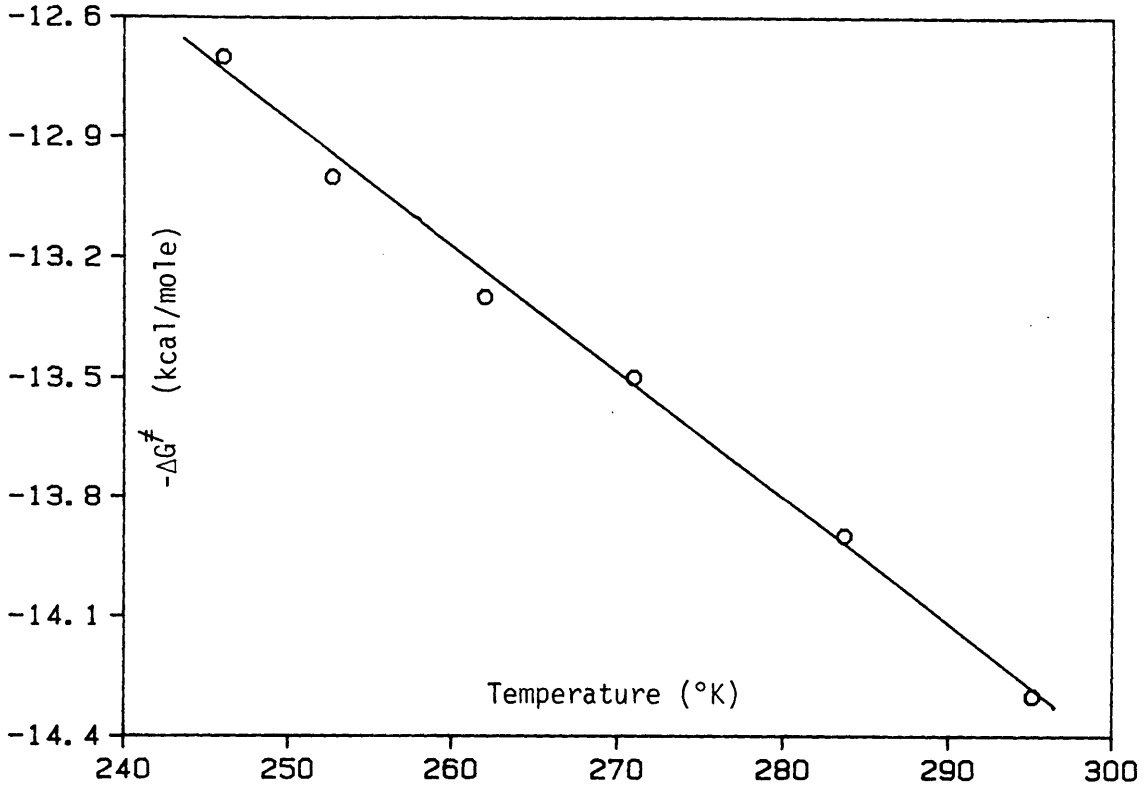

$Ti(DET)(OEt)_2$. A $\Delta S^{\neq}$ value of -31 e.u. is well in the range of that expected for a bimolecular reaction, whereas near zero entropies of activation would be expected for unimolecular processes. It is not understand why $Ti(DET)(OEt)_2$ should prefer a bimolecular route when the others show unimolecular behavior. Either bimolecular exchange is enhanced for this complex, or intramolecular exchange is disfavored, or both. $Ti(DET)(OEt)_2$ is probably much more polar than the other four complexes (all of which have tertiary or secondary alkoxide ligands), and therefore intermolecular interactions may be rendered more attractive. In any case, the concentration dependence of this process must be investigated to establish its bimolecular nature. All the complexes studied here, it should be noted, were found to be dimeric in solution by the Signer method (except $Ti(DMT)(O\underline{t}Bu)_2$, which was not examined).

d. Variable Temperature ^{13}C NMR

^{13}C NMR spectra of titanium tartrates also illustrate the fluxional

equilibration process. Figure 33 shows the temperature dependent spectra of Ti(DIPT)(O$\underline{i}$Pr)$_2$ in $CDCl_3$. Note the coalescence behavior of carbonyl groups (176.8 and 171.7 ppm at 255°K, 174.0 ppm at 320°K), Ti-O$\underline{i}$Pr methine carbons (79.0 and 78.1 ppm at 255°K, 78.7 ppm at 320°K), and isopropyl ester methine carbons (70.9 and 68.4 ppm at 255°K, 69.3 ppm at 320°K). The isopropoxide methyl resonance at 25.2 ppm shows a hint of splitting at low temperature. Curiously, the tartrate methine (carbinol) carbons provide a sharp singlet (86.0 ppm) regardless of temperature, presumably because of a very small difference in peak position between the two chemically different carbinol centers of the unsymmetrical structure. Bandshape analysis could also be applied to the ^{13}C nmr spectra, but inaccurate temperature measurement makes the resultant error limits too large.

Note that Figure 33 provides no evidence for the minor component of Ti(DIPT)(O$\underline{i}$Pr)$_2$ in solution that was observed in the proton nmr. Variable temperature ^{13}C nmr spectra of Ti(DIPT)(O$\underline{t}$Bu)$_2$ (Figure 34) and Ti(DMT)(O$\underline{t}$Bu)$_2$ (Figure 35), on the other hand, do show a second species for each, whereas their proton nmr spectra do not.

Consider the ^{13}C nmr spectrum of Ti(DIPT)(O$\underline{t}$Bu)$_2$ at 255°K, on the bottom of Figure 34. Four peaks for tartrate methine protons appear; a larger pair at 86.8 and 84.5 ppm, and a smaller pair at 85.0 and 83.1 ppm. On warming, line broadening of all four peaks occurs so that at 310°K an apparent broad doublet is present. Analogous to Ti(DIPT)(O$\underline{i}$Pr)$_2$, we assign the smaller set of resonances to a minor titanium tartrate species that undergoes chemical exchange with the major component in solution. Note also the coalescence of free and bound carbonyl resonances as temperature is increased.

A minor tartrate species is also visible in the spectra of Ti(DMT)(O$\underline{t}$Bu)$_2$ presented in Figure 35, again in the tartrate methine carbon resonances: major species at 87.7 and 83.8 ppm; minor species at 85.6 and 84.1 ppm. In this case, fluxional equilibration is manifested in the resonances of Ti-O$\underline{t}$Bu (30.9 ppm, as shown in the insets of the spectra at 271°K and 282°K), and $-CO_2CH_3$ (51.8 ppm). Because of the large value for $\Delta H^{\neq}$ (15.4 kcal/mole, Table 31), the carbonyl peaks at 174.2 and 171.2 do not reach coalescence at 308°K, but are merely broadened by exchange of bound and free ester groups.

Figure 33. Variable temperature ^{13}C NMR of Ti(DIPT)(O$\underline{i}$Pr)$_2$ in $CDCl_3$. Temperatures are reported to within ± 3°K.

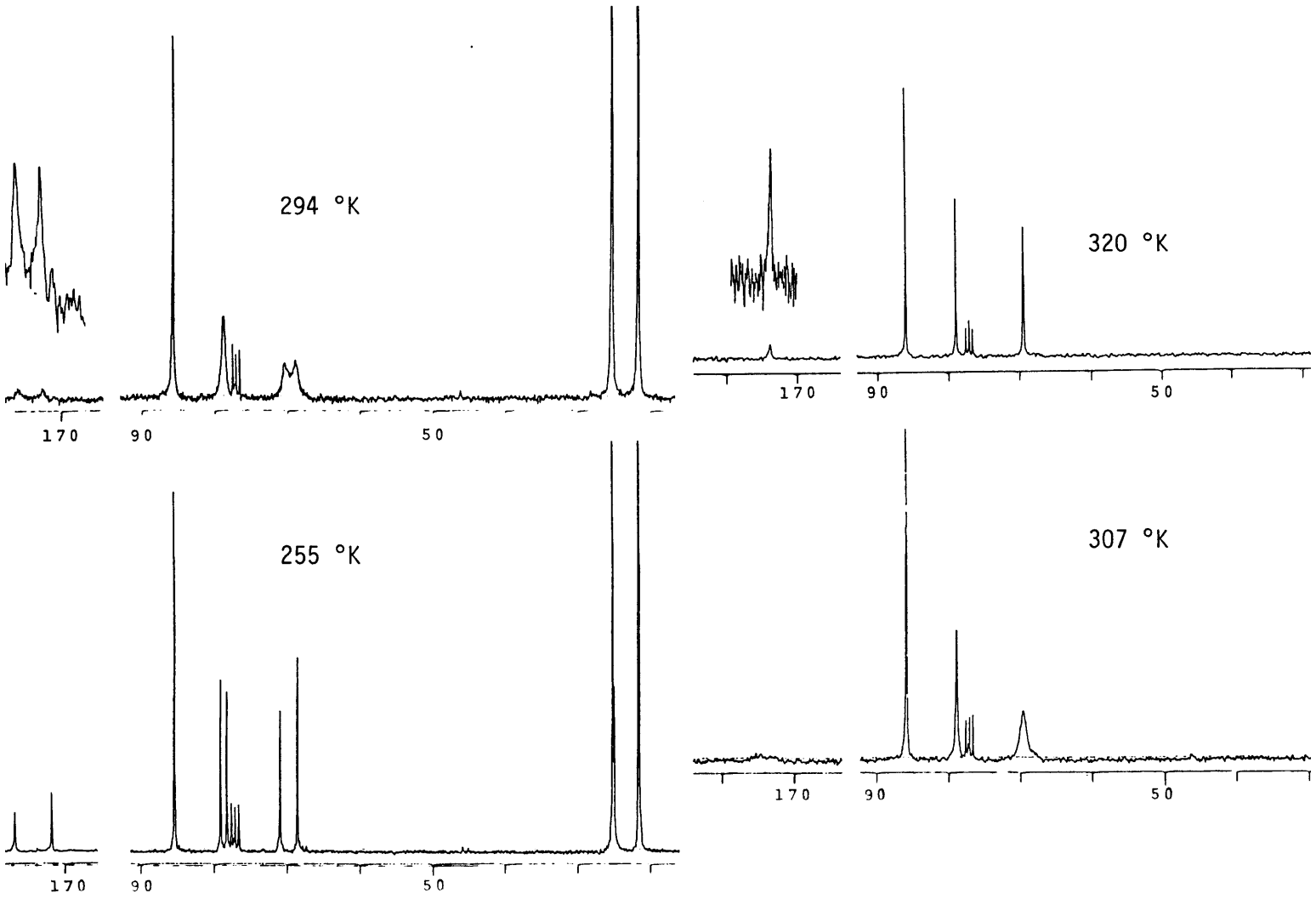

Figure 34. Variable temperature ^{13}C NMR of Ti(DIPT)(O$\underline{t}$Bu)$_2$ in $CDCl_3$. Temperatures are reported to within ± 3°K.

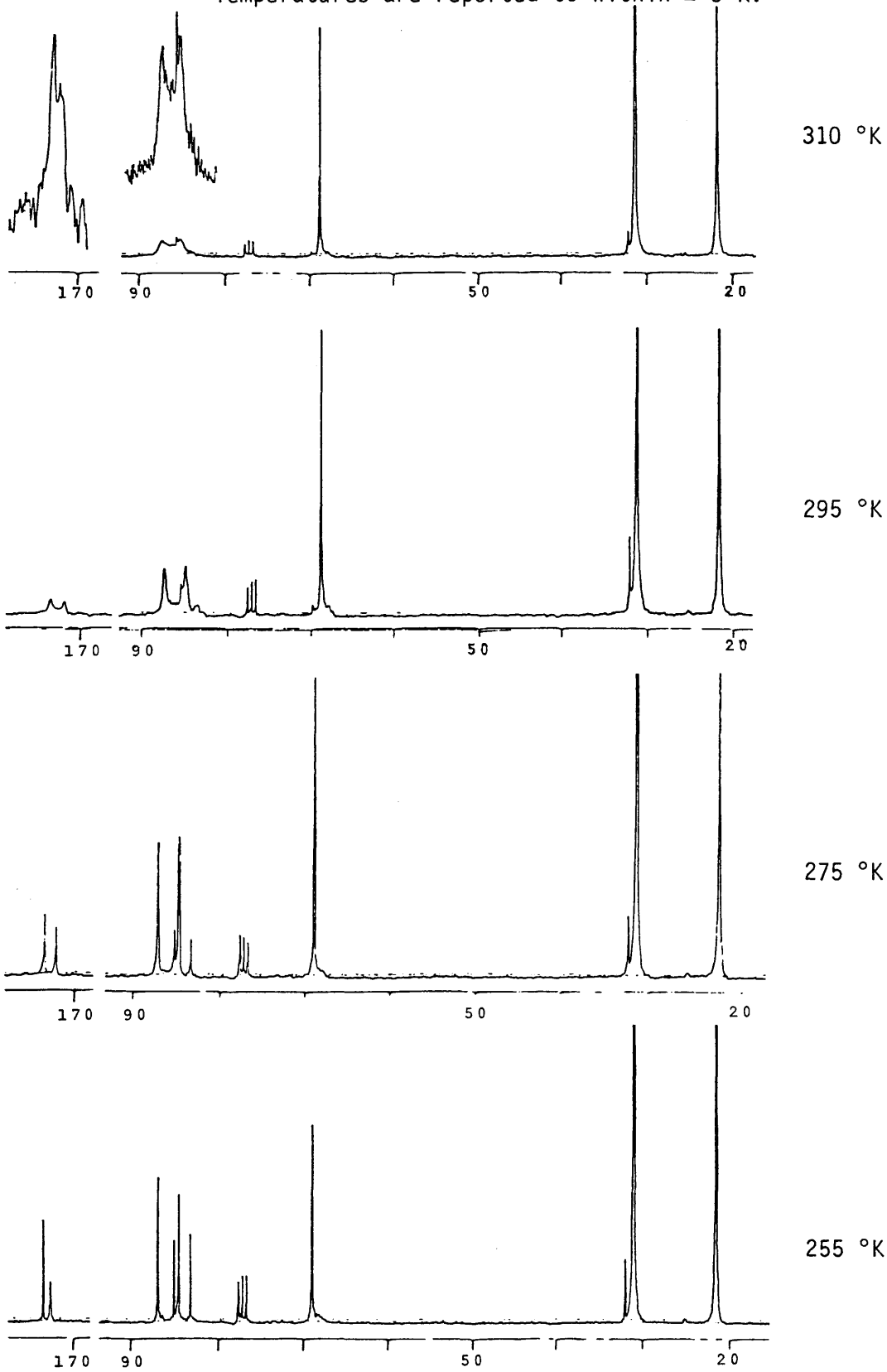

Figure 35. Variable temperature ^{13}C NMR of $Ti(DMT)(O\underline{t}Bu)_2$ in $CDCl_3$

Temperatures are ± 3°K.

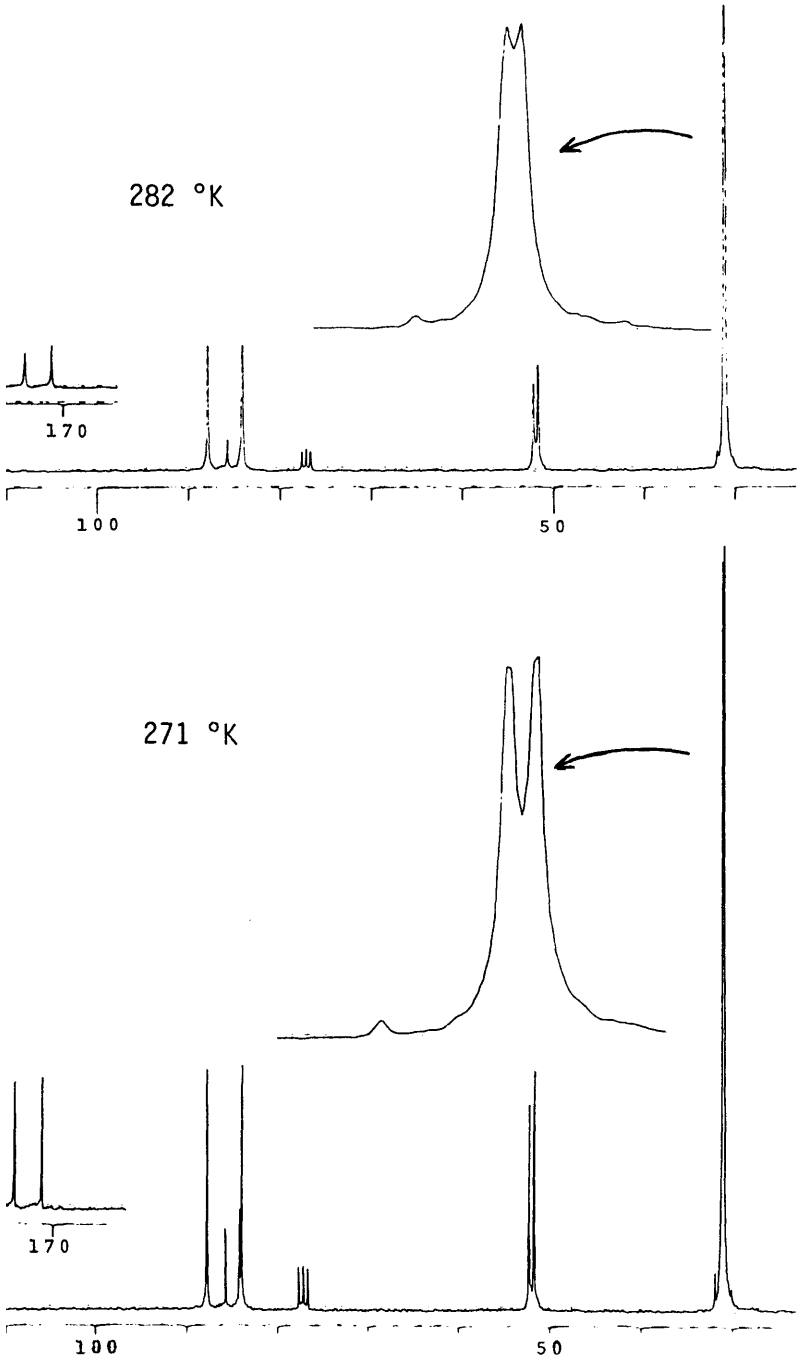

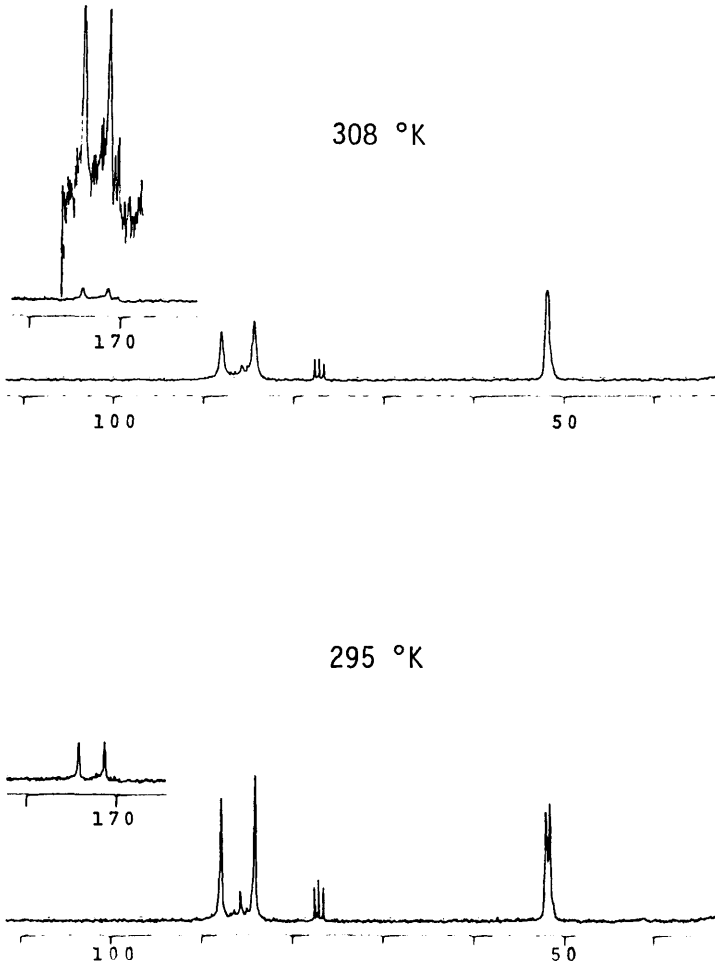

Using the proposed catalyst structure analogous to the crystal structures **13a** and **13b** (section II.C.3), Dr. Steven Pedersen originally proposed the existence of the equilibration process depicted in Figure 36. As required by the nmr spectra, the fluxional process takes bridging oxygens to terminal positions and vice versa (marked with asterisks in Fig. 36), exchanges the axial and equatorial monodentate alkoxides (diamonds), and exchanges the bound and free ester groups (triangles). Note, of course, that structures **14a** and **14b** are superimposable. For all the complexes studied except $Ti(DET)(OEt)_2$, a possible intermediate in such an exchange process could be the 10-membered ring structure **21**.

Figure 36. Proposed fluxional equilibrium of Ti-tartrates in solution.

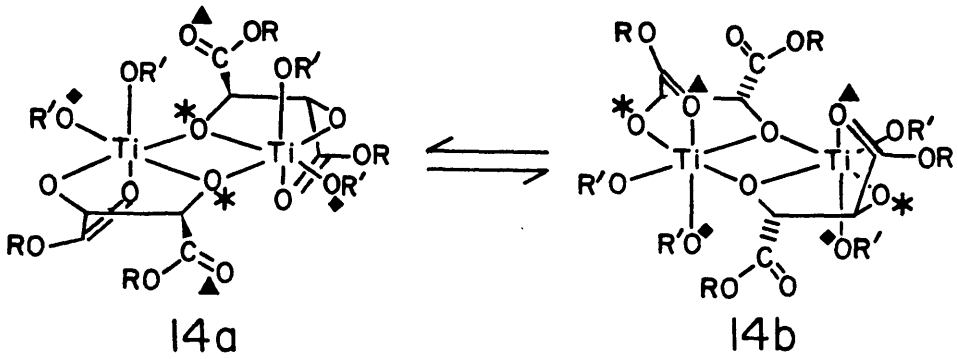

5. IR Spectroscopy in CH_2Cl_2

As first reported by Woodard, the IR spectrum of $Ti(DIPT)(O\underline{i}Pr)_2$ in CH_2Cl_2 solution shows three carbonyl stretching bands: 1738, 1683, and 1638 cm^{-1}. The first is due to an uncoordinated ester unit, the second and third to ester groups bound to titanium through the carbonyl oxygen. The band at 1685 cm^{-1} is much smaller than the other two when the Ti:tartrate ratio is 2:2. Figure 37 reproduces the IR spectra of $Ti(DIPT)(O\underline{i}Pr)_2$ in CH_2Cl_2 in the presence and absence of two equivalents of isopropanol; the carbonyl region of other standard 2:2 Ti:tartrate complexes is the same in CH_2Cl_2 solution.

Thus, the presence of free and bound ester groups is indicated by the IR, as well as the nmr, spectra, and the major IR bands at 1738 and 1638 cm^{-1} can be assigned to free and bound carbonyls of structure **14**. It appears that the 1638 cm^{-1} band is rare among complexes of Ti(IV) with α-hydroxy esters. Woodard noted that when the Ti:tartrate ratio is either greater or less than 1:1, the intensity of the 1638 cm^{-1} band is diminished

Figure 37. IR spectra of Ti(DIPT)(O$\underline{i}$Pr)$_2$ (CH_2Cl_2) in the presence (bottom) and absence (top) of $\underline{i}$PrOH.

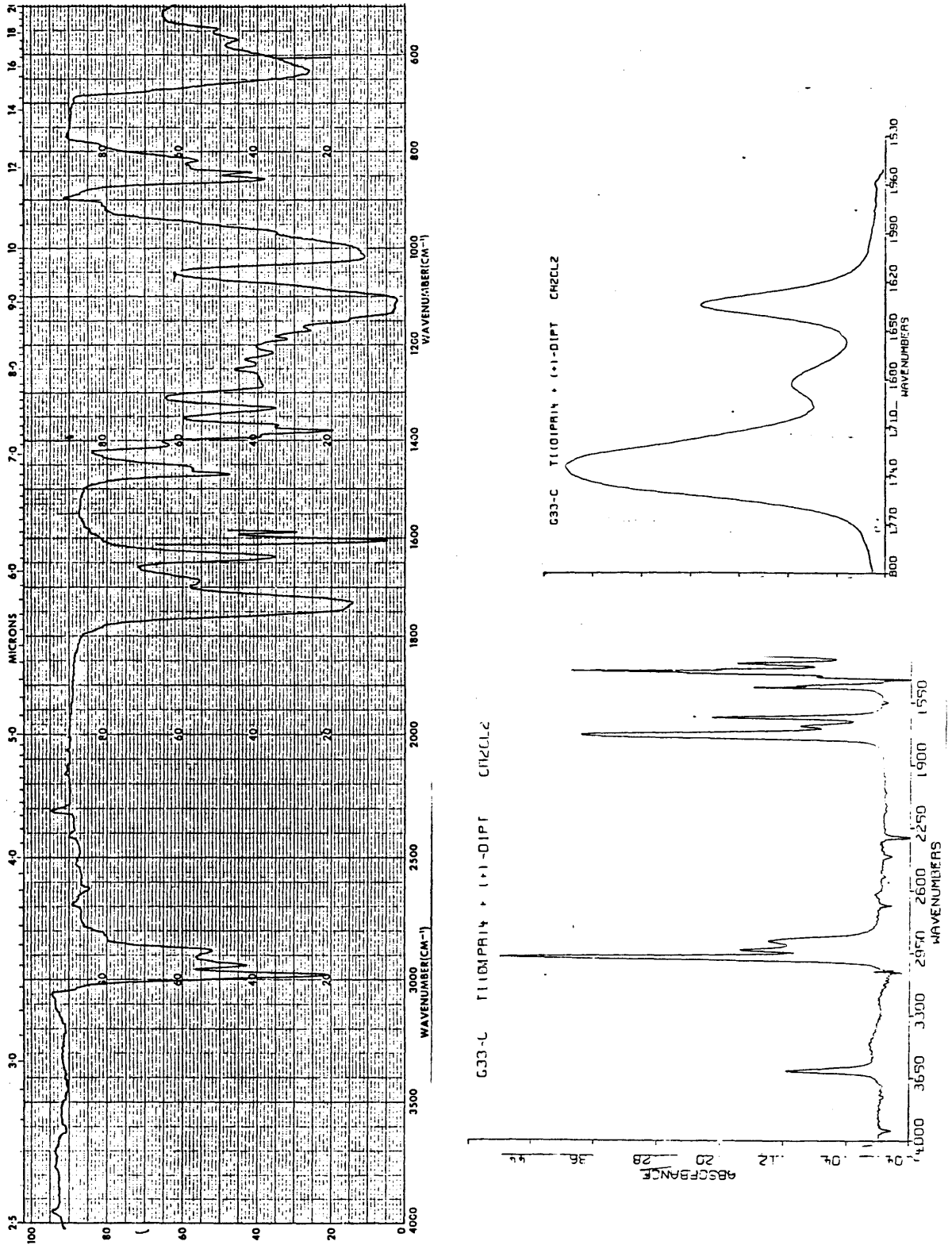

relative to that of the 1683 cm^{-1} stretch. Furthermore, we have found no complex of titanium tetraalkoxide and monobasic α-hydroxy ester in any Ti:ligand ratio that shows a band near 1640 cm^{-1}. Even $Ti(DIPT)Cl_2$, in spite of the increased Lewis acidity of the titanium center, shows a bound carbonyl stretch of 1660 cm^{-1}. Examples are shown below in Figure 38.

Both the 2:1 Ti:DIPT complex (spectrum 1) and 2:2 complex of $Ti(O\underline{i}Pr)_4$ with the tartrate analogue **15** (spectrum 4) show bands near 1635 cm^{-1}, accompanied by equally intense bands near 1680 cm^{-1}. The 2:2 complex of $Ti(O\underline{i}Pr)_4$ with the cyclohexyl-substituted tartrate analogue **16** (spectrum 5) lacks a significant 1635 cm^{-1} band. Asymmetric epoxidation using ligands **15** and **16** are discussed in section III.E.

Complexes of $Ti(O\underline{t}Bu)_4$ with both one and two equivalents of α-hydroxy ester ligand **17** (spectra 6 and 7) show bound C=O stretching at 1670 cm^{-1} only. Replacing one isopropoxide group of $Ti(DIPT)(O\underline{i}Pr)_2$ with ligand **17** eliminates the 1638 cm^{-1} band, replacing it with one at 1670 cm^{-1} (spectrum 8). In this case, we surmise that the bound ester group of tartrate is displaced from the metal by the ester group of **17**, to allow **17** to form a five-membered ring chelate.

Note also that addition of the electron withdrawing ligand pentafluorophenol to $Ti(DIPT)(O\underline{i}Pr)_2$ also causes the 1638 cm^{-1} band to be suppressed in favor of one at 1670 cm^{-1} (spectra 9 and 10). As mentioned in the introduction, both the [$Ti(DIPT)Cl_2$] and [Ti/tartrate/electron-withdrawing additive] systems mediate epoxidation in the opposite enantiomeric sense to the normal Ti:tartrate reaction (see Appendix 1). The display of a strong 1640 cm^{-1} C=O stretch (relative to the band at 1680 cm^{-1}) in CH_2Cl_2 solution, then, appears to be exclusively a property of the 2:2 Ti:tartrate complex, as is epoxidation of the pro-2<u>S</u> face of prochiral allylic alcohols to high enantiomeric excess. Perhaps the 1640 cm^{-1} band is indicative of a structural unit necessary for effective 2<u>S</u> epoxidation. From this point of view, it is comforting to consider spectrum 11 in Fig. 38, which is of $Ti(DIPT)(O\underline{i}Pr)_2$ in isopropanol. The 1635 cm^{-1} band is still prominent, which bodes well for the applicability of the pseudo-first order kinetic results (in the presence of a large excess of isopropanol) to the epoxidation under standard conditions.

Pedersen has suggested that the "effective" structural component identified by 1640 cm^{-1} band could be the one found in **14**, in which the

Figure 38. IR in CH_2Cl_2.

(1) $Ti_2(DIPT)(O\underline{i}Pr)_6$

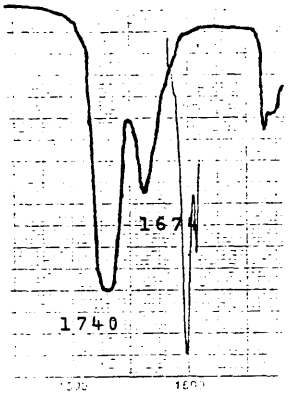

(2) $Ti(DIPT)_2$

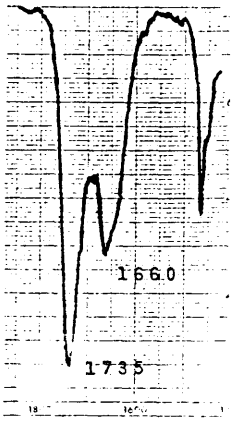

(3) $Ti(DIPT)Cl_2$

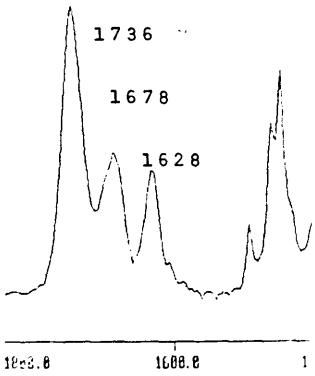

(4) $Ti(\underline{15})(O\underline{i}Pr)_2$

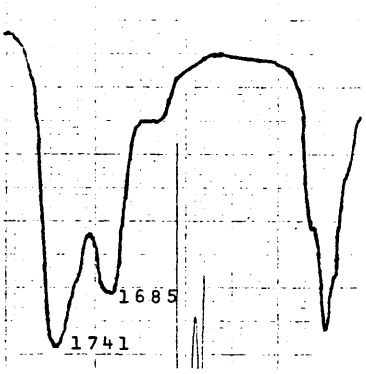

(5) $Ti(\underline{16})(O\underline{i}Pr)_2$

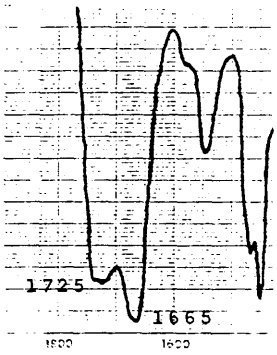

(6) $Ti(\underline{17})_2(O\underline{t}Bu)_2$

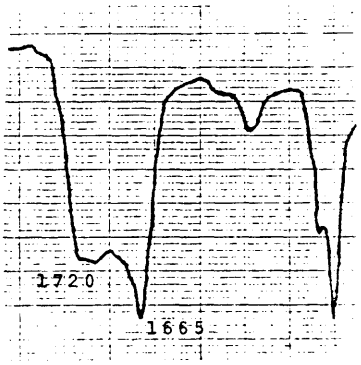

(7) $Ti(\underline{17})(O\underline{t}Bu)_3$

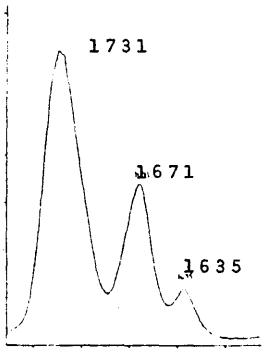

(8) $Ti(DIPT)(\underline{17})(O\underline{i}Pr)_2$

Figure 38, continued. IR in CH_2Cl_2.

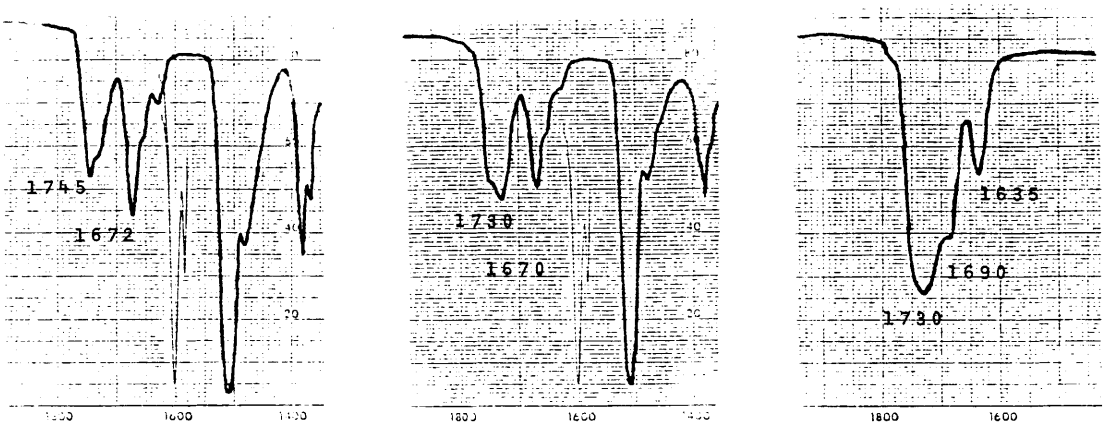

(9) Ti_2(DIPT)(O<u>i</u>Pr)$_6$ + 2 C_6F_5OH

(10) Ti(DIPT)(OiPr)$_2$ + C_6F_5OH

(11) Ti(DIPT)(OiPr)$_2$ <u>i</u>PrOH solvent

carbonyl oxygen and the terminal and bridging tartrate alkoxide oxygens adopt a facial arrangement about titanium, and that other configurations of bound carbonyl groups, such as are found in structures **13c**, **13d**, and **13e**, show C=O stretching bands in the 1680 cm^{-1} region. This would of course explain why no monofunctional α-hydroxy ester complex shows a 1640 cm^{-1} absorbance. It suggests, too, that Ti(tartrate)$_2$, Ti(tartrate)Cl_2, and Ti/DIPT/pentafluorophenol (Figure 38) adopt configurations of bound ester groups that do not match the facial arrangement of structure **14**.

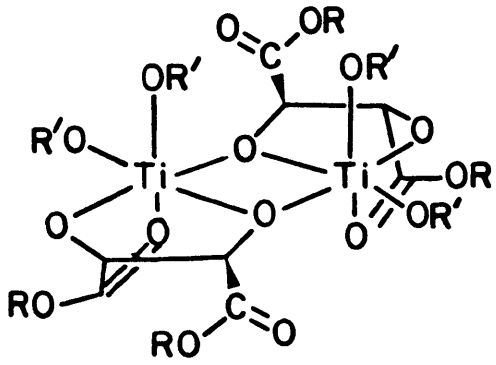

14

6. IR Spectroscopy in Other Solvents

Just as the solvent-dependent asymmetric induction (Table 15), pseudo-first order kinetic behavior, and molecular weight measurements all seem to

go hand-in-hand, IR spectra of titanium tartrates show a similar dependence on solvent. In particular, the pattern of C=O stretching bands of Ti(DIPT)(O$\underline{i}$Pr)$_2$ is similar for the two solvents that give high ee, the "normal" kinetic rate law, and dimeric species in solution - CH_2Cl_2 and ether. The C=O region in pentane and cyclopentane is different, with the 1638 cm^{-1} band diminished with respect to the 1680 cm^{-1} absorbance, as shown below in Figure 39.

Figure 39. IR spectra of Ti(DIPT)(O$\underline{i}$Pr)$_2$ in various solvents.

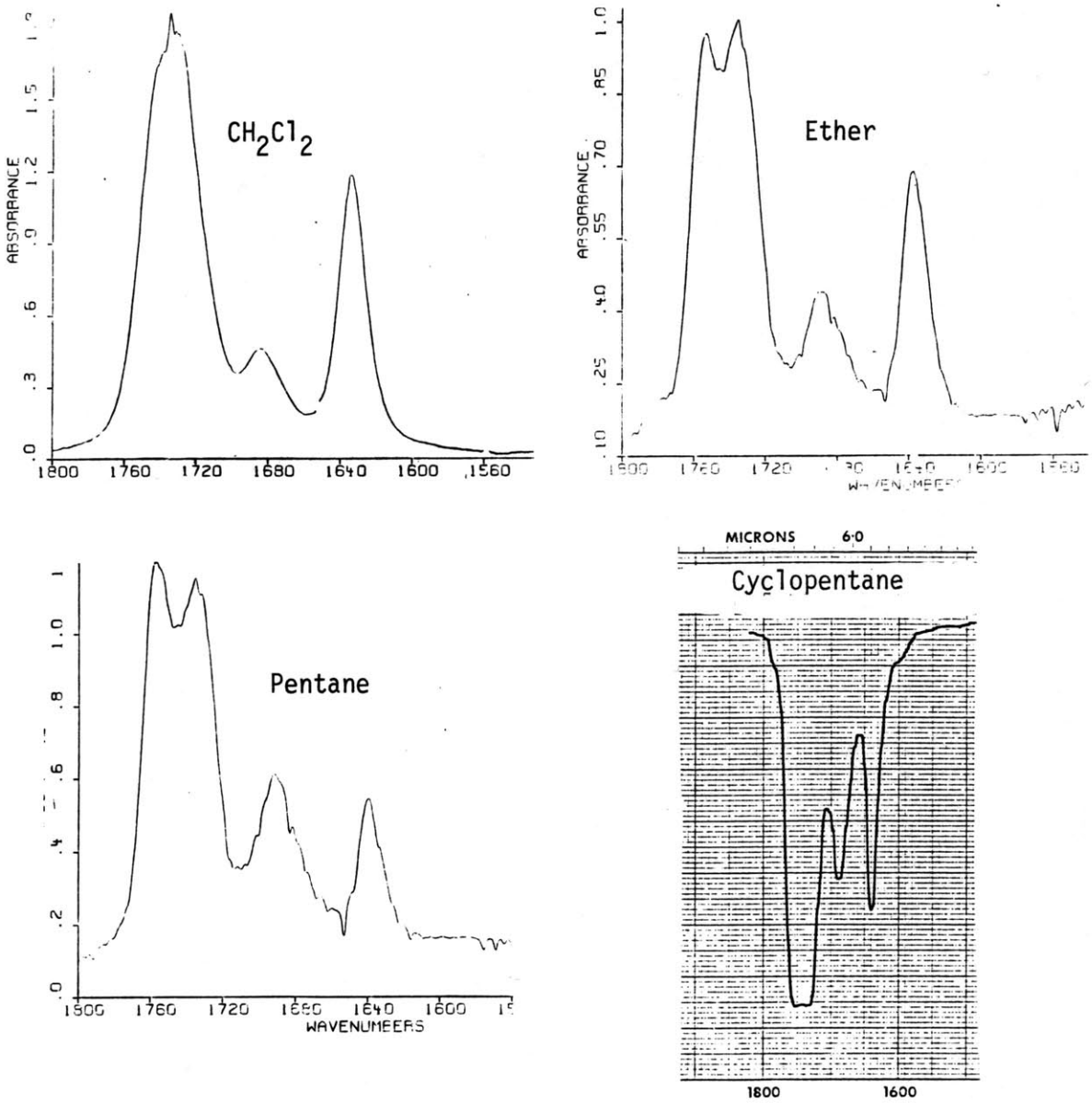

One can prepare Ti(DIPT)(O$\underline{i}$Pr)$_2$ in CH_2Cl_2, obtain spectrum 1 of Fig. 39, replace the solvent with pentane, obtain spectrum 3, and then regenerate spectrum 1 by evaporation and addition of CH_2Cl_2 again. The complex therefore does not decompose or undergo irreversible change in changing solvent.

We can offer no definite assignment for the two peaks in the free carbonyl range of spectra in ether and pentane. It may be that a second complex is represented (to go with the 1685 cm^{-1} band, perhaps), or that two conformations of free ester group are distinguished.

From the IR and NMR spectra, we have seen that there are at least two Ti-tartrate species present in solutions of Ti(tartrate)(OR)$_2$ in $CDCl_3$ and CH_2Cl_2. We assign the 1740 and 1640 cm^{-1} IR bands to the major component, and the 1680 (and probably an accompanying 1740) cm^{-1} band to the minor component. From the low temperature ^1H nmr, we see that the minor species comprises about 10-15% of the mixture. In pentane, Signer molecular weight measurements indicate the presence of significant amounts of trimeric material even at low concentrations. This is accompanied by a change in the IR and a decay in enantiomeric excess of epoxidation. An assignment of the 1691 cm^{-1} band in pentane to trimeric Ti-tartrate is therefore indicated. It still remains to assign a structure (or at least a stoichiometry) to the minor component in CH_2Cl_2 and $CDCl_3$. NMR spectra taken in different solvents proved to be very useful in this endeavor.

7. IR with Added Hydroperoxide

Addition of TBHP or trityl hydroperoxide to dilute CH_2Cl_2 solutions of Ti(DIPT)(O$\underline{i}$Pr)$_2$ produced changes in the C=O stretching region of the IR spectra as shown in Figure 40. The band at 1635 cm^{-1} diminishes and a new C=O band grows in at 1673 cm^{-1}, slightly different from that present before hydroperoxide addition (1676 cm^{-1}). An isosbestic point is found at 1645 cm^{-1} for TBHP addition and 1643 cm^{-1} for trityl hydroperoxide addition. The peak at 1604 cm^{-1} in the TBHP spectra is due to toluene from the TBHP solution; the one at 1596 in the trityl hydroperoxide experiment is from the phenyl groups of the hydroperoxide itself. The latter plot was taken from the same experiment in which the equilibrium constant for trityl hydroperoxide binding was determined, whereas the TBHP plot was not obtained in the equilibrium constant determination, but rather in a separate

Figure 40. Addition of hydroperoxides to Ti(DIPT)$(OiPr)_2$ in CH_2Cl_2.

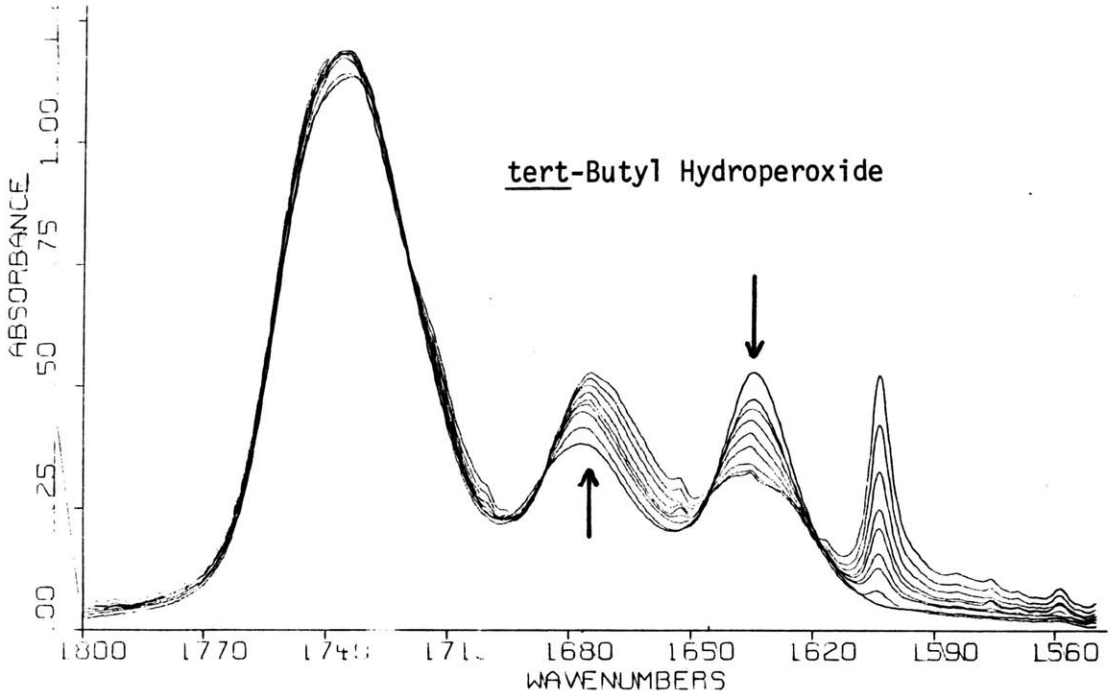

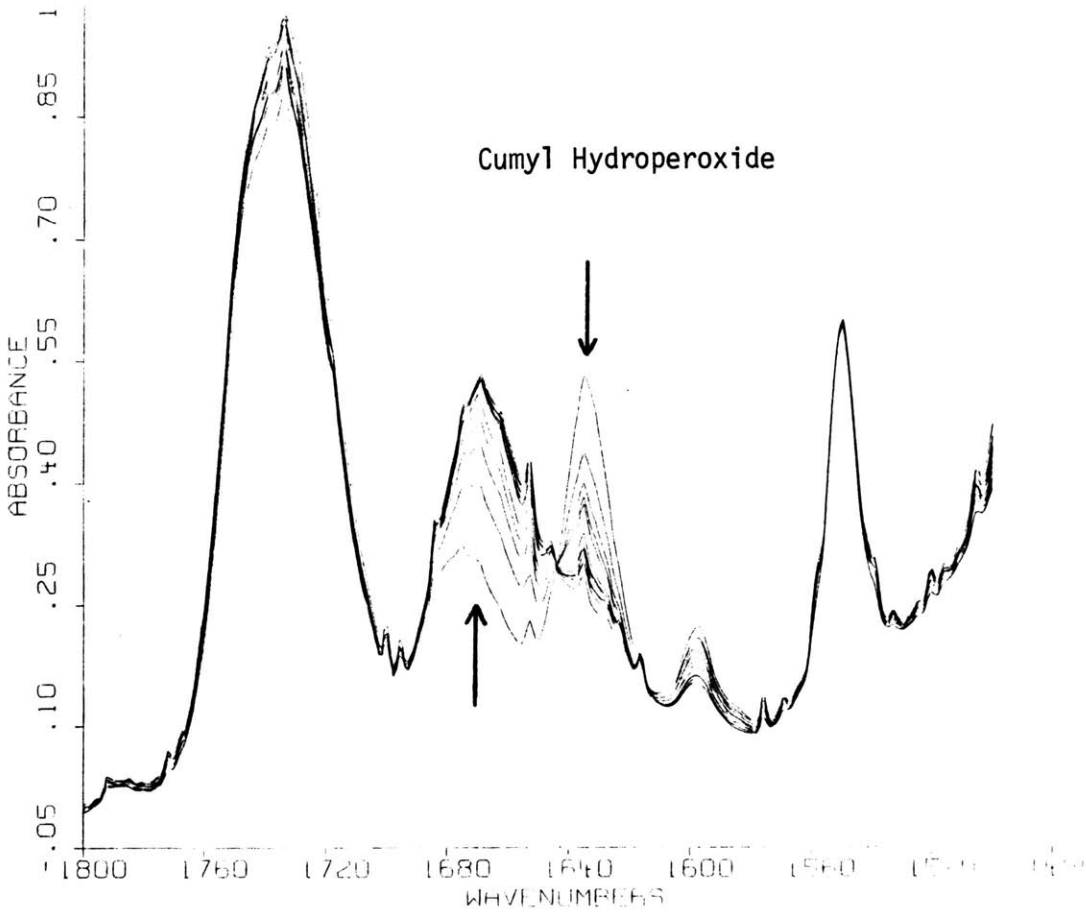

experiment. In neither case was more than one equivalent of hydroperoxide per titanium added, and, because of the small equilibrium binding constants, much less than one equivalent of hydroperoxide was actually bound. Still, the IR changes in the carbonyl region are pronounced.

Complexation of hydroperoxide clearly changes the manner of carbonyl binding, by changing either the structure of the complex or the strength of the carbonyl-titanium interaction within the same overall structure. NMR spectra of Ti-tartrate + hydroperoxide are uninformative, with broadened resonances in both ^{13}C and ^{1}H spectra. We would not expect simple monodentate coordination of hydroperoxide to effect such profound changes in the IR and nmr spectra, so we take these changes as possible evidence for bidentate interaction of bound alkylperoxide with titanium. Because we have been unable to isolate a relatively pure alkylperoxide complex of titanium-tartrate, we have no further information regarding the structure of this species. From the IR it is at least clear that one tartrate carbonyl remains bound to the metal, since the intensity of the free C=O stretch changes very little with added hydroperoxide.

8. NMR Spectroscopy in Other Solvents

a. CD_2Cl_2

In Figure 41 are ^{1}H and ^{13}C nmr spectra of an equimolar mixture of $Ti(DIPT)_2$ and $Ti(O\underline{i}Pr)_4$ in CD_2Cl_2, approximately 1 M in Ti for the top spectrum and about 0.07 M for the middle. A list of assignments appears in Table 32.

Table 32. Peak assignments for NMR spectra of $Ti(DIPT)(O\underline{i}Pr)_2$ in CD_2Cl_2.

Sample[a]	Tartrate Methine	-CO2iPr methine	Ti-OiPr (intensity ratio)
1 M	5.13 (s)	5.06 (m)	4.72 (br m)
1 M decoupled	5.13 (s)	5.06 (br s)	4.76, 4.71 (ca. 1:2.7)
0.07 M	5.15 (s)	5.08 (br m)	4.70 (m)
0.07 M decoupled	5.15 (s)	5.08 (br s)	4.77, 4.71 (ca. 1:11)
$Ti(O\underline{i}Pr)_4$			4.46 (heptet)
1 M (^{13}C)[b]	86.20	69 (v br)	79.0, 76.6 (ca. 4:1)

a. "decoupled" indicates irradiation of upfield methyl signals

b. also C=O at 177.8, 172.5; methyls at 25.6, 21.9 ppm

Figure 41. ^{1}H and ^{13}C NMR of Ti(DIPT)(O$\underline{i}$Pr)$_2$ in CD_2Cl_2.
top = 1 M Ti, middle = 0.07 M Ti

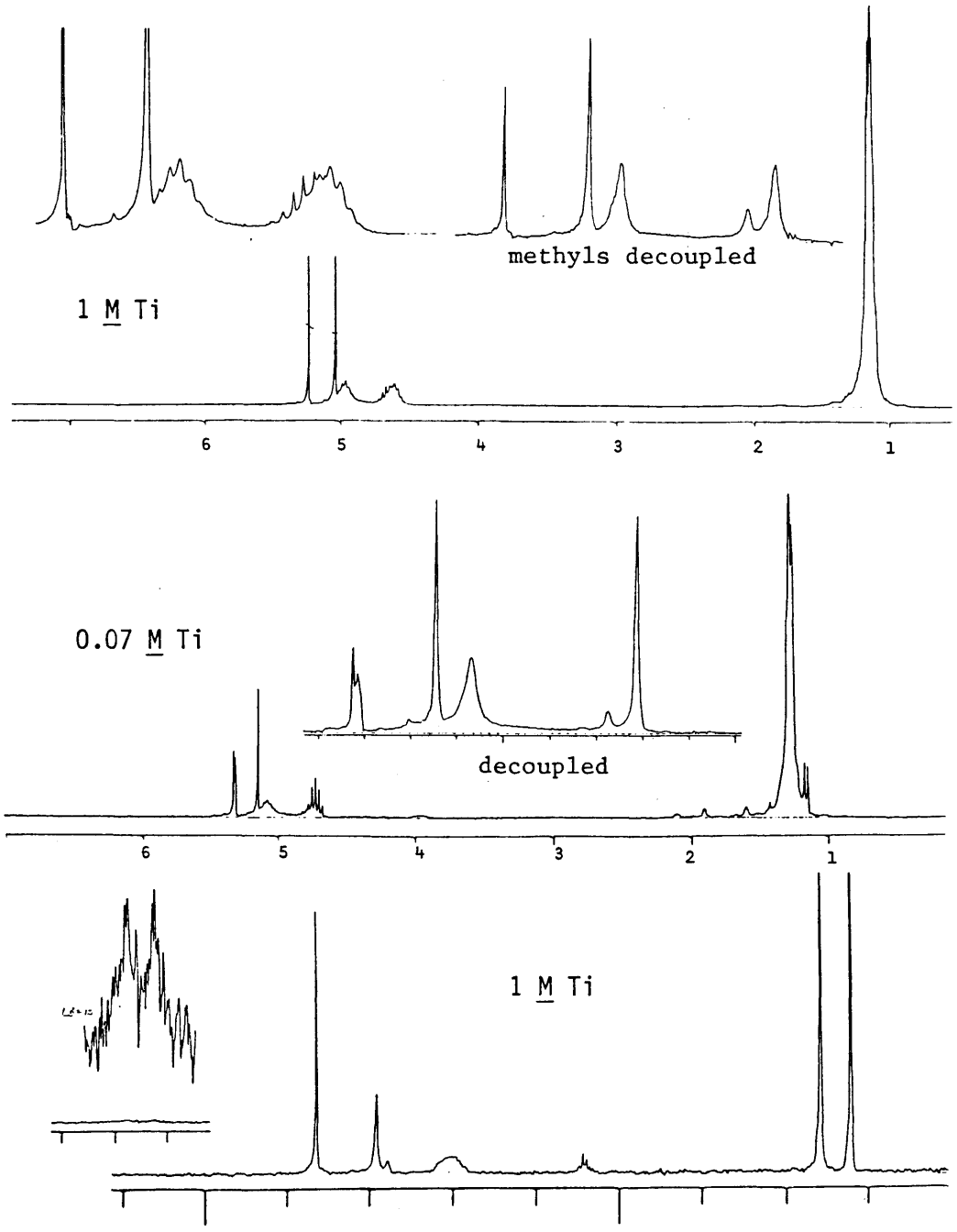

Note that both ^{1}H and ^{13}C spectra show two isopropoxide resonances; the more dilute the sample, the less of the minor component is present. We attempted (unsuccessfully) to verify the presence of another concentration-dependent species by measurements of optical rotation; see Appendix 3.

Careful variation of the amount of DIPT relative to $Ti(O\underline{i}Pr)_4$ allows us to assign the minor species as a 2:1 Ti:DIPT complex, $Ti_2(DIPT)(O\underline{i}Pr)_6$. Consider Figure 42, which presents the normal and decoupled spectra in CD_2Cl_2 for Ti:DIPT ratios of 2.0:1.95, 2.0:2.0, 2.0:2.1, and 2.0:2.4. The intensity of the resonance at 4.77 ppm varies inversely with the amount of tartrate present, indicating suppression of a 2:1 complex with added tartrate. We earlier proposed the presence of 2:1 Ti:tartrate as being responsible for the loss of enantioselectivity and rate in asymmetric epoxidation using exactly a 2:2 mixture. Figure 42 thus confirms the supposition that excess tartrate reduces the formation of less selective epoxidation catalysts in the reaction mixture.

Of course, it is easy to prepare the 2:1 complex itself and see whether its nmr resonances match those of the minor component of the 2:2 spectra. Reproduced below in Figure 43 are proton and carbon nmr spectra in CD_2Cl_2 (approximately 0.5 M in Ti) and $CDCl_3$ (0.3 M in Ti); peak positions are tabulated in Table 33.

Note first that $Ti_2(DIPT)(O\underline{i}Pr)_6$ does indeed display a strong heptet at 4.77 ppm in CD_2Cl_2 and $CDCl_3$, matching the minor resonances of $Ti(DIPT)(O\underline{i}Pr)_2$ in these solvents.

Secondly, the 2:1 mixture of $Ti(O\underline{i}Pr)_4$:DIPT displays its own family of component structures - the 2:1 complex itself, and minor amounts of the disproportionation products $Ti(O\underline{i}Pr)_4$ and $Ti(DIPT)(O\underline{i}Pr)_2$. Recall that only one of the disproportionation products of $Ti(DIPT)(O\underline{i}Pr)_2$ could be observed in the nmr (no distinct resonance for complexes like $Ti_2(DIPT)_3(OR)_2$ or $Ti_2(DIPT)_4$ could be found). In contrast, both products of $Ti_2(DIPT)(O\underline{i}Pr)_6$ disproportionation are observed, most clearly in the ^{13}C nmr spectra. See Table 33 for peak assignments.

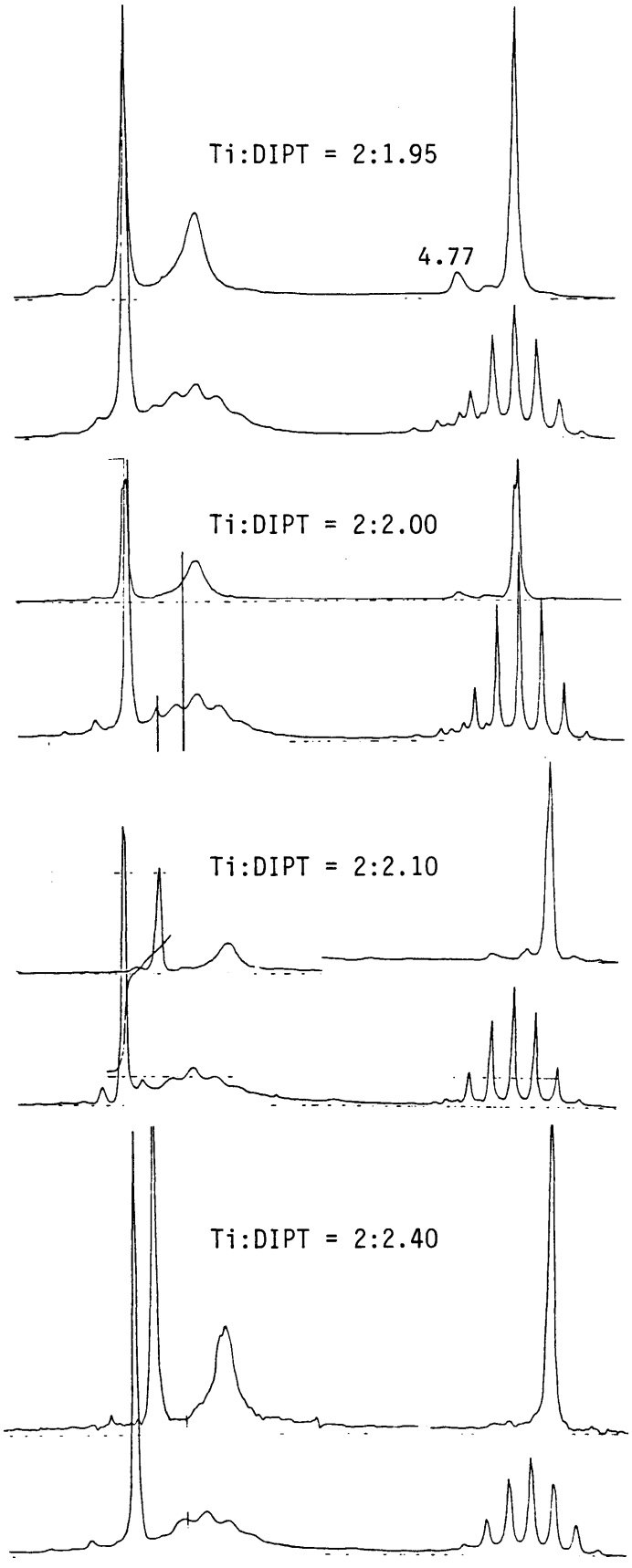

Figure 42.

^{1}H NMR of Ti(O$\underline{i}$Pr)$_4$:DIPT mixtures in CD_2Cl_2.

Normal and methyl-decoupled spectra appear for each sample.

5.5-4.5 ppm displayed

Figure 43. ^{1}H and ^{13}C NMR of $Ti_2(DIPT)(O\underline{i}Pr)_6$ in CD_2Cl_2 and $CDCl_3$.

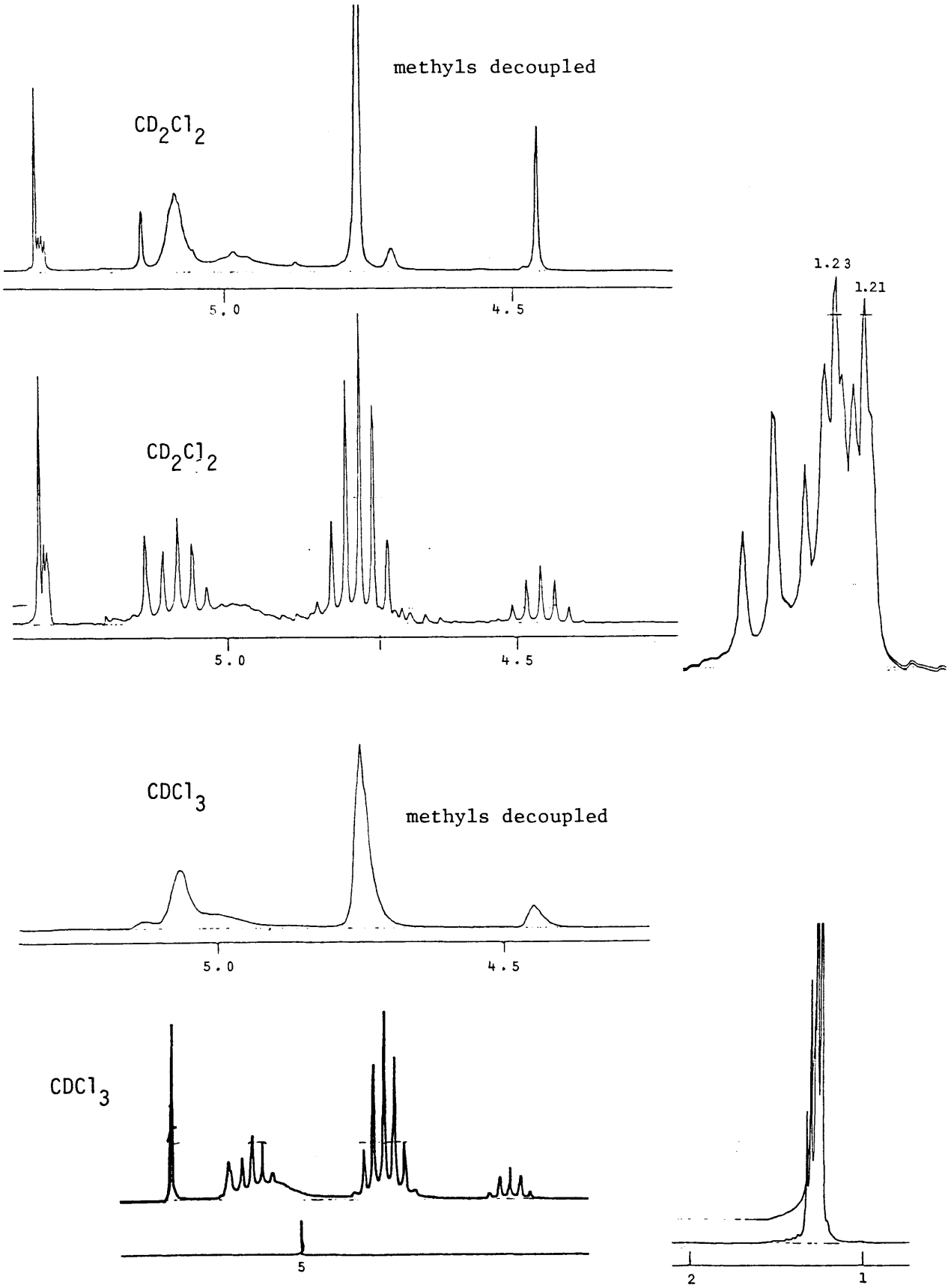

Figure 43, continued.

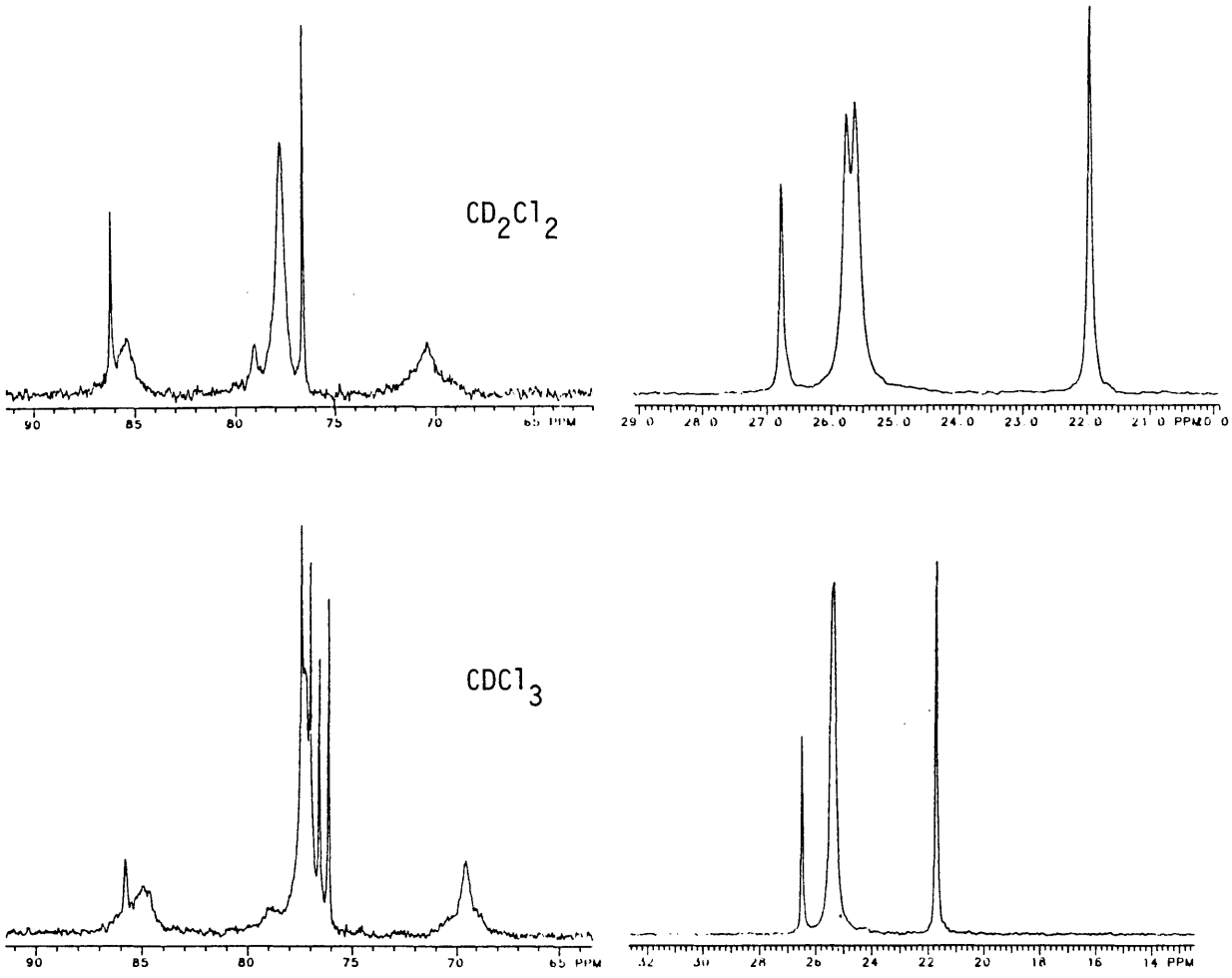

Table 33. Peak assignments for NMR spectra of 2:1 $Ti(O\underline{i}Pr)_4$:DIPT in CD_2Cl_2 and $CDCl_3$.

Nucleus[a]	Solvent	Peak position	Assignment and Notes
^1H	CD_2Cl_2	5.14 (s)	Tartrate methine
		5.09 (m)	$-CO_2\underline{i}Pr$ methine
		5.0 (broad)	$-CO_2\underline{i}Pr$ methine of 2:2 complex?
		4.77 (heptet)	$Ti-O\underline{i}Pr$ methine of 2:1 complex
		4.46 (heptet)	$Ti-O\underline{i}Pr$ methine of $Ti(O\underline{i}Pr)_4$
			Relative intensity of 4.77 to 4.46 = 5.8:1
^1H - d	CD_2Cl_2	5.14	Tartrate methine
		5.09 (br)	$-CO_2\underline{i}Pr$ methine
		4.98 (br)	
		4.77	$Ti-O\underline{i}Pr$ methine, 2:1 complex
		4.71	$Ti-O\underline{i}Pr$ methine, 2:2 complex
		4.46	$Ti-O\underline{i}Pr$ methine, $Ti(O\underline{i}Pr)_4$
^1H	$CDCl_3$	5.10 (br s)	Tartrate methine
		5.06 (m)	$-CO_2\underline{i}Pr$ methine
		5.03 (br)	$-CO_2\underline{i}Pr$ methine, 2:2 complex?
		4.75 (heptet)	$Ti-O\underline{i}Pr$ methine, 2:1 complex
		4.44 (m)	$Ti-O\underline{i}Pr$ methine, $Ti(O\underline{i}Pr)_4$
			Relative intensity of 4.75 to 4.44 = 7.8:1
^{13}C	CD_2Cl_2	ca. 176.5	C=O
		86.1 (sh)	Tartrate methine of 2:2 complex (Table 32)
		85.4 (br)	Tartrate methine of 2:1 complex
		79.0 (small)	$Ti-O\underline{i}Pr$ methine of 2:2 complex (Table 32)
		77.7 (br)	$Ti-O\underline{i}Pr$ methine of 2:1 complex
		76.6 (sh)	$Ti-O\underline{i}Pr$ methine of $Ti(O\underline{i}Pr)_4$
		70.4 (br)	$-CO_2\underline{i}Pr$ methine of 2:1 and 2:2
		26.8	$Ti-O\underline{i}Pr$ methyl of $Ti(O\underline{i}Pr)_4$
		25.7, 25.6	$Ti-O\underline{i}Pr$ methyl of 2:1 and 2:2
		21.9	$-CO_2\underline{i}Pr$ methyl
^{13}C	$CDCl_3$	176	C=O
		85.7 (sh)	Tartrate methine of 2:2 complex (Table 22)
		84.9 (br)	Tartrate methine of 2:1 complex
		77.3 (br)	$Ti-O\underline{i}Pr$ methine of 2:1 complex
		76.1 (sh)	$Ti-O\underline{i}Pr$ methine of $Ti(O\underline{i}Pr)_4$ (Table 22)
		69.6 (br)	$-CO_2\underline{i}Pr$ methine of 2:1 and 2:2
		26.4	$Ti-O\underline{i}Pr$ methyl of $Ti(O\underline{i}Pr)_4$ (Table 22)
		25.4	$Ti-O\underline{i}Pr$ methyl of 2:1 and 2:2
		21.7	$-CO_2\underline{i}Pr$ methyl

a. "d" indicates irradiation of upfield methyl signals

Unfortunately, the ^{13}C nmr spectrum of a 2:1 mixture of $Ti(O\underline{t}Bu)_4$ and DMT in $CDCl_3$ (Figure 44, below) does not match the minor peaks of $Ti(DMT)(O\underline{t}Bu)_2$ (Figure 35). Table 34 lists the resonances for each spectrum. The minor component of the $Ti(DMT)(O\underline{t}Bu)_2$ solution therefore remains unidentified.

Figure 44. ^{13}C NMR of $Ti_2(DMT)(O\underline{t}Bu)_6$ in $CDCl_3$; carbonyl peaks not shown.

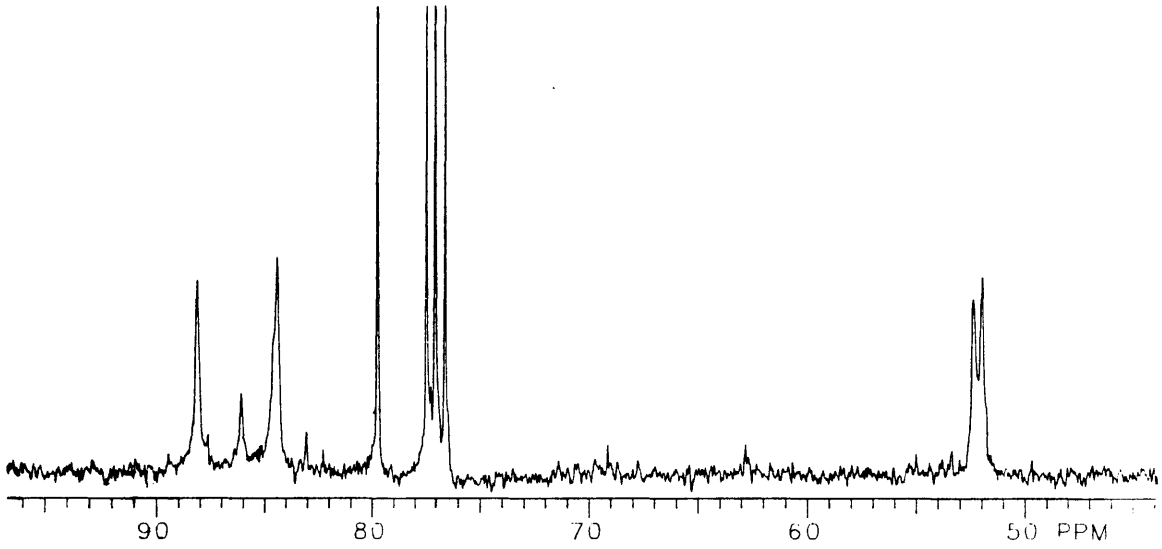

Table 34. ^{13}C NMR of $Ti(DMT)(O\underline{t}Bu)_2$ and $Ti_2(DMT)(O\underline{t}Bu)_6$ in $CDCl_3$. Both samples are free of $\underline{t}$BuOH.

Sample	Tartrate Methine Peaks	Methyl Ester	Ti-OtBu
$Ti(DMT)(O\underline{t}Bu)_2$[a]	87.7 (major)	52.1 (flux[b])	31.8 (quat)
	83.8 (major)	51.6 (flux[b])	31.0 (flux[b])
	85.6 (minor)		30.8 (flux[b])
	84.1 (minor)		
$Ti_2(DMT)(O\underline{t}Bu)_6$	88.1 (major)	52.3	32.2 (major)
	84.4 (major)	51.9	31.4 (minor)
	79.7 (sharp)		
	86.1, 83.8 (both minor)		

a. 273°K b. "flux" refers to bands that coalesce on warming

Finally, note in Figure 45 the same evidence in CD_2Cl_2 for preferential exchange of free isopropanol with one of the two bound isopropoxides of $Ti(DIPT)(O\underline{i}Pr)_2$ as was observed in $CDCl_3$ (Figure 23). Again, decoupling

of the upfield methyl signals reveals one sharpened and one broadened Ti-O<u>i</u>Pr methine signal.

Figure 45. ^{1}H NMR of Ti(O<u>i</u>Pr)$_4$ + DIPT in CD_2Cl_2, 0.2 <u>M</u> Ti

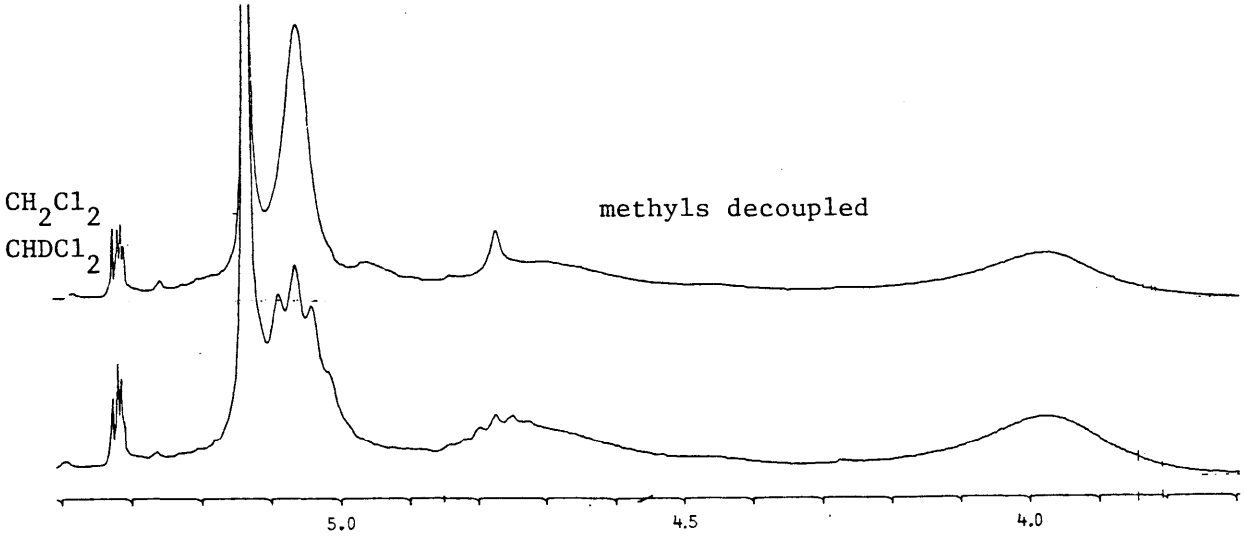

b. Benzene-d_6

The ^{1}H nmr spectrum of Ti(DIPT)(O<u>i</u>Pr)$_2$ in C_6D_6 is presented in Figure 46; peak assignments for this and related spectra in C_6D_6 are in Table 35. Note the resolution of methyl peaks: doublets for free and bound isopropyl

Figure 46. ^{1}H NMR of Ti(DIPT)(O<u>i</u>Pr)$_2$ in C_6D_6.

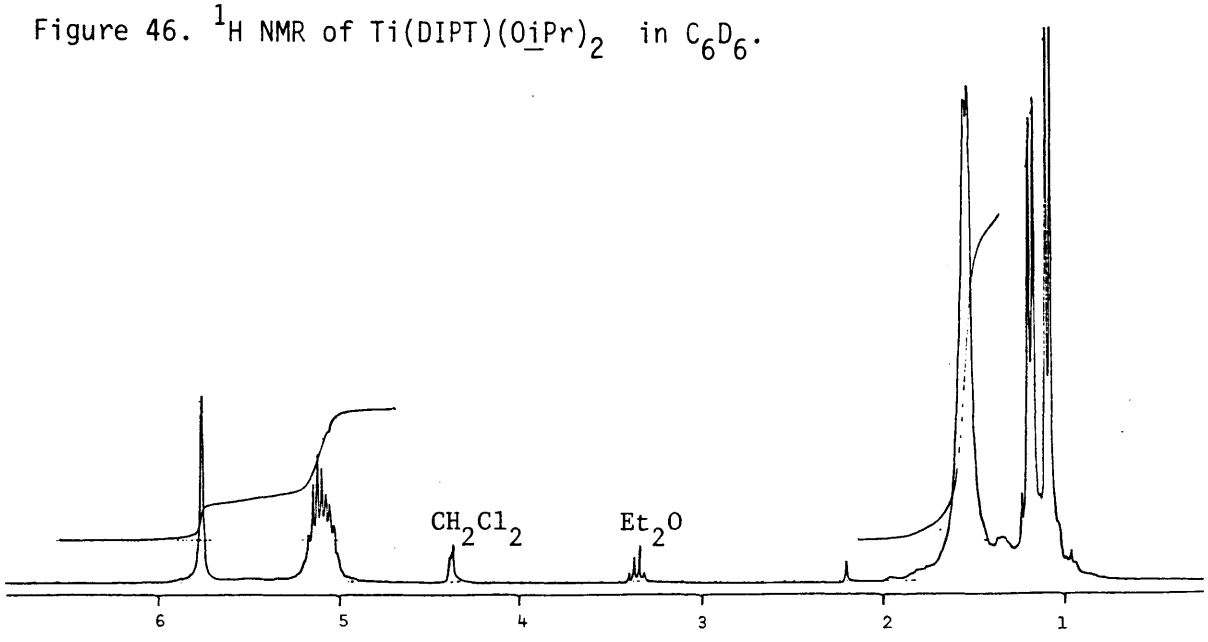

Table 35. Peak assignments for the ^1H NMR spectra in C_6D_6.

Sample	Peak Position	Assignment
Ti(DIPT)(O<u>i</u>Pr)$_2$	5.67 (s)	Tartrate methine
	5.07 (m)	-CO$_2$<u>i</u>Pr and Ti-O<u>i</u>Pr methines
	1.65 (br d)	Ti-O<u>i</u>Pr methyl
	1.10 (d, J = 7 Hz)	-CO$_2$<u>i</u>Pr methyl, bound carbonyl
	0.99 (d, J = 7 Hz)	-CO$_2$<u>i</u>Pr methyl, free carbonyl
Ti(O<u>i</u>Pr)$_4$	4.50 (heptet)	Ti-O<u>i</u>Pr methine
	1.23 (d, J = 7 Hz)	Ti-O<u>i</u>Pr methyl
DIPT	4.98 (heptet)	-CO$_2$<u>i</u>Pr methine
	4.52 (d)	Tartrate methine
	3.67 (d)	-OH
	1.00 (d, J = 6.1)	-CO$_2$<u>i</u>Pr methyl
	0.93 (d, J = 6.1)	-CO$_2$<u>i</u>Pr methyl
Isopropanol	3.91 (m)	HO<u>i</u>Pr methine
	1.13 (d)	HO<u>i</u>Pr methyl

ester groups are separated from each other and from the Ti-O<u>i</u>Pr methyl resonances. However, the methine protons of the ester and isopropoxide groups are lumped together in the multiplet at 5.07 ppm.

Another example of the increased nmr resolution in C_6D_6 is provided by Figure 47 and its associated Table 36. The spectrum of an equimolar mixture of Ti(O<u>t</u>Bu)$_4$ and DIPT, clean in $CDCl_3$, fairly teems with small peaks clustered about the major downfield resonances. We have not identified these minor bands, but our analysis of Ti(DIPT)(O<u>i</u>Pr)$_2$ spectra in $CDCl_3$ and CD_2Cl_2 would lead us to suspect the presence of 2:1 and 1:2 Ti:tartrate species in small amounts. The spectrum of a mixture of Ti(O<u>t</u>Bu)$_4$ and dineopentyl tartrate (DNePT) looks much worse but really is not, in terms of the relative intensities of major and minor resonances. Ti(DNePT)(O<u>t</u>Bu)$_2$ is probably quite sterically crowded, and we suggest that rotation about the ester C(O)-CH_2 and CH_2-<u>t</u>Bu bonds may be restricted. The strange appearance of ester methylene resonances at 3.8 ppm would then be a consequence of the presence of several neopentyl conformations, each with slightly different chemical shifts, and each with diastereotopic methylene protons.

More importantly, we do not know the origin of the prominent

Figure 47. ^{1}H NMR in C_6D_6.

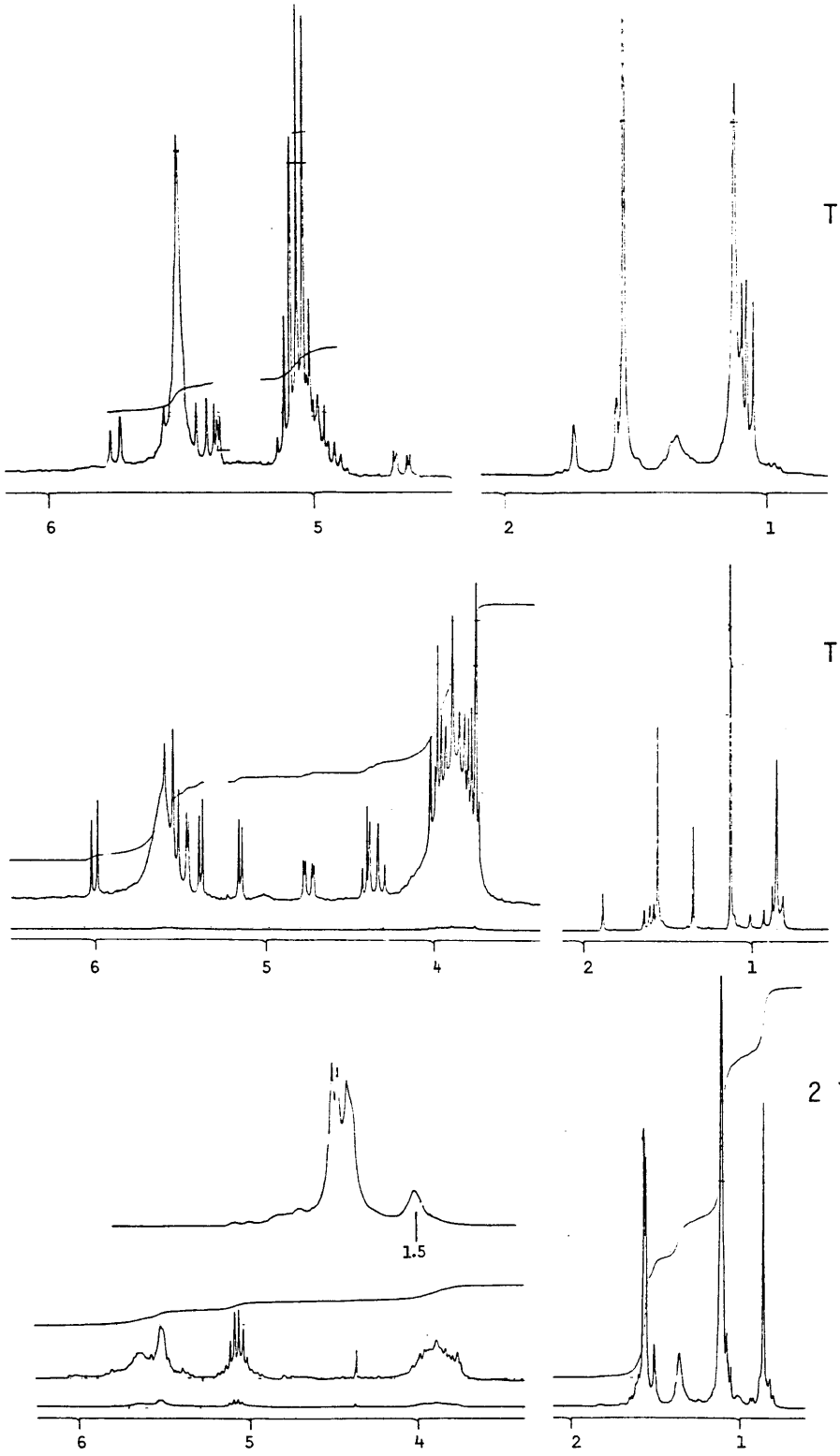

Table 36. Peak positions and assignments for $Ti(DIPT)(O\underline{t}Bu)_2$, $Ti(DNePT)(O\underline{t}Bu)_2$, $Ti_2(DIPT)(DNePT)(O\underline{t}Bu)_4$, and $Ti(O\underline{t}Bu)_4$ in C_6D_6.

Sample	Peak Position	Assignment
$Ti(DIPT)(O\underline{t}Bu)_2$	5.52 (br s)	Tartrate methine
	5.75 (d, J = 9.2 Hz)	Minor species
	5.39 (d, J = 9.2 Hz)	''
	5.37 (d, J = 6 Hz)	''
	5.56, 5.44	''
	4.67 (d), 4.62 (d)	''
	4.39 (s)	trace CH_2Cl_2
	5.06 (m)	$-CO_2\underline{i}Pr$ methine
	4.97 (m)	Minor species
	1.73 (s)	$\underline{t}BuO\underline{H}$ hydroxyl
	1.54 (s)	$Ti-O\underline{t}Bu$
	1.574, 1.567	Minor species
	1.35 (s)	$Ti-O\underline{t}Bu$, approximately 1/4 the intensity of 1.54 ppm peak
	1.11 (s)	$\underline{t}BuOH$ methyl
	1.10 (d, J = 6 Hz)	$-CO_2\underline{i}Pr$ methyl
	1.06 (d, J = 6 Hz)	$-CO_2\underline{i}Pr$ methyl
$Ti(DNePT)(O\underline{t}Bu)_2$	5.61 (br s)	Tartrate methine
	6.00 (d, J = 9.2 Hz)	Minor species
	5.54 (d)	''
	5.46 (d, J = 4 Hz)	''
	5.39 (d, J = 5 Hz)	''
	5.15 (d, J = 5 Hz)	''
	4.76 (d, J = 3 Hz)	''
	4.71 (d, J = 3 Hz)	''
	3.9-3.7 (br m)	$-CO_2CH_2\underline{t}Bu$ methylene
	4.44 (q, J = 12 Hz)	Minor species
	1.88 (s)	$\underline{t}BuO\underline{H}$ hydroxyl
	1.55 (s)	$Ti-O\underline{t}Bu$
	1.63, 1.60, 1.57	Minor species
	1.34 (s)	$Ti-O\underline{t}Bu$, approximately 1/3 the intensity of 1.55 ppm peak
	1.12 (s)	$\underline{t}BuOH$ methyl
	0.85 (s)	$-CO_2CH_2\underline{t}Bu$ methyl
	0.97, 0.92, 0.87, 0.81	Minor species
$Ti(O\underline{t}Bu)_4$	1.27	$Ti-O\underline{t}Bu$
$Ti_2(DIPT)(DNePT)(O\underline{t}Bu)_4$	(Major peaks only)	
	5.62 (v br s)	$Ti_2(DNePT)_2(O\underline{t}Bu)_4$ tartrate
	5.51 (br s)	$Ti_2(DIPT)_2(O\underline{t}Bu)_4$ tartrate
	5.06 (m)	$-CO_2\underline{i}Pr$ methine
	4.0-3.7 (br m)	$-CO_2CH_2\underline{t}Bu$ methylene
	1.568 (s)	$Ti_2(DNePT)(DIPT)(O\underline{t}Bu)_4$?
	1.562 (s)	$Ti_2(DNePT)_2(O\underline{t}Bu)_4$
	1.555 (s)	$Ti_2(DIPT)_2(O\underline{t}Bu)_4$
	1.50 (s)	$\underline{t}BuO\underline{H}$ hydroxyl
	1.10 (s)	$\underline{t}BuOH$ methyl
	1.08 (d)	$-CO_2\underline{i}Pr$ methyl
	1.05 (d)	$-CO_2\underline{i}Pr$ methyl
	0.85 (s)	$-CO_2CH_2\underline{t}Bu$ methyl

t-butoxide singlet at 1.35 ppm in the spectra of both complexes; it is not from $Ti(OtBu)_4$.

At the bottom of Figure 47 is the spectrum of an equimolar mixture of $Ti(DNePT)(OtBu)_2$ and $Ti(DIPT)(OtBu)_2$, each containing two equivalents of t-butanol. It is included because of the appearance of three major Ti-OtBu singlets around 1.56 ppm. The spectra of each reactant alone show only one major band in this region, so the appearance of a third may represent the mixed tartrate dimer, $Ti_2(DNePT)(DIPT)(OtBu)_4$. It is unlikely that DNePT and DIPT could participate in a transesterification reaction in the presence of only t-butoxide and t-butanol.

c. Toluene-d_8

Proton nmr spectra of $Ti(DIPT)(OiPr)_2$ in toluene-d_8 at several temperatures are reproduced in Figure 48; a ^{13}C nmr spectrum taken at room temperature is shown in Figure 49. Peak assignments for the room temperature spectra are in Table 37.

We do not find evidence for more than one Ti-tartrate species, but we do find remarkable resolution of methyl peaks in the low temperature proton spectra. Consider the nmr spectrum at 245°K at the bottom of Figure 48. The tartrate methine singlet has split to an AB quartet, in the same manner as in $CDCl_3$ and CD_2Cl_2. More striking is the observation of eight methyl doublets; irradiation of the methine signals at 5 ppm produces a clear eight-line pattern. This is consistent with separation of free and bound ester groups and axial and equatorial isopropoxides, each with methyl groups of nonequivalent chemical shift. The assignment of the multiplet at 4.93 to Ti-OiPr methine protons is made on the basis of its greater sensitivity to temperature than the multiplet at 5.02 ppm, and on the spectrum of $Ti(DIPT)(OtBu)_2$ presented below.

The variable temperature nmr spectra of $Ti(DIPT)(OtBu)_2$ and $Ti(DMT)(OtBu)_2$ comprise Figure 50. Again, these show predominantly one set of resonances; standard line broadening behavior characteristic of fluxional equilibration is observed with temperature. Note in particular the excellent differentiation of Ti-OtBu groups at 245°K. ^{13}C NMR spectra of these complexes are presented in Figure 51; peak assignments at room temperature in Table 38.

Figure 48. ^{1}H NMR of Ti(DIPT)(O$\underline{i}$Pr)$_2$ in toluene-d_8.

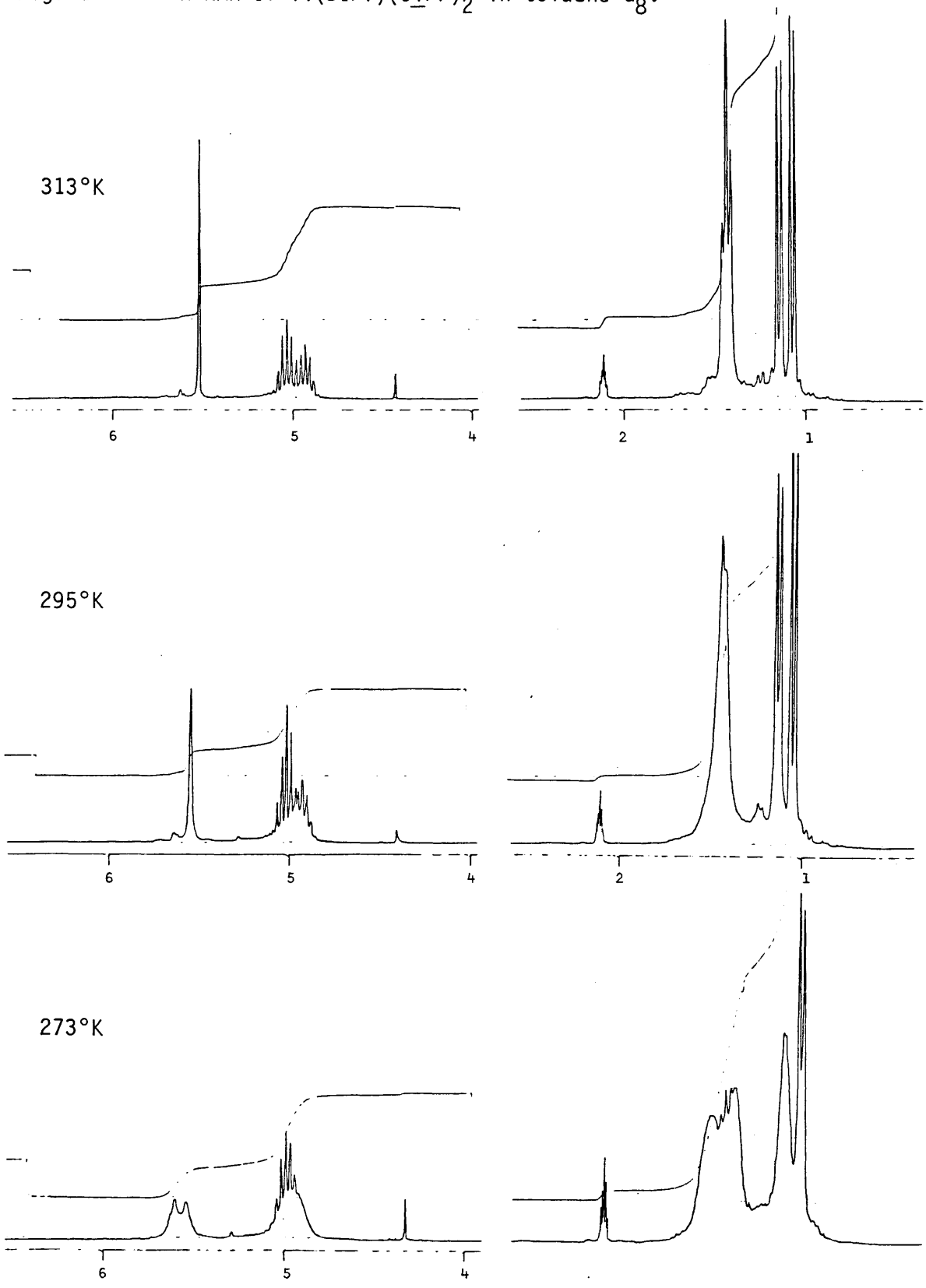

Figure 48, continued. ^{1}H NMR of Ti(DIPT)(O$\underline{i}$Pr)$_2$ in toluene-d_8.

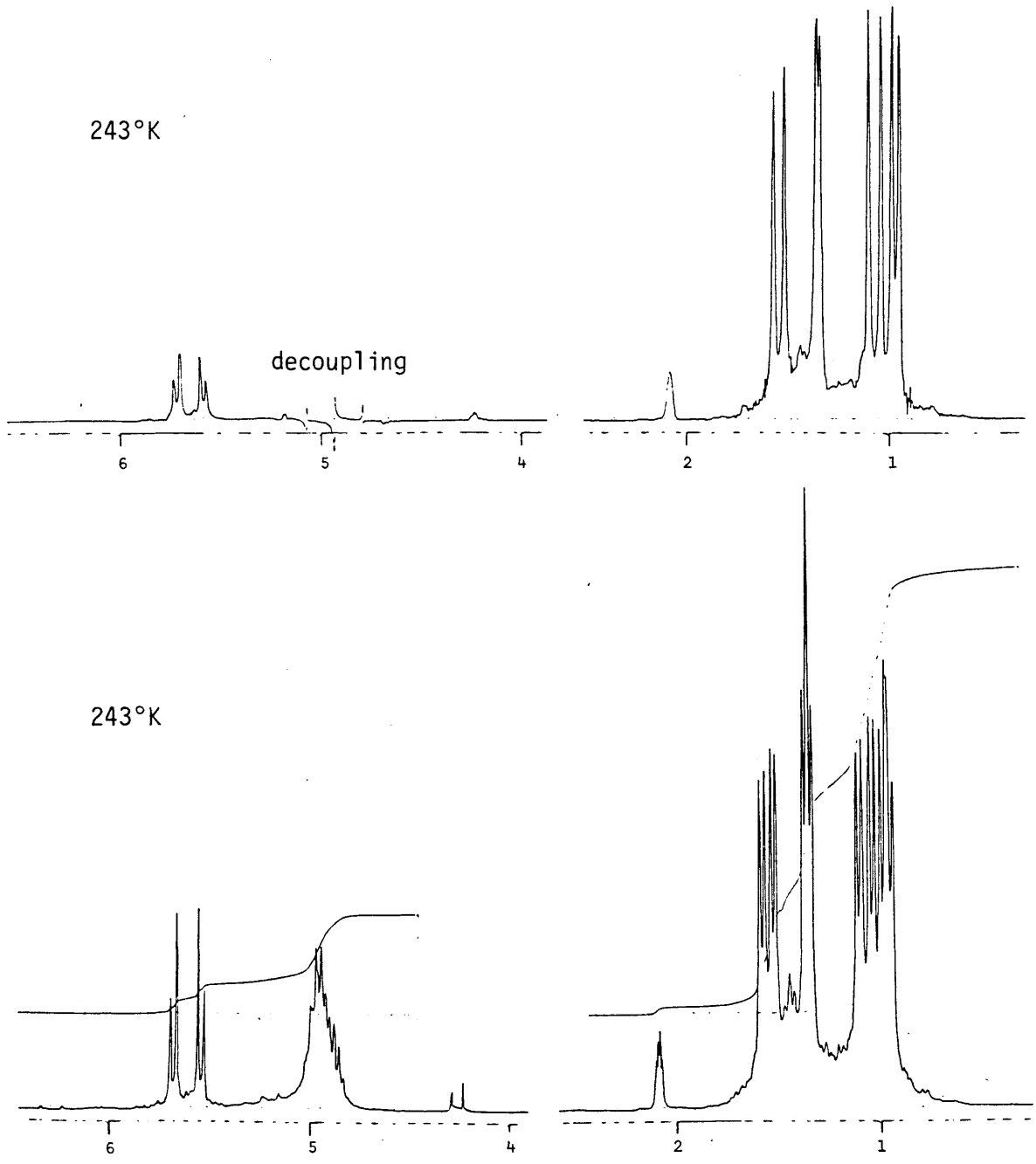

Figure 49. ^{13}C NMR of Ti(DIPT)(O$\underline{i}$Pr)$_2$ in toluene-d_8

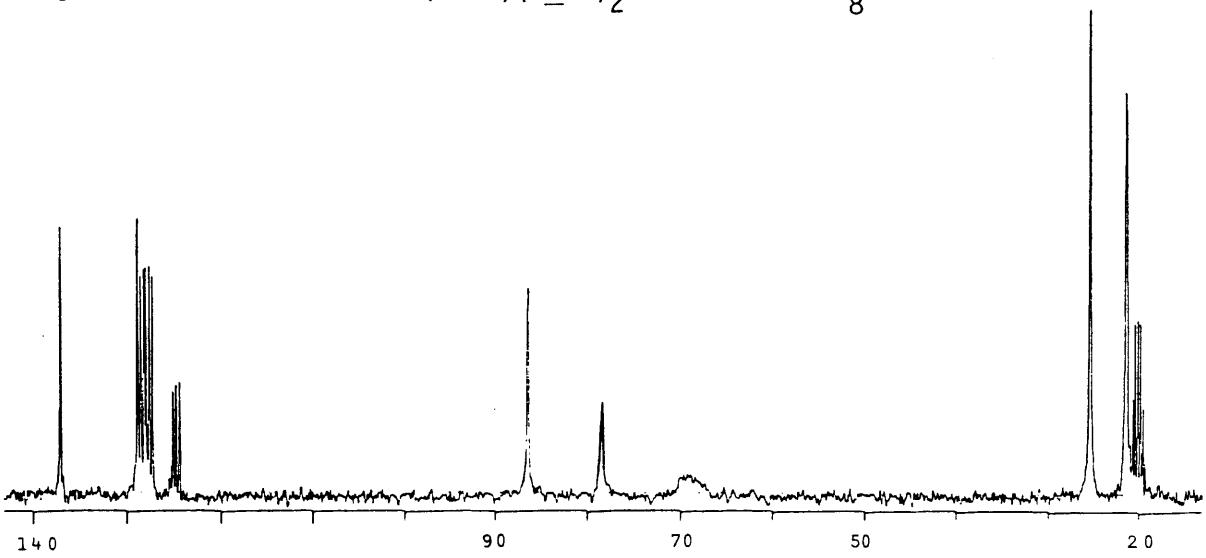

Table 37. Peak assignments for the ^1H and ^{13}C nmr spectra of Ti(DIPT)(O$\underline{i}$Pr)$_2$ in toluene-d_8 at 295°K.

^1H Peak	^{13}C Peak	Assignment
5.55 (s)	86.3	Tartrate methine
5.02 (m)	69 (br)	-CO$_2\underline{i}$Pr methine
4.93 (m)	78.3	Ti-O$\underline{i}$Pr methine
4.42 (s)		CH_2Cl_2
1.43 (br d)	25.2	Ti-O$\underline{i}$Pr methyl
1.13 (d, J = 7 Hz)	21.3	-CO$_2\underline{i}$Pr methyl (bound ester)
1.05 (d, J = 7 Hz)	21.2	-CO$_2\underline{i}$Pr methyl (free ester)

d. Cyclohexane-d_{12}

Because the kinetics, molecular weights, and IR spectra are different in pentane than in CH_2Cl_2 or $CDCl_3$, the ^1H and ^{13}C nmr spectra of Ti(DIPT)(O$\underline{i}$Pr)$_2$ were taken in the nonpolar solvent cyclohexane-d_{12}; they are shown in Figure 52. The ^1H spectrum is much like those taken in $CDCl_3$, except that the two different Ti-O$\underline{i}$Pr groups (axial and equatorial) appear to be partially resolved. Small additional peaks in both proton and ^{13}C spectra suggest the presence of a minor species in solution. See Table 39 for peak assignments.

Figure 50. ^{1}H NMR of Ti(DIPT)(O$\underline{t}$Bu)$_2$ in toluene-d_8.

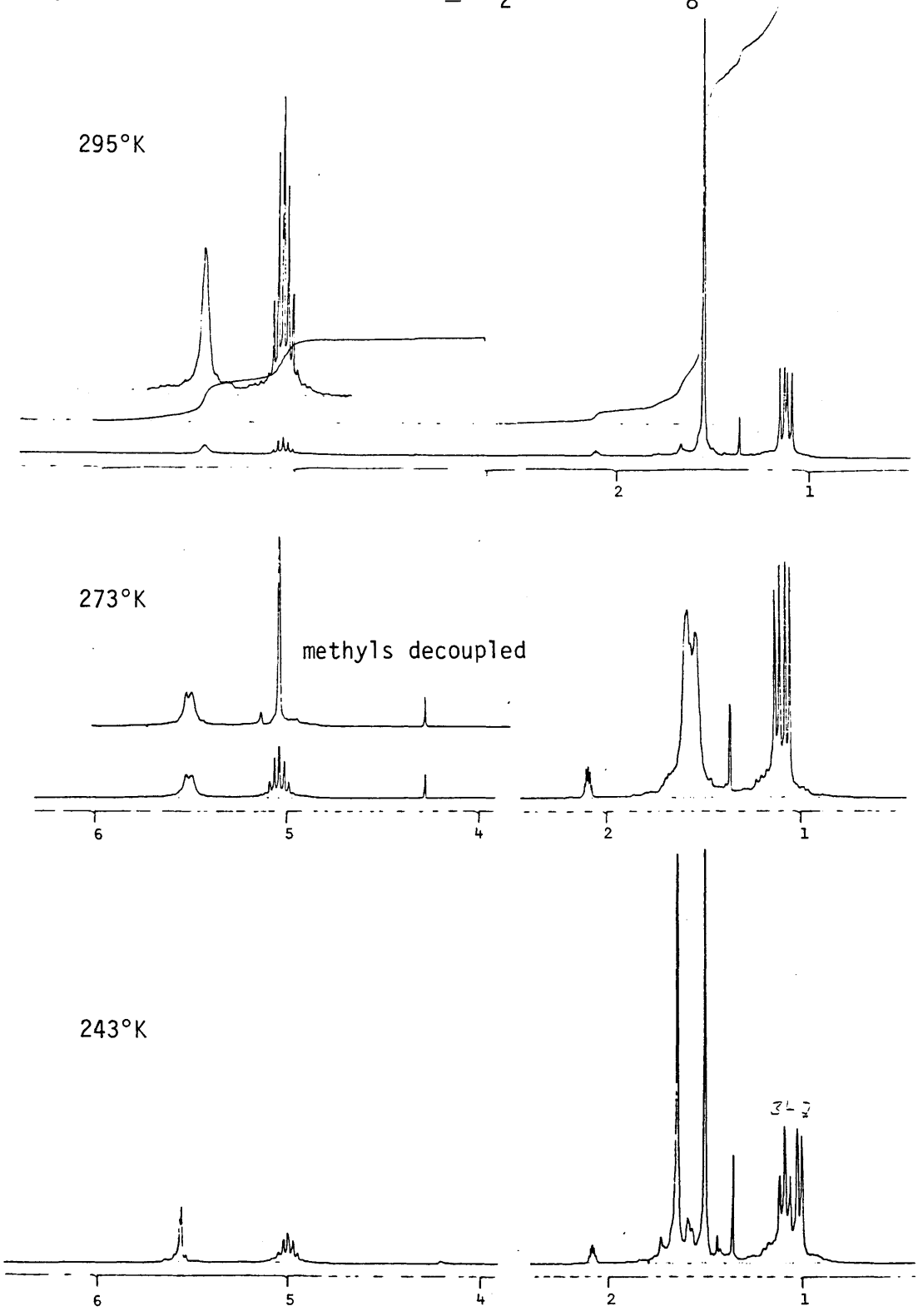

Figure 50. ^{1}H NMR of Ti(DMT)(O$\underline{t}$Bu)$_2$ in toluene-d_8.

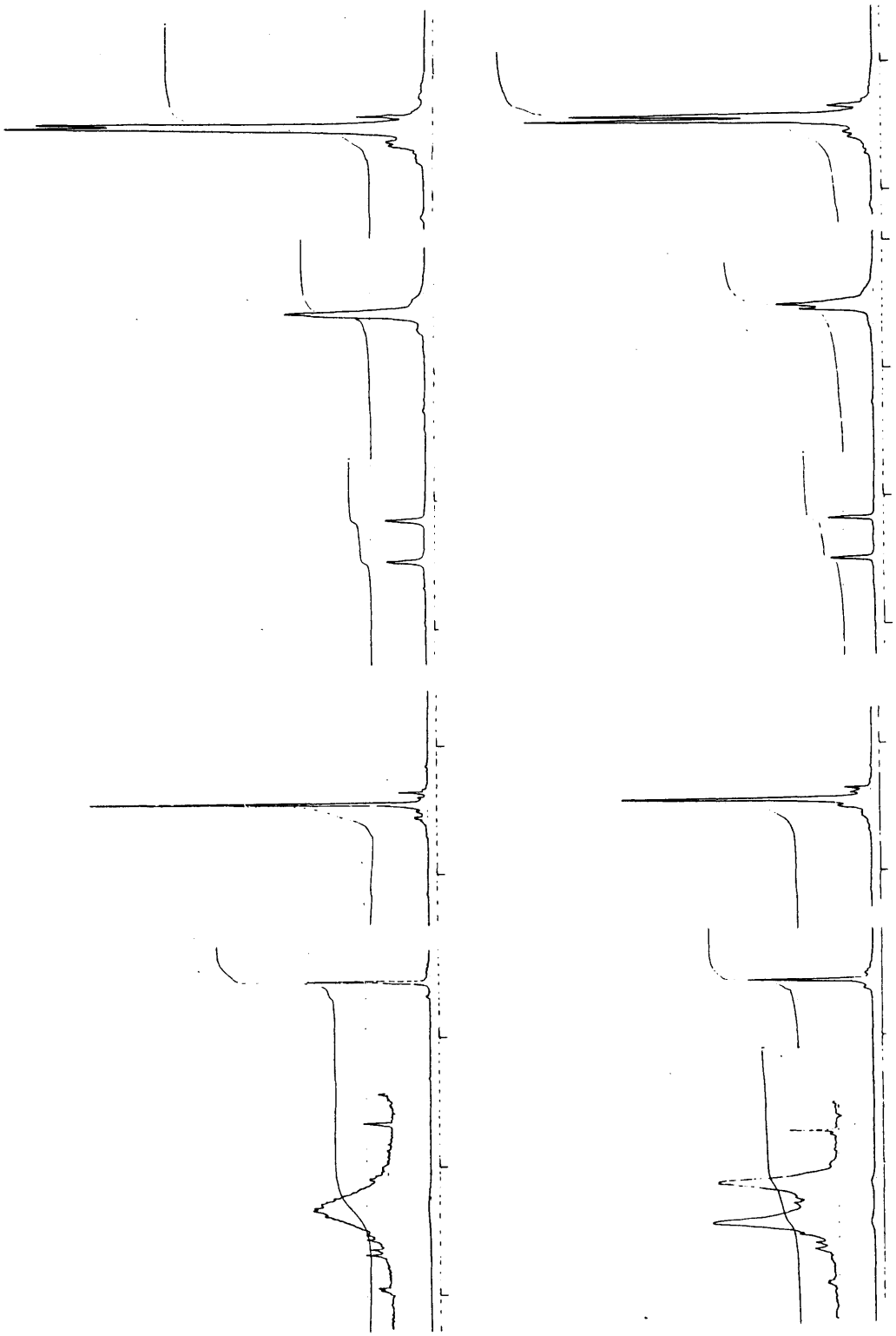

Figure 51. ^{13}C NMR of Ti(DIPT)(O$\underline{t}$Bu)$_2$ and Ti(DMT)(O$\underline{t}$Bu)$_2$ in toluene-d_8.

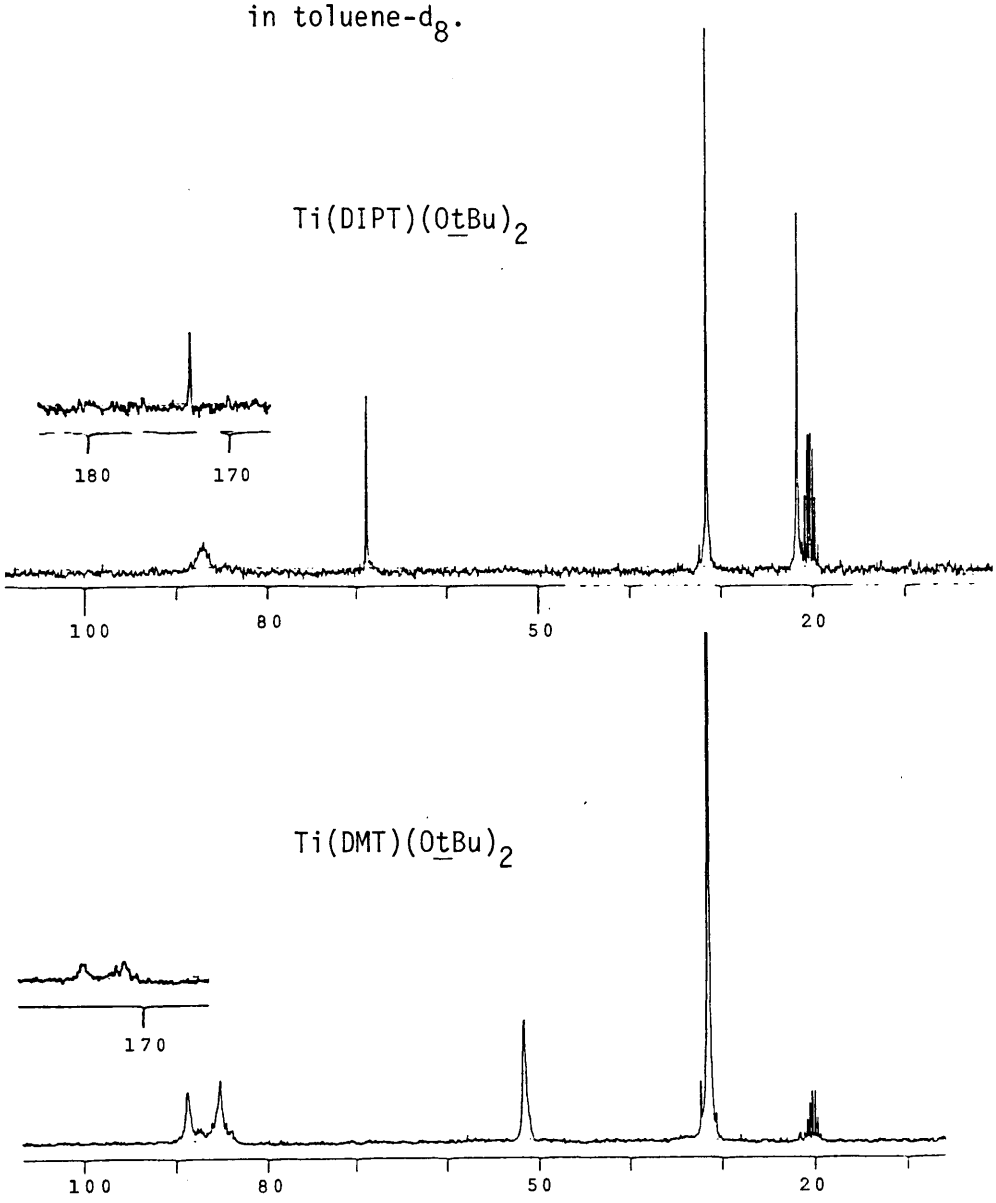

Table 38. Peak assignments for ^{1}H and ^{13}C nmr spectra of Ti(DIPT)(O$\underline{t}$Bu)$_2$ and Ti(DMT)(O$\underline{t}$Bu)$_2$ in toluene-d_8 at 295°K.

Complex	^{1}H Peak	^{13}C Peak	Assignment
Ti(DIPT)(O$\underline{t}$Bu)$_2$		172.6	C=O
	5.44 (br s)	87 (br)	Tartrate methine
	5.03 (heptet)	68.7	-CO$_2\underline{i}$Pr methine
	1.52 (s)	31.5	Ti-O$\underline{t}$Bu
	1.12 (d, J = 7 Hz)	21.6	-CO$_2\underline{i}$Pr methyl (bound)
	1.08 (d, J = 7 Hz)	21.6	-CO$_2\underline{i}$Pr methyl (free)
Ti(DMT)(O$\underline{t}$Bu)$_2$		174.2, 171.3	C=O
	5.48 (br s)	88.7	Tartrate methine
	5.15 (br s)	85.3	Tartrate methine
	4.42 (s)	51.5	-CO$_2$CH$_3$
	1.44 (s)	31.4	Ti-O$\underline{t}$Bu

Table 39. Peak assignments for ^{1}H and ^{13}C nmr spectra of Ti(DIPT)(O$\underline{i}$Pr)$_2$ in cyclohexane-d_{12} at 295°K.

^{1}H Peak	^{13}C Peak	Assignment
	174.6 (br)	C=O
5.23 (br s)	87.0	Tartrate methine
5.33, 5.29	78.1 (shoulder)	Minor species?
5.18 (m)	69.3 (br)	-CO$_2\underline{i}$Pr methine
4.90 (m)	79.0 (br)	Ti-O$\underline{i}$Pr methine
4.86 (m)	77.7 (br)	Ti-O$\underline{i}$Pr methine
4.95 (br m)		Minor species?
1.51 (br s)		cyclohexane
1.38 (m)		$\underline{i}$Pr methines
	25.8	Ti-O$\underline{i}$Pr methyl
	22.1	-CO$_2\underline{i}$Pr methyl

e. CD_3CN

Clear evidence for a minor Ti-tartrate species in the solution of Ti(DIPT)(O$\underline{i}$Pr)$_2$ in CD_3CN is provided by the spectra of Figure 53. Multiplets for isopropoxide methine protons are visible at 4.77 and 4.69 ppm, especially when methyl resonances are irradiated. Since they are not of equal intensity, they cannot be due to axial and equatorial

Figure 52. ^{1}H and ^{13}C NMR of Ti(DIPT)(O$\underline{i}$Pr)$_2$ in cyclohexane-d_{12}.

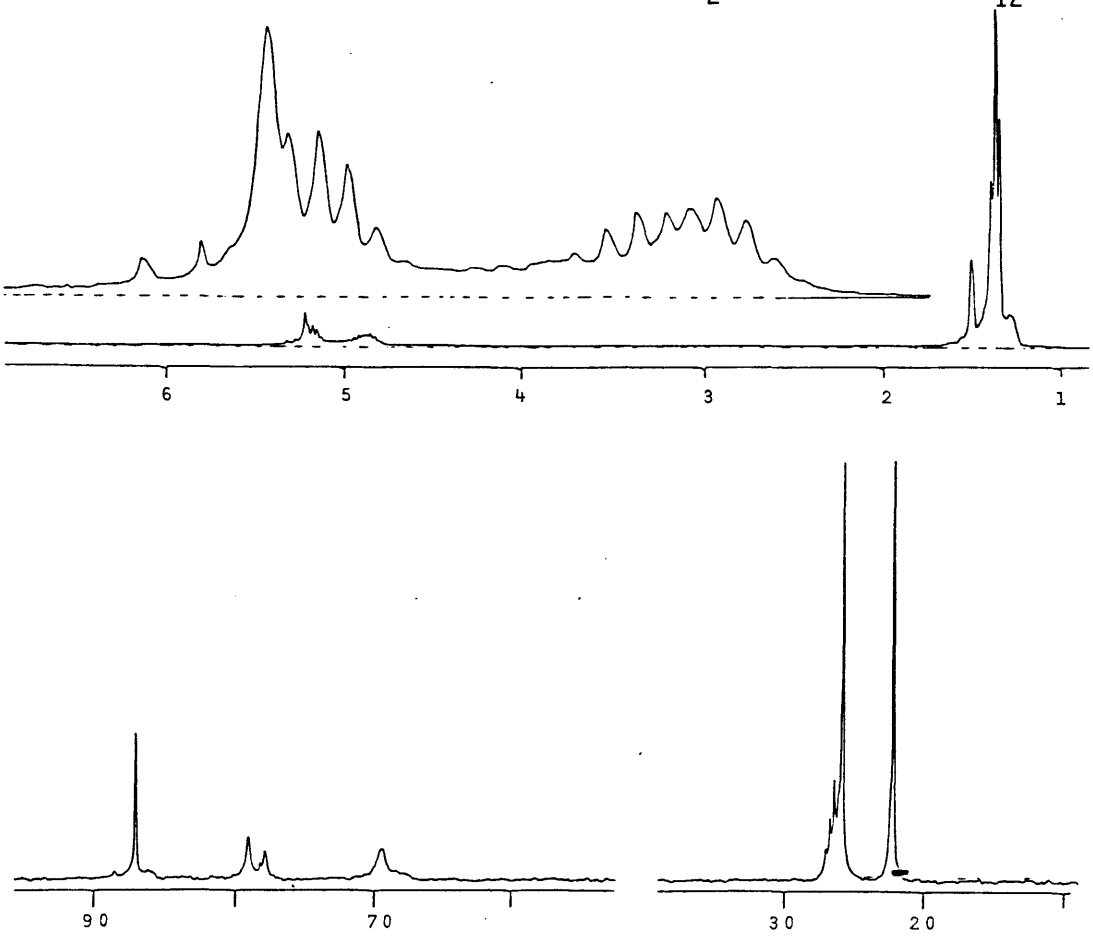

Table 40. Peak assignments for ^{1}H and ^{13}C nmr spectra of Ti(DIPT)(O$\underline{i}$Pr)$_2$ in CD_3CN at 295°K.

^{1}H Peak	^{13}C Peak	Assignment
5.14 (s)	86.7	Tartrate methine
5.05 (br m)	70.9	-$CO_2\underline{i}$Pr methine
4.77 (m)*	78.1	Ti-O$\underline{i}$Pr methine, minor species
4.69 (m)*	79.2	Ti-O$\underline{i}$Pr methine
1.26 (d)		Ti-O$\underline{i}$Pr, -$CO_2\underline{i}$Pr methyls
	25.8	Ti-O$\underline{i}$Pr methyl
	22.1	-$CO_2\underline{i}$Pr methyl

*Relative intensity of peaks at 4.69 to 4.77 ppm:
ca. 3.7:1 at 0.4 M Ti, ca. 6:1 at 0.03 M Ti

Figure 53. ^{1}H NMR of Ti(DIPT)(O$\underline{i}$Pr)$_2$ in CD_3CN.

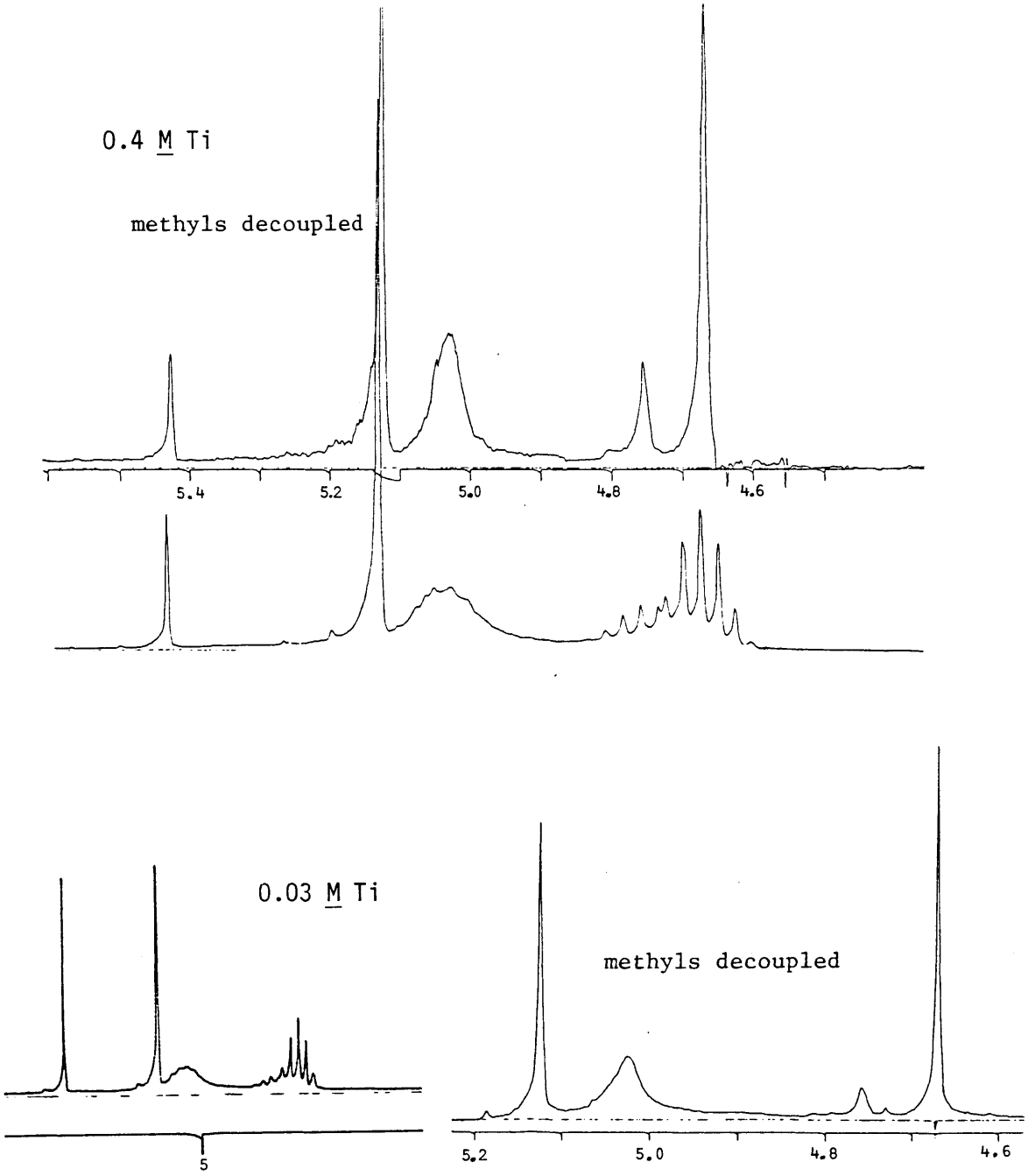

Figure 53, continued. ^{13}C NMR of Ti(DIPT)(O$\underline{i}$Pr)$_2$ in CD_3CN.

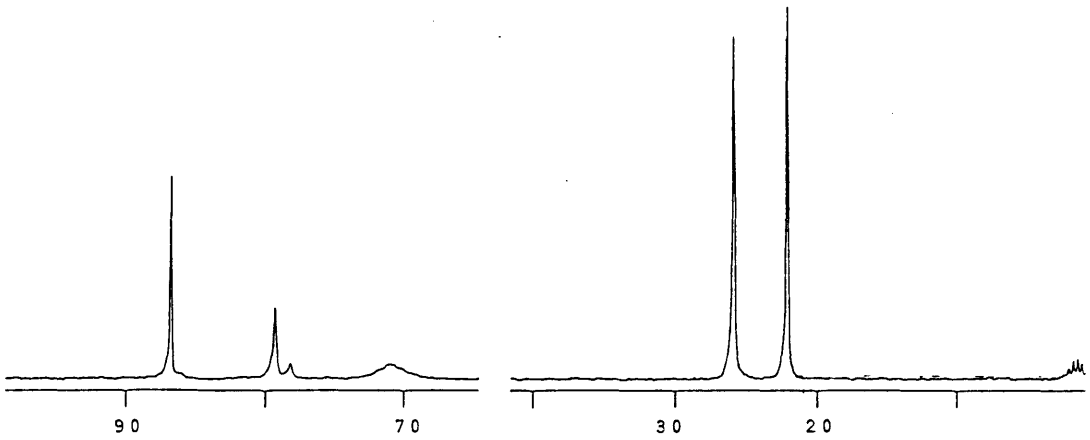

isopropoxides of the same molecule. The 4.77 band is attributed to the minor (presumably 2:1 Ti:DIPT) species, confirmed by a decrease in the relative intensity of the 4.77 to the 4.69 ppm band with a 12-fold decrease in concentration (the same trend as seen in CD_2Cl_2). The ^{13}C nmr spectrum in CD_3CN also shows a small additional isopropoxide methine resonance.

f. THF-d_8

Successful kinetics, molecular weight, enantioselection, and IR measurements obtained in ethyl ether prompted us to check the nmr behavior in an ethereal solvent. The ^1H and ^{13}C nmr spectra of Ti(DIPT)(O$\underline{i}$Pr)$_2$ in THF-d_8 are very similar to those in CD_3CN. Figure 54 and Table 41 summarize these results.

Table 41. Peak assignments for ^1H and ^{13}C nmr spectra of Ti(DIPT)(O$\underline{i}$Pr)$_2$ in THF-d_8 at 295°K.

^1H Peak	^{13}C Peak	Assignment
4.93 (s)	87.0	Tartrate methine
4.82 (br m)	70.0	-CO$_2\underline{i}$Pr methine
4.58 (m)*	77.9	Ti-O$\underline{i}$Pr methine, minor species
4.50 (m)*	79.0	Ti(O$\underline{i}$Pr)$_4$
1.05 (d)		Ti-O$\underline{i}$Pr, -CO$_2\underline{i}$Pr methyls
	25.8	Ti-O$\underline{i}$Pr methyl
	22.0	-CO$_2\underline{i}$Pr methyl

*Relative intensity of peaks at 4.50 to 4.58 ppm (0.3 M Ti) = ca. 7:1

Figure 54. ^{1}H and ^{13}C NMR of Ti(DIPT)(O$\underline{i}$Pr)$_2$ in THF-d_8.

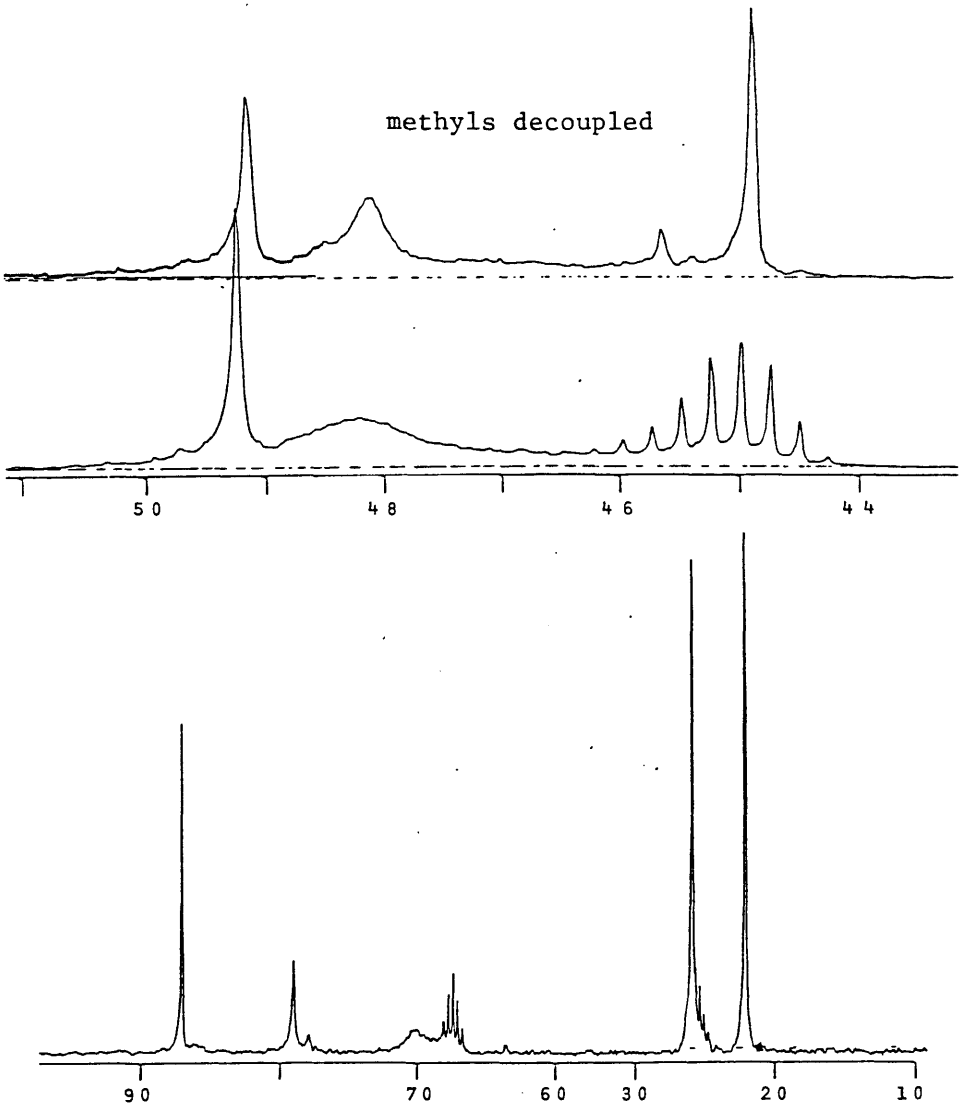

9. ^{17}O NMR

a. Introduction

Oxygen-17 has a spin of 5/2, natural abundance of 0.037%, sensitivity of 0.03 relative to ^{1}H, and a quadrupole moment of -0.026 (10^{-24} cm^2), about ten times that of ^{2}H and about ten times smaller than that of $^{47,49}Ti$.[98] Its saving grace in the face of these abysmal nmr properties is the extremely wide chemical shift range exhibited by oxygen-containing compounds. Because the nucleus relaxes extremely rapidly, pulse Fourier transform nmr data acquisition can be done quickly, and in many cases natural abundance spectra are possible. Peak widths, however, are usually broad and are very susceptible to asymmetry in the electronic environment surrounding the oxygen center. For example, natural abundance ^{17}O nmr spectra of monomeric $Ti(O\underline{t}Bu)_4$ and $Ti(O\underline{i}Pr)_4$ are easy to obtain, but trimeric $Ti(OEt)_4$ and $Ti(O\underline{n}Bu)_4$ give weak signals; it was impossible to obtain any natural abundance signal for alkoxide oxygens in Ti-tartrate complexes.

There has been rapid growth in the application of ^{17}O nmr spectroscopy to organic and inorganic structural problems, pioneered by the many studies of Klemperer's group on polyoxo anions of early transition metals.[99] Our interest in the technique was sparked by the large chemical shift variations found for terminal and different types of bridging oxo ligands in the cluster $V_{10}O_{28}^{6-}$: terminal, 1143 ppm (with respect to H_2O); OV_2, ca. 800 ppm; OV_3, 406 ppm; and OV_6, 62 ppm.[99c] In the complex $[CpTi(Mo_5O_{18})]^{3-}$, oxygens that bridge a Ti and Mo center are found over 100 ppm away from those that bridge two Mo atoms.[99d] Bercaw has measured the ^{17}O nmr spectra of oxo-bridged zirconocene and hafnocene dimers, finding a chemical shift of 581 ppm for the oxo bridge of $(Cp^*_2ZrH)_2O$, and a peak at 175 ppm for $Cp^*_2Zr(OH)_2$, for example.[100]

Studies of ^{17}O nmr spectra of substituted benzyl alcohols[101] have demonstrated a direct relationship between electron density and shielding of the ^{17}O nucleus. Thus, increasing the electron withdrawing power of the <u>para</u>-substituent on the phenyl ring of a benzyl alcohol causes the ^{17}O resonance to shift <u>upfield</u>. The trend is reversed for substituted benzoate esters,[102] indicating that a combination of inductive, resonance, and paramagnetic effects are at work in the ^{17}O nmr experiment. We have found that, while substitution of electron withdrawing groups on the carbinol

carbon increases the shielding of the ^{17}O nucleus, coordination of an alcohol to an electron deficient metal center induces a large downfield shift - the more acidic the metal, the greater the shift.

Since the chemical shift difference between bridging and terminal oxo groups is so large, we reasoned that perhaps the ^{17}O resonances of bridging and terminal alkoxide oxygens of Ti(IV) compounds could be resolved. Applied to Ti-tartrate, this represents the first method of distinguishing between our proposed structure (containing a four-membered ring core with bridging tartrate oxygens) and the two other possibilities (bridging alkoxides and the ten-membered ring structure with no bridging oxygens) in solution. We therefore prepared ^{17}O-labeled tartrate and, encouraged by our success, we have explored the ^{17}O nmr spectra of other alkoxide ligands as well.

For reference purposes, a complete list of observed ^{17}O nmr resonances is given at the end of this discussion in Table 44. Peak positions are reported relative to ethyl ether, positive values indicating resonances to lower field, negative values to higher field. Ether was chosen because an internal standard was desired for the spectra of $Ti(O\underline{t}Bu)_4$ and $Ti(O\underline{i}Pr)_4$. Chemical shifts are usually reported in the literature relative to water, but obviously water is an inappropriate internal standard here. To convert to a water reference, simply add 15.5 ppm to the values reported in Table 44. The line width at half-height, $LW_{1/2}$, is given in ppm. Oxygen resonances are broadened by fast relaxation as well as by all the chemical and fluxional exchange processes that affect proton and ^{13}C nmr of titanium alkoxide systems. Peak positions are accurate to ± 3 ppm, estimated by repeated determinations of the spectra of titanium tetraalkoxides and ^{17}O-labeled alcohols.

Discussion of ^{17}O nmr spectra will be divided into five sections: alcohols and Ti tetraalkoxides, tartrate complexes, α-hydroxy ester complexes, benzyl alcohol complexes, and complexes of cumyl hydroperoxide.

b. Alcohols and Titanium Tetraalkoxides

The chemical shift trend of the alcohols follows that of the substituted benzyl alcohols mentioned above; electron-withdrawing substituents on the carbinol carbon bring the ^{17}O resonance upfield. Thus, cumyl alcohol is found at 44.5 ppm, $\underline{i}$PrOH at 21.7 ppm, and α-hydroxy esters at -7.1 (**18**)

and -10.4 (**17**). The chemical shift of tartrate hydroxylic oxygens is found the farthest upfield, -20 ppm, as befits the electron-deficient nature of its carbinol centers. Benzyl alcohol in $CDCl_3$ is found at -6.8 ppm, close to the literature value[101] (-9.5 ppm in toluene), indicating a significantly more electron-deficient oxygen center than in isopropanol. (This has unfortunate consequences for the intepretation of the ^{17}O nmr of titanium benzyloxide complexes.)

The ^{17}O nmr spectra of ^{17}O-enriched alcohols are fairly narrow singlets, as listed in Table 44.

Natural abundance ^{17}O nmr spectra were obtained for titanium tetraalkoxides in concentrated $CDCl_3$ solution (typically 30-40% by volume); they are shown below in Figure 55. A sharp resonance at 288 ppm is found for $Ti(O\underline{t}Bu)_4$, strictly a monomer in solution. $Ti(O\underline{i}Pr)_4$, having an average aggregation state slightly greater than 1.0 in solution,[103] shows a strong resonance at 280 ppm. In contrast, the ^{17}O signal of $Ti(OEt)_4$ at room temperature is very weak and broad, consistent with the trimeric structure of the complex in solution. Heating the sample to 320°K greatly increases the signal to noise ratio. The same phenomenon was observed for $V_2W_4O_{19}^{4-}$ and $(OC)_3ReNb_2W_4O_{19}^{3-}$ by Klemperer;[99a,b] he suggested that a decrease in the rate of quadrupole relaxation with an increase in temperature was responsible for the enhanced signal. Increasing the temperature also speeds the rate of ethoxide scrambling between terminal and bridging positions of $Ti(OEt)_4$, which undoubtedly contributes to a sharper averaged signal.

More importantly, the chemical shift of $Ti(OEt)_4$, representing an average of bridging and terminal alkoxide resonances, is at 252 ppm, 36 ppm upfield from $Ti(O\underline{t}Bu)_4$. If the assignment by Russo and Nelson of a trimeric structure is correct,[104] $Ti(OEt)_4$ contains eight terminal ethoxides and four bridging ones. Taking the resonance of $Ti(O\underline{t}Bu)_4$ as that of a "pure" terminal alkoxide, a bridging alkoxide should be found at approximately 180 ppm, or about 100 ppm upfield from a terminal alkoxide resonance.

$Ti(O\underline{n}Bu)_4$, having much less oxygen per mole than $Ti(OEt)_4$, gave a very weak ^{17}O signal (not shown in Figure 55). Consistent with the observed effect of electron-withdrawing substituents on the carbinol carbon, a peak at 212 ppm is found for titanium tetrahexafluoroisopropoxide,

Figure 55. ^{17}O NMR of metal tetraalkoxides in $CDCl_3$.

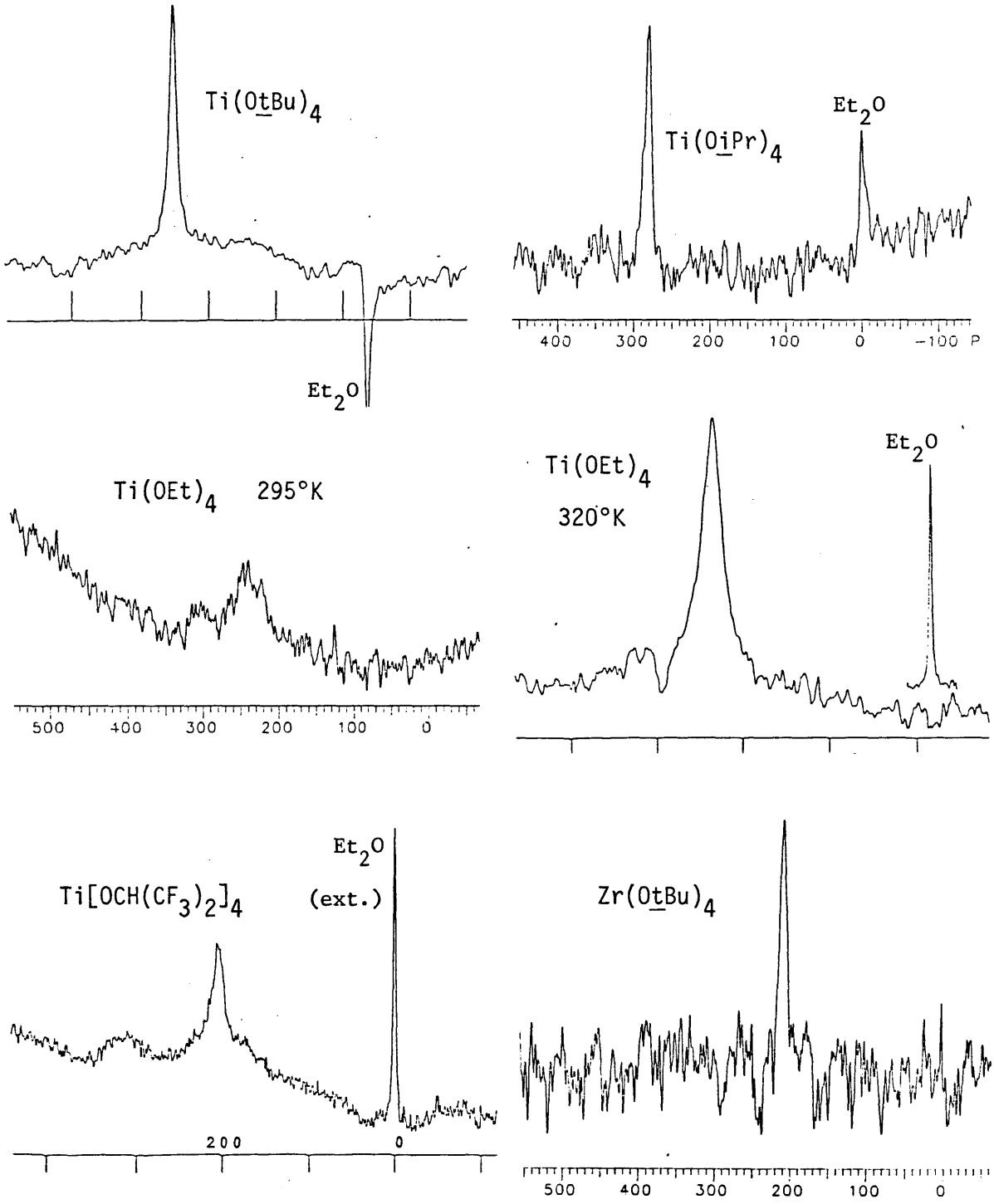

$Ti[OCH(CF_3)_2]_4$. $Zr(O\underline{t}Bu)_4$ has a sharp resonance at 209 ppm, characteristic of a metal center less Lewis acidic than Ti(IV).

c. Titanium Tartrates

In Figure 56 are the ^{17}O nmr spectra of $Ti(DIPT)(O\underline{i}Pr)_2$ containing labeled tartrate hydroxylic oxygens. Two bands are observed for spectra in $CDCl_3$ and C_6D_6, with an increase in signal strength at 310°K in C_6D_6. Peak positions are slightly different in the two solvents. In $CDCl_3$, the peak maxima are 88 ppm apart and in C_6D_6, 116 ppm separates the resonances, both close to the 100 ppm chemical shift difference between bridging and terminal alkoxides estimated from the titanium tetraalkoxide spectra. It is unlikely that terminal tartrate oxygens in different coordination sites (such as axial and equatorial) could have such different chemical shifts. With this assumption, we assign the band at lower field to the terminal tartrate alkoxide oxygen and the higher field band to the bridging oxygen in structure **14**.

The spectra of $Ti(DIPT)(O\underline{t}Bu)_2$ display an interesting temperature dependence (Figure 57). At ambient temperature in $CDCl_3$, one broad band at 190 ppm ($LW_{1/2}$ = 100 ppm) is observed. At approximately 315°K, two bands are seen (229 and 165 ppm), but at 330°K, the peaks coalesce again. Exactly this sort of behavior was reported for $(HMPA)CrO(O_2)_2$: the ^{17}O nmr spectrum is a singlet at low temperature and a doublet at higher temperature.[105b] Increased resolution at higher temperature is attributed to the decrease in spin-lattice relaxation rate that accompanies a decrease in solution viscosity.

We believe the two $Ti(DIPT)(O\underline{t}Bu)_2$ peaks coalesce at higher temperature for the same reason that ^1H and ^{13}C nmr peaks coalesce - fluxional exchange between terminal and bridging sites. Below about 0°C, signals for all the ^{17}O-labeled tartrate complexes disappeared entirely. The ^{17}O signals of Ti-tartrates are much broader than the tetraalkoxides because of an increased sensitivity to quadrupole relaxation, since the oxygen atoms are in an asymmetric environment.

Figure 56. ^{17}O NMR of Ti(DIPT)(O$\underline{i}$Pr)$_2$; external Et_2O = 0.0 ppm.

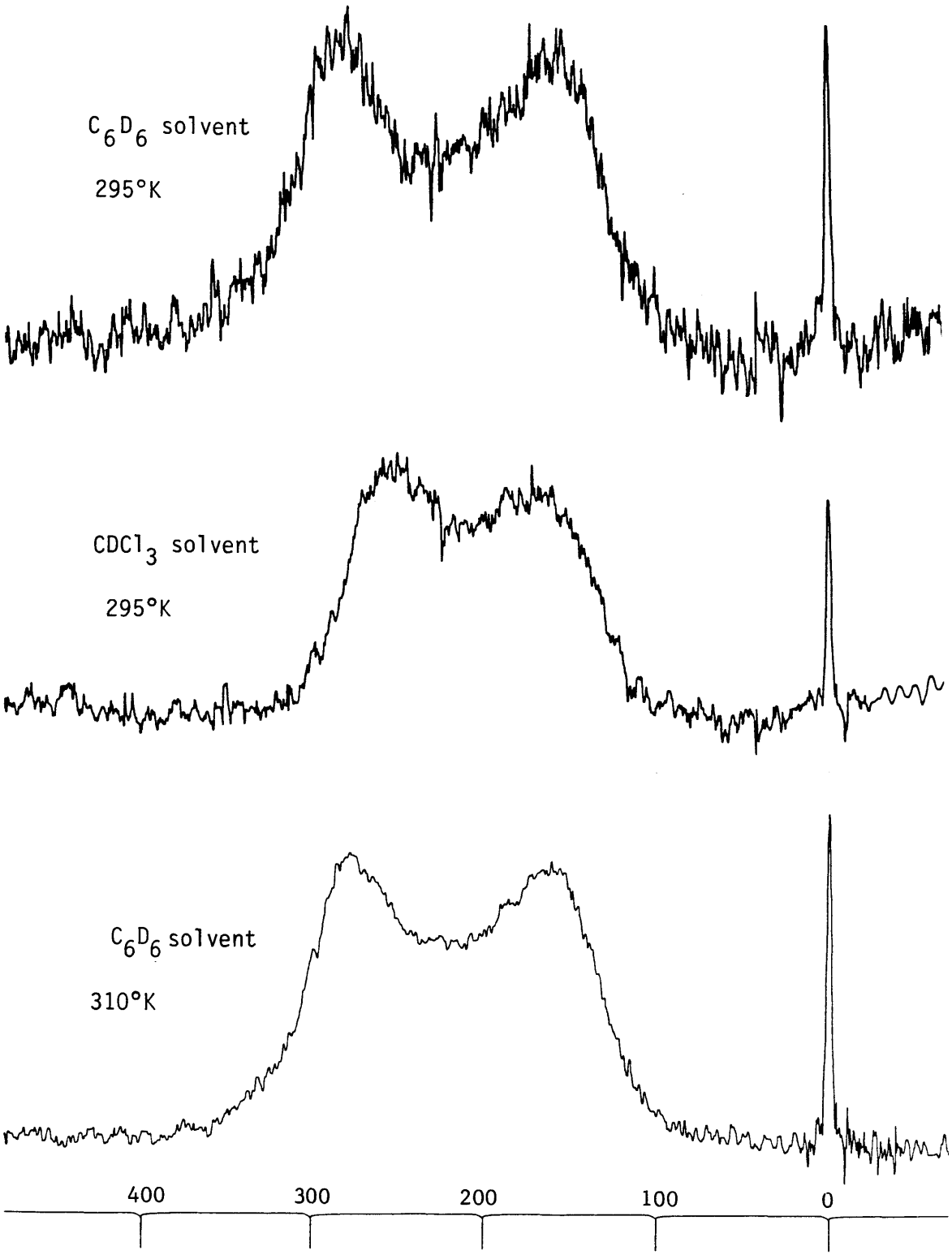

Figure 57. Temperature dependent ^{17}O NMR spectra of Ti(DIPT)(O$\underline{t}$Bu)$_2$.

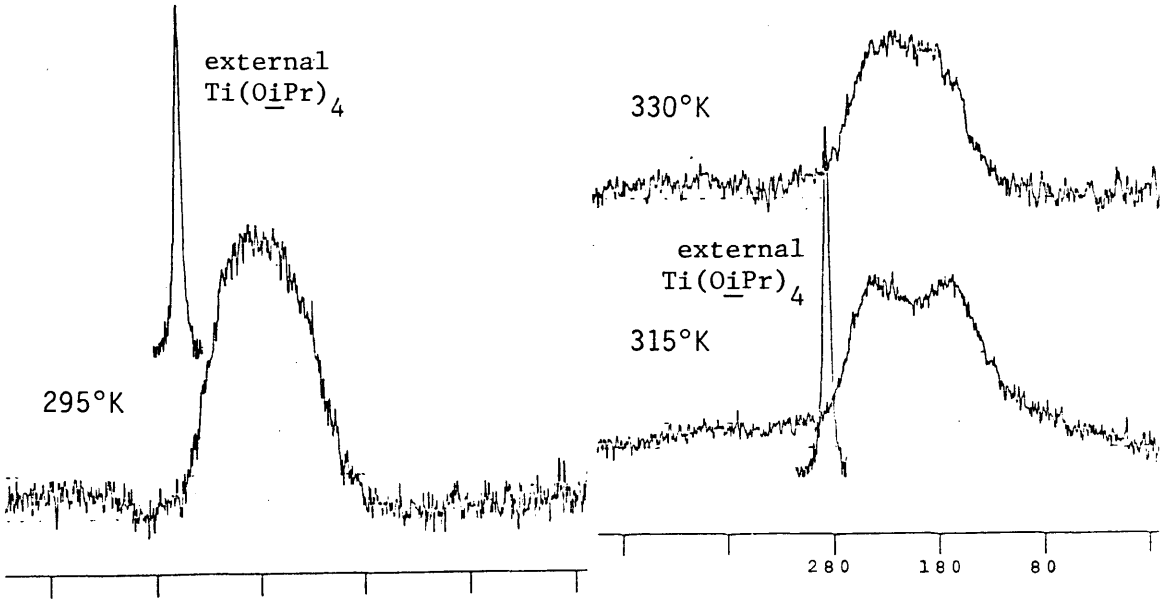

The 2:2 complex of Ti(O$\underline{i}$Pr)$_4$ and di-l-menthyl tartrate (DMnT) shows a very well resolved two-line spectrum, 285 and 140 ppm (Figure 58).

Secondary alkoxides are much poorer at bridging than primary alkoxides, as demonstrated by the molecularities of Ti(O$\underline{i}$Pr)$_4$ vs. Ti(OEt)$_4$. In using only isopropoxide and $\underline{t}$-butoxide as monodentate ligands, we may be forcing the complex to adopt a tartrate-bridged configuration by making the alkoxide-bridged one inaccessible. We therefore measured the ^{17}O nmr spectrum of Ti(DMnT)(OEt)$_2$. This is a complex of a bulky tartrate (but one that is nevertheless effective in asymmetric epoxidation) and primary monodentate alkoxides; it should be biased toward formation of an alkoxide bridged structure, if anything. Figure 58 shows the appearance of bands at 304 and 154 ppm in the nmr spectrum, just as for all the other Ti-tartrates examined.

Temperature-dependent ^{17}O nmr of 2:1 Ti(O$\underline{t}$Bu)$_4$:DIPT is the same as the 2:2 complex. One broad band at 198 ppm is seen at 295°K, while two peaks are mildly resolved at 318°K (231 and 164 ppm). See Figure 59 for these spectra.

Since the x-ray crystal structure of the tartramide complex Ti(D$\underline{N}$BnT)(O$\underline{i}$Pr)$_2$ has been determined, its ^{17}O nmr provides something of a test of the applicability of the method to structure determination. The

Figure 58. ^{17}O NMR of Dimenthyltartrate complexes.

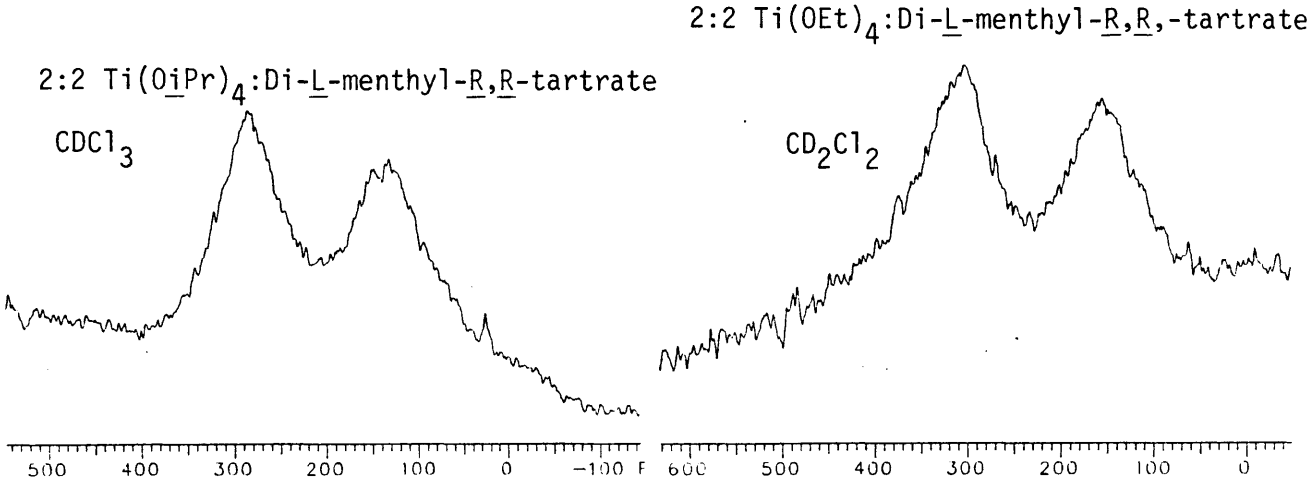

Figure 59. Temperature dependent ^{17}O NMR of $Ti_2(DIPT)(O\underline{t}Bu)_6$ in $CDCl_3$.

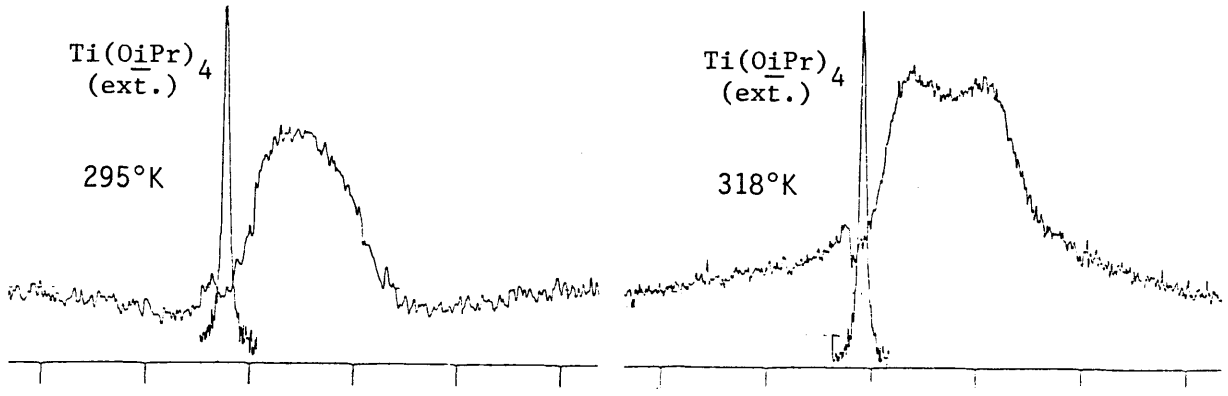

labeled tartramide ligand was prepared from labeled dimenthyl tartrate, and the ^{17}O nmr of its 1:1 complex with $Ti(O\underline{i}Pr)_4$ is recorded in Figure 60. Two bands are observed, but they are not found in equal intensities, as expected. Since the proton nmr of the labeled complex was identical to that of unlabeled material, we are confident that both bands are the product of the proper species. We do not know why the bands are of unequal intensity, and so we cannot confidently assign them to bridging and

Figure 60 . ^{17}O NMR of Ti(DNBnT)(O$\underline{i}$Pr)$_2$ in $CDCl_3$ at 295°K.

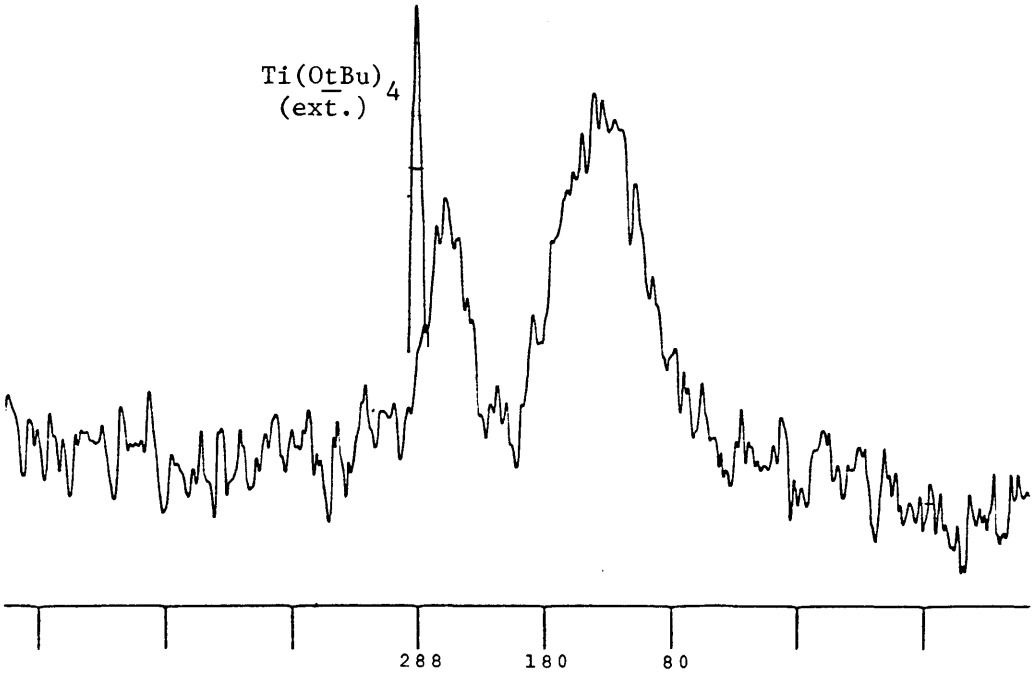

terminal oxygens. Heating the sample results in a more intense signal, but no change in peak positions or relative size.

d. Complexes of Monobasic α-Hydroxy Esters

While they may provide some indication of the expected chemical shift difference between bridging and terminal oxygens, Ti(O$\underline{i}$Pr)$_4$ and Ti(OEt)$_4$ are not very suitable model compounds for Ti-tartrate. We therefore prepared ^{17}O-labeled α-hydroxy esters to see if we could resolve bridging and terminal sites in titanium complexes of these ligands. Signer molecular weight measurements were made of some representative cases; the results are given below in Table 42.

(i) Ethyl Lactate, **18**

No clear evidence for bridging and terminal oxygens was observed. Figure 61 shows the ^{17}O nmr spectra of the following samples:

(a) a 1:1 mixture of Ti(O$\underline{i}$Pr)$_4$ and **18**;

(b) a 1:2 mixture of Ti(O$\underline{i}$Pr)$_4$ and **18**;

(c) a 1:1 mixture of Ti(O$\underline{t}$Bu)$_4$ and **18**, from which free alcohol was removed *in vacuo*, giving a complex of composition Ti(O$\underline{t}$Bu)$_{3.7}$(**18**)$_{0.3}$, as determined by proton and ^{13}C nmr;

(d) 1:3 mixture of $Ti(O\underline{t}Bu)_4$ and **18**, affording, after high-vacuum pumping, $Ti(O\underline{t}Bu)_{2.5}(\underline{18})_{1.5}$; which posesses two resolvable lactate ligands and two different t-butoxides by nmr; and

(e) a 1:1 mixture of $Ti(OEt)_4$ and **18**, affording $Ti(OEt)_3(\underline{18})$ after high vacuum evaporation of free alcohol.

Table 42. Molecular weight determinations by the Signer method of titanium complexes with L-(+)-Ethyl Lactate, **18** and (dl)-Ethyl-α-hydroxycyclohexyl Acetate, **17**.

Entry	Sample	Solvent	Conc.[a]	MW_{obs}	N[b]	MW_{calc}[c]
1.	1:1 $Ti(O\underline{t}Bu)_4$: **17**	CH_2Cl_2	0.31	414	0.92	452
2.	$Ti(DIPT)(O\underline{i}Pr)Br$ + **17**	CH_2Cl_2	0.31	774	1.48	524
3.	''	CH_2Cl_2	0.21	1063	3.04	1049
4.	1:1:1 $Ti(O\underline{i}Pr)_4$:DIPT:**18**	CH_2Cl_2	0.23	700	1.54	913
5.	$Ti(O\underline{t}Bu)_2(\underline{18})_2$ prepared from $Ti(O\underline{t}Bu)_4$ + $Ti(\underline{18})_4$	CH_2Cl_2	0.29	398	0.93	428
6.	1:1 $Ti(OtBu)_4$: **18**	CH_2Cl_2	0.29	343	0.90	383
	$Ti(O\underline{t}Bu)_3(\underline{18})$ prepared from $Ti(O\underline{t}Bu)_4$ + $Ti(\underline{18})_4$	CH_2Cl_2	0.30	395	1.03	383
7.	$Ti(OEt)_3(\underline{18})$	CH_2Cl_2	0.29	452	1.51	300

a. Concentration (moles/L) of titanium at equilibrium.

b. Average degree of association.

c. Molecular weight of closest oligomer to that observed value.

Samples (c) and (d) should be monomeric, as indicated by entries 5 and 6 of Table 42. Sample (e) was found to have an average molecularity of 1.5, and so should contain some bridging lactate oxygen centers. All the ^{17}O signals are clean singlets, however, with the exception of sample (d), which displays a lopsided peak that is probably composed of two overlapping bands. Although the ^{13}C and ^{1}H nmr spectra of this complex show two different types of bound lactate (discussed in the experimental section), the monomeric molecular weight findings for $Ti(O\underline{t}Bu)_2(\underline{18})_2$ and $Ti(O\underline{t}Bu)_3(\underline{18})$ make it unlikely that bridging oxygens are being observed. Rather, we may be seeing slightly different chemical shifts for terminal alkoxide bonds in different environments. The fact that only one signal is present for $Ti(OEt)_3(\underline{18})$ is disappointing, but does not invalidate the

technique. It is possible that the observed band is an average of bridging and terminal positions, which exchange much more rapidly than those in the more rigid tartrate complexes. Note that as electron-withdrawing lactate ligands replace t-butoxide groups, the ^{17}O resonance moves slightly downfield as a consequence of the greater Lewis acidity of the metal center [compare 214 ppm for $Ti(O\underline{t}Bu)_{3.7}(\underline{\mathbf{18}})_{0.3}$ and 221 ppm for $Ti(O\underline{t}Bu)_{2.5}(\underline{\mathbf{18}})_{1.5}$].

The addition of 1 equivalent per titanium of labeled ethyl lactate, **18**, to a solution of $Ti(DIPT)(O\underline{t}Bu)_2$ results in the ^{17}O nmr spectrum of Figure 62. One broad band at 282 ppm for bound lactate is accompanied by a smaller one at -7 ppm for free lactate, indicating that most, but not all, of the α-hydroxy ester is bound. The ^{17}O chemical shift is moved roughly 60 ppm downfield from those in Fig. 60, indicating binding to a more electron-deficient metal center. This supports our longstanding suspicion that tartrate is a much more electron-withdrawing ligand than normal alkoxides (or even α-hydroxy esters such as lactate). The spectrum of a 1:1 mixture of $Ta(O\underline{i}Pr)_5$ with **18** is also shown in Figure 62. In this case, the less Lewis acidic metal causes the ^{17}O chemical shift to appear at higher field than the titanium complexes (approximately 176 ppm downfield from ether).

(ii). Ethyl-α-hydroxycyclohexyl acetate, **17**

The greater size of the cyclohexyl group manifests itself in a smaller binding constant of **17** for titanium than of **18** for titanium, as shown in the ^{17}O nmr spectra of Figure 63. Mixing 0.5 equivalents of $Ti(O\underline{t}Bu)_4$ with 1.0 equivalent of ligand **17** (spectrum a) leaves about 60% of the ligand free in solution; addition of another 0.5 equivalents of $Ti(O\underline{t}Bu)_4$ causes more α-hydroxy ester to bind. These complexes are monomeric as indicated by a Signer molecular weight determination (entry 1, Table 42). The chemical shift (207 ppm) is 7-13 ppm upfield from the lactate resonances.

Figure 61. ^{17}O NMR of ethyl lactate (L) complexes in $CDCl_3$.

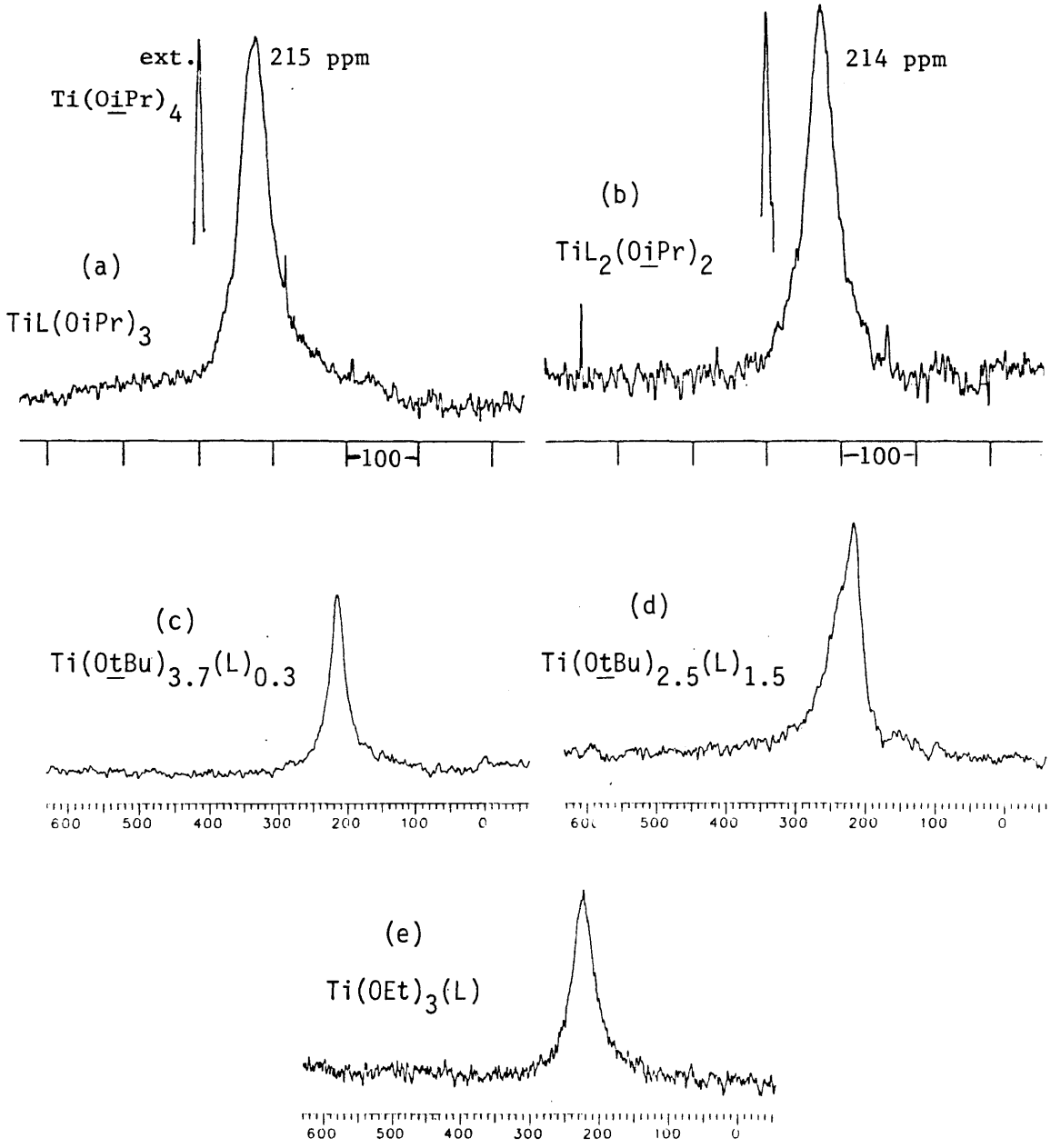

Figure 62. ^{17}O NMR of equimolar mixtures of labeled ethyl lactate with $Ti(DIPT)(O\underline{t}Bu)_2$ (a), and $Ta(O\underline{i}Pr)_5$ (b).

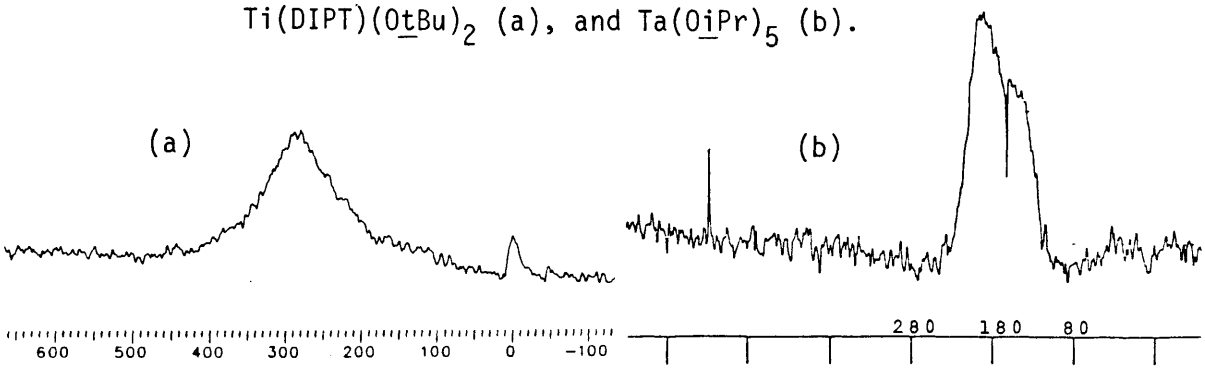

Figure 63. ^{17}O NMR of mixtures of ethyl-α-cyclohexylacetate (L) with $Ti(O\underline{t}Bu)_4$.

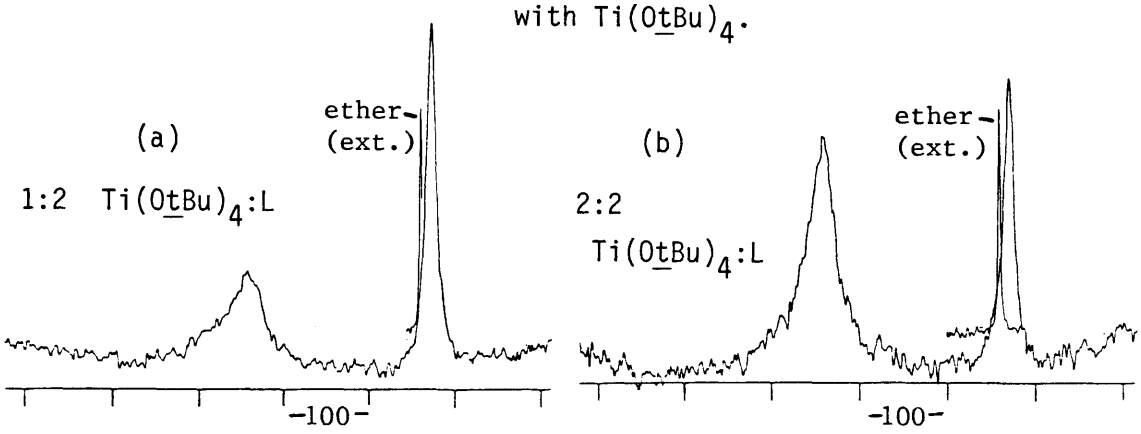

e. Titanium Benzyloxide Complexes

The preparation of ^{17}O labeled benzyl alcohol was conveniently accomplished by reduction of labeled benzaldehyde. The ^{17}O nmr of $Ti(tartrate)(*OBn)_2$ should give a single peak in the terminal alkoxide region (that is, downfield) if our proposed tartrate-bridged dimer structure is correct. Therefore, five benzyloxide complexes were prepared and their ^{17}O nmr spectra recorded; they appear in Figure 64. Pertinent Signer molecular weight determinations are listed below in Table 43.

Figure 64 . ^{17}O NMR of titanium benzyloxide complexes in $CDCl_3$. (L = ethyl lactate-^{16}O)

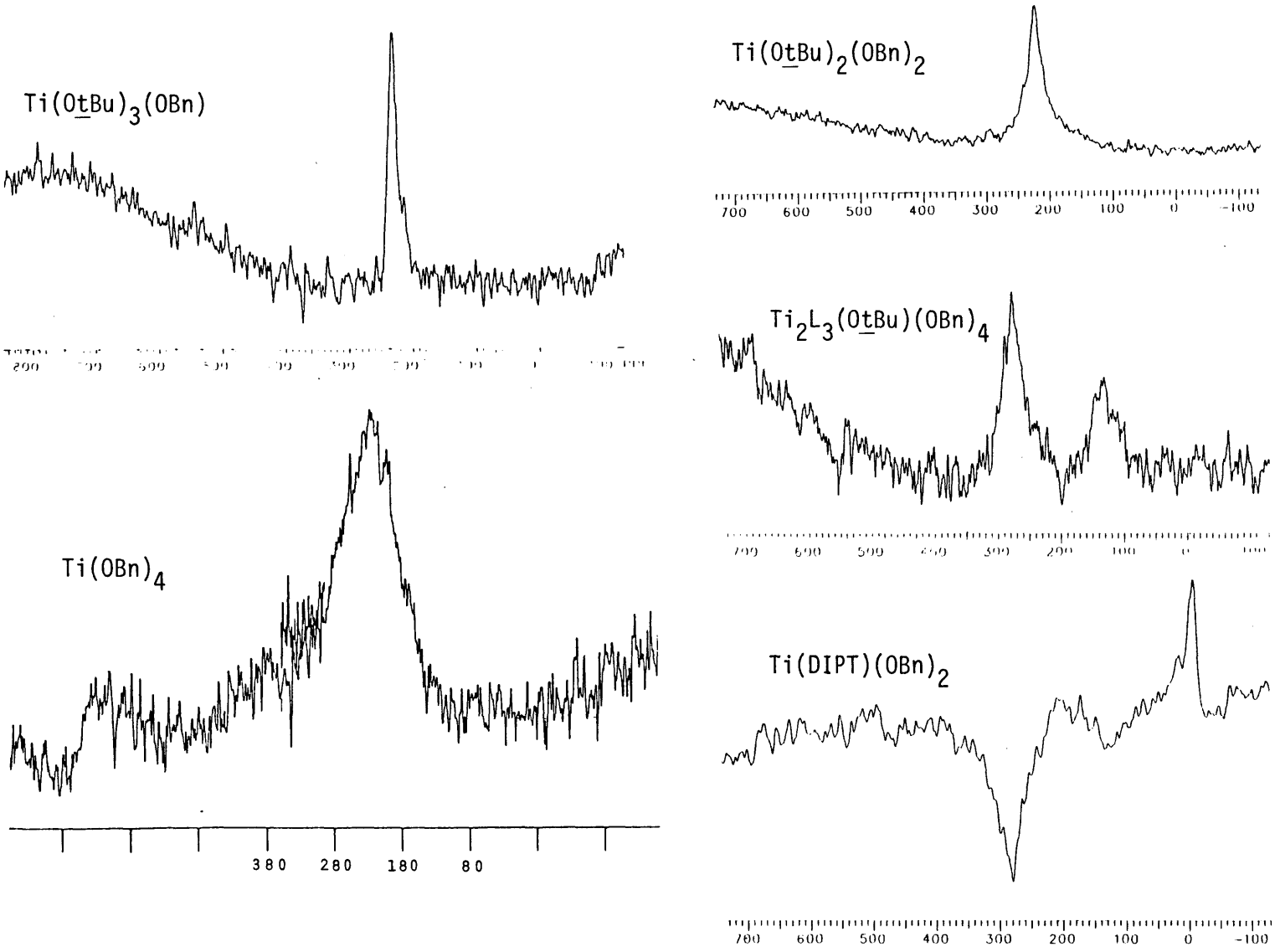

Table 43. Molecular weight determinations by the Signer method of titanium benzyloxide complexes in CH_2Cl_2.

Entry	Sample	Conc.[a]	MW_{obs}	N[b]	MW_{calc}[c]
1	$Ti(OBn)_4$	0.27	840	1.76	953
2	$Ti(O\underline{t}Bu)_3(OBn)$	0.32	354	0.95	374
3	$Ti(O\underline{t}Bu)_2(OBn)_2$	0.32	423	1.04	408

a. Concentration (moles/L) of titanium at equilibrium.

b. Average degree of association.

c. Molecular weight of closest oligomer to that observed value.

It is a bit surprising that $Ti(O\underline{t}Bu)_2(OBn)_2$ is monomeric in CH_2Cl_2 solution (entry 3), but its ^{17}O nmr signal is strong, only slightly wider than that of $Ti(O\underline{t}Bu)_3(OBn)$, and at the same chemical shift as $Ti(O\underline{t}Bu)_3(OBn)$ (223 and 221 ppm, respectively). $Ti(OBn)_4$ (with ^{17}O-enriched benzyloxy groups) displays a broadened, weaker resonance 12 ppm downfield from $Ti(O\underline{t}Bu)_2(OBn)_2$. An upfield shift would be expected solely on bridging/terminal alkoxide considerations, since $Ti(OBn)_4$ is dimeric (Table 43, entry 1) and therefore posesses at least two bridging benzyloxide groups. We can speculate that $Ti(OBn)_4$, having two more electron withdrawing benzyloxy ligands[106] than $Ti(O\underline{t}Bu)_2(OBn)_2$, has a more electron deficient metal center, which is responsible for a net downfield shift of the O^{17} resonance.

An equimolar mixture of $Ti(O\underline{t}Bu)(\underline{\mathbf{18}})_3$ and $Ti(*OBn)_4$ was prepared to model Ti(tartrate)$(OBn)_2$. A downfield shift in the benzyloxy resonance of 53 ppm from that of $Ti(O\underline{t}Bu)_2(OBn)_2$ was observed (276 ppm), consistent with the replacement of t-butoxide with lactate, a relatively electron deficient ligand. It is likely that this mixture contains mostly monomeric species, and therefore defines the likely area for terminal Ti-OBn groups to appear in a spectrum of Ti(tartrate)$(OBn)_2$. Thus, a mixture of $Ti(O\underline{i}Pr)_4$, $Ti(OBn)_4$, and two equivalents of (+)-DIPT was prepared, giving Ti(DIPT)$(OR)_2$ + ROH, where R is either benzyl or isopropyl. The O^{17} nmr spectrum of this mixture shows a single benzyloxide peak at 278 ppm.

The bands that appear at approximately 130 ppm in the spectra of $Ti_2(\underline{\mathbf{18}})_3(O\underline{t}Bu)(OBn)_4$ and Ti(DIPT)$(OR)_2$ come about by virtue of transesterification of lactate and tartrate, respectively, with benzyloxide. They are the acyl oxygen resonances of the product benzyl esters. The band at

Figure 65. ^{17}O NMR of cumyl hydroperoxide (a), cumyl methyl peroxide (b), and cumyl methyl peroxide + $Ti(O\underline{i}Pr)_4$ (c).

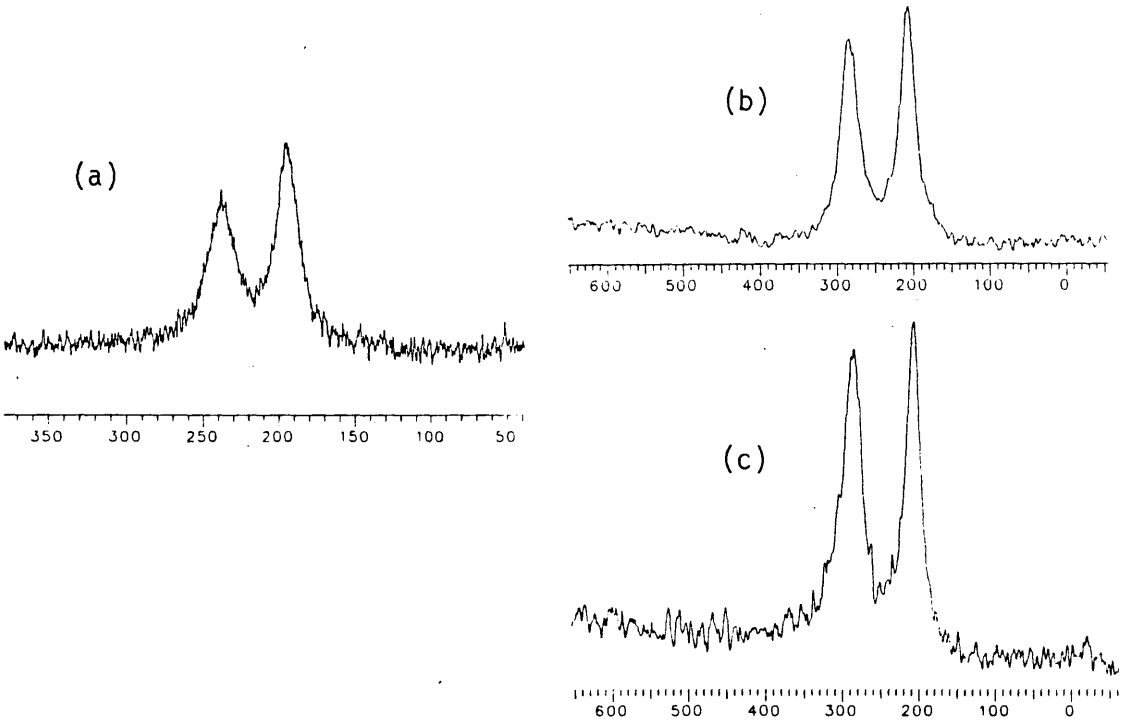

Figure 66. ^{17}O NMR of $Hf(O\underline{i}Pr)_4 \cdot HO\underline{i}Pr$ + Cumyl hydroperoxide.

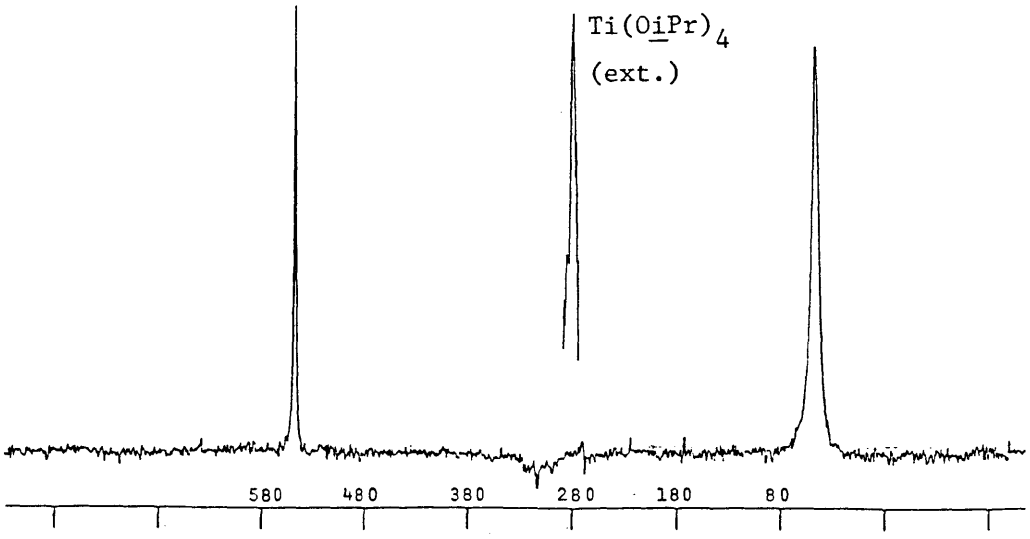

-7 ppm in the latter spectrum is from free benzyl alcohol. The reason for the phase inversion of the benzyl alcohol peak is unknown, but it is at the correct chemical shift.

f. Hydroperoxide Complexes

Covalent mononuclear d^0 metal oxo-peroxo complexes have recently been examined by ^{17}O nmr spectroscopy.[105] Signals for tert-butyl hydroperoxide[105b] and cumene hydroperoxide[105c] have been observed, but complexes of hydroperoxide with d^0 transition metals have heretofore been unexplored.

The nmr spectrum of ^{17}O-labeled cumene hydroperoxide is shown in Figure 65. Both oxygen resonances are visible, at 200 and 242 ppm, close to the chemical shifts of 206 and 239 ppm (with respect to ether) reported for TBHP.[105b] Their different lineshapes betoken slightly different relaxation rates. The lower-field band (242 ppm) is tentatively assigned as the distal hydroperoxide oxygen (R-O-O-H) because of its greater linewidth, possibly the result of ^{17}O-^{1}H coupling.[107] Cumyl methyl peroxide, prepared by reaction of the hydroperoxide with diazomethane,[108] shows bands at 207 and 283 ppm. Note that the lineshapes are more nearly the same than for cumyl hydroperoxide.

The spectrum of cumyl methyl peroxide in the presence of 1.0 equivalents of $Ti(OiPr)_4$ is also shown in Figure 65 (peroxide concentration = 0.2 M in $CDCl_3$). The oxygen peaks are found at 207 and 286 ppm - suggesting a very weak association with the metal, but certainly not proving the existence of such an interaction.

Consider the ^{17}O nmr spectrum of $Hf(OiPr)_4 \cdot HOiPr$ plus 1.0 equivalent of cumyl hydroperoxide (Figure 66), taken after approximately two hours at room temperature following hydroperoxide addition. (The nmr solution was a light amber color.) The peak at 51 ppm is assigned to cumyl alcohol (2-phenyl-2-propanol, 44.5 ppm in $CDCl_3$ alone). The peak at 545 ppm is probably from an oxo-bridged structure (Hf-O-Hf), in the same range as that observed for $(Cp^*_2ZrH)_2O$ (566 ppm relative to ether).[100] These products arise from the oxidation of isopropanol to acetone according to Figure 67; one equivalent of acetone with respect to cumyl hydroperoxide added was observed in the proton nmr of the reaction mixture.

Figure 67. Oxidation of isopropoxide by ^{17}O-labeled hydroperoxide.

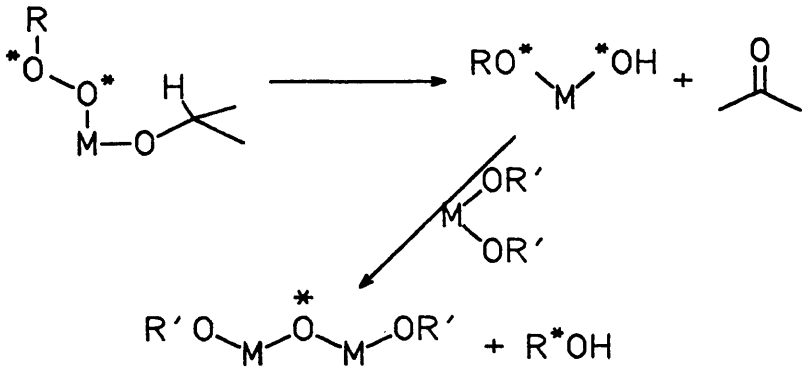

Following the reaction of $Ta(O\underline{i}Pr)_5$ with cumyl hydroperoxide by ^{17}O nmr was more informative. At the top of Figure 68 is a 4 minute scan of the reaction mixture several minutes after hydroperoxide addition. A large, broad signal at 226 ppm dominates the spectrum, representing bound cumyl hydroperoxide (Ta-OOR), and perhaps some free hydroperoxide as well. A sharp resonance is visible at 419 ppm, and free cumyl alcohol makes a token appearance at approximately 50 ppm.

The second spectrum is from an additional 7 minutes of data accumulation, added onto the FID of the first spectrum. Notice the growth of both the free cumyl alcohol resonance and the peak at 419 ppm, at the expense of Ta-OOR. The final spectrum, taken after an additional 15 minutes at room temperature, is identical to the hafnium spectrum above (Figure 66), showing just the μ-oxo oxygen (Ta-O-Ta) and free cumyl alcohol. The 419 ppm band is then thought to be from bound cumyl alcohol, $Ti-OC(Me)_2Ph$. The alkoxide is an initial product of isopropanol oxidation, but is displaced from the metal because its equilibrium constant for binding must be far lower than for formation of the μ-oxo unit, or even for binding of isopropanol. Again, proton nmr showed the clean production of an equivalent of acetone.

Addition of one equivalent of cumyl hydroperoxide to a $CDCl_3$ solution of $Zr(O\underline{t}Bu)_4$ produced the ^{17}O nmr spectrum of Figure 69. A single band at 171 ppm is observed from Zr-OOR. Very small bands at 400 and 509 ppm may represent Zr-OR and Zr-O-Zr groups, respectively (R = cumyl), from a minor

Figure 68. ^{17}O NMR of $Ta(O\underline{i}Pr)_5$ + Cumyl Hydroperoxide in $CDCl_3$.

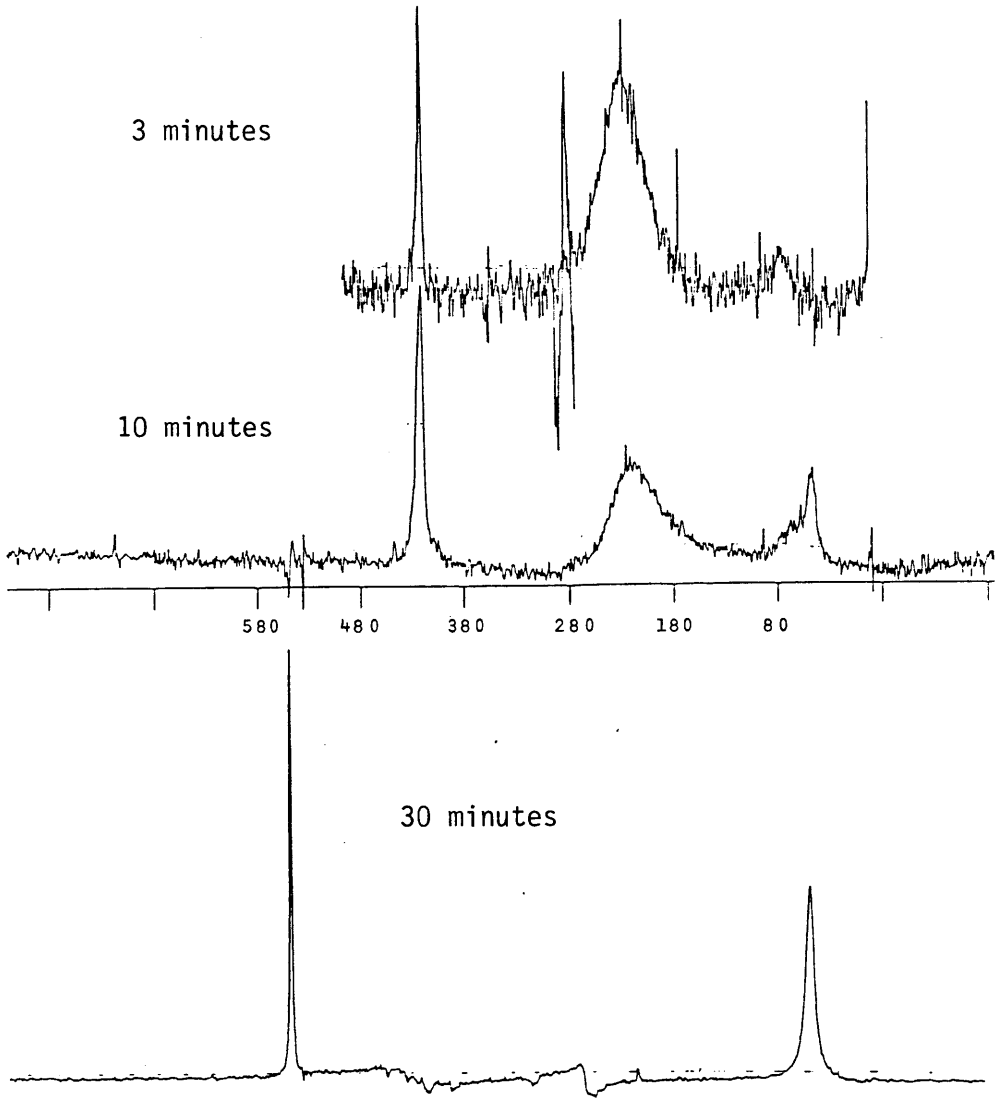

Figure 69. ^{17}O NMR of $Zr(O\underline{t}Bu)_4$ + Cumyl hydroperoxide in $CDCl_3$.

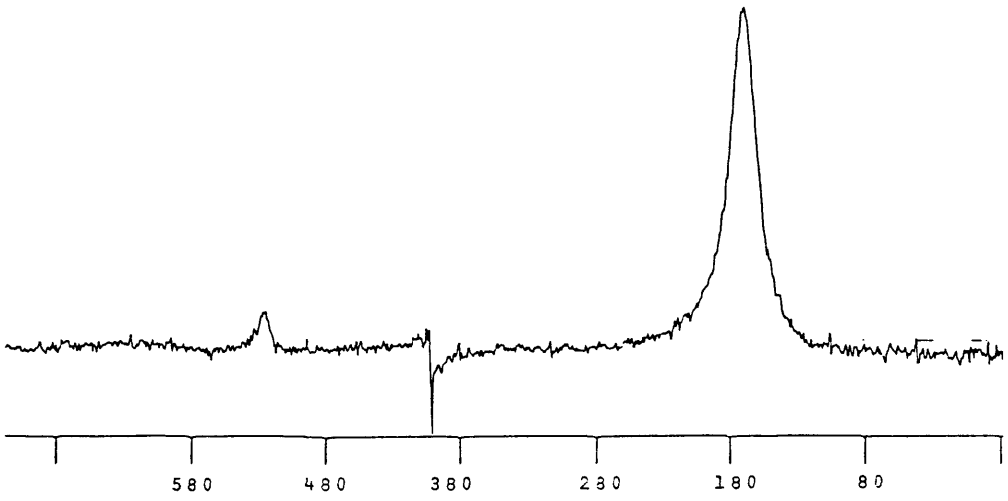

decomposition pathway. No change in the nmr spectrum is observed after 20 minutes at room temperature and an additional three hours at -10°C.

Addition of 1.0 equivalent of cumyl hydroperoxide to a pre-cooled $Ti(O\underline{i}Pr)_4$ solution in $CDCl_3$ results in warming of the solution and an immediate color change to light amber. ^{17}O nmr of the reaction mixture shows a large band at 278 ppm (Ti-OOR), smaller peaks at 49 ppm (cumyl alcohol) and 546 ppm (sharp, Ti-O-Ti), and minor bands at 493 and 521 ppm (tentatively assigned to different Ti-OR groups). The oxidation of isopropanol to acetone therefore seems to be faster in the presence of Hf or Ta, by this very rough comparison of nmr spectra.

On the other hand, cumyl hydroperoxide appears to be much less stable in the presence of $Ti(O\underline{t}Bu)_4$ than $Zr(O\underline{t}Bu)_4$ at room temperature. The ^{17}O nmr of a mixture of 0.8 equivalents of cumyl hydroperoxide and 1.0 equivalents of $Ti(O\underline{t}Bu)_4$ appears on the bottom of Figure 70. Again, the large 268 ppm band is assigned to Ti-OOR and the band at 44 ppm to free ROH, but the pattern of downfield peaks is different from the $Ti(O\underline{i}Pr)_4$ spectrum on the top of Figure 70. The 546 ppm band is much smaller, perhaps reflecting steric hindrance to the formation of an oxo-bridged dimer $(\underline{t}BuO)_3Ti\text{-}O\text{-}Ti(O\underline{t}Bu)_3$. The bands at 526 and 533 ppm, on the other hand, are much larger than their $Ti(O\underline{i}Pr)_4$ counterparts, reflecting the increased stability of $Ti\text{-}OC(Me)_2Ph$ with respect to a μ-oxo dimer. We have no assignment for the sharp peak at 60.1 ppm, and more experiments are needed

to elucidate the hydroperoxide decomposition pathway.

Figure 70. Titanium tetraalkoxides + Cumyl hydroperoxide, $CDCl_3$.

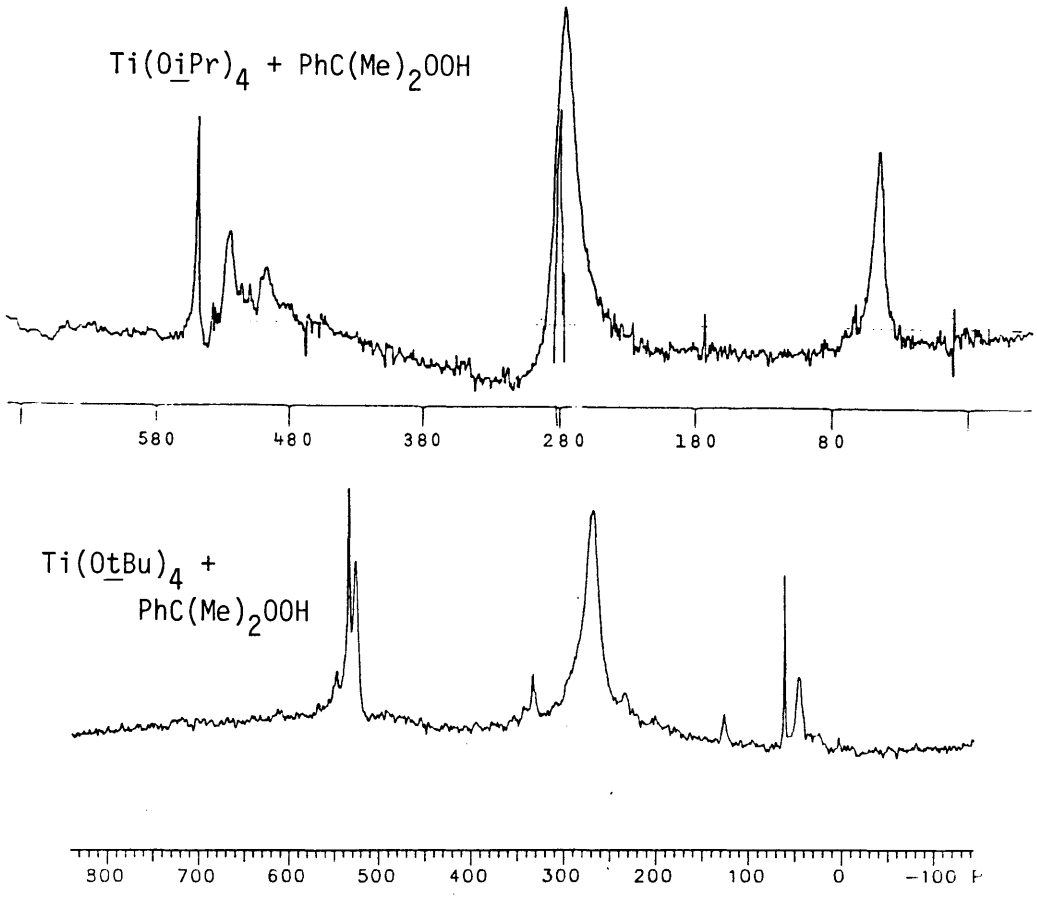

Finally, we come to the rather anticlimactic spectra of Ti-tartrate plus cumyl hydroperoxide, displayed in Figure 71. Because of the small binding constant of cumyl hydroperoxide for Ti(DIPT)(O<u>t</u>Bu)$_2$ (probably smaller than the value of 0.35 for TBHP), the ^{17}O nmr spectrum of a 1:1 mixture of these components is essentially that of cumyl hydroperoxide alone. Addition of 1.2 equivalents of (<u>E</u>)-2-hexen-1-ol directly to the nmr sample produced the middle spectrum of Figure 71 after a few minutes at room temperature. Note the disappearance of hydroperoxide bands, the appearance of a strong cumyl alcohol peak, and a new resonance at -11.3 ppm assigned to the epoxide oxygen of coordinated epoxy alcohol (since epoxy alcohol should be a much better ligand than <u>t</u>-butanol or cumyl alcohol). Again, we don't know the origin of the sharp band at 59.6 ppm.

Figure 71. ^{17}O NMR; Ti(DIPT)(O$\underline{t}$Bu)$_2$ + Cumyl hydroperoxide, $CDCl_3$.

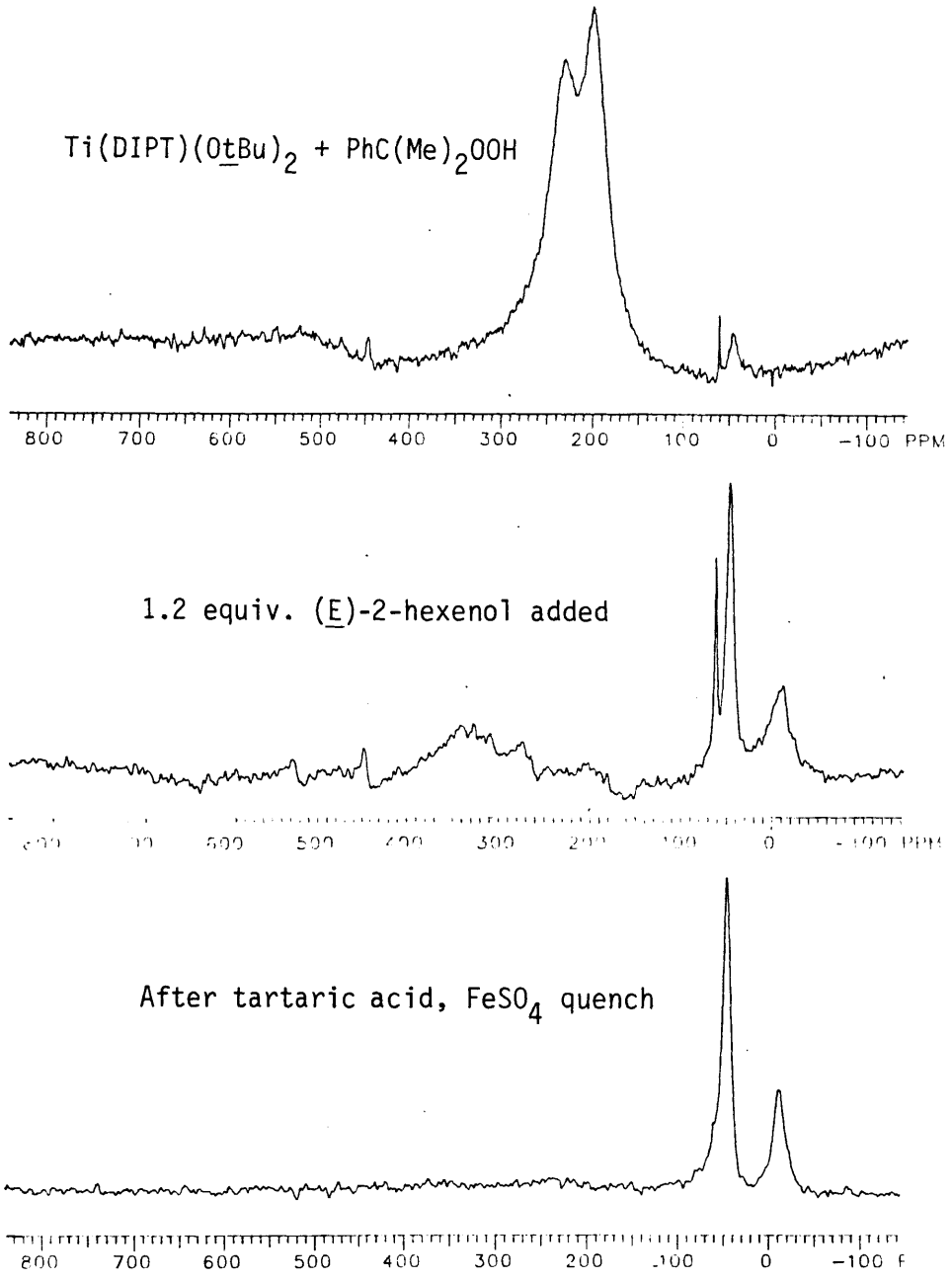

This asymmetric epoxidation reaction in the nmr tube was quenched by addition of 1 mL of aqueous $FeSO_4$/tartaric acid solution with vigorous shaking. The $CDCl_3$ layer was then removed by pipette and filtered into another nmr tube, which gave the bottom spectrum of Figure 71. Only cumyl alcohol (44.1 ppm) and free epoxy alcohol (-12.5 ppm) are found.[109]

Thus, we see that coordination of cumyl hydroperoxide to $Ti(OR)_4$ results in only a modest downfield shift of 50-70 ppm with no resolution of the different oxygen atoms. For tantalum, no chemical shift difference is seen at all between bound and free cumyl hydroperoxide, merely the coalescence of the signal to one broad peak upon coordination. Binding to $Zr(OR)_4$ causes an <u>upfield</u> shift of alkylperoxide resonances, again to a single broad band. In the absence of structurally characterized model compounds, we can draw no conclusions concerning the mode of alkylperoxide binding.

Figure 72. ^{17}O NMR of C=O-labeled DIPT and its Ti complex.

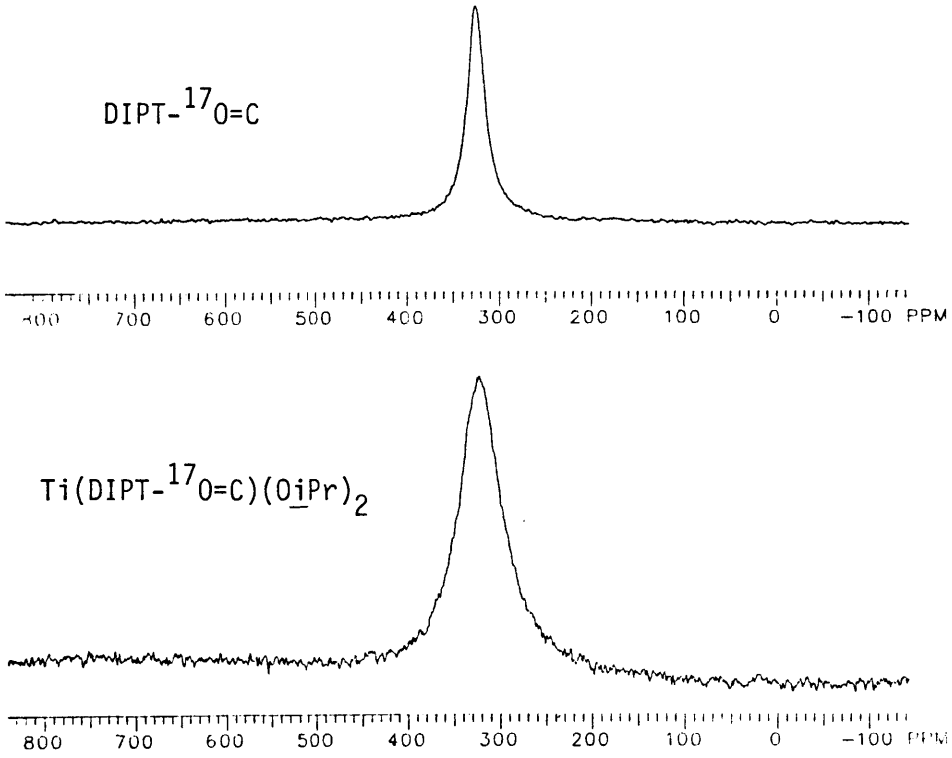

g. ^{17}O=C Labeled Tartrate

The carbonyl oxygens of DIPT were enriched in ^{17}O by exchange of tartaric acid with $O^{17}H_2$, followed by esterification. It was hoped that ester coordination to titanium could be observed by ^{17}O nmr. The spectra of DIPT-C=*O alone and its complex with $Ti(O\underline{i}Pr)_4$ are shown in Figure 72; the results are less than spectacular. The peak positions of both spectra are the same; only the linewidths differ. For free ligand, $LW_{1/2}$ = 22 ppm; for $Ti(DIPT)(O\underline{i}Pr)_2$, $LW_{1/2}$ = 48. This does not constitute definitive proof of the coordination of ester carbonyl oxygens to titanium in solution.

Table 44. ^{17}O NMR.

Entry	Sample	Peak Position	$LW_{1/2}$ (ppm)	Notes
Standards				
1	Ether	0.0	5	
2	D_2O	-15.5	2	
3	iPrOH	21.7	11	
4	Cumyl alcohol	44.5		
5	Benzyl alcohol $-^{17}OH$	-6.8	4.5	
6	DIPT-^{17}OH	-20.6	19	
7	Di-l-menthyl-(2R,3R)-tartrate	-18.7	25	
8	Di-l-menthyl-(2S,3S)-tartrate	-18.1	24	
8	Ethyl Lactate $-^{17}OH$	-7.1		
9	Ethyl Perydromandelate-^{17}OH	-10.3	10	Hydroxyl
		142	23	-C(O)-OEt
		324	10	-C(O)-OEt
10	Ph-C$^{17}O_2$H	220	6	-C(O)-OH
		892	17	-C(O)-OH
11	DIPT -C(^{17}O)-OiPr	325	18	
Metal Alkoxides				
12	Ti(OtBu)$_4$	288	8	
13	Ti(OiPr)$_4$	279.5	6	
14	Ti(OEt)$_4$	252	31	weak signal
15	Ti(OnBu)$_4$	245	ca. 40	very weak
16	Ti[OCH(CF$_3$)$_2$]$_4$	212	18	
17	Zr(OtBu)$_4$	209	19	
Tartrate-^{17}OH Complexes				
18	Ti(*DIPT)(OiPr)$_2$	252, 164		$CDCl_3$
		277, 161		C_6D_6
19	Ti(*DIPT)(OtBu)$_2$	229, 165	133	325°K
20	Ti$_2$(*DIPT)(OiPr)$_6$	231, 164		318°K
21	Ti(*DMnT)(OiPr)$_2$	285, 140		CD_2Cl_2
22	Ti(*DMnT)(OEt)$_2$	304, 154		CD_2Cl_2
23	Ti(*DNBnT)(OiPr)$_2$	196		295°K
		279, 164	34, 64	320°K
		264, 146	31, 74	310°K
Tartrate-^{17}O=C Complexes				
24	Ti(*DIPT)(OiPr)$_2$	323	42	$CDCl_3$
		330	44	Pentane solvent

Table 1. Continued.

Entry	Sample	Peak Position	$LW_{1/2}$ (ppm)	Notes
Benzyl Alcohol-^{17}OH Complexes				
25	$Ti(*OBn)_4$	235	98	Molecularity = 1.76
26	$Ti(O\underline{t}Bu)_3(*OBn)$	221, 202	13, shoulder	Monomer
27	$Ti(O\underline{t}Bu)_2(*OBn)_2$	223	23	Monomer
28	$Ti(DIPT)(*OBn)_2$	278	25	
29	$Ti_2(\#300\#)_3(O\underline{t}Bu)(*OBn)_4$	276	18	
Ethyl Lactate-^{17}OH, 18 Complexes				
30	1:1 $Ti(O\underline{i}Pr)_4$:**18**	215	39	
31	1:2 $Ti(O\underline{i}Pr)_4$:**18**	214	37	
32	$Ti(O\underline{t}Bu)_{3.7}(\underline{\mathbf{18}})_{0.3}$	214	23	
33	$Ti(O\underline{t}Bu)_{2.5}(\underline{\mathbf{18}})_{1.5}$	ca. 221	48	
34	$Ti(OEt)_3(\underline{\mathbf{18}})$	223	31	
35	$Ti(DIPT)(O\underline{t}Bu)_2$ + **18**	282	90	
36	$Ta(O\underline{i}Pr)5$ + **18**	ca. 178	76	

10. IR Spectroscopy of Deuterium-Labeled Alkoxides

Since our model studies for ^{17}O nmr were not completely satisfying, we desired another method of distinguishing bridging from terminal alkoxides in solution. The availability of Fourier transform IR spectrometers able to obtain difference spectra prompted us to explore the changes in C-H bending modes accompanying substitution of deuterium for hydrogen on the carbinol carbon of secondary alkoxides. We anticipated that the H-D (or D-H) difference spectra for terminal alkoxides would be different from bridging alkoxides. By "H-D" or "difference" spectrum, we mean the subtraction of the IR spectrum of the deuterium-labeled complex (labeled at only one site, such as the methine proton of isopropanol) from that of the same molecule under the same conditions but containing unlabeled (protio) alkoxide.

Furthermore, we hoped to be able to show that the technique could be applied for any single alkoxide to a variety of d^0 metal complexes. For example, if a titanium complex containing only terminal isopropoxide groups were prepared and its difference spectrum measured, we thought it possible that a vanadium or hafnium complex containing only terminal isopropoxides would show a very similar H-D spectrum. By the same token, a purely bridging alkoxide would have a characteristic difference spectrum that, if observed in another structure containing the same alkoxide, would signal the presence of exclusively bridging modes of complexation.

We have not progressed very far in this endeavor, but our initial results are encouraging. 4-Heptanol-4-d was prepared by reduction of 4-heptanone with $LiAlD_4$. Deuterium substitution is indicated in the IR by C-D stretching bands centered at 2120 cm^{-1}. Titanium tetra-4-heptoxide, $Ti[OCH(C_3H_7)_2)]_4$, and its d-labeled analogue were prepared by the quantitative reaction of the alcohols with $Ti(NMe_2)_4$. The H-D difference spectrum of the tetraalkoxides is plotted in Figure 73, along with the difference spectrum for the alcohols. Titanium tetra-4-heptoxide is a monomer in solution, as reported by Mehrotra.[79]

The Ti-tartrate complexes of 4-heptoxide, $Ti(DIPT)[OCH(C_3H_7)_2]_2$ and $Ti(DIPT)[OCD(C_3H_7)_2]_2$, were then prepared by reaction of the tetraalkoxides with $Ti(DIPT)_2$. A good example of the difference spectrum technique is provided by Figure 74, showing the protio, deuterio, and H-D difference spectra together. Note that the C=O stretching pattern is the same as observed for

Figure 73. H-D Difference IR spectra for methine substitution in 4-heptanol and titanium tetra-4-heptoxide, CH_2Cl_2.

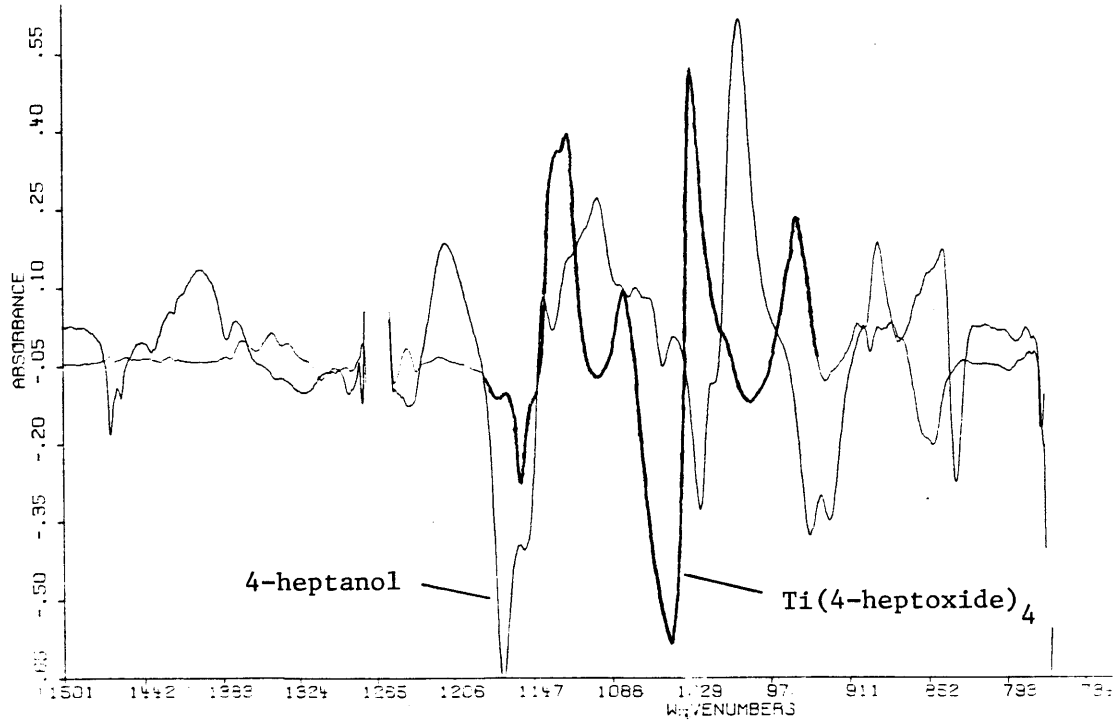

Figure 74. H-substituted, D-substituted, and H-D difference spectra of Ti(DIPT)(4-heptoxide)$_2$ in CH_2Cl_2. Asterisks mark the difference IR plot.

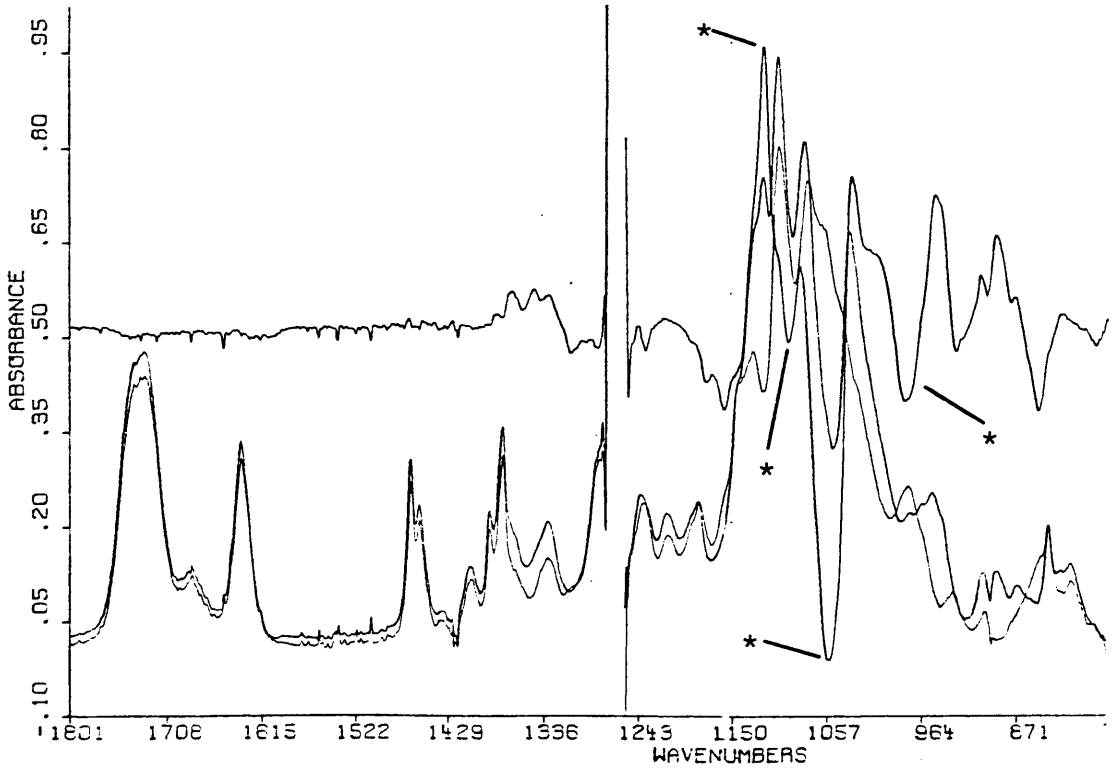

other Ti-tartrates in CH_2Cl_2, and is the same for both samples (deuterium substitution should have no effect on carbonyl stretching).

Overlaying the H-D spectrum for the titanium tetra-4-heptoxides with that of the Ti-DIPT bis-4-heptoxides shows them to be virtually identical (Figure 75), despite the fact that titanium is bound by tartrate in one case and only by 4-heptoxide ligands in the other. This provides evidence in the solution phase that 4-heptoxide occupies a terminal position in the $Ti(DIPT)[OCH(C_3H_7)_2]_2$ structure.

Figure 75. H-D Difference IR spectra for Ti(4-heptoxide)$_4$ (a), and Ti(DIPT)(4-heptoxide)$_2$ (b).

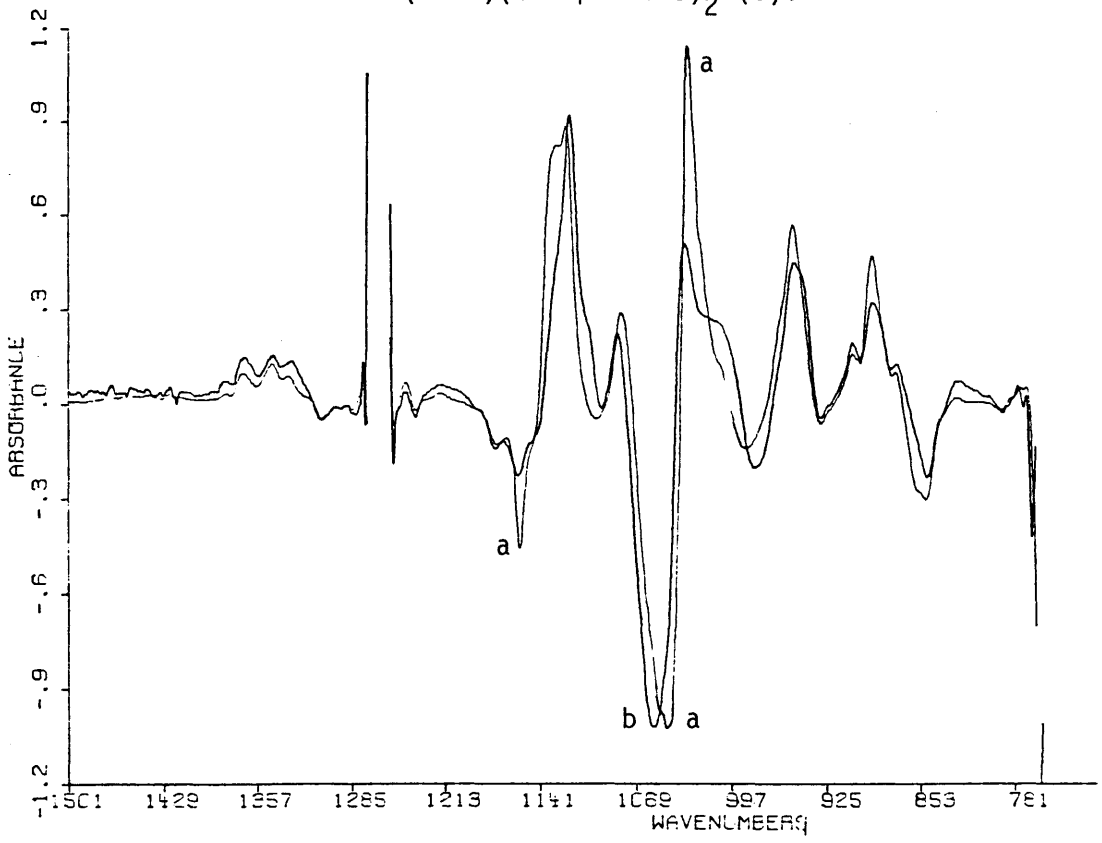

Since Ti(O$\underline{i}$Pr)$_4$ is largely a monomer, an identical experiment was performed with isopropanol-2-d, obtained from KOR Isotope Laboratories. The overlay of H-D difference spectra for Ti(O$\underline{i}$Pr)$_4$ and Ti(DIPT)(O$\underline{i}$Pr)$_2$ is displayed in Figure 77, again showing a good match, though not as close as the 4-heptoxide case (perhaps because of the small amount of oligomeric material present in Ti(O$\underline{i}$Pr)$_4$).

Figure 76. H-D Difference IR spectra for $Ti(O\underline{i}Pr)_4$ (a), and $Ti(DIPT)(O\underline{i}Pr)_2$ (b).

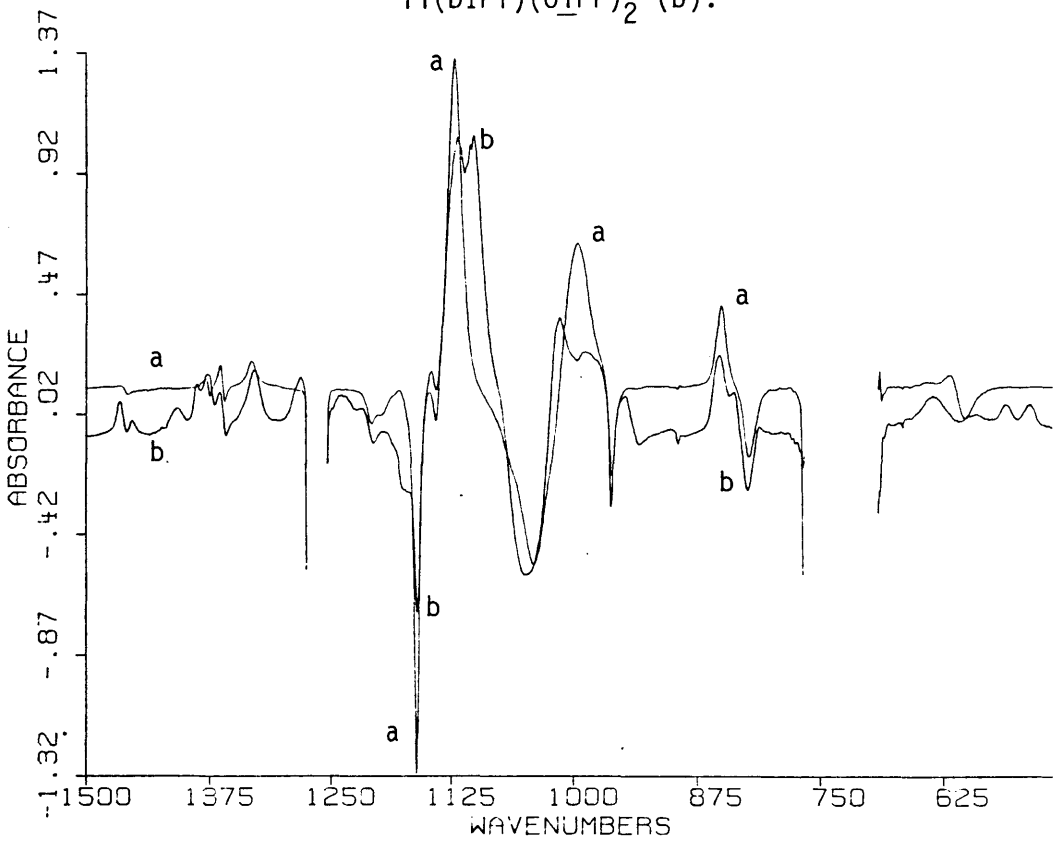

The difference spectra of titanium tetraisopropoxide and titanium tetra-4-heptoxide are not the same, as shown in Figure 77. Since the experiment measures differences in C-H and C-D bending modes, which are subject to interactions with adjacent substituents, we would not expect isopropoxide and 4-heptoxide to give the same pattern. On the other hand, 4-heptoxide and, say, 5-nonoxide ligands should produce similar H-D difference spectra.

To complement the observation of a reproducible terminal secondary alkoxide pattern, we have prepared the trimeric compound $Zr(O\underline{i}Pr)_4$, with deuterium substitution at the isopropyl methine position. If our hypothesis is correct, the H-D spectrum of $[Zr(O\underline{i}Pr)_4]_3$ should be much different than that of $Ti(O\underline{i}Pr)_4$. Indeed, an overlay of the two shows them to have few features in common (Figure 78).

Figure 77. H-D Difference IR spectra for $Ti(O\underline{i}Pr)_4$ (a), and $Ti(4\text{-heptoxide})_4$ (b).

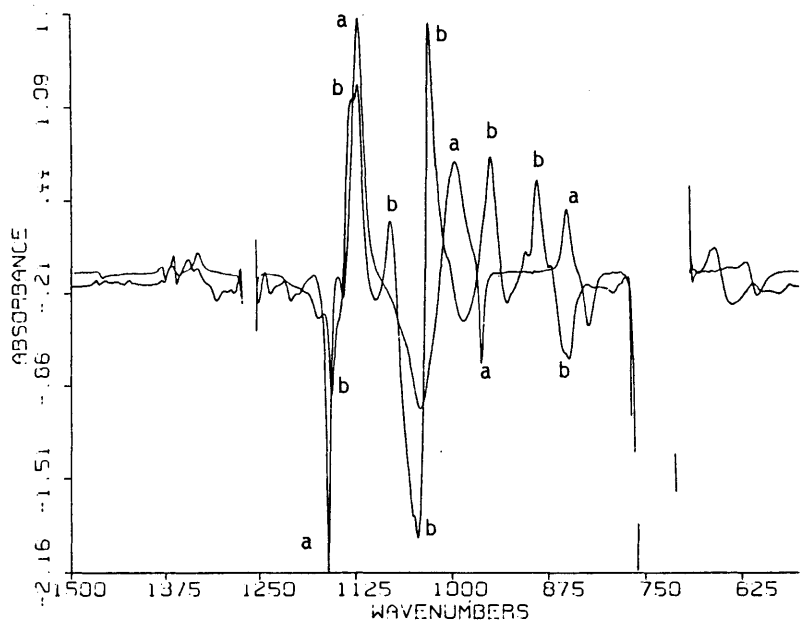

Figure 78. H-D Difference IR spectra for $Ti(O\underline{i}Pr)_4$ (a), and $Zr(O\underline{i}Pr)_4$ (b).

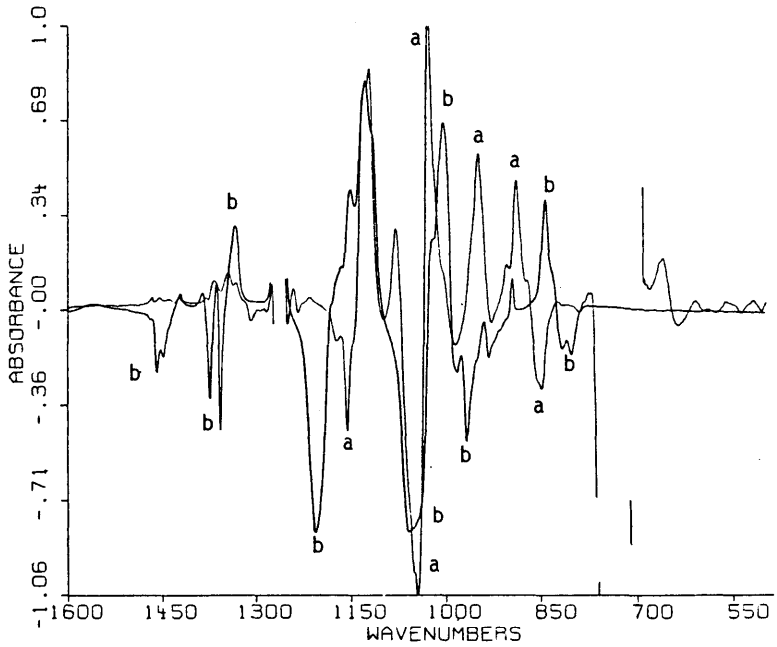

Many potential applications can be seen because the concept of "model compounds" takes on a new meaning in this experiment. For example, rather than having to synthesize a ligand model for tartrate (that looks and acts as much like tartrate as possible, but isn't), tartrate itself serves as its own model. The problem is changed to finding a tartrate complex of known structure with a d^0 transition metal. In many cases, this will be easier than preparing ligand analogues, the complexes of which have to be structurally characterized anyway.

11. Conclusion

We list here the most important evidence supporting our assignment of **14** as the structure of the asymmetric epoxidation catalyst in solution, as well as in the solid state.

For the following four reasons, the active catalyst is believed to be a dimer:

a. The average molecularity of $[Ti(tartrate)(OR)_2]_x$ in solution is 2.

b. NMR measurements in different solvents show that a single structure comprises at least 80% of the total mixture in solution. Therefore, this major structure must be a dimer.

c. NMR spectra also identify at least one of the minor species in solution as the 2:1 Ti:tartrate complex. This material has been shown to be a much more sluggish epoxidation catalyst than the 2:2 complex. Species containing more tartrate than titanium have also been shown to be poor catalysts for epoxidation of allylic alcohols.

d. The pseudo-first order rate of epoxidation varies linearly with Ti-tartrate concentration over a 10-fold range, suggesting that the active catalyst does not participate in a bimolecular equilibrium reaction with a species of different aggregation state. That is, the dominant dimeric species does not give rise to a trace amount of active reagent by dissociation to two monomers or by association to higher aggregates. The only way for a non-dimeric species to be the epoxidation catalyst is for it to be present in trace amounts and for it to be inert to aggregation equilibria. The existence of such a substitutionally moribund Ti-tartrate complex is very unlikely. Ti-tartrate is, after all, a Ti(IV) tetraalkoxide, and tartrate ligands are subject to exchange among metal atoms just like mono-

dentate alkoxides, albeit at a slower rate. (Indeed, the temperature dependent nmr spectra of $Ti(DET)(OEt)_2$ suggest that bimolecular tartrate exchange reactions can be quite fast.) A Ti-tartrate complex inert to equilibration with other structures in solution would probably be slow to exchange monodentate alkoxides as well, and thus would be a poor epoxidation catalyst.

So, we have concluded that the dominant species in solution is a dimer and the active catalyst is a dimer; there is no evidence that they are the same molecule. There always remains the possibility that a trace amount of a dimer of different structure is the actual asymmetric epoxidation catalyst, in the same way that a minor component of the asymmetric hydrogenation reaction mixture was found to be the active species.[110] But unlike asymmetric hydrogenation, the structure of the major species is consistent with (or at least allows the rationalization of) the results of asymmetric epoxidation. Because we have no reason to say that the observed dimer is not the active catalyst, we shall proceed on the assumption that it is the active catalyst.

For the following reasons, the catalyst structure in solution is believed to be the same as indicated by the x-ray crystal structures:

a. NMR and IR spectra, including the observation of fluxional equilibration and different exchange rates of the two alkoxides with free alcohol, are consistent with such a structure.

b. ^{17}O NMR spectra show resonances of two different tartrate alkoxide oxygens and only one type of monodentate alkoxide, consistent with the tartrate-bridged dimer structure and inconsistent with the ten-membered ring structure **321** (Figure 19) which has only terminal alkoxide bonds.

c. Difference FTIR spectra of deuterium-labeled alkoxide complexes show the presence of only terminal isopropoxides in $Ti(DIPT)(O\underline{i}Pr)_2$, ruling out an isopropoxide-bridged structure analogous to **20** (Fig. 19).

Section III.

Proposed Mechanism

A. Introduction

The proposed catalyst structure, **14**, is reproduced below. By virtue of the C_2 symmetry axis, each titanium center is equivalent. A striking feature of the structure is that the two axial monodentate alkoxides are found on the same side of the Ti_2O_2 core, which would allow an allylic alcohol and alkylperoxide bound to two different Ti atoms to reach each other. Since this is a property not shared by the other catalysts we have considered (such as $Ti(O\underline{i}Pr)_4$ alone or 2:1 Ti-tartrate) and since 2:2 Ti:tartrate is uniquely effective, such a bimetallic scheme seems an attractive possibility. At this point, however, we are not able to see how enantioselectivity and kinetic resolution might be achieved from such a mechanism. We have recently returned to a closer inspection of the binuclear epoxidation scheme, and we are renewing our attempts at proving whether or not it is viable.

We now consider how the chirality of tartrate is expressed if the reaction occurs on one metal center. This is most clearly appreciated when either Ti atom is viewed from a perspective in the plane of the Ti_2O_2 core. Structure **15** in Figure 79 shows this perspective for L-(+)-tartrate. Notice how the tartrate ester groups provide steric bulk in a pseudo-C_2 relationship by blocking two diagonal quadrants of space around the metal center. A D-(-)-tartrate complex has the mirror-image local C_2 symmetry.

Figure 79. Pseudo-C_2 arrangement of ester groups about titanium.

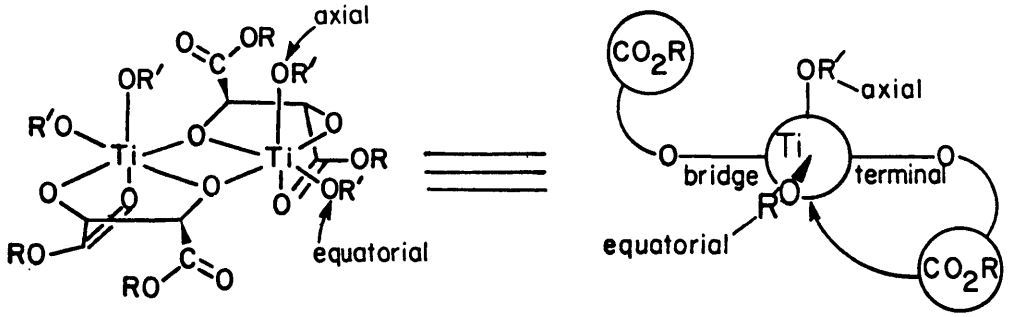

14 15

Allyl alcohol is epoxidized under catalytic conditions in 89% ee and 90% yield at 0°C,[111] representing a value of 1.58 kcal/mole for the

difference in energies of the two competing diastereomeric transition states. Placing alkyl groups at four of the five possible positions of allyl alcohol results in little or no loss in enantioselectivity (Tables 1 and 2). This suggests that allyl alcohol is subject to a set of enantioselective interactions that are not substantially perturbed by substitution on the carbon skeleton. Therefore, at least some of these controlling interactions cannot be steric in nature. We will start, however, by taking a lock-and-key analysis as far as possible, since steric effects are easier to understand.

B. "Mapping" the Transition State

We have attempted to define the steric aspects of selectivity by selected variations in the structures of allylic alcohol, tartrate, and hydroperoxide.

The most spectacular of these effects, of course, is the result of substitution at C1 of the allylic alcohol. Each enantiomer of secondary allylic alcohols is reactive with only one enantiomer of tartrate catalyst. Thus it is the C1 position that must experience the greatest steric crowding. Since relative rates of kinetic resolution increase dramatically with the size of the tartrate ester group, the steric interactions at C1 probably involve the tartrate ester functionality.

Recall also that substitution of chiral fragments for hydrogen at the C2 and (Z)-C3 positions also results in good kinetic resolution, but most chiral substituents at (E)-C3 are not kinetically resolved by asymmetric epoxidation. Thus, in the transition state the allyloxy moiety experiences some crowding at the C2 and (Z)-C3 positions, but not at the (E)-C3 site.

A similar set of experiments was performed by Schweiter for asymmetric epoxidation of a series of prochiral substrates having tert-butyl substituents at each position of the allylic alcohol skeleton;[3j] the results appear in Table 45.

Consistent with the kinetic resolution results, the (E)-C3 position was found to be the least sensitive to steric hindrance (substrate **23**), (Z)-C3 the most sensitive (**25**), and C2 moderately encumbered (**24** and **25**). The poor kinetic resolution observed when a t-butyl group is placed at the carbinol carbon was quite surprising, since a cyclohexyl group causes no

Table 45. Asymmetric epoxidation of t-butyl substituted allylic alcohols.[3j]

Substrate	$Ti(OR)_4$/(+)-tartrate	% e.e.	Reaction Time	Major Product Enantiomer
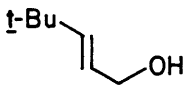 **23**	$Ti(OiPr)_4$/DET	95	96 h	2S
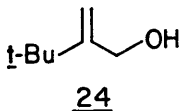 **24**	$Ti(OtBu)_4$/DET	85	15 h	2S*
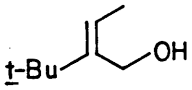 **25**	$Ti(OtBu)_4$/DET	60	15 h	2S*
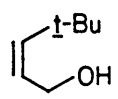 **26**	$Ti(OiPr)_4$/DET $Ti(OtBu)_4$/DET	25 25	192 h 192 h	2S 2S

Substrate	$Ti(OR)_4$/(+)-tartrate	% e.e. Recovered Substrate	% Completion
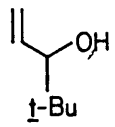 **27**	$Ti(OiPr)_4$/DET	0-10	25-60
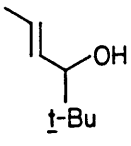 **28**	$Ti(OiPr)_4$/DET $Ti(OiPr)_4$/DMT	0 0	40-80

*The major enantiomer (predicted to be 2S by the tartrate selection rule of Figure 1) has been correlated with a chiral alcohol, the absolute configuration of which was assigned by the application of Prelog's (reference 3f) and Eliel's (Eliel, E.L.; Lynch, J.E. Tetrahedron Lett. 1981, 2855-2858) rules of enantioselective addition to carbonyl groups. The three enantioselection rules agree on the 2S assignment, but a rigorous correlation has not yet been performed.

problems.

In order to explore the steric environment of the C1 position in greater detail, we attempted the kinetic resolution of (3S)-4-phenyl-1-penten-3-ol, **29**, at -20°C with Ti-(+)-DIPT (see below). The (3S) configuration is the faster-reacting one with (+)-tartrate, so this experiment explores the kinetic resolution at C4 within the favored epoxidation transition state of secondary allylic alcohols.

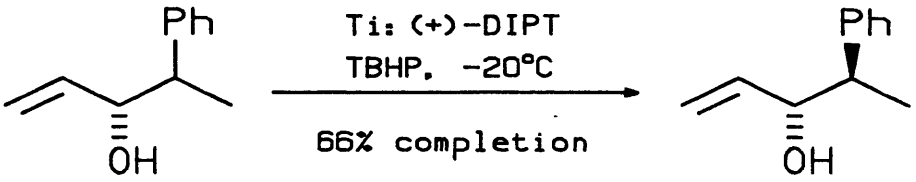

29 71% de

As detailed in the experimental section, a relative rate of 2.15 was observed for kinetic resolution of the phenethyl center, translating to a difference in energies of diastereomeric transition states of only 0.38 kcal/mole, a very mild steric effect. The (4S)-epimer was the faster-reacting configuration.

The ability of C4 (to the carbinol carbon in secondary allylic alcohols) to tolerate secondary but not tertiary substitution indicates that there is one particular area of space that is blocked near that center in the transition state. Primary and secondary groups can fit by placing a hydrogen atom in this region, but tertiary substituents cannot.

Consider Pedersen's observation that trityl hydroperoxide is an effective oxidant in asymmetric epoxidation.[91] We assume, in accordance with the theoretical studies mentioned in the introduction, that both oxygens of the alkylperoxide are associated with titanium in the transition state (and, as shown by equilibrium constants and IR spectra, possibly in the ground state as well). Therefore, there must be a lot of room available in some area around the metal if the trityl group is to fit. This also suggests that steric bulk in the hydroperoxide alkyl group is an important element for success of the reaction, for there appears to be not all that much room available around certain positions of the allylic alkoxide. If the alkylperoxide group were smaller, it might allow the allylic alkoxide to occupy the open area to the detriment of enantioselectivity and kinetic

resolution.

In undesired support of these ideas, we obtained poor kinetic resolution of phenethyl hydroperoxide in the asymmetric epoxidation reaction, with relative rates k_{fast}/k_{slow} not greater than 1.44. A list of results appears in the experimental section. Had the trityl hydroperoxide result been known at the time, this experiment might not have been attempted.

We also tried n-butyl hydroperoxide in the asymmetric epoxidation of (E)-α-phenylcinnamyl alcohol and (E)-2-hexen-1-ol. As expected, asymmetric induction was reduced with the smaller hydroperoxide: 92% ee for the former and 75% ee for the latter, in epoxidations at -20°C using 2:2.4 $Ti(OiPr)_4$:DIPT in CH_2Cl_2.

C. Oxygen Transfer

The two monodentate alkoxides on a titanium atom in structure **14** occupy axial and equatorial ligand sites. The replacement of these nonreactive ligands by the epoxidation reactants can place either allylic alkoxide or alkylperoxide in the axial position. Space-filling molecular models of the crystal structure **13a** and of **14** indicate that O^1 of the alkylperoxide ($R-O^2-O^1-Ti$) should occupy the equatorial position to give the alkyl group enough room to accomodate the steric bulk of a trityl group on coordination of O^2. We believe that the bound carbonyl of **14** is released from the metal in the transition state in response to the greater steric congestion and greater electron donating ability of bidentate peroxide.

In considering the orientation of the reactants for oxygen transfer, we make two additional assumptions:

(1) the peroxo oxygen distal to the alkyl group (O^1) is transferred to the nucleophilic olefin,[12f, 33] and (2) the most favorable approach of olefin to the coordinated peroxide is along the axis of the O-O bond being broken.

With alkylperoxide in the equatorial site, the O-O bond can be oriented in the equatorial plane (the plane of the Ti_2O_2 ring), perpendicular to that plane, or at an intermediate angle. For a given coordination geometry, the possible peroxide orientations will be restricted to those that can accomodate a near linear attack by olefin on the O-O bond.

In Section I, we mentioned Hanzlik's observation that the secondary deuterium isotope effect in epoxidation of styrene by peracid was greater for the β-carbon than the α-carbon, indicating that Cβ-O bond formation is faster than C_α-O bond formation (k_D/k_H = 1.22 for β,β-d_2 and 1.01 for α-d).[53] As this is a crucial point in our detailed mechanism, we performed a similar experiment for the epoxidation of (E)-2-decen-1-ol by Ti(DIPT)(O<u>i</u>Pr)$_2$ + TBHP, Ti(O<u>i</u>Pr)$_4$ + TBHP, and <u>m</u>CPBA. We also tested the epoxidation of (E)-2-decenyl acetate by <u>m</u>CPBA. The results, summarized below in Table 46 and described in detail in the experimental section, showed small but equal (within experimental error) rate accelerations when deuterium was substituted for hydrogen at C2 or C3. Thus, bond formation to C2 and C3 occurs simultaneously, and we assume that the midpoint of the C=C bond is aligned with the O-O axis, to make for an extended linear transition state.

Table 46. Secondary deuterium isotope effects in epoxidation reactions.

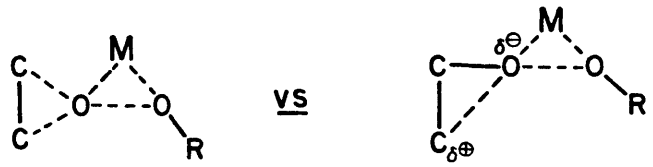

Substrate	Oxidant	D Position	k_D/k_H
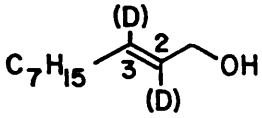	Ti–DIPT–TBHP	C2	1.017, 1.002
		C3	1.043, 1.044
	Ti(OiPr)$_4$–TBHP	C2	1.031, 1.029
		C3	1.049, 1.056
	<u>m</u>CPBA	C2	1.064, 1.091
		C3	1.106, 1.052
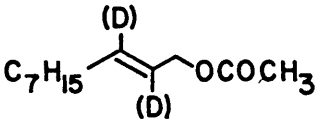	<u>m</u>CPBA	C2	1.050, 1.056
		C3	1.029, 1.038

Recall that the tartrate ligands are believed to impose steric congestion in a C_2-like relationship on two of the four quadrants of space surrounding the Ti center. We suggest that the reactants in the linear epoxidation transition state are constrained on steric grounds to occupy the open quadrants around the Ti atom. With the use of space-filling models, we rule out a transition state configuration in which the peroxide O-O bond lies in the equatorial plane, since that would place the olefin also in the plane and result in severe steric crowding. A model in which the peroxide O-O bond is nearly perpendicular to the equatorial plane appears to be the least crowded one, resulting in a "meridional" (linear) alignment of allylic alkoxide and alkylperoxide oxygen atoms and a roughly octahedral titanium coordination geometry as represented in structure **16**.

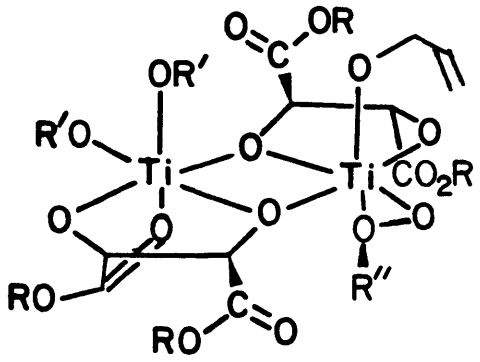

16

For the meridional arrangement of **16**, there are four allylic alkoxide conformations that allow the olefin to attack the peroxide in an S_N2 fashion; these are depicted in Figure 80. The C_2 environment of the catalyst serves to disfavor structures **16c** and **16d** by virtue of a steric interaction involving a tartrate ester group and C1 of the allylic alkoxide.

The two remaining conformations, **16a** and **16b**, present opposite enantiofaces of the olefin to the peroxide O-O bond, so the source of enantioselectivity is not identified by ruling out **16c** and **16d**. Notice, however, that the high level of kinetic resolution at C1 is explained by the selection of arrangements **16a** or **16b**, in which substituent R' is pointed away from the catalyst into a relatively open region of space,

Figure 80.

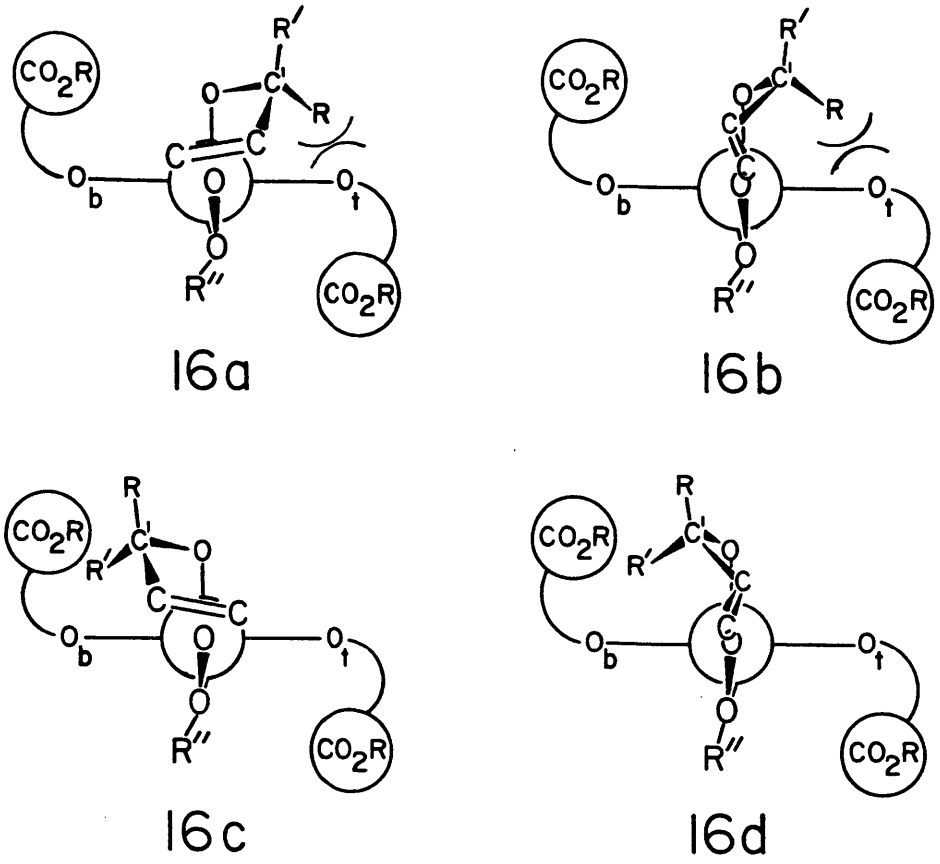

while R is forced into an area occupied by a tartrate ligand. When R = H, this steric interaction is small, but when R = alkyl, structures **16a** and **16b** become unfavorable. The epoxidation of these slower reacting isomers of secondary allylic alcohols (in which R = alkyl, R' = H) proceed with little diastereoselectivity.[3c,112] For the same reason, tertiary allylic alcohols also fail to undergo effective asymmetric epoxidation (e.g., entry 4 in Table 3).

Since both models **16a** and **16b** account for kinetic resolution behavior at C1, it is not, in principle, necessary for good kinetic resolution to be accompanied by good diastereofacial selectivity. Uncoupling of the two effects has been observed for (Z)-4-undecen-3-ol, **17**, which undergoes asymmetric epoxidation at a slower than usual rate to give unreacted allylic alcohol in 82% ee at 53% completion (k_{rel} = 16 at -20°C) and product epoxy alcohol with only a 4:6 ratio of erythro to threo isomers.[3c] Thus, the faster reacting enantiomer is epoxidized to approximately 20% diastereomeric excess in the abnormal direction (i.e., contrary to the

usual selection rule of Figure 1.[113] The kinetic resolution, while effective and consistent with all other cases in the absolute configuration of the slow- and fast-reacting enantiomers, is worse than usual in this case (relative rates of 50-100 are routine), so the phenomena of kinetic resolution and asymmetric epoxidation may not be entirely independent. In the language of our transition state model, the arrangement **16** represents the favored placement of allylic alcohol **17** and TBHP on the metal (as it does with most substrates), but neither conformation within that arrangement (**16a** or **16b**) is significantly favored over the other. Furthermore, it must be the Z-alkyl substituent that prevents attainment of the normal alignment of olefin to peroxide, since secondary allylic alcohols without cis-alkyl groups combine good kinetic resolution with good diastereofacial selectivity.

The observed enantioselection in all prochiral cases is consistent with structure **16a** of Figure 80 being preferred. There seems to be no steric interactions responsible for this preference, and the enantioselection is virtually the same regardless of the substitution pattern on the allylic alcohol: this is the point at which lock-and-key considerations no longer avail. We believe that a stereoelectronic factor determines which prochiral face of the olefin receives the oxygen atom by substantially favoring the reaction from the olefin orientation in **16a** over that in **16b**.

Unfortunately, identification of this putative stereoelectronic effect must be left to speculation; we have found no way to examine it directly. A simple geometric difference may be responsible: the required S_N2 approach of olefin to peroxide can be reached more easily by the allylic alkoxide conformation in structure **16a** than in **16b**. With crystal structures in hand, simple geometric effects such as this may be meaningfully evaluated by means of molecular mechanics calculations.

In Section I we cited two other possible modes of stereoelectronic selection that have been suggested in the literature: a difference between spiro and planar transition states (in this case, model **16a** can achieve the spiro orientation and **16b** the planar, so spiro would have to be preferred to rationalize the observed enantioselectivity); and alignment of a lone pair with the olefin π^* orbital.[3e] No support for either of these suggestions has been offered by the theoretical community, either in the litera-

ture or in private communications. Indeed, Bach's calculations show forcefully that no selectivity can be expected on a spiro/planar basis.

Another simple and attractive suggestion has been made to us independently by Professors A. Eschenmoser and J.K. Whitesell.[114] Assuming that the initial product of oxygen transfer is an epoxy alkoxide with the epoxide oxygen bound to titanium, they note an essential difference in the spiro and planar orientations of olefin and alkylperoxide. As shown below, oxygen transfer from a spiro geometry (as in transition state **16a**) yields an epoxide with a lone pair already directed toward the titanium atom, perfectly disposed for dative coordination. The direct product from the planar orientation involves a Ti atom that lies well away from the epoxide oxygen lone pairs, so that the incipient epoxy alkoxide moiety can only be envisioned as bound to the metal center in a badly distorted fashion; this should disfavor transition state **16b**. To the extent that the transition state resembles the bound epoxy alkoxide product, this difference provides a compelling rationale for oxygen transfer through a spiro geometry in the metal-catalyzed case. It appears, however, that the transition state is an early one, resembling reactants more than products.[115]

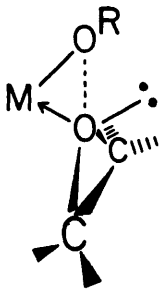

spiro

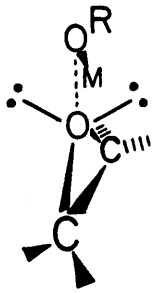

planar

Finally, the different allylic alcohol conformations of **16a** (O-C-C=C dihedral angle of approximately 30°) and **16b** (dihedral angle ≅ 120°) may be responsible for the enantioselection. It has been suggested to us by several groups that the olefin in conformation **16b** is deactivated toward reaction with coordinated peroxide with respect to **16a** by virtue of an overlap of the allylic C-O bond with the olefin π system (maximum when the O-C-C=C dihedral angle = 90°).[116] Bach has calculated that the initial four-electron interaction that drives the molecular orbital reorganization

in epoxidation is adversely affected by an allylic alkoxide dihedral angle of 90°.[17] Professor Andrzej Cieplak has suggested that an overall shift of olefin electron density into the allylic C-O bond results from this alignment (citing reference 116b). Professor K.N. Houk has published ab initio calculations that support this latter view.[117]

Hill and Sharpless have tested this proposition by measuring the relative rate of epoxidation of two allylic ethers that are similar in steric hindrance but have different O-C-C=C dihedral angles. The dihedral angle of olefin **18a** is 178° and for olefin **18b** it is 58° (by molecular mechanics calculations). Substrate **18b**, having a dihedral angle closer to 90° , is expected to be epoxidized at a slower rate by peracid. Indeed, it reacts at a rate 13 times slower than **18a** at room temperature,[118] representing a value of approximately 1.5 kcal/mole for the difference in energies of activation for epoxidation of the two substrates.

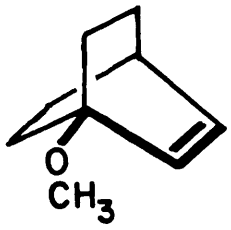

18a

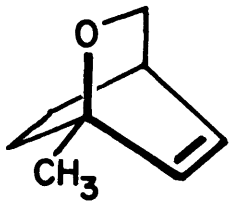

18b

Whatever the ultimate source of stereoelectronic selection, the identification of **16a** as the favored transition state model allows us to rationalize many other features of the asymmetric epoxidation reaction.

Kinetic resolutions at positions other than C1 of the allylic alcohol can be explained using model **16a**.[3d,k] For example, 2-(1'-phenethyl)-2-propen-1-ol, **19**, should adopt a conformation in which the hydrogen substituent on the chiral center is directed toward the sterically demanding Ti-tartrate catalyst as shown below. Based on the resulting steric interactions of the phenyl (larger) or methyl (smaller) group with the olefinic moiety, structure **19a** is expected to be favored. Indeed, it is found that the S enantiomer remains in ca. 80% ee after asymmetric epoxidation of a racemic mixture of **19** with 0.6 equiv. of TBHP.

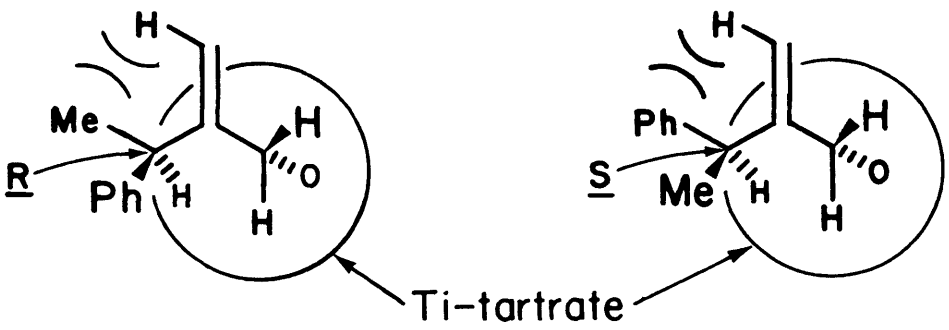

19a **19b**

Also correctly predicted by the favored transition state **16a** (and not by **16b**) is the decreased selectivity observed when the olefin has a substituent cis to the hydroxymethyl group. When the allylic alcohol is in the conformation shown in **16a** (dihedral angle = 30°), the dominant steric interaction is that of the cis substituent with the coordinated allyloxy oxygen. The interaction is small when the cis substituent is hydrogen. With substitution ofa primary alkyl in the (Z)-position, the steric interactions are evident in diminished rates but the asymmetric induction remains high. When a large group (e.g., cyclohexyl or phenyl) is present cis to the hydroxymethyl functionality, the rates diminish further and the enantiomeric excess falls off dramatically. Kinetic resolution of a (Z)-C3 substituent, as in 4-phenyl-(Z)-2-penten-1-ol, is similarly rationalized: orientation of the hydrogen atom of the (Z)-α-phenethyl group toward the allylic oxygen places either a phenyl or methyl group over the preferred olefin diastereoface. The remaining enantiomer after kinetic resolution is therefore predicted to have the S configuration, which is indeed the enantiomer isolated in 95% ee.

With our transition state model we can identify no diastereoselective interactions involving an (E)-α-phenethyl group at C3 of an allylic alcohol. Indeed, kinetic resolution at that position is found to be very poor while the facial selectivity remains high. It takes the substitution of a very large, branched structure at the (E)-C3 position to perturb the asymmetric epoxidation to a signficant extent. In such cases (entries 8 and 19 in Table 3, for example), the (E)-C3 substituent interacts with the tartrate ester group in the upper left quadrant of structure **16a**, so reducing the bulk of the tartrate ester group should help.

As yet unexplained is the poor kinetic resolution exhibited by 3-phenylpropen-3-ol (entry 16 in Table 3). A phenyl group is certainly no larger in a steric sense than a cyclohexyl group, which causes no problems in kinetic resolution (entries 4, 7, and 10 of Table 2). We therefore suspect a stereoelectronic cause, and the suggestion of Bach that olefin electron density as a function of O-C-C=C dihedral angle is important provides a possible clue. When the faster-reacting enantiomer of a secondary allylic alcohol adopts the favored configuration **16a** (for (+)-tartrate), the O-C-C=C dihedral angle is 30° and the dihedral angle with the α-substituent (C4-C-C=C) is 90°. Placement of an aryl group at C4 should have a different electronic effect than an alkyl group, though we cannot estimate its magnitude *a priori*. If the electron-withdrawing ability of an allylic substituent is the important factor, the substitution of electron-donating substituents at the *para*-position of the aryl ring would be expected to increase the effectiveness of kinetic resolution. Such an experiment has not yet been performed.

D. Orthoester Mechanism

Another possible mechanistic pathway for the asymmetric epoxidation involves the formation of an orthoester intermediate **29** from attack of an allylic alcohol on the carbonyl group of a tartrate ligand as depicted below. This pathway is kinetically indistinguishable from the allylic alkoxide pathway we have been discussing. An orthoester is presumably an intermediate in the Ti-catalyzed transesterification reaction which tartrates undergo at a rate usually much slower than that of epoxidation of an allylic alcohol.

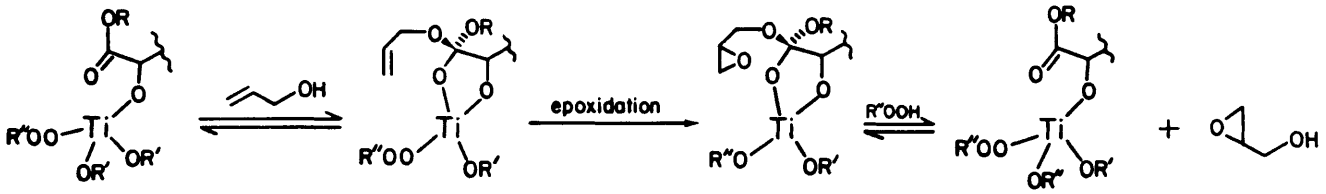

29

For epoxidation to take place through an orthoester intermediate, without transesterification being observed, requires that the ejection of the tartrate OR group from the orthoester be much slower than loss of the product epoxy alcohol from the orthoester. As an indirect test of this

idea, we prepared the digeranyl ester of L-tartrate (DGT) and subjected it to standard epoxidation conditions in the presence of an equivalent of $Ti(OiPr)_4$. The 2,3-double bond of the geranyl group was epoxidized exclusively, but at a rate far slower than asymmetric epoxidation of geraniol itself. No transesterification was observed during the reaction at -20°C. Interestingly, on base hydrolysis of the tartrate, geraniol epoxide was isolated in 95% ee in the same configuration (2S) as that formed in the standard asymmetric epoxidation.

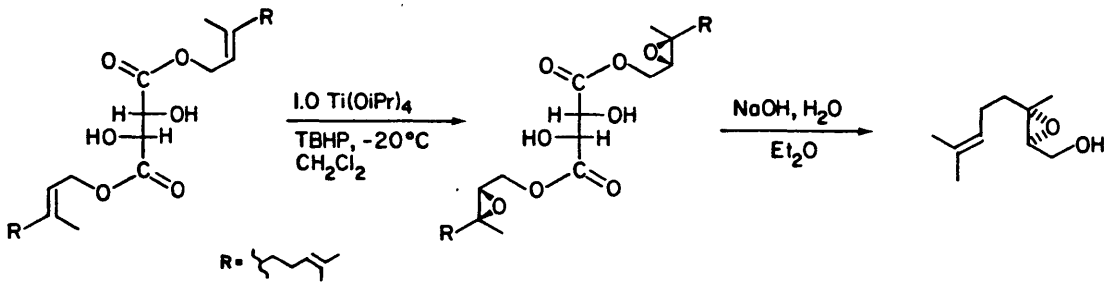

Because of the slow rate and lack of appearance of free geraniol epoxide during the DGT reaction, we do not assign a common orthoester mechanism to epoxidation of geraniol and digeranyl tartrate. Rather, we regard the DGT reaction as an example of a different mechanism altogether. The geranyl ester group, when introduced into a model of the catalyst structure appears able to reach a bound alkylperoxide without the need for an orthoester form, though we cannot identify a reason for the high enantioselectivity without further experiments. The epoxidation of allylic tartrate ester groups may prove to be a useful adaptation of the asymmetric epoxidation reaction in cases in which product epoxy alcohols are sensitive to opening, or for homoallylic alcohols which give poor enantiomeric excess in the standard procedure.

E. Asymmetric Ligands Other Than Tartrate

In reference 3j are listed the results of asymmetric epoxidations with $Ti(OiPr)_4$ and a selection of 50 chiral ligands. We have reproduced a few of these in Table 47 for discussion.

The first two entries, DET and DNBnT respectively, show good asymmetric induction in the 2:2.4 system and opposite selectivity in the 2:1 regime. Entry 3 shows that the benzyl group of the tartramide can be

replaced by a butyl group with the same general results. On the other hand, a secondary alkyl amide group is harmful (entry 4) whereas secondary tartrate ester groups perform well (DIPT and entries 5-6). So the tartramide-mediated epoxidation is more sensitive both to amide group and substrate structure.[84]

Entry 7 shows the substitution of methyl groups on the tartrate skeleton to be harmful. In a structure analogous to **13a**, these methyl groups would be in a gauche arrangement (Me-C(OTi)-C(OTi)-Me dihedral angle of approximately 60^{o}). Release of the bound ester carbonyl from the metal, as envisioned for the transition state, would tend to push the methyl groups toward an unfavorable eclipsed conformation. Replacement of the methyl groups by a four-carbon linkage would produce a 1,2-cyclohexanediol diester, which would not suffer a bad eclipsing interaction. Our prediction that such a ligand should be successful in asymmetric epoxidation is currently being tested.

Entries 8-12 show that a diol ester functionality is necessary for good asymmetric induction, but the results at the end of Table 47 show that both ester groups of tartrate are apparently not needed. In entries 13 and 14, one ester group of tartrate is replaced by a phenyl group (ligand **15**) or a cyclohexyl group (**16**) to give epoxidation in the same sense of asymmetric induction as tartrate itself. The better performance of the cyclohexyl substituent in asymmetric epoxidation is seen also in kinetic resolution (entries 15 and 16), though **16** is not as effective in this regard as tartrate.

No other single result more effectively highlights the unique activity of the asymmetric epoxidation catalyst than entry 14 in Table 47, for the IR (Figure 16) and nmr spectra (not shown) of 2:2 mixtures of **16** with $Ti(O\underline{i}Pr)_4$ indicate the presence of more than one major species in solution. In the presence of probably several complexes in roughly equal amounts, asymmetric induction remains high. Each of the Ti-ligand species could be an enantioselective catalyst, but this is unlikely when the presence of minor species in Ti-tartrate reaction mixtures cause enantiomeric excess to fall. If only one of the complexes in solution is an enantioselective catalyst, it must be a far more active catalyst as well. We suggest that this is indeed the case, and that the selective species is a complex of

Table 47. Ligands used in the epoxidation of (E)-α-phenylcinnamyl alcohol by $Ti(OiPr)_4$ and TBHP at 0°C in CH_2Cl_2.

Entry	Ligand	Ti:Ligand	% ee	C2 Configuration
1	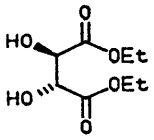	1.0:1.2	> 98	S
		1.0:0.5	80	S
2	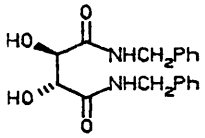	1.0:1.2	96	S
		1.0:0.5	82	R
3	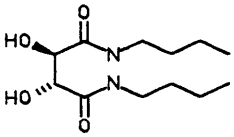	1.0:1.2	96	S
		1.0:0.5	61	R
4	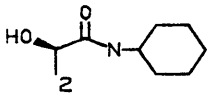	1.0:0.5	35	R
5	Di-l-menthyl-(R,R)-tartrate	1:1	70	S
6	Di-l-menthyl-(S,S)-tartrate	1:1	87	R
7	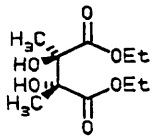	1:1	13	S
8	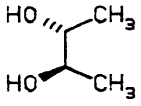	1:1.2	5	R
9	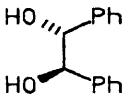	1:1	0	
10	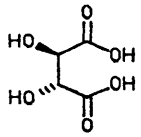	1:1	8	S
		1:0.5	1	
11	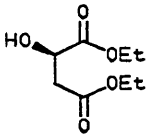	1:1	0	

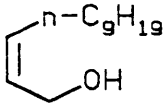

substrate

Table 47. Continued.

Entry	Ligand	Ti:Ligand	% ee	C2 Configuration
12	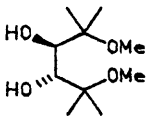	1:1.2	28	S
13	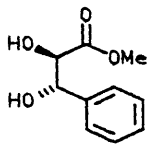	1.0:1.2	80	S
14	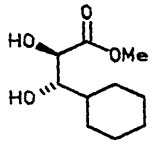	1.0:1.2	> 98	S

Kinetic resolution of (E)-cyclohexylpropenyl carbinol, 1:1.2 Ti:Ligand, -20°C.

		k_{rel}	Slower-reacting enantiomer configuration
15	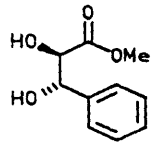	1.36	R
16	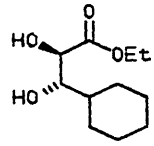	6.1	R
17	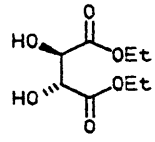	36	R

structure analogous to **14**, with the free ester groups replaced by the cyclohexyl substituent of **16**.

Having developed some ideas about the source of asymmetric induction, an understanding of the reasons for the unique kinetic activity of the enantioselective catalyst is just as important for the design of new oxidation systems. While we do not have a single explanation for the catalyst's robust behavior, we can identify three important properties possessed by structure **14** that are not all shared by any other potential catalyst:

(1) Three tartrate oxygen atoms bound per Ti center. By virtue of the electron-withdrawing ester groups, tartrate is a fairly acidic alkoxide, which serves to activate the titanium center toward peroxidic oxygen transfer. Perhaps epoxidation activity increases with an increasing number of bound tartrate oxygens, keeping two monodentate alkoxides available for exchange with hydroperoxide and allylic alcohol. Tartrates with electron-deficient ester groups should provide even more active systems if this concept is valid.

(2) A facile mechanism for monodentate alkoxide exchange. The reactants first have to reach the metal, so rapid exchange of alkoxides is important. Release of the bound ester carbonyl provides an easy way for an associative exchange mechanism to operate.

(3) A restrictive ligand environment to ease the entropic burdens of oxygen transfer. Metal-mediated epoxidation involves the assembly of five atoms in a close, well-ordered arrangement (M, O-O, and C=C), giving rise to a large entropic barrier to reaction. When allylic alcohol and hydroperoxide find themselves bound to the same titanium atom in structure **14**, they are already in close proximity to each other. Part of the unfavorable entropy change for reaction has therefore been distributed among steric and torsional interactions in the entire complex. Structure **14** has a firm tartrate skeleton (recall the unusual 1640 cm^{-1} IR band characteristic of this complex), and is able to absorb the additional energy cost of forcing the reactants into close quarters. The combination of a restrictive ligand environment with rapid ligand exchange is unique to this structure among epoxidation catalysts.

Section IV.

Appendices

Appendix 1. "Reversed" Enantioselective Systems Based on 2:1 Ti:Tartrate

In the introduction we mentioned the 2:1 Ti:tartramide and 2:1 (or 2:2) $TiCl_2(OR)_2$:tartrate systems that produce epoxide products of opposite configuration than those produced by the normal asymmetric epoxidation reaction. Both the tartramide and $TiCl_2(O\underline{i}Pr)_2$ systems are characterized by a stronger Ti-carbonyl interaction - the first by increasing the Lewis basicity of the carbonyl group,[119] and the second by increasing the Lewis acidity of the metal. We therefore reasoned that increasing the Lewis acidity of the metal by other means might produce the same inverse enantioselection. Thus, the addition of electron-withdrawing additives to the 2:1 Ti:tartrate system results in the reversal of enantioselectivity from 80% (2S) to 80-90% ee (2R). The results of an exhaustive study on the effects of various additives on the asymmetric epoxidation of α-phenylcinnamyl alcohol conducted by Mr. Jonathan Ellman appear below in Table 48.

The additives p-nitrophenol (pK_a = 7.2-7.5), pentafluorophenol (pK_a = 5.5), and hexafluoroisopropanol (pK_a = 9.3)[120] were successful at reversing the sense of asymmetric induction. The importance of the electron-withdrawing ability of the additive is emphasized by the use of phenol itself (pK_a = 9.9), which, though it binds well to Ti(IV),[79a,b] gives (2R)-epoxy alcohol in only 6% ee (entry 8).

The importance of binding affinity is emphasized by the hexafluoroisopropanol results in entry 10. At the 1:0.5:1 stoichiometry ratio, the enantiomeric excess was not reproducible. Doubling the amount of catalyst with respect to substrate dramatically improved the ee, while reducing Ti-tartrate to catalytic concentrations resulted in poor asymmetric induction. These results show that hexafluoroisopropanol is not an exceptionally good ligand for titanium and is being displaced by other alcohols present in equal or greater amounts. When the electron-withdrawing additive is washed off the catalyst, the reversed enantioselectivity is lost.

Addition of pentafluorophenol and hexafluoroisopropanol served to raise the enantioselectivity of the 2:1 Ti:tartramide epoxidations slightly (entries 41-45).

Entries 14-22 explore the effects of adding water to the Ti-tartrate

Table 48. Epoxidation of α-phenylcinnamyl alcohol by the given reagents and TBHP; CH_2Cl_2, -20°C.

Entry	$Ti(O\underline{i}Pr)_4$:DET:Additive[a]	Additive	% ee (config.)	% Yield	Rxn. Time
1	10 : 12 : 0	---	>98 (2S)	90-95	15 min.
2	5 : 10 : 0	---	80 (2S)	90-95	15 min.
3	10 : 12 : 10	p-NO_2-Phenol	79 (2S)		15 min.
4	10 : 5 : 5	''	51 (2R)		15 min.
5	10 : 5 : 10	''	80 (2R)		15 min.
6	10 : 5 : 15	''	68 (2R)		15 min.
7	1 : 0.5 : 1	''	84 (2R)	40	
8	10 : 5 : 10	Phenol	6 (2R)	70	15 min.
9	10 : 5 : 10	$(F_3C)_2CHOH$	77 (2R)		0°C
10	1 : 0.5 : 1	''	50 (2R)	78	
	''	''	45 (2R)	59	
	''	''	70 (2R)	67	
	2 : 1 : 2	''	84 (2R)	88	15 min.
	0.1 : 0.05 : 0.1	''	15 (2R)	75	15 min.
11	2 : 1 : 2	Pentafluorophenol	90 (2R)	93	15 min.
12	1 : 0.5 : 1	2,4-Dinitrophenol	2 (2S)	66	slow
13	1 : 0.5 : 1	1,4-Dinitro-o-cresol	79 (2S)		slow
Addition of Water					
14	10 : 12 : 5	H_2O	97 (2S)		50%, 15 min.
15	10 : 12 : 7.5	''	92 (2S)		
16	10 : 12 : 9	''	77 (2S)		
17	10 : 12 : 10	''	48 (2S)		> 24 h
18	10 : 12 : 20	''	9 (2S)		25%, 48 h
19	10 : 5 : 5	''	86 (2S)		
20	10 : 5 : 10	''	14 (2S)		75%, 3 h
21	10 : 5 : 20	''	6 (2S)		> 24 h
22	10 : 12 : 10	''	62 (2S)		DIPT used

a. With respect to 1.0 equivalent of allylic alcohol.

Table 48. Continued.

Entry	$Ti(OiPr)_4$:DET:Additive[a]	Additive	% ee (config.)	% Yield	Rxn. Time
Other Additives					
23	10 : 12 : 10	Benzamide	98 (2S)		15 min.
24	10 : 5 : 5	''	45 (2S)		30 min.
25	10 : 5 : 10	''	44 (2S)		30 min.
26	10 : 12 : 10	p-Toluenesulfonamide	>98 (2S)		15 min.
27	10 : 5 : 10	''	58 (2S)		30 min.
28	10 : 5 : 5	''	59 (2S)		30 min
29	10 : 12 : 10	Benzylamine	93 (2S)		100 min.
30	10 : 5 : 10	''	17 (2S)		120 min.
31	10 : 5 : 5	''	16 (2S)		120 min.
32	2 : 2 : 2	Triethylamine	94 (2S)	91	30 min.
33	10 : 12 : 5	Ethylene Glycol	>98 (2S)		15 min.
34	10 : 12 : 10	''	92 (2S)		3 h
35	10 : 5 : 5	''	86 (2S)		15 min.
36	10 : 12 : 5	Pinacol	>98 (2S)		15 min.
37	10 : 12 : 5	2,2-Dimethylpropanediol	94 (2S)		15 min

Reactions using DNBnT (prepared from L-tartrate)

Entry	$Ti(OiPr)_4$:DNBnT:Add.[a]	Additive	% ee (Configuration)	% Yield	Rxn. Time
38	10 : 12 : 0	---	98 (2S)	90	1 h
39	10 : 5 : 0	---	82 (2R)	90	30 min
40	1 : 0.5 : 1	p-NO_2-Phenol	60 (2R)		
41	1 : 0.5 : 1	$(F_3C)_2CHOH$	89 (2R)	75	
42	2 : 1 : 2	''	91 (2R)	82	
43	2 : 1 : 2	Pentafluorophenol	90 (2R)	94	
44	0.1 : 0.05 : 0.1	''	91 (2R)	90	
45	0.02 : 0.01 : 0.02	''	83 (2R)	95	Overnight
46	10 : 5 : 5	H_2O	62 (2R)		66%, 2 h
47	10 : 5 : 10	''	15 (2R)		50%, 2 h

a. With respect to 1.0 equivalent of allylic alcohol.

system, experiments inspired by the observation of Kagan and Pitchen that the 2:2:2 Ti:tartrate:H_2O system is a highly enantioselective reagent for the oxidation of sulfides.[87] As expected, water reduces both the rate and enantioselectivity of asymmetric epoxidation. Interestingly, the addition of 0.5 equivalents of water (relative to Ti) to the 2:1 system causes a slight increase in the (2S) selectivity of that reagent (entry 19).

To test the substrate dependence and epoxide opening activity of the electron-withdrawing additive systems, epoxidations were attempted on 2-phenylpropenol with various reagents. Only mixtures containing DNBnT allowed the isolation of epoxy alcohol: the 2:2 Ti:DNBnT reagent gave epoxy alcohol in 62% ee, and the 2:1:2 Ti:DNBnT:pentafluorophenol reagent afforded epoxy alcohol of the opposite configuration in 65% ee (absolute configurations were not assigned).

In the epoxidation of para-nitrocinnamyl alcohol with the 2:1:2 Ti:DET:$(F_3C)_2CHOH$ system, epoxy alcohol was produced in only 13% ee (2R) and 90% yield. The substrate 2-tetradecylpropenol was epoxidized in 71% ee (2R) and 90% yield by the same reagent. Thus, the additive systems are more sensitive to substrate structure than the standard asymmetric epoxidation, much like the other reversed-selectivity catalysts.[3j,84]

Burns and Sharpless have discovered that the use of electron-deficient hydroperoxides results in reversal of asymmetric induction by 2:1 Ti:tartrate catalysts.[121] Thus, in the epoxidation of α-phenylcinnamyl alcohol with 2:1 $Ti(OiPr)_4$:DET, 2-cyanopropyl-2-hydroperoxide (**30**) affords epoxy alcohol in 80% ee (2R) and tris(p-nitrophenyl)methyl hydroperoxide (**31**) gives (2R) product in 36% ee.

Burns has also measured the pseudo-first order rate of epoxidation of the standard 2:2 system with a series of other hydroperoxides, confirming the suggestion that greater electron deficiency boosts the rate.[121] Under a set of standard conditions (Ti:DIPT = 1:1.2, 0°C, CH_2Cl_2 solvent, (E)-2-decenol substrate), the following relative rates were observed:

Hydroperoxide	Relative Rate
TBHP	1.00
31	0.86
Trityl (Ph_3COOH)	0.31
32	0.86

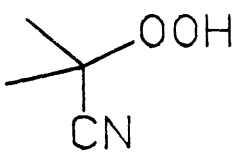

30

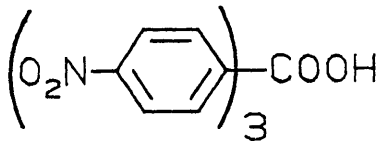

31

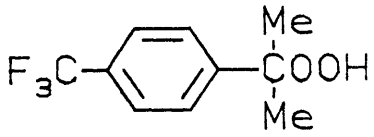

32

Note the rate increase obtained on substituting a nitro group on each aromatic ring of trityl hydroperoxide.

Appendix 2. NMR of Ti:(dl)-DIPT Mixtures

The proton nmr spectrum of a 1:0.5:0.5 mixture of $Ti(OiPr)_4$:(+)-DIPT:(-)-DIPT is shown below in Figure 81. In addition to the normal Ti-tartrate resonances at 5.16 (ester methine) and 4.76 (Ti-OiPr methine) are found multiplets at 5.10 and 4.67; these are assigned to the (dl)-tartrate complex Ti_2(d-DIPT)(l-DIPT)$(OiPr)_4$. On irradiation of the upfield methyl signals, the bands at 5.16, 5.10, and 4.76 collapse to singlets, while the 4.76 band resolves into a major resonance plus two shoulders, which may represent different isopropoxides of one or more Ti-(dl)-DIPT complexes. Major and minor resonances are present in approximately a 65:35 ratio, so we can say that the homochiral tartrate dimer is somewhat more stable than the dl-DIPT complex.

The spectrum of a 1.0:0.7:0.3 mixture of $Ti(OiPr)_4$:(+)-DIPT:(-)-DIPT shows a smaller amount of the bands assigned to the (dl)-DIPT complex, as expected.

Figure 81. ^1H NMR of $Ti(OiPr)_4$ complexes with (dl)-DIPT and 40% ee DIPT in $CDCl_3$ at 295°K; 5.5-4.3 ppm.

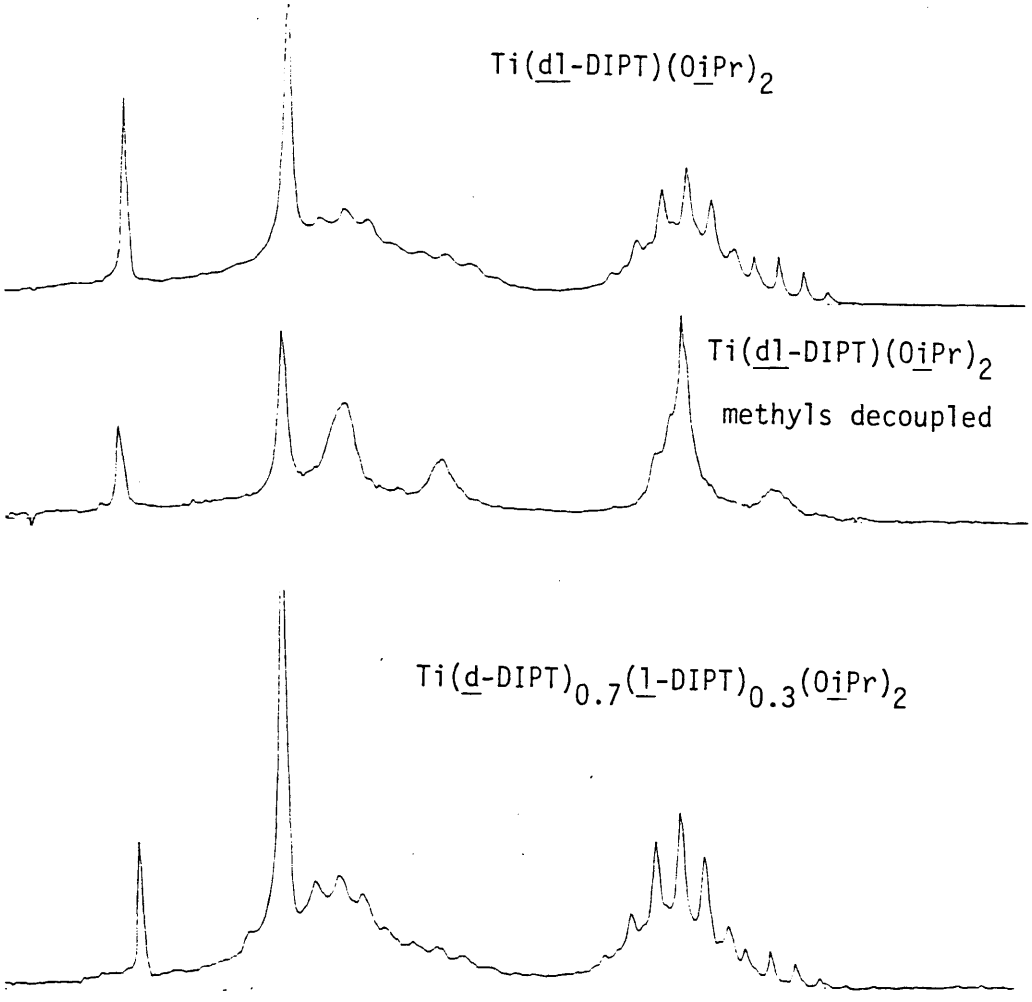

Appendix 3. Optical Rotation vs. Concentration of $Ti(DIPT)(O\underline{i}Pr)_2$

In section II, we discussed nmr and IR evidence for the presence of a second Ti-tartrate species in 1:1 mixtures of $Ti(OR)_4$ and dialkyl tartrate. Since the amount of this complex appeared to depend on concentration, we measured the optical rotation of $Ti(DIPT)(O\underline{i}Pr)_2$ as a function of concentration in three different solvents. If the optical rotation of the minor species were significantly different from the major one, we would expect a non-linear plot of rotation vs. total concentration. The results below show that linear plots were found within the error limits of the mesurement.

Two experiments in isopropanol were performed, one with $Ti(DIPT)(O\underline{i}Pr)_2$ prepared from $Ti(DIPT)(O\underline{i}Pr)Br$ and the other prepared from $Ti(O\underline{i}Pr)_4$ plus DIPT. The slopes and y-intercepts for these two experiments are not the same. A systematic error in the measurement of concentration is the most likely reason for this discrepancy, since the IR and nmr

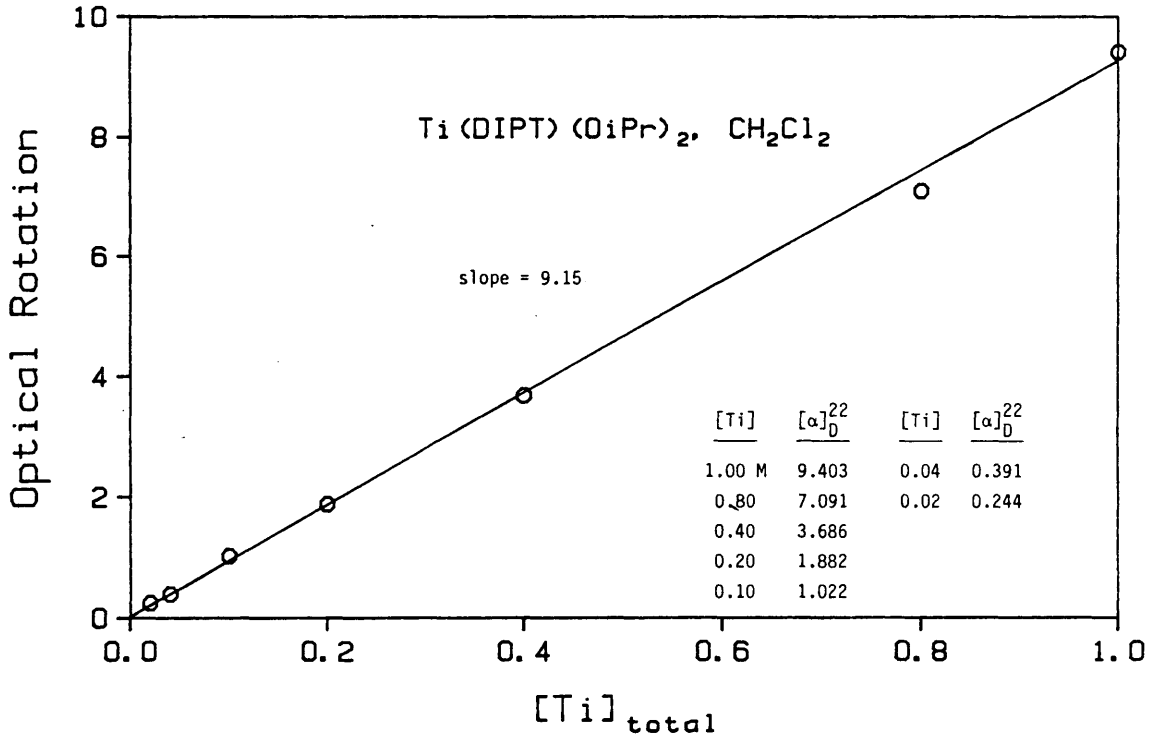

spectra were identical for these two preparations. Non-zero y-intercepts (with otherwise linear plots) also indicate an error in concentration measurement for these solutions.

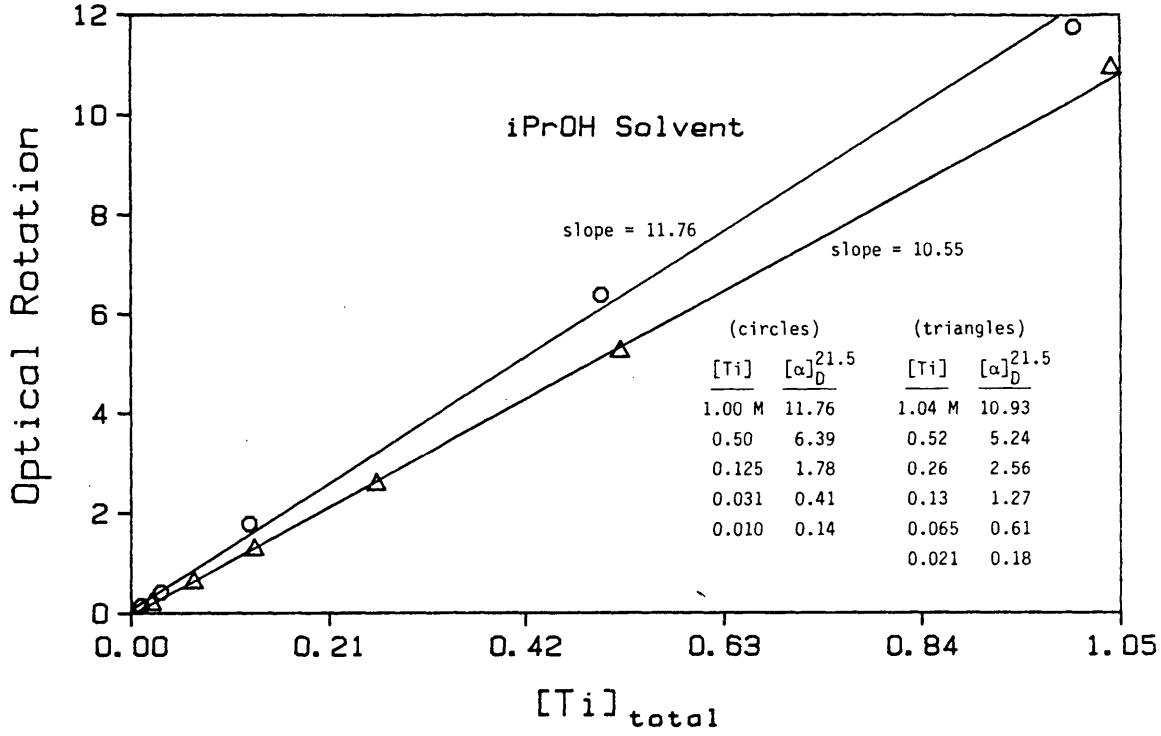

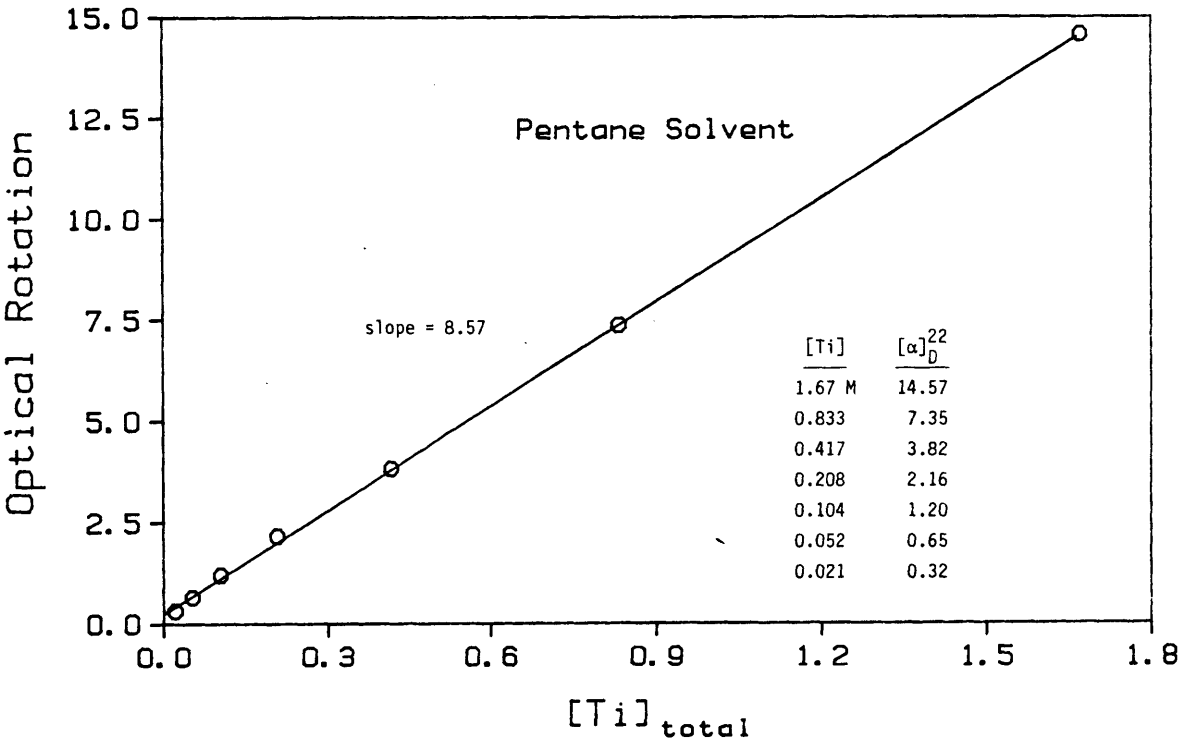

Optical rotations were measured at ambient temperature; the temperatures given are accurate to ± 0.3 degrees in comparison between experiments and ± 0.2 degrees within each experiment. A typical procedure for sample preparation follows:

To a solution of 0.845 g Ti(DIPT)(O*i*Pr)Br (0.00201 mol) in 15 mL ether was added 0.34 mL triethylamine (0.0024 mol) followed by 0.30 mL isopropanol (0.0039 mol). A white precipitate immediately formed and the reaction was allowed to stand with occasional shaking for 45 minutes. After filtration and washing of the filtrate with ether (3 x 10 mL), removal of solvent from the combined solutions afforded a clear oil and 0.358 g of recovered $Et_3NH^+Br^-$ (99%). The oil was taken up in 10 mL of CH_2Cl_2 and evaporated *in vacuo* to remove excess *i*PrOH. This process was repeated twice more and the product was transferred to a 2.0 mL volumetric tube and diluted to the mark, to afford a solution of Ti(DIPT)(O*i*Pr)$_2$ that was 1.0 M in Ti.

The 1.0 M solution was diluted by removal of 0.80 mL with a volumetric pipette into another 2.0 mL volumetric tube, with dilution up to the mark (taking care to rinse the pipette into the solution) to afford a 0.40 M solution. Solutions of 0.10 M and 0.02 M concentration were similarly prepared by dilution. A solution 0.8 M in Ti was prepared from Ti(DIPT)(O*i*Pr)Br as above, and used to prepare solutions of 0.2 M and 0.04 M.

Solutions for the first *i*PrOH experiment above were prepared from Ti(DIPT)(O*i*Pr)Br in the same way, omitting the CH_2Cl_2/vacuum cycles. For the second experiment in *i*PrOH, 0.592 g Ti(O*i*Pr)$_4$ (0.00208 mol) and 0.488 g (+)-DIPT (0.00208 mol) were mixed in a 2.0 mL volumetric tube in dry isopropanol, to afford a solution 1.04 M in titanium. All the other solutions were prepared by dilution.

Appendix 4. Circular Dichroism of Titanium Tartrates.

CD measurements were made on a Jasco CD instrument at ambient temperature. The results show different patterns for 2:2 and 2:1 Ti:ligand systems. We cannot interpret them in detail, since very little is known about the relationship of CD spectra to structure for d^0 transition metal complexes.[122] Note the differences in 2:2 and 2:1 Ti:ligand spectra.

Spectrophotometric grade cyclopentane (C_5H_{10}) was dried with activated 3A molecular sieves; CH_2Cl_2 was reagent grade solvent distilled under nitrogen from CaH_2 and stored over sieves. The ligands used were (+)-DIPT and DNBnT prepared from (-)-tartrate. Pentafluorophenol was dissolved in toluene and stored over molecular sieves; nmr was used to determine the concentration of pentafluorophenol in the stock solution.

Circular Dichroism

Spectrum	Sample	Solvent	Conc.(mg/mL)	Path	Wavelength	Δε (mdeg)
1	(+)-DIPT	C_5H_{10}	6.5×10^{-3}	1 mm	209 nm	-21.5
2	(+)-DIPT	CH_2Cl_2	1.47	0.1 mm	209	-23
3a	Ti[DIPT](O<u>i</u>Pr)$_2$	C_5H_{10}	1.69	0.1 mm	231	+5.0
					ca. 267	shoulder
					205	-9.2
3b	Ti_2(DIPT)(O<u>i</u>Pr)$_6$	C_5H_{10}	0.155	1 mm	269	+0.7
					237	-1.9
					204	-4.8
4a	Ti(DIPT)(O<u>i</u>Pr)$_2$	CH_2Cl_2	9.12	0.1 mm	240	+30
4b	Ti_2(DIPT)(O<u>i</u>Pr)$_6$	CH_2Cl_2	1.09	1 mm	264	+9.2
					235	-9.2
5	Ti(DIPT)(OC_6F_5)(O<u>i</u>Pr)	CH_2Cl_2	1.29	1 mm	320	-8.5
					252	+16
6	Ti_2(DIPT)(OC_6F_5)$_2$(O<u>i</u>Pr)$_4$	CH_2Cl_2	0.70	1 mm	309	-6
					246	-11
7a	Ti(D<u>N</u>BnT)(O<u>i</u>Pr)$_2$	CH_2Cl_2	1.01	1 mm	245	-18.5
7b	Ti_2(D<u>N</u>BnT)(O<u>i</u>Pr)$_6$	CH_2Cl_2	9.84	0.1 mm	280	+4.7
					249	-13.0

Circular Dichroism

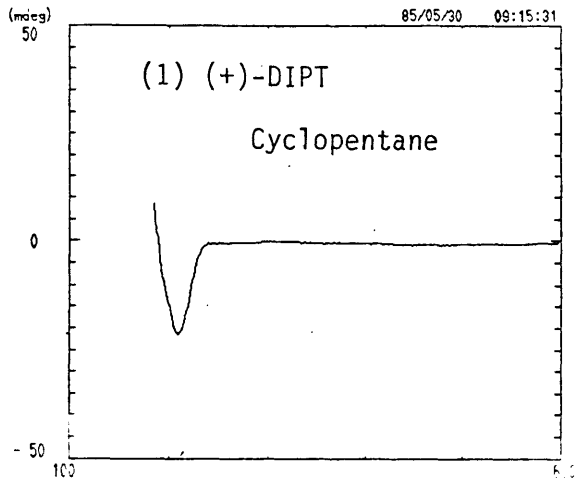

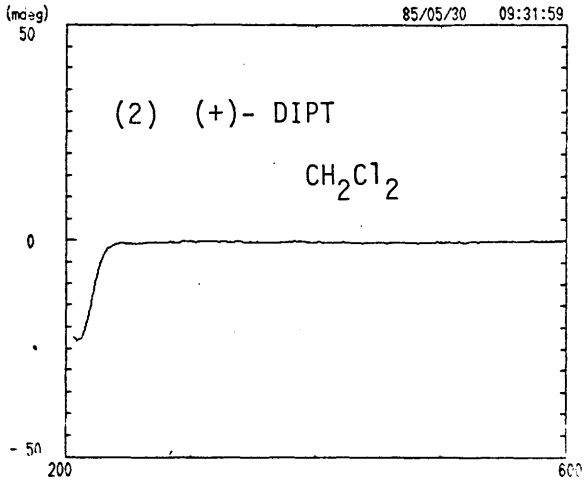

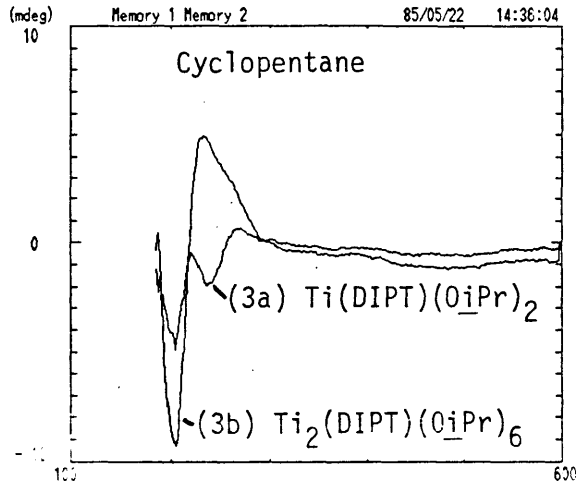

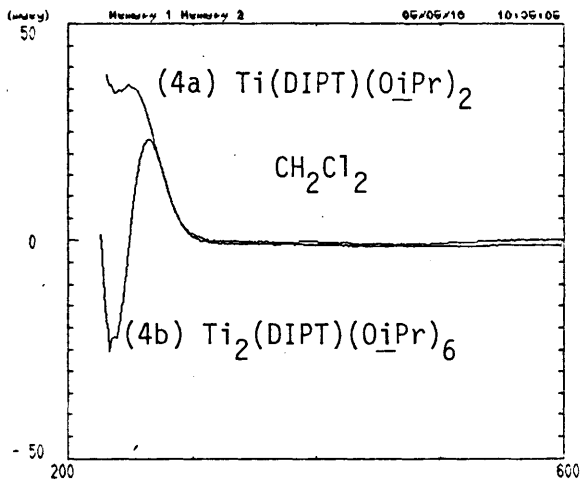

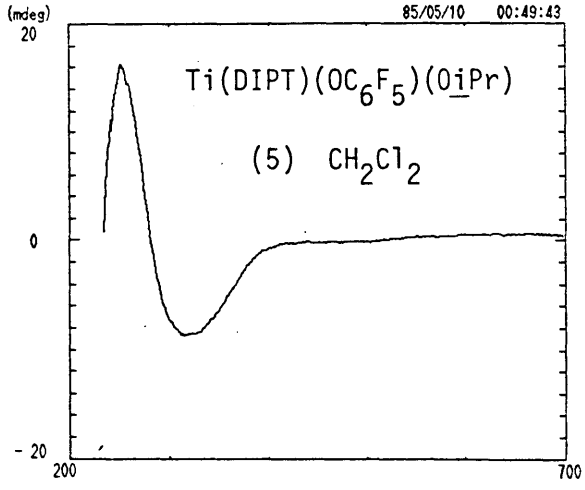

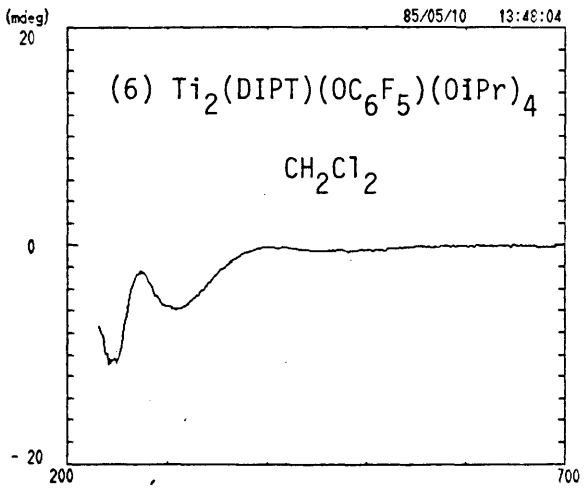

Appendix 5. Kinetics of 1% Catalyst Epoxidations.
Kinetics of Epoxidation by $OV(OR)_3$.

Table 49. Entries 71-73. Table 50. Entries 66-67.

One of the earliest indications that such a reaction as asymmetric epoxidation was possible came in Dr. Tsutomu Katsuki's observation in 1979 that the rate of epoxidation of an allylic alcohol by $Ti(dipic)(O\underline{i}Pr)_2$ was faster than that of $Ti(O\underline{i}Pr)_4$ itself (dipic = 2,6-dipicolinic acid). This was a rare case in which a chelating ligand caused the activity of the complexed metal to <u>increase</u>. A more rigorous kinetics experiment was undertaken to confirm this observation. The results appear in Table 49.

Table 49. Kinetics of the epoxidation of <u>E</u>-2-hexenol by 1 mol% catalysts. Solvent = CH_2Cl_2 (distilled from CaH_2). Oxidant = TBHP in toluene.

Entry	Catalyst	(M) [Catalyst]	(M) [Hexenol]	(M) [TBHP]	(M^{-1} sec^{-1}) k_1[a]	k_2[a]
71	$Ti(O\underline{i}Pr)_4$	0.00060	0.0593	0.119	0.10	0.12
72	$OV(OEt)_3$	0.00060	0.0593	0.119	0.51	0.42
73	$Ti(dipic)(O\underline{i}Pr)_2$	0.00086	0.086	0.154	0.04	

dipic = 2,6-dipicolinic acid

a. k_1 = rate constant from disappearance of hexenol,
k_2 = from appearance of 2,3-epoxy-1-hexanol.

Note that Katsuki's initial observation was incorrect: the initial rate of epoxidation by $Ti(O\underline{i}Pr)_4$ is about twice as fast as by $Ti(dipic)(O\underline{i}Pr)_2$. However, the gc data reported below shows that the $Ti(O\underline{i}Pr)_4$ stopped after about an hour, whereas $Ti(dipic)(O\underline{i}Pr)_2$ remained an active catalyst for many hours. Coordination of dipicolinate, then, <u>stabilizes</u> the catalyst, but does not increase its rate of reaction.

While $OV(OEt)_3$ is the most active of the three catalysts at the 1% level, Table 50 shows $OV(O\underline{i}Pr)_3$ to be a sluggish catalyst under pseudo-first order conditions. These results are included because of an interesting observation in entry 68: the use of ethanol in place of isopropanol as an inhibitor actually <u>raises</u> the rate of epoxidation. Since $OV(O\underline{i}Pr)_3$ is a monomer and $OV(OEt)_3$ is a trimer, this points out that aggregation can

dramatically change the behavior of a catalyst, in this case by increasing the rate (possibly because of favorable epoxidation reactions requiring two metal centers).

Table 50. Pseudo-first order kinetics.

Substrate = trans-2-hexenol. Catalyst = $OV(OiPr)_3$.

Solvent = CH_2Cl_2 (distilled from CaH_2). Oxidant = TBHP in toluene.

Entry	(M) $[OV(OiPr)_3]$	(M) [iPrOH]	(M) [TBHP]	(10^{-4} sec^{-1}) $Rate_{obs}$	Sieves
66	0.0138	0.204	0.0150	0.45	none
67	0.0133	0.107	''	1.2	''
68	0.0131	0.054 iPrOH 0.056 EtOH	''	1.57	''

Pseudo-first order kinetics measurements for Table 50 were performed exactly as for the other epoxidations of (E)-2-hexen-1-ol by titanium catalysts.

1% Catalysis

The following stock solutions were prepared and used immediately: (a) 5.9363 g $Ti(OiPr)_4$ (0.0208 mol) in 51.52 g CH_2Cl_2 (total volume = 45.0 mL, 0.465 M), (b) 5.0749 g $OV(OEt)_3$ (0.0251 mol) in 62.10 g CH_2Cl_2 (total volume = 51.5 mL, 0.488 M), and (c) 1.674 g $Ti(OiPr)_4$ (0.00589 mol) and 0.984 g 2,6-dipicolinic acid (0.00589 mol) were stirred overnight in 100.0 mL solution (toluene) in a dry 100 mL volumetric flask; the mixture remained slightly cloudy, suggesting the presence of a slight excess of dipicolinic acid.

Entry 71: A dry, 100 mL volumetric flask equipped with a stir bar was charged with 0.900 mL of a 7.0:2.0 (v:v) mixture of trans-2-hexen-1-ol and n-hexadecane (0.594 g allylic alcohol, 0.00593 mol) and ca. 50 mL CH_2Cl_2; 0.128 mL of the $Ti(OiPr)_4$ stock solution (0.000060 mol) was then added by gastight syringe, followed by CH_2Cl_2 to approximately 95 mL. A small amount of this solution (0.4 mL) was removed and subjected to the workup conditions as a t_0 sample. To begin the reaction, 0.0119 mol TBHP was added by cannula (3.23 mL of a 3.68 M solution in heptane) with rapid stirring, followed immediately by CH_2Cl_2 to the 100.0 mL mark. Aliquots of

10-20 mL were removed through a teflon tube into 10 mL of an aqueous $FeSO_4$/tartaric acid quench solution. After stirring vigorously for 5 minutes, 30 mL of ether were added and the organic layer was separated, dried ($MgSO_4$) and removed directly for gc analysis. The results are summarized below. Note that the reaction was run at room temperature (ca. 23°C).

Entry 72: In an identical procedure to entry 71, the same amounts of reagents were used except for $OV(OEt)_3$ (0.122 mL of the stock solution, 0.000060 mol) instead of $Ti(O\underline{i}Pr)_4$.

Entry 73: A dry 50 mL round-bottomed flask was charged with 0.2050 g trans-2-hexen-1-ol (0.00205 mol), 0.1 mL n-hexadecane, and 30.353 g CH_2Cl_2 (22.8 mL). To this solution was added 0.348 mL of the $Ti(dipic)(O\underline{i}Pr)_2$ stock solution (0.000020 mol). After working up a small amount of the solution for a t_0 sample, TBHP was added to begin the reaction (1.00 mL of a 3.68 M solution in heptane). Thus, the total volume of the solution was 23.8 mL, making the reaction 0.00086 M in catalyst, 0.086 M in substrate, and 0.154 M in TBHP. Aliquots of 2-4 mL were removed by cannula into a test tube with 1 mL $FeSO_4$/tartaric acid quench solution. After vigorous shaking for one minute, the organic layer was removed by pipette into a test tube with 0.5 g $MgSO_4$ and approximately 10 mL ether was added. After shaking, the supernatant was removed for gc injection.

The gc results are given below:

Entry	Catalyst	Time (min)	GC (hexenol/std)	GC (product/std)
71	$Ti(O\underline{i}Pr)_4$	0.00	2.560	---
		7.33	2.196	0.310
		17.58	1.945	0.557
		28.92	1.733	0.742
		38.67	1.616	0.825
		48.00	1.544	0.873
		58.92	1.477	0.884

If we assume a steady-state condition for the catalyst, and we examine only the early part of the reaction, we can treat the epoxidation as a standard bimolecular process: $A + P \longrightarrow E$, where A = hexenol, P = TBHP, and E = 2,3-epoxy-1-hexanol. The rate expressions for the disappearance of

A and the appearance of E are given below:

Disappearance of A: $[A_0 - P_0]kt = \ln[(P_0)(A)/(A_0(P_0 - A_0 + A))]$.

Thus, a plot of time vs. $\ln[(P_0)(A)/(A_0(P_0 - A_0 + A))]$ should be a straight line with slope = $k[A_0 - P_0]$.

Appearance of E: $[A_0 - P_0]kt = \ln[(A_0-E)/(P_0-E) - \ln(A_0/P_0)$.

A plot of time vs. $\ln[(A_0-E)/(P_0-E)$ should be a straight line with slope = $k[A_0 - P_0]$.

For the above equations, A_0 = [hexenol] at the start of the reaction

P_0 = [TBHP] at the start of the reaction

A = [2-hexenol] at time t

E = [2,3-epoxy-1-hexanol] at time t

If we assume that the gc response factor of hexenol/hexadecane is linear, then the gc data gives us the concentration of A in each aliquot. Using this information, we can estimate the gc response factor for 2,3-epoxy-1-hexanol and hexadecane, and thus obtain the concentration of E in each aliquot. The necessary logarithmic expressions are then easily calculated, as shown below.

Catalyst	Time	GC (A/std)	GC (E/std)	[A]	[E]	$\ln(X_A)^a$	$\ln(X_E)^b$
$Ti(O\underline{i}Pr)_4$	0.00	2.560	---				
	7.33	2.196	0.310	0.0509	0.0084	-0.0796	-0.773
	17.58	1.945	0.557	0.0451	0.0152	-0.147	-0.852
	28.92	1.733	0.742	0.0401	0.0202	-0.214	-0.923
	38.67	1.616	0.825	0.0374	0.0224	-0.256	-0.959
	48.00	1.544	0.873	0.0358	0.0237	-0.284	-0.981

a. $X_A = \ln[(P_0)(A)/(A_0(P_0 - A_0 + A))$

b. $X_E = \ln[(A_0-E)/(P_0-E)$

The first three data points provide passable linear plots:

time vs. $\ln(X_A)$: $R^2 = 0.993$, slope = -0.006,

$k = -0.006/(0.0593 - 0.119) = 0.10\ M^{-1}sec^{-1}$

time vs. $\ln(X_E)$: $R^2 = 0.996$, slope = -0.007

$k = -0.007/(0.0593 - 0.119) = 0.12\ M^{-1}sec^{-1}$

The same analysis is applied to the data for entries 72 and 73:

Catalyst	Time	GC (A/std)	GC (E/std)	[A]	[E]	$\ln(X_A)^a$	$\ln(X_E)^b$
$OV(OEt)_3$	0.00	2.560	---				
	9.33	1.396	1.021	0.0323	0.0278	-0.349	-1.058
	19.92	0.858	1.40	0.0199	0.0381	-0.689	-1.33
	29.33	0.600	1.60	0.0139	0.0435	-0.968	-1.56
	39.08	0.442	1.77	0.0102	0.0482	-1.223	-1.85
	60.00	0.249	1.96	0.0058	0.0533	-1.73	-2.39

For the first three data points:

time vs. $\ln(X_A)$: $R^2 = 0.9997$, slope = -0.031,

$k = -0.031/(0.0593 - 0.119) = 0.51\ M^{-1}sec^{-1}$

time vs. $\ln(X_E)$: $R^2 = 0.9994$, slope = -0.025

$k = -0.025/(0.0593 - 0.119) = 0.42\ M^{-1}sec^{-1}$

Catalyst	Time	GC (A/std)	[A]	$\ln(X_A)^a$
$Ti(dipic)(O\underline{i}Pr)_2$	0.0	2.010	0.086	
	3.0	1.984	0.085	-0.0058
	6.0	1.949	0.083	-0.014
	9.0	1.941	0.083	-0.016
	12.0	1.896	0.081	-0.026
	15.0	1.85	0.079	-0.038
	30.0	1.69	0.072	-0.080
	60.0	1.45	0.062	-0.157
	overnight	0.72	0.031	-0.583

For the data points from 3.0 to 60.0 minutes,

time vs. $\ln(X_A)$: $R^2 = 0.997$, slope = -0.0027,

$k = -0.0027/(0.086 - 0.154) = 0.040\ M^{-1}sec^{-1}$

Appendix 6. Decomposition of 1,2-Epoxy-3-nonenol, **11**, with Ti-tartrate.

The decomposition, as well as the preparation, of 2,3-epoxy alcohols on Ti-tartrate can be a selective process.[123] We demonstrated this by exposing a racemic mixture of 1,2-epoxy-3-nonenol to Ti-tartrate under standard epoxidation conditions. As detailed below, the threo epoxy alcohol diastereomer decomposes at a rate about twice that of erythro epoxy alcohol, and the threo diastereomer undergoes some enantiomeric kinetic resolution, leaving the S enantiomer with (+)-tartrate and the R enantiomer with (-)-tartrate in greater than 95% ee. Both enantiomers of the erythro material, on the other hand, are opened at about the same (slow) rate.

Erythro-**11** is the diastereomer produced selectively by asymmetric epoxidation. If it binds to Ti-tartrate in the configuration indicated by our transition state model **16a**, the alkyl group at C1 points away from the catalyst and over the back of the epoxide group, shielding it from external nucleophilic attack. It makes sense, then, for the favored product of epoxidation to be the disfavored substrate for opening. Experimental details follow:

A racemic mixture of epoxy alcohols **11** in a 42:58 ratio of erythro:threo isomers was prepared by m-chloroperbenzoic acid epoxidation of racemic 1-nonen-3-ol; the nmr spectra and gc properties match those reported previously.[3c]

A solution of 1.0771 g **11** (6.81 mmol), 0.2529 g pentadecane, and 1.7540 g (+)-DIPT (7.49 mmol) in 38 mL CH_2Cl_2 was cooled to 0°C under argon; a small amount (ca. 0.5 mL) was removed and subjected to the workup conditions below as a t_0 sample. To the cooled solution was added 1.9349 g $Ti(OiPr)_4$ (6.80 mmol) by gastight syringe. A second solution was similarly prepared with 1.0645 g epoxy alcohols (6.73 mmol), 0.2499 g pentadecane, 1.7334 g (-)-DIPT (7.40 mmol), and 1.9122 g $Ti(OiPr)_4$ (6.72 mmol). The reaction flasks were stored in a refrigerator at 2°C, and transferred to an ice bath for monitoring of the reaction. Aliquots of 3-5 mL were transferred by cannula into a 1:1 acetone:water solution (10 mL), stirred vigorously for 2 h, filtered through Celite, and evaporated. The residue was taken up in 20 mL ether and stirred at 0°C for 20 minutes with 6 mL of a 1N NaOH solution in saturated NaCl. The organic phase was then washed with water, dried over $MgSO_4$, and evaporated to give a clear oil, which was taken up in 1 mL ether

for gc analysis.

At 141 h, each reaction solution was quenched as above and a small amount removed for gc. The remaining residue was chromatographed (15:85 EtOAc:hexane) to isolate unreacted epoxy alcohol (erythro and threo isomers did not separate) and the major decomposition product. The epoxy alcohol was peracetylated (Ac_2O, pyridine) and subjected to medium pressure liquid chromatography (15:85 EtOAc:hexane) to isolate samples of pure erythro and threo epoxy acetates for each reaction. NMR spectra in C_6D_6 in the presence of $Eu(hfc)_3$ cleanly resolve the acetate methyl resonances due to each enantiomer; the results are tabulated below.

Tartrate	Epoxy alcohol diastereomer	% ee	Absolute configuration at C1
(+)-DIPT	Erythro	11.5 %	R
(+)-DIPT	Threo	95 %	S
(-)-DIPT	Erythro	13.5 %	S
(-)-DIPT	Threo	95 %	R

To assign absolute configurations, (R)-1-nonen-3-ol was prepared by the published kinetic resolution procedure using (+)-DIPT.[3c] The homochiral allylic alcohol was then epoxidized by mCPBA and acetylated. The resulting R-erythro and R-threo epoxy acetates were separated by medium pressure liquid chromatography as above. NMR samples enriched in the 1R enantiomer were prepared by mixing the resolved epoxy acetates with (dl)-erythro and (dl)-threo samples. Addition of chiral shift reagent $Eu(hfc)_3$ to C_6D_6 solutions of the racemic epoxy acetates produced baseline resolution of the acetate singlets from each enantiomer. The R-enriched erythro diastereomer displayed a more intense upfield acetate signal; the R-enriched threo diastereomer a more intense downfield acetate peak.

Section V.
Experimental Section

1. General Remarks

Nuclear magnetic resonance (NMR) spectra were measured with Bruker 250-MHz or 270-MHz spectrometers, or with a Varian 300-MHz instrument. For titanium samples, residual solvent bands served as internal standards: 7.24 ppm for $CDCl_3$, 7.15 ppm for C_6D_6, 5.32 ppm for CD_2Cl_2. NMR spectra of organic compounds were referenced to tetramethylsilane. Chemical shifts are given in ppm downfield from Me_4Si and coupling constants are in hertz. Infrared spectra (IR) were measured with a Perkin-Elmer Model 597 grating spectrophotometer; Fourier transform IR spectra (FTIR) were obtained on Nicolet 7199 or 60-SX instruments. Melting points were determined with a Thomas-Hoover capillary melting point apparatus and are uncorrected. Optical rotations were measured with a Perkin-Elmer Model 241 polarimeter using a 1 cm^3 capacity (1 dm path length) quartz cell. Analytical thin-layer chromatograhy was performed using aluminum paltes coated with 0.20 mm thickness of Merck silica gel 60 F-254. Flash chromatography was performed using Merck silica gel 60 (230-400 mesh) as described by Still.[124] Elemental analyses were performed by the Robertson Laboratory Inc., Florham Park, N.J.

All water-sensitive manipulations were performed in a Vacuum Atmospheres inert atmosphere drybox, with a recirculating dry-train composed of one-third Ridox oxygen-scrubbing catalyst and two-thirds activated 13X molecular sieves. Nitrogen for the drybox was bled from liquid nitrogen tanks. Glassware was oven-dried (160°C) before use; gastight syringes were dried over $CaSO_4$ in a vacuum dessicator.

Methylene chloride was distilled from CaH_2 or dried over 3A molecular sieves, as discussed in the text. Toluene, pentane, ether, and THF were distilled from Na-benzophenone ketyl under nitrogen.

Gas chromatogrphy (gc) was performed on Perkin Elmer Model 990, 3920, 3920b, or Sigma-10 gas chromatography instruments using 1/4" o.d. packed glass columns of Carbowax-20M (10% on GasChrom-Q) or SE-30 (5-10% on Chromosorb W). Capillary gc was performed using 20-30 meter fused silica columns of Carbowax-20M or SE-30 supplied by J&W Products.

General Procedures for NMR of Titanium Tartrates

$CDCl_3$ was usually dried by distillation onto activated 4A molecular sieve beads. In several cases, $CDCl_3$ was satisfactorily dried with two successive treatments of 4A sieves without distillation. Other deuterated solvents were passed through a pipette filled with activity-I grade neutral alumina before use. Isopropanol-d_8 was dried over 3A sieves (two treatments).

Ti-tartrates were usually prepared by simply mixing the appropriate molar equivalents of titanium tetraalkoxide and tartrate diester in CH_2Cl_2 at room temperature in the drybox. For alcohol-free samples, three repeated cycles of dissolution in CH_2Cl_2 followed by evaporation *in vacuo* were performed, before the sample was dissolved in the nmr solvent of choice.

It should be noted that complexes prepared from commercially available DIPT and DET, purified by distillation, invariably gave a yellow color when mixed with titanium tetraalkoxides. When tartrates were synthesized by other means (by esterification of tartaric acid, or as for the ^{17}O labeled samples), no yellow color was observed in the titanium complexes. Since the yellow impurity led to no differences in the NMR and IR spectra, nor in enantioselectivity of epoxidation under stoichiometric conditions (catalytic has yet to be tested), it was ignored. In the case of $Ti(DET)(OAd)_2$, the yellow color of the crude product could be eliminated by recrystallization. It was found late in this work that simple chromatography of the commercial DIPT is sufficient to eliminate the yellow color of its complex with $Ti(O\underline{i}Pr)_4$.[125]

Alcohol-free samples were also prepared by mixing appropriate amounts of $Ti(tartrate)_2$ and $Ti(OR)_4$. The bis tartrate complexes were prepared by mixing two equivalents of tartrate with the tetraalkoxide of the same R group; DIPT with $Ti(O\underline{i}Pr)_4$ and DET with $Ti(OEt)_4$.

General Procedure for Asymmetric Epoxidation of Prochiral Allylic Alcohols.

Into the oven-dried reaction flask were placed a dry stir bar, the allylic alcohol (1.0 equivalent), and dialkyl tartrate (1.2 equivalents). The flask was capped with a septum and flushed with argon. Methylene chloride was then added and the solution cooled under argon to 0^oC or below, as appropriate, before addition of titanium tetraalkoxide (1.0

equivalent). Keep in mind that we now recommend the use of activated 3A molecular sieve powder (0.2-0.4 g per 10 mL of solution) in routine asymmetric epoxidations. After 15-30 minutes, TBHP was added by gastight syringe to initiate the reaction. After monitoring by TLC, excess hydroperoxide was quenched and titanium removed by addition of an aqueous solution of tartaric acid (10% by weight) saturated in $FeSO_4$, with rapid stirring or shaking.

General Procedure for Kinetic Resolution of Secondary Allylic Alcohols

Unless otherwise noted, kinetic resolutions were performed with stoichiometric amounts of Ti-ligand complexes in the published manner.[3c] Typically, a solution of allylic alcohol (1.0 equivalent), ligand (1.2 equivalents), and saturated hydrocarbon (gc internal standard) was treated with titanium tetraalkoxide (usually $Ti(O\underline{i}Pr)_4$) under inert atmosphere and allowed to stir for about 10 minutes at room temperature. During this time, a small aliquot was removed into the quench solution for a t_0 gc sample. The reaction mixture was then cooled to the desired temperature (usually -20^oC) and was then treated with TBHP (0.25 or 0.6 equivalents) dropwise by gastight syringe. The reaction was monitored if necessary by gc and was quenched by addition to a stirred aqueous solution of $FeSO_4$ and tartaric acid (about 5% and 10% by weight, respectively). The crude product was usually peracetylated (Ac_2O, pyridine) since the epoxy acetates were used for determination of the ratio of erythro to threo diastereomers by gc; the enantiomeric excess of unreacted starting material was determined by nmr of the allylic acetate with the chiral shift reagent $Eu(hfc)_3$ in C_6D_6. Flash chromatography was used to purify the acetylated products.

The important parameters of a kinetic resolution are temperature, percent completion (percent consumption of allylic alcohol), ee of recovered allylic alcohol, and erythro/threo ratio of the product epoxy alcohols.

2. Pseudo-first order kinetics

The general method used here was developed by Dr. Scott Woodard.[78] Comments concerning the procedure for each of the kinetics tables are recorded below.

DIPT was stored under argon after distillation under vacuum; before

each reaction the tartrate was stirred for 1 h at 0.1 mm Hg to eliminate dissolved gases and prevent the buildup of water in the viscous oil. This procedure is more important for diethyl tartrate, since DET is considerably more hygroscopic than DIPT. trans-2-Decen-1-ol was prepared as described in Section V.6. E-2-Hexen-1-ol was purchased from Aldrich Chemical Company, distilled, and stored at 4°C over activated 3A sieves. $Ti(O\underline{i}Pr)_4$ was purified by distillation under vacuum and stored in a flask equipped with a teflon stopcock placed in a dessicator or the inert atmosphere drybox. $OV(O\underline{i}Pr)_3$ and $OV(OEt)_3$ were purified by distillation under vacuum. Isopropanol was dried by distillation from $Mg(O\underline{i}Pr)_2$ and storage over powdered 3A molecular sieves.[125] A freshly opened bottle of absolute ethanol was dried by three sequential treatments with, and storage over, activated 3A molecular sieve powder. N,N'-Dibenzyltartramide was prepared by the literature procedure,[84] recyrstallized from hot toluene, and dried under vacuum. Isopropanol-d (Cambridge Isotope Laboratories) was dried by two sequential treatments with, and storage over, powdered 3A molecular sieves. 2,6-Dipicolinic acid was ground to a fine powder and dried in a vacuum oven at 150°C and 0.2 mm Hg for 24 h. The molecular sieves were obtained, allegedly in activated form, from Aldrich Chemical Company and were stored in a vacuum oven at 160°C and 0.1-0.5 mm for at least 24 h before use.

Volumetric flasks were cleaned of adsorbed metal ions by soaking in 95/5 H_2SO_4/HCl for 6 h and then 10% HF for six hours, followed by rinsing with base and then water. Thereafter, all glassware, teflon tubing, and syringes were carefully washed with dilute HF after every use to prevent the accumulation of metal contaminants (see the notes for entries 24 and 25, below).

Table 6, Entry 5.

A dry 100 mL volumetric flask was charged with a stir bar and 0.550 g powdered, activated 4A molecular sieves while still hot and was allowed to cool to room temperature under vacuum. (+)-DIPT (0.6373 g, 0.00272 mol) was then added by tared gastight syringe, followed by approximately 102 mL CH_2Cl_2 (freshly distilled from CaH_2 under nitrogen). The flask was then immersed in a 0.0-0.3°C ice/water bath up to the 100.0 mL mark and the solution was allowed to cool with stirring under argon. CH_2Cl_2 at 0°C is about 5% more dense than at room temperature, so the volume of the CH_2Cl_2

solution was approximately 97 mL at this stage. To the solution was then added 0.5897 g $Ti(O\underline{i}Pr)_4$ (0.002075 mol) by tared gastight syringe, and the mixture was allowed to stir for 15 minutes. This provides a $Ti(O\underline{i}Pr)_4$:DIPT ratio of 1:1.31, and an active Ti concentration of 0.0143 M, correcting for the production of 0.00064 mol of inactive $Ti(DIPT)_2$, as described by Woodard. Isopropanol (1.5029 g, 0.02501 mol) was then added by tared gastight syringe, followed by 0.015 mL of a 3:2 (v:v) mixture of trans-2-decen-1-ol and n-heptadecane (approximately $5x10^{-5}$ mol decenol, providing a 40-fold excess of Ti-tartrate and TBHP with respect to substrate). A small amount of CH_2Cl_2 was then added to bring the solution up to the 100.0 mL mark. If too much solvent was present, the excess solution was removed by cannula into a graduated cylinder, and the calculated concentrations of reagents were adjusted accordingly. After stirring for an additional 5 minutes, the reaction was initiated by the rapid injection of 0.00151 mol of TBHP (0.380 mL of a 3.98 M solution in toluene) to the vigorously stirred reaction mixture. A 0.50 mL gastight syringe was used with a needle sufficiently long to extend about one inch below the surface of the reaction mixture for injection, so that mixing was instantaneous. The added volume of TBHP solution compensates for the volume of the stir bar to bring the total volume very close to 100.0 mL.

Aliquots of 10-20 mL were removed by rapid cannula transfer through a teflon tube into a vigorously stirred mixture of 10 mL aqueous quench solution (10% tartaric acid plus 5-15% $FeSO_4$) and 10 mL ether. Control experiments determined that quenching the aliquots at 0^oC and room temperature produced identical results. The resulting mixtures were stirred for 5 minutes and the organic layer was separated, dried with $MgSO_4$, filtered, and evaporated at room temperature and reduced pressure on the rotary evaporator. The resulting clear oil was taken up in 1 mL ether for gc analysis.

Control experiments were performed for each different solvent to verify that the workup did not change the decenol:heptadecane ratio. Thus, a mixture of reactants prepared as above (except for the addition of TBHP) was subjected to the workup procedure. The gc ratios of decenol to heptadecane were identical before and after workup.

For the reaction summarized in Table 6, the $Ti(O\underline{i}Pr)_4$:DIPT ratio ranged from 1:1.10 to 1:1.31. No systematic effect of Ti:DIPT ratio on

rate was observed. See, however, entries 26 and 27 for the rate of 1.0:1.0 Ti:DIPT.

Gas chromatographic analysis was performed on either a 6' packed column (10% Carbowax 20-M on GasChrom-Q) or a fused-silica capillary column (Carbowax 20-M, 20 meter, J&W Scientific). When both columns were used to analyze the same set of aliquots, identical results were obtained.

Aliquots were taken at 1.58, 7.40, 12.92, 18.12, 24.05, and 30.65 minutes; 2-4 injections for each aliquot were averaged:

Time (min)	GC ratio (Decenol/Std)	ln (GC ratio)
1.58	1.0355	0.0349
7.40	0.6503	-0.4303
12.92	0.4353	-0.8317
18.12	0.2849	-1.256
24.05	0.1800	-1.715
30.65	0.1063	-2.242

A plot of time vs. ln(GC ratio) is a line with $R^2 = 0.9998$, and slope = $-0.0781\ min^{-1}$. The slope is reported as $Rate_{obs}$:

$$R_{obs} = 0.0781/60 = 1.30 \times 10^{-3}\ sec^{-1}.$$

Table 9, Entry 18.

With the same procedure as for entry 5, above, the following reagents were used: 4A powdered sieves (0.525 g), (+)-DIPT (1.0356 g, 0.004421 mol), $Ti(O\underline{i}Pr)_4$ (1.1025 g, 0.003879 mol), $\underline{i}PrOH$ (1.2763 g, 0.02124 mol), and decenol/heptadecane (0.015 mL). This produced $[Ti]_{active} = 0.0334$ M, and a $Ti(O\underline{i}Pr)_4$:DIPT ratio of 1:1.14.

A plot of the data below (time vs. ln(GC ratio)) is a line with $R^2 = 0.9999$, and slope = $-0.168\ min^{-1}$. $R_{obs} = 0.168/60 = 2.80 \times 10^{-3}\ sec^{-1}$.

Time (min)	GC ratio (Decenol/Std)	ln (GC ratio)
0.53	1.1557	0.1447
2.62	0.8081	-0.2131
4.85	0.5470	-0.6033
6.90	0.3887	-0.9449
9.34	0.2595	-1.349
13.17	0.1375	-1.984

For entry 21, we relied on Woodard's determination of a first order

dependendence on [TBHP], and correct for use of half the normal concentration by multiplying (R_{obs}x[iPrOH]^2) by 2.0. In this reaction, the amount of (E)-2-decen-1-ol/heptadecane mixture used was reduced to 0.012 mL to assure a 20-fold excess of TBHP with respect to allylic alcohol.

Entries 21 and 22 represent the approximate practical limit in observed rate that can be accomodated by this technique. Aliquots were taken 30 seconds after TBHP injection, and then at 90 second intervals; only the first four data points were usable (R^2 = 0.997) since the allylic alcohol was consumed within 6.5 minutes.

Table 8, Entries 24-25.

Entry 24: A 100 mL volumetric flask was charged with a stir bar and 0.600 g powdered 4A molecular sieves. The flask and sieves were then dried under vacuum (0.2 mm) by heating with a Bunsen burner for a few minutes and were then allowed to cool to room temperature under vacuum. Approximately 105 mL of distilled CH_2Cl_2 were added followed by 0.015 mL of a trans-2-decen-1-ol/heptadecane mixture. The solution was cooled to 0°C and TBHP (0.38 mL of 3.98 M solution in toluene) was added as above. Four aliquots were taken and worked up in the usual way.

Time (min)	GC ratio (Decenol/Std)	ln (GC ratio)
2.83	0.8954	-0.1105
31.92	0.8811	-0.1266
87.00	0.8601	-0.1507
114.7	0.8433	-0.1704

For the plot of time vs. ln(GC ratio), R^2 = 0.992, slope = -5.17×10^{-4} min^{-1}. $R_{obs} = 0.086 \times 10^{-4}$ sec^{-1}.

Entry 25: A 100 mL volumetric flask was soaked in 95/5 H_2SO_4/HCl for six hours, followed by 10% HF for six hours. It was then was rinsed with KOH/EtOH and copious quantities of water before drying in an oven at 165°C. With the same procedure as for entry 24 (0.630 g 4A molecular sieves), a poor line for the plot of time vs. ln(GC ratio) was obtained:

Time (min)	GC ratio (Decenol/Std)	ln (GC ratio)
2.18	0.9666	-0.0340
20.62	0.9531	-0.0480
66.33	0.9294	-0.0732
119.7	0.9383	-0.0637

R^2 = 0.6, slope = ca. 2.5 x 10^{-4} min^{-1}, R_{obs} = ca. 0.042 x 10^{-4} sec^{-1}. Note that acid washing reduced the rate of disappearance of allylic alcohol by about half. No epoxy alcohol was detected on gc for either entries 24 or 25.

Table 8, Entries 26 and 28.

Entry 26: In the drybox, 0.605 g Ti(DIPT)(O<u>i</u>Pr)Br (0.00144 mol) was dissolved in 5 mL ether in a reaction vial and treated with 0.175 g Et_3N (0.00173 mol), followed by 0.110 g <u>i</u>PrOH (0.00183 mol). An immediate white precipitate was formed. The vial was capped and allowed to stand with occasional shaking for 45 minutes. The white precipitate was the filtered and washed with ether (3 x 10 mL). The precipitate dried <u>in vacuo</u> to afford 0.256 g $Et_3NH^+Br^-$ (98%). The ether solutions were combined and the solvent evaporated. The resulting clear oil was dissolved in 8 mL CH_2Cl_2 and the solvent was again removed; this was repeated once more to yield alcohol-free Ti(DIPT)(O<u>i</u>Pr)$_2$ (0.00144 mol) with no excess DIPT present.

The Ti-tartrate complex was taken up in CH_2Cl_2 and quantitatively transferred to a dry 100 mL volumetric flask, to which was added 1.800 g <u>i</u>PrOH (0.0300 mol). The flask was removed from the drybox and cooled to 0°C under argon as before. The substrate/standard mixture (0.015 mL) was added and the total volume of the solution after cooling was found to be

<u>Time (min)</u>	<u>GC ratio (Decenol/Std)</u>	<u>ln (GC ratio)</u>
2.27	0.8848	-0.1224
9.25	0.5941	-0.5207
14.38	0.4492	-0.8003
20.55	0.3154	-1.154
26.92	0.2236	-1.498
33.75	0.1521	-1.883

101 mL. After removal of the excess 1 mL of solution by cannula, the reaction was performed in the usual manner.

Plotting the data above (time vs. ln(GC ratio)): R^2 = 0.99995, slope = -0.0558 min^{-1}. R_{obs} = 0.0558/60 = 9.30 x 10^{-4} sec^{-1}.

Entry 28: Generation of Ti(DIPT)(O<u>i</u>Pr)$_2$ was performed as for entry 26 in the drybox with the following reagents: Ti(DIPT)(O<u>i</u>Pr)Br (0.733 g, 0.0175 mol), Et_3N (0.206 g, 0.0020 mol), and <u>i</u>PrOH (0.156 g, 0.0026 mol). Filtration, evaporation, and two CH_2Cl_2/vacuum cycles were done as before to generate 0.0175 mol of Ti(DIPT)(O<u>i</u>Pr)$_2$, which was transferred to a dry

100 mL volumetric flask. To this solution was added 0.071 g (+)-DIPT (0.00030 mol), to provide an overall Ti:DIPT ratio of 1:1.17. After addition of iPrOH (1.766 g, 0.0294 mol), the flask was removed from the drybox, cooled to 0°C, and substrate and standard were added as before. The reaction was then performed in the usual way.

Time (min)	GC ratio (Decenol/Std)	ln (GC ratio)
2.03	0.8979	-0.1077
7.05	0.6177	-0.4813
12.65	0.3829	-0.9601
18.12	0.2538	-1.380
24.88	0.1464	-1.924
29.38	0.1050	-2.254

R^2 = 0.9997; slope = -0.0791 min^{-1}; R_{obs} = 0.0791/60 = 1.32 x 10^{-3} sec^{-1}.

Table 10. Kinetics in ether.

These reactions were performed in the usual way. DIPT was added in 10-30% excess with respect to $Ti(OiPr)_4$; no systematic effect of Ti:DIPT ratio on the rate of epoxidation was observed.

It should be noted that commercially available absolute ether (freshly opened under argon) was decidedly unsuitable for pseudo-first order kinetics measurements. Observed rates were on the order of 2-3 times less (and were far less reproducible) in the commercial solvent than in ether dried by distillation from either $LiAlH_4$ or Na/benzophenone ketyl. The asymmetric epoxidation is thus able to function as a sensitive indicator of water content; I suspect it could even be calibrated!

Tables 7 and 11. Kinetics with (E)-2-hexen-1-ol.

The procedure for epoxidation of hexenol was the same as for decenol, with one exception. Since hexenol is more volatile than decenol, evaporation under reduced pressure was not done. Rather, after quenching with the $FeSO_4$/tartaric acid solution and ether, the organic phase was simply separated, dried with $MgSO_4$, and used directly for gc analysis. The internal standard was n-hexadecane.

Table 12. Kinetics in pentane.

These reactions were performed in exactly the same manner as for CH_2Cl_2.

Table 14. Kinetics using Ti_2(DIPT)(OiPr)6 (2:1 Ti:DIPT).

The 2:1 catalyst was prepared by mixing $Ti(OiPr)_4$ and DIPT in a 2:1

molar ratio. Unlike the 2:2 reactions, DIPT was not present in excess and there are no inactive Ti complexes present. Therefore, $[Ti]_{active}$ was the concentration of $Ti(O\underline{i}Pr)_4$ used to prepare the 2:1 mixture. The pseudo-first order kinetics reactions were performed in the usual manner.

Table 18. Primary deuterium isotope effect determination; pseudo-first order kinetics in the presence of iPrOD.

Entry 70: A CH_2Cl_2 solution of 0.640 g (+)-DIPT (0.00273 mol) and 0.595 g $Ti(O\underline{i}Pr)_4$ (0.00209 mol) was prepared in the drybox, and subjected to four CH_2Cl_2/vacuum cycles to produce a yellow foam. The product was taken up in CH_2Cl_2 and an IR spectrum showed it to be free of isopropanol. The solution was transferred to a 100 mL volumetric flask, to which 0.580 g of 3A powdered sieves and 1.222 g iPrOD were added; the total volume of the solution at room temperature was approximately 104 mL. The flask was then removed from the drybox and cooled to 0°C under argon. A mixture of trans-2-decen-1-ol and n-heptadecane (3:2 v:v) was added (0.020 mL). The volume of the solution at 0°C was 99.5 mL. The reaction was initiated by the addition of 0.400 mL of a 3.744 M solution of TBHP in heptane (0.00150 mol) by gastight syringe, as usual. The molar ratio of O-D to O-H groups in the reaction was therefore [0.201 M (iPrOD)/0.0150 M (TBHP)] = 13.4. Aliquots were quenched and worked up in the usual manner.

Time (min)	GC ratio (Decenol/Std)	ln (GC ratio)
0.80	1.099	0.0944
4.45	0.619	-0.480
6.75	0.442	-0.816
9.48	0.297	-1.214
12.63	0.187	-1.677

Plotting time vs. ln(GC ratio), $R^2 = 0.9997$; slope = -0.149.

$R_{obs} = 0.149/60 = 2.48\ sec^{-1}$.

Entry 69: The reaction was performed exactly as in entry 70, with the following reagents: (+)-DIPT (0.640 g, 0.00273 mol), $Ti(O\underline{i}Pr)_4$ (0.595 g, 0.00209 mol), iPrOH (1.202 g, 0.0200 mol), decenol/heptadecane (0.020 mL), and TBHP (0.400 mL of a 3.744 M solution in heptane, 0.00150 mol). The total volume of the solution at 0°C was 103.0 mL; the extra 3.0 mL were removed before the addition of TBHP.

Time (min)	GC ratio (Decenol/Std)	ln (GC ratio)
0.77	1.039	0.0383
3.43	0.6895	-0.372
6.40	0.4253	-0.855
8.88	0.2929	-1.228
12.20	0.1731	-1.754

R^2 = 0.99995, slope = -0.157, R_{obs} = 0.157/60 = 2.61 x 10^{-3} sec^{-1}.

3. Determination of hydroperoxide binding constants.

Equilibrium constants were determined by FTIR monitoring of the intensity of the RO-H (ca. 3610 cm^{-1}) and ROO-H (3490 cm^{-1}) bands in dilute CH_2Cl_2 solution with added aliquots of hydroperoxide solution.[78] TBHP solutions were in toluene of the indicated molarity; trityl hydroperoxide (Ph_3COOH) solutions were in CH_2Cl_2. The experimental apparatus, designed by Woodard, allows the bulk reaction solution to be mixed and then drawn into the IR cell (KBr) by means of a teflon tube and a Luer-lock syringe; all manipulations done under a positive pressure of argon supplied by a balloon. Spectra were recorded approximately two minutes after addition of each hydroperoxide aliquot; no change occurred with time.

The solutions examined were as follows (reagents in mmol, CH_2Cl_2 in mL):

Sample	$Ti(OiPr)_4$	$Ti(OtBu)_4$	DIPT	iPrOH	tBuOH	CH_2Cl_2	ROOH
1						150.0	TBHP
2					1.28	70.0	TBHP
3						5.96	Ph_3COOH
4	1.40					103.0	TBHP
5	1.63		1.63			150.0	TBHP
6	2.56		2.56	5.12		168	TBHP
7		0.687	0.687			100.0	TBHP
8		0.640	0.640	1.28		70.0	TBHP
9	0.197					6.93	Ph_3COOH
10	0.209		0.209			8.52	Ph_3COOH

Trityl hydroperoxide solutions used were 0.231 M (sample 3), 0.162 M (sample 9), and 0.211 M (sample 10) in CH_2Cl_2. TBHP solutions were 2.80 M or 3.98 M in toluene.

The data is presented below. From the first three experiments,

extinction coefficient values of 8.8 for TBHP and 5.8 for Ph_3COOH were taken for use in calculting $[ROOH]_{free}$ in the subsequent tables.

Calibration

TBHP

Sample	mL ROOH	Abs_{3610}	Abs_{3490}	$[ROOH]_{total}$	Ext. Coeff.
1	0.10		0.017	0.00187	8.9
	0.30		0.051	0.00559	9.2
	0.50		0.085	0.00930	9.1
	0.70		0.119	0.0130	9.2
	1.00		0.170	0.0185	9.2
	1.40		0.234	0.0259	9.0
	1.80		0.299	0.0332	9.0
	2.20		0.351	0.0405	8.7
	2.60		0.411	0.0477	8.6
	3.20		0.502	0.0585	8.6
	3.60		0.565	0.0656	8.6
	4.00		0.628	0.0727	8.6
	4.60		0.713	0.0833	8.6
	5.20		0.804	0.0938	8.6
	5.60		0.820	0.1008	8.5
	6.00		0.919	0.1077	8.5

TBHP in the presence of tBuOH.

Sample	mL ROOH	Abs_{3610}	Abs_{3490}	$[ROOH]_{total}$	Ext. Coeff.
2	0.00	0.132	0.0	0.0	
	0.08	0.133	0.043	0.00454	9.5
	0.12	0.133	0.064	0.00681	9.3
	0.16	0.134	0.084	0.00908	9.3
	0.24	0.132	0.123	0.0136	9.1
	0.32	0.135	0.163	0.0181	9.0
	0.40	0.133	0.207	0.0226	9.1
	0.48	0.133	0.243	0.0271	9.0
	0.56	0.135	0.279	0.0316	8.8
	0.64	0.133	0.317	0.0361	8.8
	0.80	0.133	0.392	0.0450	8.7
	0.88	0.134	0.429	0.0494	8.7
	0.96	0.137	0.466	0.0538	8.7
	1.04	0.138	0.500	0.0583	8.6
	1.20	0.137	0.575	0.0671	8.6
	1.36	0.142	0.644	0.0759	8.5
	1.52	0.143	0.717	0.0846	8.5
	1.68	0.141	0.784	0.0933	8.4
	1.92	0.147	0.887	0.1063	8.4

Trityl Hydroperoxide

Sample	mL ROOH	Abs_{3610}	Abs_{3490}	$[ROOH]_{total}$	Ext. Coeff.
3	0.05		0.011	0.00192	5.7
	0.10		0.021	0.00381	5.5
	0.20		0.042	0.00749	5.6

Sample	mL ROOH	Abs_{3610}	Abs_{3490}	$[ROOH]_{total}$	Ext. Coeff.
3	0.30		0.066	0.0111	6.0
	0.40		0.087	0.0145	6.0
	0.60		0.129	0.0211	6.1
	0.80		0.170	0.0273	6.2
	1.00		0.205	0.0332	6.2
	1.20		0.238	0.0387	6.2
	1.40		0.270	0.0439	6.1

Equilibrium Constant Determinations

$Ti(OiPr)_4$ + TBHP

Sample	mL ROOH	Abs_{3610}	Abs_{3490}	$[ROOH]_{free}$	$[Ti]_{total}$	$[ROOH]_{total}$
4	0.25	0.0494	v. small	v. small	0.0136	0.00676
	0.50	0.0971	0.0216	0.00245	0.0135	0.0135
	0.75	0.146	0.0463	0.00526	0.0135	0.0202
	1.00	0.186	0.0768	0.00873	0.0134	0.0268
	1.25	0.222	0.113	0.0128	0.0134	0.0335
	1.50	0.248	0.145	0.0165	0.0134	0.0401
	2.00	0.303	0.236	0.0268	0.0133	0.0531
	2.50	0.342	0.302	0.0343	0.0133	0.0661
	3.00	0.385	0.394	0.0448	0.0132	0.0790
	3.50	0.403	0.490	0.0557	0.0131	0.0917
	4.00	0.418	0.590	0.0671	0.0131	0.104

$Ti(DIPT)(OiPr)_2$ + TBHP

Sample	mL ROOH	Abs_{3610}	Abs_{3490}	$[ROOH]_{free}$	$[Ti]_{total}$	$[ROOH]_{total}$	K_1
5	0.20	0.017	0.020	0.0022	0.0108	0.00373	0.12
	0.30	0.021	0.021	0.0024	0.0108	0.00559	0.56
	0.40	0.026	0.030	0.0024	0.0108	0.00745	0.64
	0.50	0.030	0.041	0.0046	0.0108	0.00930	0.79
	0.60	0.035	0.052	0.0059	0.0108	0.0112	0.87
	0.70	0.037	0.062	0.0071	0.0108	0.0130	1.00
	0.80	0.041	0.074	0.0084	0.0108	0.0149	1.16
	0.90	0.044	0.086	0.0105	0.0108	0.0167	0.80
	1.00	0.049	0.112	0.0128	0.0108	0.0185	0.50
	1.20	0.056	0.136	0.0154	0.0107	0.0222	0.77

$K_1 = 0.72 \pm 0.3$

$Ti(OiPr)_4$ + DIPT + TBHP

Sample	mL ROOH	Abs_{3610}	Abs_{3490}	$[ROOH]_{free}$	$[Ti]_{total}$	$[ROOH]_{total}$	K_1
6	0.0	0.266	0.0				
	0.20	0.279	0.022	0.0025	0.0153	0.00333	0.72
	0.45	0.288	0.055	0.0063	0.0153	0.00756	0.45
	0.68	0.295	0.077	0.0088	0.0153	0.0113	0.73
	0.91	0.301	0.106	0.0120	0.0152	0.0151	0.70
	1.37	0.308	0.159	0.0180	0.0152	0.0226	0.84
	1.82	0.317	0.220	0.0250	0.0152	0.0300	0.69
	2.28	0.325	0.276	0.0314	0.0151	0.0374	0.76

$K_1 = 0.70 \pm 0.12$

$Ti(DIPT)(OtBu)_2$ + TBHP

Sample	mL ROOH	Abs_{3610}	Abs_{3490}	$[ROOH]_{free}$	$[Ti]_{total}$	$[ROOH]_{total}$	K_1
7	0.06	0.015	0.009	0.0011	0.00687	0.00239	0.27
	0.09	0.020	0.016	0.0018	0.00687	0.00358	0.35
	0.135	0.027	0.029	0.0033	0.00687	0.00537	0.27
	0.180	0.032	0.038	0.0043	0.00686	0.00715	0.47
	0.270	0.043	0.062	0.0071	0.00686	0.0107	0.56
	0.360	0.047	0.094	0.0107	0.00685	0.0143	0.37

$K_1 = 0.38 \pm 0.2$

$Ti(OtBu)_4$ + DIPT + TBHP

Sample	mL ROOH	Abs_{3610}	Abs_{3490}	$[ROOH]_{free}$	$[Ti]_{total}$	$[ROOH]_{total}$	K_1
8	0.0	0.169	0.0	0.0	0.00915	0.0	
	0.08	0.197	0.033	0.0037	0.00914	0.00454	0.52
	0.12	0.212	0.051	0.0058	0.00913	0.00681	0.41
	0.16	0.219	0.070	0.0080	0.00913	0.00908	0.32
	0.24	0.235	0.111	0.013	0.00912	0.0136	0.10
	0.32	0.239	0.150	0.017	0.00911	0.0181	0.16

$K_1 = 0.30 \pm 0.2$

$Ti(OiPr)_4$ + Ph_3COOH

Sample	mL ROOH	Abs_{3610}	Abs_{3490}	$[ROOH]_{free}$	$[Ti]_{total}$	$[ROOH]_{total}$	K_1
9	0.10	0.016	0.007	0.0011	0.0280	0.00230	0.05
	0.20	0.039	0.012	0.0020	0.0276	0.00454	0.13
	0.30	0.053	0.018	0.0030	0.0273	0.00672	0.20
	0.40	0.064	0.026	0.0045	0.0269	0.00884	0.19
	0.50	0.083	0.030	0.0050	0.0265	0.0109	0.34
	0.60	0.123	0.038	0.0066	0.0262	0.0129	0.31

$K_1 = 0.20 \pm 0.1$

$Ti(DIPT)(OiPr)_2$ + Ph_3COOH

Sample	mL ROOH	Abs_{3610}	Abs_{3490}	$[ROOH]_{free}$	$[Ti]_{total}$	$[ROOH]_{total}$	K_1
10	0.05	0.041	0.004	0.0007	0.0243	0.00123	0.017
	0.10	0.087	0.012	0.0021	0.0242	0.00245	0.002
	0.15	0.114	0.019	0.0032	0.0241	0.00365	0.003
	0.20	0.142	0.026	0.0066	0.0236	0.00718	0.002
	0.30	0.165	0.040	0.0088	0.0234	0.00946	0.002
	0.40	0.169	0.053	0.0110	0.0231	0.0139	0.038
	0.50	0.172	0.066	0.0133	0.0229	0.0160	0.027
	0.60	0.176	0.080	0.0172	0.0226	0.0181	0.002
	0.70	0.177	0.093	0.0198	0.0224	0.0202	0.0004
	0.80	0.177	0.103	0.0204	0.0221	0.0222	0.008

$K_1 = 0.010 \pm 0.03$

Data Analysis

For a titanium tetraalkoxide, the binding of successive molecules of hydroperoxide is governed by a separate equilibrium constant, K_1 for the replacement of the first alkoxide with alkylperoxide, K_2 for the second, and so on. In principle, with at least four data points the values of each equilibrium constant can be calculated. However, for all samples but $Ti(O\underline{i}Pr)_4$, only the first binding constant was considered. At the higher concentrations necessary to obtain accurate information for the evaluation of the second, third, and fourth equilibrium constants, TBHP in the presence of titanium begins to decompose at a significant rate at room temperature (producing acetone for isopropoxide samples, as observed in the nmr and in attempted vapor phase gc determinations of equilibrium constants phase). Also, at higher concentrations the linear relationship between concentration and intensity of the O-H bands breaks down. $Ti(O\underline{i}Pr)_4$ was unique in its ability to show binding of more than one TBHP per titanium under acceptably dilute conditions. Even so, only K_1 and K_2 (and not K_3 and K_4) were evaluated for the same reasons as above.

For samples other than $Ti(O\underline{i}Pr)_4$, the equilibrium constant was evaluated from the simple equation:

$$K_1 = \frac{[TiL_2(OR)(OOR)] \times [\underline{i}PrOH]_{free}}{[TiL_2(OR)_2] \times [ROOH]_{free}}$$

The concentration $TiL_2(OR)(OOR)$ was calculated by subtracting the value of $[ROOH]_{free}$ (determined by the 3490 cm^{-1} absorbance) from that of the total amount of hydroperoxide added. For samples lacking free alcohol at the start of the reaction, the concentration of free alcohol simply equals the concentration of bound alkylperoxide.

Values of K_1 are listed in the last column of the tables above, the averaged value is reported.

For $Ti(O\underline{i}Pr)_4$, calculation of K_1 as above gives negative numbers, a consequence of greater than one equivalent of peroxide per Ti center being bound. In this case, a function relating the average number of peroxide ligands bound per metal, n_B, to the first two equilibrium constants, K_1 and K_2, is derived from the equation for K_1 above and the corresponding expression for K_2 as follows:

$$n_B = \frac{[Ti(L_2)(OR)(OOR)] + 2[Ti(L_2)(OOR)_2]}{[Ti(L_2)(OR)(OOR)] + [Ti(L_2)(OOR)_2] + [Ti(L_2)(OR)_2]} \quad (a)$$

By substituting expressions for $[Ti(L_2)(OOR)_2]$ and $[Ti(L_2)(OR)_2]$ in terms of $[Ti(L_2)(OR)(OOR)]$ into equation (a), and factoring out $[Ti(L_2)(OR)(OOR)]$, we obtain:

$$n_B = \frac{K_1C + 2K_1K_2C^2}{1 + K_1C + K_1K_2C^2}, \qquad \text{where } C = [ROOH]_{free} / [ROH]_{free}.$$

Rearranging, we obtain an expression for K_1 in terms of K_2, C, and n_B:

$$K_1 = \frac{n_B}{C(1 - n_B) + K_2C^2(2 - n_B)} \quad . \quad (b)$$

From each data point in the $Ti(O\underline{i}Pr)_4$ + TBHP reaction, C and n_B were obtained. With equation (b), a curve relating K_1 to K_2 for each data point can be constructed. The curve is made up of K_1,K_2 points that satisfy the observed concentrations of species for that data point. That is, for every single data point, a range of K_1 and K_2 values are possible. The point at which two curves intersect describes a unique pair of K_1 and K_2 values that satisfies the observed binding for two different aliquots of TBHP addition.

Curves for the second, third, fourth, and fifth data points are plotted below. Data points beyond the fifth one cannot be treated in this way because more than two equivalents of TBHP per titanium are bound, so K_3 would have to be brought into play, and the analysis would be complicated. As it is, the curve for the fifth data point is far from the other three because an average of 1.8 alkylperoxides per Ti center are found, which is too high a value to be treated by ignoring K_3.

Intersection points occur at $K_1 = 4.1$, $K_2 = 2.8$ in one case, and $K_1 = 2.8$, $K_2 = 4.2$ in the other, a fortuitous juxtaposition of values. Averaging these numbers, we obtain $K_1 = K_2 = 3.5 \pm 1$, as a reasonable estimate.

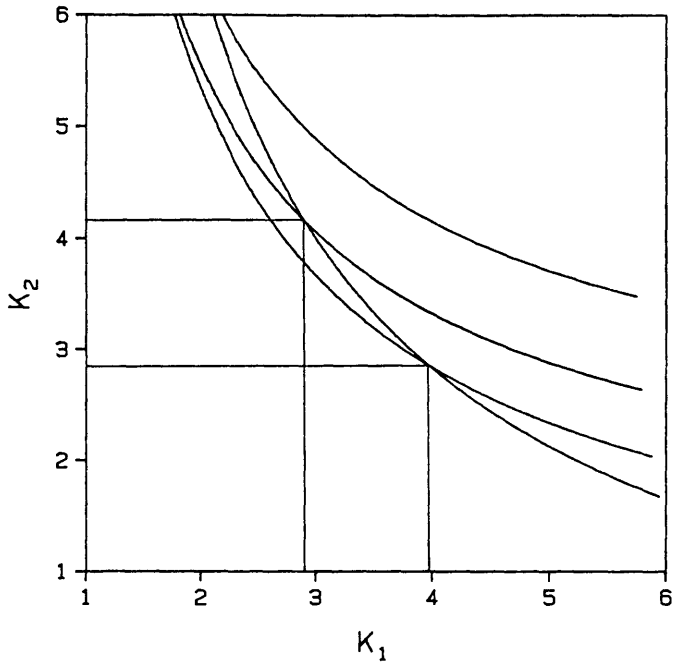

4. ^{17}O NMR

General Procedures

^{17}O nmr spectra were recorded at 33.89 MHz on a Bruker WM-250 spectrometer and at 40.67 MHz on a Varian 300-MHz instrument. Spectral parameters were as follows:

Bruker: 50^{o} pulse; sweep width, 42000 Hz; acquisition delay, 0.16 μsec; pulse delay, 0.02 sec; acquisition time, 0.098 sec; 4K data points; no zero-filling; an exponential multiplication factor of 50-100 was applied to the FID.

Varian: 45^{o} pulse; sweep width, 40000Hz; acquisition delay, 0.20 μsec; plse delay, 0.02 sec; acquisition time, 0.375 sec; 30K data points; no zero-filling; an exponential multiplication factor of 50-100 was applied to the FID.

Signal strength was found to be almost completely insensitive to acquisition delay. However, pulse breakthrough was a problem that could only be addressed by increasing the receiver delay at the expense of signal strength. If too short a receiver delay was used, the baseline signal became erratic to the point of completely masking real signals. A

compromise value was chosen so that weak resonances requiring long acquisitions still had some waviness to the baseline. No proton decoupling was done.

Chemical shifts were referenced to external ether, $Ti(O\underline{t}Bu)_4$, or $Ti(O\underline{i}Pr)_4$. At least one and usually two of these standards were run at the beginning of every session and the peak positions were found to be very reliable. For peaks of less than 40 ppm line width, an error of ± 2 ppm was found; for wider bands, an error of ± 5 ppm is more appropriate.

Preparation of ^{17}O Labeled Cumyl Hydroperoxide

Autoxidation of cumene is discussed in reference 12a; I thank Dr. Stelios Sifniades of Allied Chemical Company for helpful suggestions on the practical aspects of the reaction. $^{17}O_2$ gas (1 L, 20% ^{17}O) was purchased from Cambridge Isotope Laboratories.

Reagent grade cumene (100 g) was cleansed of trace phenols by passage through a column of silica gel (240 mesh, 20 cm long, 1 cm diameter); the product was stored under argon. A 100 mL round-bottomed flask was charged with 24.0 g of cumene (0.20 mol), capped with a reflux condenser, and placed on a volumetric gas buret apparatus. After flushing with $^{16}O_2$, the apparatus was evacuated and then filled with 60 mL $^{17}O_2$ at room temperature (Cambridge Isotope Laboratories, 20% $^{17}O_2$, lecture bottle containing 1L of gas at STP). The reaction flask was then heated to 80°C with vigorous stirring. After 12 h with no reaction, the temperature of the heating bath was increased to 87-88°C; $^{17}O_2$ uptake began after an additional 3 h and slowly accelerated. At reaction times of 24 h, 36 h, 46 h, and 62 h, the gas buret was re-filled with approximately 150 mL O_2. After 72 h, the lecture bottle was opened to the system, and a final pressure of 480 mm was reached after 77 h total reaction time. Assuming the apparatus and lecture bottle have a combined volume of 0.2 L, approximately 0.87 L of O_2 gas was consumed.

After cooling to room temperature, the reaction mixture was flash chromatographed in 1:9 EtOAc:hexane (20 x 5 cm diameter column). The solvent was removed <u>in vacuo</u> and the clear oil was taken up in 30 mL CH_2Cl_2 and transferred to a brown bottle containing activated 3A sieve beads. After standing for 3 h at room temperature, the solution was transferred to a fresh batch of sieves. On washing the first batch of sieves with CH_2Cl_2,

it was found that some hydroperoxide remained adsorbed to the sieves; washing three times with CH_2Cl_2 (10 mL each) retrieved most of the adsorbed material. The solution was again filtered, the remaining sieves washed with CH_2Cl_2 (3 x 10 mL), and the solvent removed to afford 4.05 g (69% based on O_2) of neat cumene hydroperoxide as a clear oil.
^1H NMR ($CDCl_3$) δ 7.63 (s, 1H, -OOH), 7.45-7.20 (m, 5H), 1.55 (s, 6H); IR (film) 3410 (br), 3100, 3070, 3040, 2990, 2940, 1950 (w), 1880 (w), 1810 (w), 1605, 1500, 1450, 1380, 1365, 1330, 1270, 1205, 1155, 1110, 1080, 1033, 952 (w), 913 (w), 812 O-O, 767, 702 cm^{-1}.

For ^{16}O cumyl hydroperoxide, the O-O stretch is found at 835 cm^{-1}. Complete ^{17}O substitution would result in a O-O stretch of approximately 814 cm^{-1}; the observation of a band at 812 cm^{-1} indicates the presence of ^{18}O in the enriched gas.

Preparation of ^{17}O Labeled (Hydroxyl) Tartrate

A 500 mL round-bottomed flask was charged with 250 mL toluene, 21.56 g l-menthol (0.138 mol), and 29 g polyvinylpyridine (Reilly Tar & Co., ca. 0.27 mol nitrogen). A solution of fumaryl chloride (9.59 g, 0.0627 mol) in 5 mL toluene was added by pipette with stirring; the reaction mixture turned light pink. The reaction mixture was heated to reflux for 2 days, after which it was cooled and filtered to afford a light brown solution. Removal of solvent in vacuo and flash chromatography (5x20 cm, 5:95 EtOAc:hexane) afforded 16.39 g of di-l-menthyl fumarate as a yellow oil; $[\alpha]_D^{25}$ -84.7° (c 6.03, 95:5 EtOH:H_2O)
^1H NMR ($CDCl_3$) δ 6.83 (s, 2H), 4.78 (dt, J_1 = 10.4, J_2 = 4.4 Hz, 2H), 2.04 (dm, J_1 = 10 Hz, 2H), 1.88 (doublet of quintets, J_1 = 7.4, J_2 = 2 Hz, 2H), 1.71 (br d, 4H), 1.59-1.35 (m, 4H), 1.27 (t, J = 7.4 Hz, 2H), 1.07 (m, 6H), 0.92 (dd, J_1 = 6.8, J_2 = 3 Hz, 12H), 0.77 (d, J = 6.8 Hz, 6H); IR ($CHCl_3$) 2960, 2940, 2880, 1712 (s, C=O), 1640 (w, C=C), 1460, 1370, 1300 (s), 1265 (s), 1165, 1010, 990 cm^{-1}.

It was found that the quinuclidine adduct of OsO_4 undergoes exchange with $^{17}OH_2$ readily in THF or t-butanol. While the initial dihydroxylations of dimenthyl fumarate were done with stoichiometric quantities of labeled OsO_4·quinuclidine, the following catalytic procedure based on that of Van Rheenan, et. al.[127] was far superior.

A 100 mL round-bottomed flask was charged with a stir bar and N-methylmorpholine-N-oxide monohydrate (Fluka Chemicals, 3.70 g, 0.0274 mol). The solid was heated in a 90-95°C bath with stirring under vacuum (0.15 mm) overnight, after which some of the material had sublimed to the upper part of the flask. After cooling to room temperature, dry tert-butanol was introduced (7 mL), followed by $^{17}OH_2$ (Monsanto Research Corp., Mound Facility, 23% ^{17}O, 61.5% ^{18}O; 1.00 g; 0.0514 mol) - driving most of the N-oxide into solution - and OsO_4 (0.63 mL of a 0.1 g/mL solution in hexane, 0.000243 mol). The reaction vessel was heated to 35-40°C with stirring while a viscous solution of 4.80 g di-l-menthyl fumarate (0.0122 mol) in 3 mL tert-butanol was then added to the reaction flask over 12 hours by a syringe pump. TLC (1:9 EtOAc:hexane) showed the olefin to be oxidized very rapidly upon addition, so that no unreacted olefin builds up during the addition. Assuming that the ^{17}O label is therefore completely incorporated in the OsO_4 at every instant in the reaction, it is easy to calculate the expected level of incorporation as a function of the amount of olefin consumed. Since ^{16}O is bled into the reaction mixture from the N-oxide only as fast as the olefin is consumed, this method makes the greatest possible use of the ^{17}O label: after 1 mmol of substrate consumed, the product should be 22.5% enriched in ^{17}O (from $^{17}OH_2$ of 23.0% enrichment); after 5 mmol, 22.48%; and after complete reaction (12.2 mmol), the label should be present in 22.38%.

Following addition of the substrate, the reaction mixture was degassed by two freeze/pump/thaw cycles and the solvent was removed by bulb-to-bulb distillation under vacuum in order to recover unused ^{17}O label. The resulting brown sticky solid was taken up in 160 mL CH_2Cl_2 and washed with 80 mL aqueous $NaHSO_3$ (1.8 M). The aqueous phase was extracted with CH_2Cl_2 (3 x 30 mL). Ether (300 mL) was added and the combined organic phases washed with 80 mL $NaHSO_3$ solution until the disappearance of the brown color. The aqueous phase was extracted with CH_2Cl_2 (60 mL) and the combined organic phases were washed with saturated NaCl and dried ($MgSO_4$). The solvent was removed to afford 5.19 g of crude product as a yellow oil. The diastereomeric diols have R_f values of 0.75 and 0.71 on tlc in 1:9 EtOAc:hexane. Flash chromatography twice (5:95 EtOAc:hexane) afforded 1.87 g of the less polar diastereomer, (2R,3R)-di-l-menthyl tartrate, **33a**, 0.45 g of the more polar diastereomer, (2S,3S)-di-l-menthyl tartrate, **33b**, and

2.02 g of a mixture of diols (total 4.34 g, 82%). These colorless diol diesters are very viscous oils that foam dramatically under vacuum. The absolute configuration assignments are derived from the optical rotations of DIPT generated by transesterification of these menthyl esters, described below.

Data for **33a**: ^{1}H NMR ($CDCl_3$) δ 4.84 (dt, J_1 = 13.3, J_2 = 5.0 Hz, 2H), 4.35 (d, J = 8.4 Hz, 2H), 3.11 (d, J = 8.4 Hz, 2H, -OH), 2.07 (br d, 2H), 1.96 (m, 2H), 1.72 (br d, 4H), 1.6-1.4 (m, 4H), 1.07 (m, 4H), 0.92 (t, 14H), 0.77 (d, J = 6.2 Hz, 6H); ^{13}C NMR (CD_2Cl_2) 171.7, 77.0, 72.4, 47.4, 41.0, 34.5, 31.8, 26.7, 23.7, 22.1, 20.9, 16.3; IR (CH_2Cl_2) 3521, 2960, 2940, 2880, 1740 (s, C=O), 1465, 1455, 1390, 1370, 1265, 1114, 1078, 950, 911 cm^{-1}.

Anal. Calcd for $C_{24}H_{42}O_6$: C, 67.57; H, 9.92. Found: C, 67.23; H, 9.68.

Data for **33b**: ^{1}H NMR ($CDCl_3$) δ 4.88 (dt, J_1 = 13.3 Hz, J_2 = 4.7 Hz, 2H), 4.49 (d, J = 7.3 Hz, 2H), 4.14 (d, J = 7.3 Hz, 2H, -OH), 2.05 (br d, 2H), 1.88 (m, 2H), 1.72 (br d, 6H), 1.6-1.4 (m, 4H), 1.08 (m, 4H), 0.92 (d, 14H), 0.79 (d, J = 7 Hz, 6H). ^{13}C NMR (CD_2Cl_2) δ 171.7, 77.2, 72.6, 47.4, 41.1, 34.5, 31.8, 26.3, 23.4, 22.1, 20.9, 16.0; IR (CH_2Cl_2) same as for **33a**. Anal. Calcd for $C_{24}H_{42}O_6$: C, 67.57; H, 9.92. Found: C, 67.42; H, 9.89.

The presence of ^{17}O in the hydroxylic positions was indicated by the difference in IR spectra of labeled and unlabeled dimenthyl tartrate. The O-H stretch appears at 3528 cm^{-1} for unlabeled **33a** and at 3521 for the labeled compound. Of greater interest is the fingerprint region. Below appears the IR spectra of labeled and unlabeled **33b** in CH_2Cl_2. Bands due to C-O bending modes are highlighted by the difference spectrum (^{17}O - ^{16}O) which also appears below.

The transesterification of the dimenthyl ester proved to be somewhat difficult. Of several acid catalyzed methods tried, transesterification with $Ti(O\underline{i}Pr)_4$ in isopropanol proved to be the best. Thus, samples of **33a** or **33b** were placed in a 50 mL round bottomed flask with a stir bar and 35 mL of dry isopropanol. Approximately 0.5 equivalent of $Ti(O\underline{i}Pr)_4$ was then

FTIR of Di-l-menthyl-(2S,3S)-tartrate

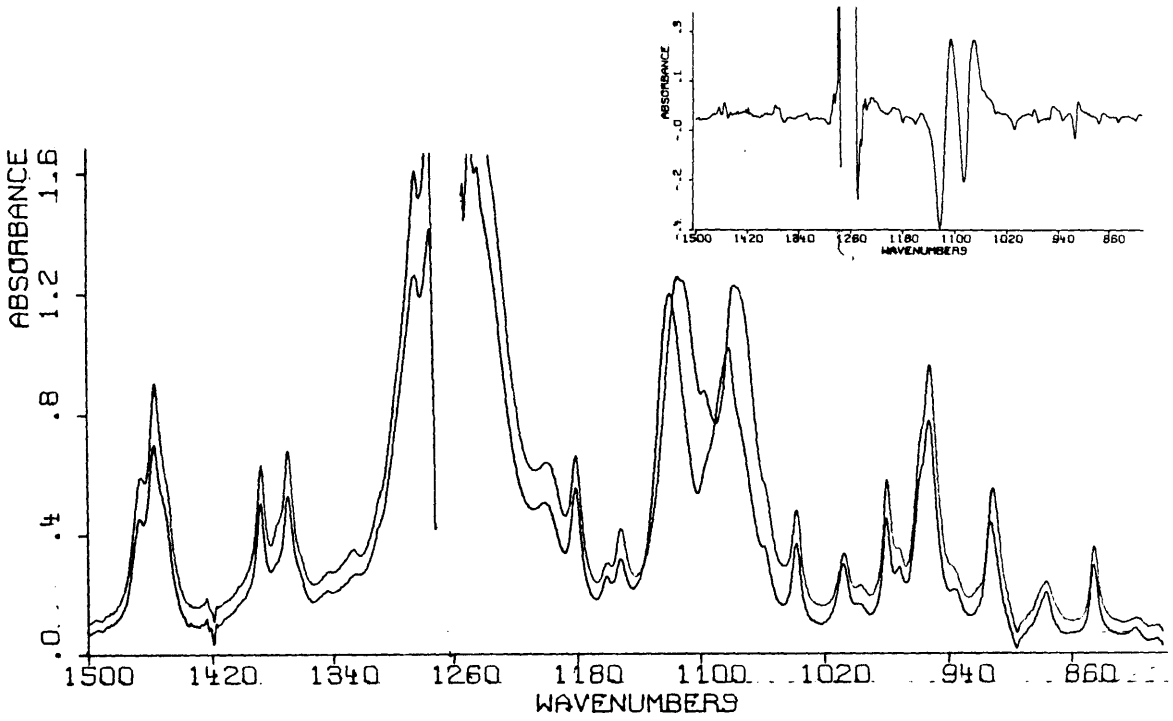

added by syringe, and the reaction mixture was refluxed for 12 hours. After cooling to room temperature, the reaction solution was transferred to a stirred mixture of 20% aqueous tartaric acid (approximately 20 mL) and ether (50 mL). Saturated NaCl (20 mL) was added to break up the resulting emulsion and the aqueous layer was extracted with ether (twice) and then with CH_2Cl_2 (once). The combined organic phases were dried ($MgSO_4$) and solvent removed to give a mixture of menthol, DIPT, and partially transesterified material (menthyl isopropyl tartrate). Flash chromatography (2:3 EtOAc:hexane) afforded 50-70% yields of DIPT. The less polar dimenthyl tartrate, **33a**, afforded (+)-DIPT: $[\alpha]_D^{25}$ +13.00° (c 6.2, CCl_4). The more polar dimenthyl tartrate, **33b**, afforded (-)-DIPT: $[\alpha]_D^{25}$ -13.06° (c 10.25, CCl_4). For comparison, commercially available (+)-DIPT shows $[\alpha]_D^{25}$ +13.08° (c 5.85, CCl_4); $[\alpha]_D^{25}$ +7.87° (c 6.67, $CHCl_3$); and $[\alpha]_D^{25}$ +12.74° (c 8.94, 95:5 EtOH:H_2O). ^1H and ^{13}C NMR spectra of the labeled DIPT were identical to those of commercially available material. For (+)-DIPT from **33a**: Anal. Calcd for $C_{10}H_{18}O_6$: C, 51.27; H, 7.75. Found: C, 51.09; H, 7.73.

It was later discovered that base catalyzed transesterification of DIPT to DET (EtOH solvent, catalytic NaOMe, room temperature, 12 h) resulted in only about 1% epimerization of the tartrate by optical rotation. This method, then, may be superior to titanium catalyzed transesterification for the production of DET from dimenthyl tartrate.

Preparation of ^{17}O Labeled (2R, 3R)-N,N'-Dibenzyltartramide.

In a variation of the published procedure,[84] a 25 mL round bottomed flask was charged with (2R, 3R)-di-l-menthyl tartrate **33a** (0.62 g, 0.00145 mol), and 5 mL benzyl amine. After heating to reflux for 14 hours, the solvent was removed *in vacuo* to afford a white solid. Recrystallization from hot toluene afforded 0.30 g (63%) of the labeled (2R, 3R)-N,N'-dibenzyltartramide as white crystals; mp. 201-202°C (lit.[84] mp 202-203°C). Anal. Calcd for $C_{18}H_{20}N_2O_4$: C, 65.84; H, 6.14; N, 8.53. Found: C, 65.63; H, 6.22; N, 8.29.

Preparation of ^{17}O Labeled (Carbonyl) Tartrate.

A 15x1 cm threaded high pressure reaction tube with teflon stopper was charged with L-(+)-tartaric acid (1.108 g, 0.00738 mol) and $^{17}OH_2$ (23% ^{17}O, 0.575 g, 0.00295 mol). The tube was placed in an oil bath at 125°C for five minutes, at which time the oil bath was allowed to cool to room temperature over 2 hours. The solution was then transferred to a dry 200 mL round bottomed flask and dry isopropanol (150 mL) and p-toluenesulfonic acid (0.03 g) were added. The reaction was refluxed for 3 h, and then distilled to reduce the volume to 40 mL. Addition of more isopropanol (150 mL) followed by distillation again to 40 mL was required to drive the reaction to completion. The remaining solvent was removed *in vacuo* and the crude product subjected to flash chromatography on a short column (1:1 EtOAc:hexane) to isolate (+)-DIPT-^{17}O (C=O), as a clear oil (1.636 g, 95% yield). The NMR spectrum was identical to ^{16}O DIPT; the IR spectrum differed only in the position of the C=O stretch, 1730 cm^{-1} (compared to 1740 cm^{-1} for ^{16}O DIPT).

Preparation of Benzoic Acid-^{17}O.

According to the literature procedure,[128] α,α,α-trichlorotoluene (Aldrich, distilled, 2.50 g, 0.0128 mol) and $^{17}OH_2$ (23% ^{17}O, 1.00 g, 0.0514

mol) were combined in a dry 25 mL pear-shaped flask. The flask was capped with a reflux condenser and $CaSO_4$ drying tube, and the reaction mixture was heated at a bath temperature of 140°C. After 12 h, white solid had sublimed to the upper part of the flask and the lower part of the reflux condenser. The entire apparatus was evacuated to remove volatile components and the solid was washed with hexane (3 x 10 mL). The solid was dissolved in ether (10 mL), filtered, and solvent removed to afford 1.520 g (97%) of benzoic acid-^{17}O as a white solid, mp 120-122°C (lit.[128] mp 122.4°C). IR (CH_2Cl_2) 3200-2800 (br), 2660, 2520, 1672, 1605, 1583, 1450, 1410, 1318, 1280-1250, 1180, 1115, 1070, 1029, 940 (br), 897, 755, 700 (br,s) cm^{-1}. The IR spectrum in CH_2Cl_2 of ^{16}O benzoic acid (Aldrich) shows a band at 1690 cm^{-1} for the C=O stretch, indicating successful isotopic labeling of the carboxylate group.

Preparation of ^{17}O Labeled (dl)-Ethyl-α-hydroxycyclohexyl Acetate, 17.

The Mitsunobu reaction[129] with labeled benzoic acid was used to introduce ^{17}O to this α-hydroxy ester system. Unfortunately, the cyclohexyl group of ethyl-α-hydroxycyclohexyl acetate makes the carbinol center too hindered for successful Mitsunobu displacement. Thus, the reaction had to be performed on ethyl mandelate with subsequent hydrogenation of the phenyl group to afford **17**.

A 100 mL round bottomed flask was charged with 40 mL THF, 0.607 g (dl)-ethyl mandelate (0.00337 mol) 0.884 g triphenyl phosphine (0.00337 mol), 0.411 g benzoic acid-^{17}O (0.00336 mol), and a stir bar. Diethylazodicarboxylate (0.539 mL, 0.587 g, 0.00337 mol) was then added by syringe under Ar atmosphere. TLC showed the reaction to have stopped after 4 h, with some starting material remaining. It is useful to note that while ethyl mandelate is visualized under uv radiation on the TLC plate, the product benzoate ester is not; it must be stained with phosphomolybdic acid. After 12 h, the solvent was removed in vacuo and the solid product flash chromatographed (CH_2Cl_2) to afford 0.575 g (60%) (dl)-ethyl- -benzoyloxyphenylacetate, **34**, as a colorless oil.

^1H NMR ($CDCl_3$) δ8.11 (m, 2H), 7.73 (m, 2H), 7.44 (m, 6H), 6.15 (s, 1H), 4.21 (m, 2H), 1.24 (t, J = 6.7 Hz, 3H); IR (film) 3070, 3040, 2990, 2940, 2910, 1753, 1715, 1604, 1588, 1500, 1455, 1372, 1350, 1320, 1280-1250, 1215, 1180, 1110, 1072, 1040, 1030, 735, 718, 702 cm^{-1}.

The benzoate ester **34** (0.572 g, 0.0020 mol) was taken up in 15 mL absolute ethanol and treated with 0.1 g NaOMe at room temperature. After 7 h, the reaction was treated with 15% 1N HCl and extracted with CH_2Cl_2 (4 x 30 mL). The combined organic phases were dried ($MgSO_4$) and solvent was removed to afford a clear oil. Column chromatography (1:4 EtOAc:hexane) provided ^{17}O labeled ethyl benzoate (C=O labeled) and ethyl mandelate (OH labeled). The latter was taken up in 10 mL methanol; 2 drops of glacial acetic acid and 0.1 g Rh/Al_2O_3 powder (Aldrich, 5% Rh) were added. The mixture was hydrogenated at 53 psi for 2 hours. Filtration through Celite and removal of solvent under vacuum afforded clean (dl)-ethyl-α-hydroxy-phenyl acetate-^{17}O, **17**, (0.243 g, 65% for two steps) as a colorless oil.
^1H NMR ($CDCl_3$) δ 4.26 (q, J = 7.3 Hz, 2H), 4.00 (d, J = 4 Hz, 1H), 3.5 (br s, 1H, -OH), 1.7 (m, 4H), 1.29 (t, J = 7.3 Hz, 3H), 1.2 (m, 6H); IR (film) 3500 (br), 2980, 2930, 2850, 1730, 1450, 1390, 1370, 1260, 1220, 1148, 1118, 1080, 1030, 980, 940, 895, 865 cm^{-1}.

Preparation of ^{17}O Labeled Ethyl Lactate, 18.

The Mitsunobu reaction [129] using ^{17}O-benzoic acid was performed with (+)-ethyl lactate as above, using the following reagents: (+)-ethyl lactate (1.460 g, 0.0124 mol), benzoic acid-^{17}O (1.520 g, 0.0124 mol), triphenylphosphine (4.86 g, 0.0185 mol), diethylazodicarboxylate (3.23 g, 0.0185 mol), and THF (50 mL). The azodicarboxylate was added portionwise by syringe; the reaction solution went clear after each addition but the final one of 0.5 mL. After standing at room temperature for 6 h, the solvent was removed to afford a viscous yellow oil. Flash chromatography (5x15 cm column, 1:4 EtOAc:hexane) afforded 2.39 g (87% based on benzoic acid and ethyl lactate) of ethyl-2-benzoyloxy-propionate, **35**, as a clear oil.
^1H NMR (neat) δ 8.14 (m, 2H), 7.45 (m, 3H), 5.32 (q, J = 7.4 Hz, 1H), 4.17 (q, J = 6.5 Hz, 2H), 1.64 (d, J = 7.4 Hz, 3H), 1.24 (q, J = 6.5 Hz, 3H).

The benzoate **35** (2.35 g, 0.0114 mol) dissolved in 100 mL absolute ethanol and 0.1 g NaOMe was added. The reaction mixture was allowed to stand at room temperature for 12 hours and then at 4°C for 3 days. Ether (60 mL) and 1 N HCl (60 mL) were then added. The aqueous layer was extracted with ether (5 x 60 mL) and the combined organic phases dried ($MgSO_4$) and

evaporated to afford a clear oil. Flash chromatography (CH_2Cl_2) provided a solution of purified ethyl lactate-^{17}O in CH_2Cl_2. The volume of the solution was reduced to approximately 5 mL and activated 3A sieve beads were added. After standing at room temperature for 3 h, the solution was transferred to a fresh batch of sieves; washing the first batch with dry CH_2Cl_2 brought the solution volume up to 10 mL. NMR of a small portion of this product was identical to that of commercially available ethyl lactate; because of compound's volatility (bp = 154°C) the bulk of the material was not freed of solvent. NMR of the CH_2Cl_2 solution showed there to be 1 mmol of ethyl lactate present for every 1.36 g of solution (assuming the solution density to be the same as that of CH_2Cl_2 alone). Since there was 10 mL (13.3 g) of this solution present, the transesterification proceeded in approximately 86% yield. IR (CH_2Cl_2) was also identical to that of the ^{16}O material (Aldrich), except for the O-H stretching band at 3528.4 cm^{-1} for **18** vs. 3541 cm^{-1} for ^{16}O-ethyl lactate, and for several bands in the fingerprint region, as shown below by the IR spectrum and the ^{17}O-^{16}O difference spectrum. Approximately 1 g of the lactate solution was evaporated on high vacuum to afford 20 mg of solvent-free sample: Anal. Calcd for $C_5H_{10}O_3$: C, 50.84; H, 8.53. Found: C, 50.61; H, 8.51.

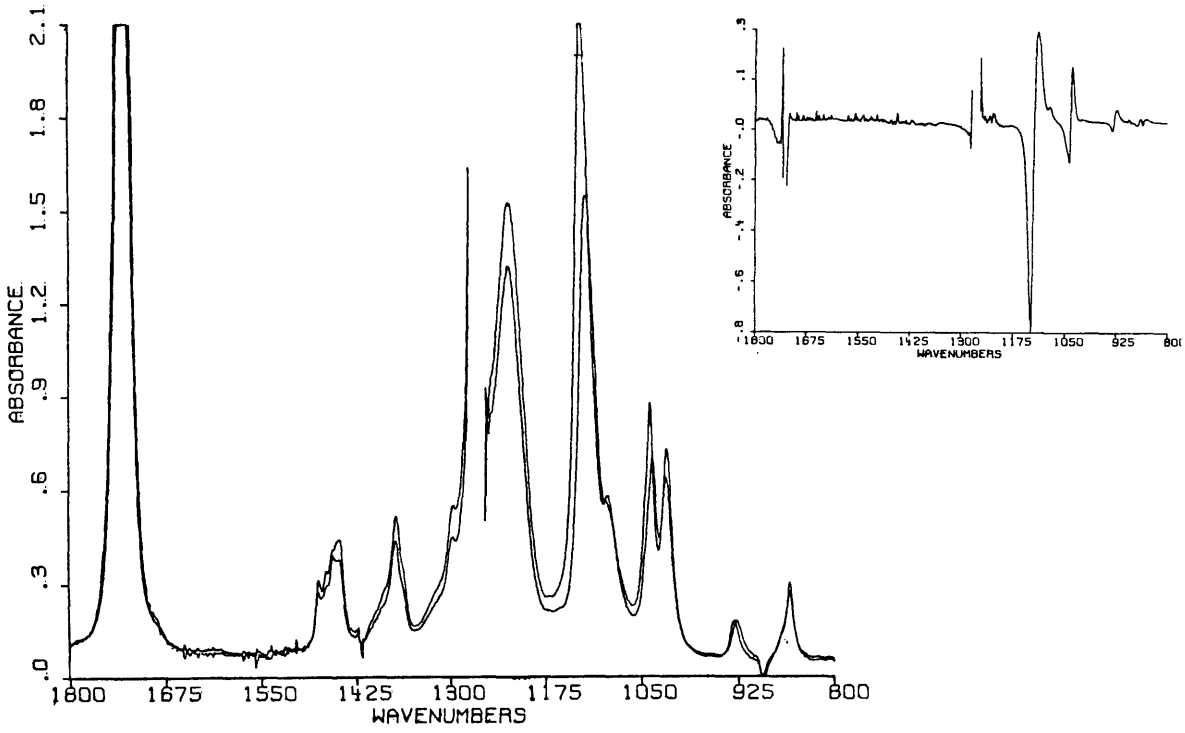

Preparation of ^{17}O Labeled Benzyl Alcohol.

To a dry, 200 mL round bottomed flask charged with 50 mL THF, benzaldehyde (2.00 g, 0.0187 mol), approximately 20 mg p-toluenesulfonic acid, and a stir bar was added 1.00 g (0.0516 mmol) of $^{17}OH_2$ by syringe. After stirring for 2 h at room temperature, the reaction mixture was cooled to -20°C and a suspension of 2.7 g $LiAlH_4$ (0.071 mol) in 100 mL ether cooled to -20°C was added portionwise by cannula. After the addition was complete, the reaction mixture was allowed to stir for 2 h while warming to room temperature. Workup by the Steinhardt method[130], filtration of the precipitate, drying of the organic phase ($MgSO_4$), and evaporation afforded 1.96 g benzyl alcohol-^{17}O as a colorless oil. Distillation at atmospheric pressure (bp = 204°C) afforded 1.85 g (91%) of dry benzyl alcohol an estimated 17% ^{17}O enrichment. Anal. Calcd for C_7H_8O: C, 77.75; H, 7.46. Found: C, 77.49; H, 7.53.

5. Mass Spectroscopy of Titanium-Tartrates

Low resolution electron impact mass spectroscopy was done on a Varian MAT-44 instrument at 22.3 eV. Solutions of approximately 0.4 M in titanium were prepared in CH_2Cl_2, transferred to dry capillary tubes, and sealed with vacuum grease in the dry box. To obtain the spectrum, a sample tube was placed in the probe holder, the seal was broken, and the probe was quickly placed in the instrument and evacuated. After the solvent was removed, the probe was heated slowly to volatilize the sample. Peak positions were accurate to only ± 1 amu.

6. Formation of Ti-tartrate in Pentane Monitored by Vapor Phase GC

A solution of $Ti(O\underline{i}Pr)_4$ (0.816 g, 0.00287 mol), (+)-DIPT (0.672 g, 0.00287 mol), toluene (0.572 g) as an internal standard, and pentane (25.0 mL) was prepared in a 50 mL Ehrlenmeyer flask in the drybox, and was capped with a rubber septum. For analysis, 0.250 mL of the vapor above the solution was removed by gastight syringe and injected into the gc. Before each injection 0.25 mL of argon was added by the same syringe to the reaction flask to maintain a constant pressure. Nine injections were averaged to obtain a gc ratio of iPrOH/toluene of 72.56/27.44.

Calibration was performed by vapor phase gc analysis of a solution of isopropanol (0.3456 g, 0.00575 mol) and toluene (0.5732 g) in 25.0 mL pentane. Note that the amount of isopropanol used for calibration was exactly that expected for release of two equivalents into solution in the first experiment. Also note that the amount of internal standard was the same for both experiments. An average of six injections of the calibration sample gave a iPrOH/toluene ratio of 73.12/26.88, indicating the release of 2.00 ± 0.03 moles of iPrOH into solution per mole of DIPT added.

$Ti(O\underline{i}Pr)_4$ (0.500 mL, 0.0017 mol) was then added to the calibration sample to see if the presence of titanium tetralkoxide changes the observed ratio by dative coordination of isopropanol. An average of four gc injections gave a iPrOH/toluene ratio of 72.58/27.42, the same as in the absence of $Ti(O\underline{i}Pr)_4$.

An identical experiment was performed with $Ti(OEt)_4$ (0.509 g, 0.00223 mol), (+)-DET (0.460 g, 0.00223 mol), toluene (0.693 g) and pentane (25.0 mL). Averaging 18 injections gave an EtOH/toluene ratio of 71.61/28.39. A calibration run performed with ethanol (0.2054 g, 0.00446 mol), toluene (0.6930 g), and pentane (25.0 mL) gave an EtOH/toluene ratio of 72.26/27.74 after averaging of 9 injections. Adding 0.50 mL of $Ti(OEt)_4$ gave a ratio of 72.33/27.67 after 7 injections. Thus, the release of 1.98 ± 0.04 moles of ethanol is observed upon addition of 1 mole of DET to $Ti(OEt)_4$.

Gas chromatography was performed on a 20 meter Carbowax 20-M fused silica column with helium carrier gas. Retention times were as follows: isopropanol, 2.42 min (flow rate = 40 mL/min); toluene, 4.28 min (flow = 40); ethanol, 2.82 min (flow = 35); toluene, 4.84 min (flow = 35).

7. Determination of Secondary Deuterium Isotope Effects in Epoxidations of 2-Decen-1-ol Substrates.

Preparation of (E)-2-decen-1-ol, 36.

The $LiAlH_4$/NaOMe reduction scheme used here is that of Corey, et. al.[131]

To 200 mL dry THF in a dry, 300 mL round-bottomed flask was added 0.688 g (0.0182 mol) $LiAlH_4$ powder, followed by NaOMe 1.960 g (0.0364 mol) with stirring, taking care to vent the septum-stoppered flask through a wide-bore needle to accomodate the release of some H_2 gas. To the stirred reaction mixture under Ar atmosphere was added 2.00 g 2-decyn-1-ol (0.0130 mol) by syringe. After stirring for 30 minutes, the septum was replaced by a reflux condenser, and the reaction was heated to reflux for 3 hours. The solution was then cooled to -78°C and is transferred by cannula into a slurry of 3 mL of water in 100 mL of THF at -78°C with vigorous stirring. The stirred reaction mixture was allowed to warm to room temperature, and 100 mL of ether was added. The organic phase was then dried ($MgSO_4$) and solvent was removed to afford a colorless oil. Flash chromatography (15:85 EtOAc:hexane) produced 1.91 g (94%) of (E)-2-decen-1-ol as a colorless oil. GC analysis indicated the absence of (Z)-allylic alcohol.
^1H NMR ($CDCl_3$) δ 5.66 (m, 2H), 4.09 (d, J = 4.0 Hz, 2H), 2.05 (q, J = 7.0 Hz, 2H), 1.49 (br s, 1H), 1.25 (m, 10H), 0.90 (t, J = 7.1 Hz, 3H); ^{13}C NMR ($CDCl_3$) 133.0, 128.8, 63.3, 32.1, 31.7, 29.1, 22.5, 13.9.

Since the allylic alcohol itself was found to give irreproducible mass spectra, the t-butyldimethylsilyl ether was made by the following general method: to a solution of one equivalent of **36** and three equivalents of triethyl amine was added two equivalents t-butyldimethylsilyltrifluoromethane sulfonate (TBDMS-OTf) at 0°C. The reaction was complete in 10 minutes, and was quenched by the addition of 1 mL of water, followed by 5 mL of 0.5N HCl. The organic phase was dried (Na_2SO_4) and the solvent removed to give a colorless oil. Flash chromatography (1:5 EtOAc:hexane) yielded the pure silyl ether, **37**.
^1H NMR ($CDCl_3$) δ 5.64 (m, 2H), 4.09 (d, J=4.2 Hz, 2H), 2.05 (q, J = 7.0 Hz, 2H), 1.25 (m, 10H), 0.91 (s, 9H), 0.89 (t, 3H), 0.05 (s, 6H).

Preparation of (E)-3-deuterio-2-decen-1-ol, 38.

A sample of $LiAlH_4$ powder was titrated by hydrolysis with dilute HCl on a gas buret, revealing it to contain about 75% of the theoretical amount of active hydride. The $LiAlH_4$/NaOMe reduction was carried out as above with the following reagents: 150 mL dry THF, 1.40 g of the $LiAlH_4$ powder (approximately 0.028 mol), 3.02 g NaOMe powder (0.0559 mol), and 3.23 g of 2-decyn-1-ol (0.0201 mol). The reaction was quenched with iodine as follows. In a separate dry flask was placed 100 mL THF and 31 g of I_2 (0.122 mol); this solution was also cooled to -78°C under inert atmosphere. The reaction mixture was added by cannula to the iodine solution with rapid stirring. After 15 minutes at -78°C, the reaction mixture was allowed to stir overnight, slowly warming to room temperature. The solution was then transferred to a separatory funnel, 150 mL of ether was added, and the mixture washed with 0.7 M Na_2SO_3 until the iodine color disappeared (4 x 100 mL). The combined aqueous phases were extracted with ether (2 x 80 mL), and the combined organic phases were then dried ($MgSO_4$) and solvent removed to give a yellow oil. Flash chromatography (1:4 EtOAc:hexane) gave 1.959 g (E)-3-iodo-2-decen-ol **39** as a colorless oil (33%) plus approximately 0.6 g of **39** contaminated with a small amount of (E)-2-decen-1-ol.

Data for **39**:

^1H NMR ($CDCl_3$) δ 5.86 (t, J = 6.2 Hz, 1H), 4.21 (d, J = 6.2 Hz, 2H), 2.51 (t, J = 7.0 Hz, 2H), 1.55 (m, 3H), 1.28 (m, 8H), 0.88 (t, J = 7 Hz, 3H); ^{13}C NMR ($CDCl_3$) 133.4 (d), 110.3 (s), 67.1, 45.1, 31.7, 29.2, 29.0, 28.1, 22.5, 14.0.

In a 50 mL round-bottomed flask was placed 1.910 g of **39** (0.0688 mol) and a stir bar. THF (10 mL) was added, followed by 1 mL D_2O. After stirring briefly, the solvent was removed under high vacuum. This process of THF and D_2O addition followed by evaporation under vacuum was repeated twice more with 3-4 mL THF and 0.8 mL D_2O. The colorless oil was taken up in 25 mL THF and cooled to -78°C under Ar. t-BuLi (10 mL of a 1.9 M solution in hexane, 0.019 mol) was added dropwise by syringe. After the addition was complete, the reaction was stirred at -78°C for 15 minutes and then quenched by cannula transfer into a solution of 4 mL D_2O in 30 mL THF cooled to -70°C. The reaction mixture was stirred while warming to room

temperature and 100 mL ether was added. The aqueous phase was dried ($MgSO_4$) and solvent was removed. Flash chromatography of the crude product (1:4 EtOAc:hexane) gave 0.9083 g (84%) of **38** as a colorless oil. ^1H NMR (below) showed approximately 20% of the product to be (E)-2-decen-1-ol, that is, the protonated, not deuterated, allylic alcohol. Since the deuterated substrate was meant to be used in competition with the protonated one, this product was used as obtained, and the competition experiment simply adjusted for an 80% deuterium content. GC analysis showed no (Z)-allylic alcohol to be present.

Data for **38**:

^1H NMR ($CDCl_3$) δ 5.69 (m, 0.2H), 5.64 (m, sharpens to br s upon irradiation at 4.09 δ, 1H), 4.09 (d, J = 5.7 Hz, 2H), 2.05 (t, J = 7.3 Hz, 2H), 1.25-1.38 (m, 9H), 0.90 (t, J = 6.7 Hz, 3H); ^{13}C NMR ($CDCl_3$) 133.26 (d, small), 128.7 (d), 63.5, 32.1, 31.8, 29.1, 22.6, 14.0. Anal. Calcd for $C_{10}H_{19}OD$: C, 76.87; H, 12.90. Found: C, 76.78; H, 12.62.

The TBDMS ether of **38** was prepared in the usual way to afford a colorless oil, **40**:

^1H NMR ($CDCl_3$) δ 5.69 (m, 0.2H), 5.64 (m, 1H), 4.09 (d, J = 6.0 Hz, 2H), 2.02 (t, J = 7 Hz, 2H), 1.27 (m, 8H), 0.91 (s, 9H), 0.89 (t, 3H), 0.05 (s, 6H).

Preparation of (E)-2-deuterio-2-decen-1-ol, 41.

The reaction sequence was identical to that for (E)-3-deuterio-2-decen-1-ol **38** above, with the following reagents:

$LiAlD_4$ (98 atom % D, 0.975 g, 0.0233 mol), 150 mL THF, NaOMe (2.51 g, 0.0465 mol), 2-decyn-1-ol (2.87 g, 0.0186 mol), and I_2 (30 g, 0.12 mol) in 100 mL THF. Flash chromatography yielded 2.261 g (43%) of (E)-3-iodo-2-deuterio-2-decen-1-ol **42** as a colorless oil.

^1H NMR ($CDCl_3$) δ 4.20 (d, J = 6.0 Hz, 2H), 1.50 (t, J = 7.4 Hz, 2H), 1.52 (m, 3H), 1.29 (br s, 8H), 0.89 (t, J = 6.7 Hz, 3H); ^{13}C NMR ($CDCl_3$) δ 133.1 (t, J_{CD} = 23 Hz), 110.1 (s), 67.0, 45.0, 31.6, 29.1, 28.9, 28.1, 22.5, 14.0.

Lithiation and hydrolysis of **42** was performed (without deuterium exchange of the alcohol with D_2O) in the same way as for **39**, with the

following amounts of reagents: **42** (2.250 g, 0.00797 mol), t-BuLi (0.019 mmol, 10 mL of a 1.9 M solution), 30 mL THF, and 4 mL H_2O in 30 mL THF. Flash chromatography provided 1.176 g (94%) of (E)-2-deuterio-2-decen-1-ol as a colorless oil.

^1H NMR ($CDCl_3$) δ 5.69 (br t, collapses to br s on irradiation at 4.09 , 1H), 4.09 (d, J = 6.0 Hz, 2H), 2.05 (q, J = 6.7 Hz, 2H), 1.28 (m, 9H), 0.89 (t, J = 6.7 Hz, 3H); ^{13}C NMR ($CDCl_3$) 132.9, 128.5 (very weak t), 63.2, 32.1, 31.7, 29.0, 22.5, 14.9. Anal. Calcd for $C_{10}H_{19}OD$: C, 76.87; H, 12.90. Found: C, 76.67; H, 13.08.

The TBDMS ether was prepared in the usual way to afford a colorless oil, **43**.

^1H NMR ($CDCl_3$) δ 5.69 (m, 1H), 4.08 (s, 2H), 2.00 (q, J = 6.8 Hz, 2H), 1.27 (m, 8H), 0.91 (s, 9H), 0.89 (t, 3H), 0.05 (s, 6H).

Mass Spectra of tert-Butyldimethylsilyl Ethers, 37, 40, and 43.

Low resolution electron impact mass spectra were performed on a Finnigan MAT 8200 spectrometer at 70 eV. For the TBDMS ethers, small peaks corresponding to the M^+ ion (at m/v=270 or 271), but the intensities were too small to give reproducible mass ratios. The $[M-57]^+$ (M - t-Bu) peak, however, was the second largest in each spectrum, providing ample intensity to extract H/D ratios. The precision of the measurements was improved by limiting the scanning region to m/e values of 208-218, and by averaging 95-100 spectra taken in succession at a period of steady overall ion abundance; standard deviations for the intensities of the peaks of interest were ±2% (relative).

For the diprotio allylic silyl ether (**37**) the calculated ratio of 213 to 214 peaks matched the observed spectrum nicely. In the following discussion, let $[A]^+$ stand for the $[M-t\text{-}Bu]^+$ ion. For $C_{12}H_{25}OSi$, the relative intensities should be: $[A]^+$=100, $[A+1]^+$=18.34, $[A+2]^+$=5.07, [A+3]=0.45; the observed intensities were [213]=100, [214]=18.34, [215]=5.36, [216]=0.45. For **43**, the C2-d derivative, the observed intensities did not match so well: [213]=1.5, [214]=100, [215]=27.53, [216]=6.93, [214]=1.08. It is the [213] and [214] peaks that were used in the H/D determination, and these are acceptable, the 1.5% intensity of the [213] peak arising from the fact that the $LiAlD_4$ used in preparing **43** was 98% isotopically enriched in deuterium.

For **40**, the C3-d compound, the mass spectrum confirms the presence of approximately 20% of the diprotio allylic alcohol indicated by the NMR spectrum: [213]=19.31, [214]=100, [215]=19.44, [216]=5.16. The procedure used to determine the H/D ratio (that is, the ratio of diprotio/deuterated allylic alcohols) here is the same procedure used in the determination of relative rate constants in the competition experiments described below. Assuming that the [213] peak is entirely due to the $[A]^+$ of the diprotio substrate, its contribution to the [214] peak must be (19.31)x(18.34%)=3.54. Therefore, the contribution of the deuterated substrate to the [214] peak is 100-3.54=96.46, and the H/D ratio (the ratio of the $[A]^+$ ions of each molecule) is 19.31/96.46 = 1.00/5.00; the diprotio allylic alcohol therefore comprises 16.7% of the total.

Determination of the Relative Rate of Epoxidation of (E)-3-deuterio-2-decen-1-ol 38, and (E)-2-deuterio-2-decen-1-ol 41, with respect to (E)-2-decen-1-ol 36.

A typical procedure (for epoxidation by TBHP and Ti-tartrate) is presented here, followed by a table of the reagents used for each of the competition experiments.

A dry 25 mL round-bottomed flask was charged with 0.067 mL (E)-2-decen-1-ol (57 mg, 0.36 mmol), 0.078 mL (E)-3-deuterio-2-decen-1-ol [66 mg = 11 mg (E)-2-decen-1-ol (0.07 mmol) + 55 mg d-labeled allylic alcohol (0.35 mmol)], and 40 mg heptadecane as internal gc standard. CH_2Cl_2 (10 mL) was added, of which 1 mL was then removed as a t_0 sample for gc and, after silylation, for mass spectroscopy. It should be noted that a known amount of 2-decen-1-ol and heptadecane was subjected to the workup conditions below with no change in the gc ratio of allylic alcohol to internal standard. To the reaction mixture under argon was added (+)-DIPT (0.208 g, 0.888 mmol). The flask was then cooled to -17°C and $Ti(O\underline{i}Pr)_4$ was added (0.200 g, 0.704 mmol). After stirring for 5 minutes, TBHP (0.544 mmol, 0.151 mL of a 3.60 M solution in heptane) was added. After 4 hours at -17 to -20°C, a small aliquot was quenched by transfer into a $FeSO_4$/tartaric acid solution (10%/10% by weight) with rapid mixing; gc indicated that the reaction was 80.8% complete. After 4.5 hours reaction time, the reaction mixture was poured into a mixture of 1 mL of the aqueous quench solution and 40 mL ether. The aqueous layer was extracted with 40 mL ether and the

combined organic phases dried with $MgSO_4$ and the solvent removed to a yellow oil.

GC of an ether solution of the crude product indicated 82.4% ± 0.3% completion. The error limits here represent twice the standard deviation for a collection of at least four gc injections; it is worth noting that in the calculation of k_{rel} below, a variation of ±0.3% completion gives rise to a change of only ± 0.001 in k_{rel}. After flash chromatography (15:85 EtOAc:hexane), the pure allylic alcohol was taken up in 5 mL CH_2Cl_2 and treated with 0.04 mL Et_3N (29 mg, 0.3 mmol) and 70 mg TBDMS-OTf (0.27 mmol). After 10 minutes, the solvent was removed and the crude product flash chromatographed (hexane for the first 25 mL to remove heptadecane, then 1:9 EtOAc:hexane) to afford 33.4 mg of the TBDMS ether (0.12 mmol, approximately 95% based on percent completion and the removal of a t_0 sample). Four-fifths of the t_0 sample was silylated in the same way.

Mass spectra of the two TBDMS ether samples provided the following relative values of [213] and [214] peaks: for the t_0 sample, [213] = 93.96 ± 1.50, [214] = 100.00; for recovered substrate, [213] = 99.69 ± 1.45, [214] = 100.00. Again, the error limits represent twice the standard deviation for the 95-100 spectra averaged. The ratios of diprotio to deuterated allylic alcohols are therefore found to be: for the t_0 sample, H/D = 1.137 ± 0.025; for the recovered substrate, H/D = 1.223 ± 0.020.

Calculation of the relative rate relies upon the equation:

$$k_{rel} = \ln(D/D_0)/\ln(H/H_0)$$

where D_0 = initial amount of the d-labeled substrate,

D = amount of the d-labeled substrate after the reaction

H_0,H = initial and final amounts of diprotio allylic alcohol.

From the mass spectra values, recalling that the reaction was 82.4% complete, we calculate: D_0=100, H_0=113.7 ± 2.5, D=16.92, H=20.69±0.4. From these values, k_{rel} = 1.043 ± 0.025.

The same reaction sequence was performed for (E)-2-deuterio-2-decen-1-ol **41** (0.074 mL, 63 mg, 0.40 mmol) and (E)-2-decen-1-ol **36** (0.074 mL, 63 mg, 0.40 mmol). The other reagents used were (+)-DIPT (0.207 g, 0.884 mmol), $Ti(OiPr)_4$ (0.200 g, 0.704 mmol), heptadecane (40 mg), and TBHP (0.544 mmol, 0.151 mL of a 3.60 M solution in heptane). After 5.5 hours, the reaction was quenched and found to have proceeded to 83.6 % completion.

Standard workup and silylation yielded 30.4 mg of the TBDMS ether (ca. 98%), as well as the TBDMS ether of the starting substrate mixture. For the t_0 sample, [213]=86.66 ± 1.45, and [214]=100.00; for the recovered substrate, [213]=88.86±0.76, and [214]=100.00. These values lead to the determination of k_{rel} = 1.017 ± 0.023.

The oxidations by mCPBA were performed as follows. A 25 mL round-bottomed flask was charged with the mixture of diprotio and deuterated decenols plus approximately 42 mg of heptadecane. About 1 mL of ether was added to completely mix the reagents, the ether was removed *in vacuo*, and approximately 23 mg of the mixture was removed as a t_0 sample. CH_2Cl_2 (15 mL) was added, and the reaction mixture was cooled to -20°C. The oxidant was then added by uncapping the flask and quickly pouring in the solid mCPBA (Aldrich, 80-85%) all at once. The reaction was monitored by injecting aliquots directly from the reaction mixture. After 16 hours at -10°C, the reaction was worked up by addition of 15 mL of a 0.7 M aqueous solution of Na_2SO_3 with vigorous shaking for 5 minutes. Ether (40 mL) was added, the organic phase was washed with 1 N $NaHCO_3$ (20 mL), the combined aqueous phases were extracted with 20 mL ether, and the combined organic phases were dried over $MgSO_4$. A small amount of this solution was removed for gc analysis to determine the final extent of reaction, and the remainder was evaporated to afford a yellow oil. The crude product was then treated as above, with chromatography, silylation, and chromatography to yield the pure TBDMS ether.

A summary of the competition reactions involving the epoxy alcohols is presented below; the first table contains the amounts of reagents used (in mmols), the second table the results of each reaction.

Reaction	C2-d	C3-d	C2,C3-H	Ti(OiPr)$_4$	(+)-DIPT	TBHP	mCPBA
1		0.35	0.43	0.704	0.888	0.544	
2	0.40		0.40	0.704	0.884	0.544	
3		0.40	0.38	0.800	0.960	0.523	
4	0.40		0.40	0.800	0.960	0.544	
5		0.41	0.42	0.772		0.577	
6	0.41		0.44	0.792		0.602	

Reaction	C2-d	C3-d	C2,C3-H	$Ti(OiPr)_4$	(+)-DIPT	TBHP	mCPBA
7		0.38	0.48	0.741		0.593	
8	0.42		0.41	0.720		0.576	
9		0.34	0.41				0.55
10	0.41		0.39				0.57
11		0.34	0.44				0.57
12	0.39		0.39				0.56

Reaction	% Completion	$[213]_0$	$[214]_0$	$[213]_p$	$[214]_p$	k_{rel}
1	82.4	93.96	100.00	99.69	100.00	1.043 ± 0.025
2	83.6	86.66	100.00	88.86	100.00	1.017 ± 0.023
3	69.7	74.87	100.00	78.27	100.00	1.044 ± 0.028
4	87.9	87.32	100.00	87.68	100.00	1.002 ± 0.023
5	82.9	78.60	100.00	84.38	100.00	1.049 ± 0.025
6	81.9	90.87	100.00	94.86	100.00	1.031 ± 0.025
7	83.2	91.02	100.00	98.72	100.00	1.056 ± 0.025
8	83.4	85.20	100.00	88.95	100.00	1.029 ± 0.025
9	82.5	91.22	100.00	100.00	94.92	1.106 ± 0.025
10	81.4	83.74	100.00	91.36	100.00	1.064 ± 0.025
11	86.7	95.51	100.00	100.00	96.39	1.052 ± 0.025
12	86.5	81.69	100.00	94.54	100.00	1.091 ± 0.025

Determination of the Relative Rate of Epoxidation of (E)-3-deuterio-2-decen-1-ol Acetate 44, and (E)-2-deuterio-2-decen-1-ol Acetate 45, with respect to (E)-2-decen-1-ol Acetate, 46.

The allylic acetates were prepared and epoxidized *in situ* as follows. A 25 mL round-bottomed flask was charged with 0.082 mL (E)-3-deuterio-2-decen-1-ol (containing 58 mg of the 3-deuterio substrate, 0.37 mmol; and 12 mg of the diprotio allylic alcohol, 0.08 mmol), 0.070 mL (E)-2-decen-1-ol (60 mg, 0.38 mmol), and 44 mg of heptadecane. To this mixture was added 2 mL pyridine and 1 mL acetic anhydride; the reaction was allowed to stand at room temperature for two hours, after which time tlc (3:7 EtOAc:hexane) showed the acetylation to be complete. The volatile components of the reaction (pyridine, Ac_2O, and acetic acid) were removed *in vacuo* (0.1 mm). CCl_4 (2 mL) was added, the solution swirled to mix, and the solvent

evaporated *in vacuo* to remove the last traces of the acetylation by-products; 28 mg of the resulting oil was removed as a t_0 samples. The mixture was taken up in 15 mL CH_2Cl_2 and, at room temperature, 0.155 g *m*CPBA was added as a solid (80-85% pure, 0.74 mmol). After standing at room temperature for 12 hours, the reaction was quenched with Na_2SO_3, extracted with ether, washed with saturated $NaHCO_3$, and dried ($MgSO_4$) as above. GC of a small portion of the crude product compared to the t_0 sample disclosed 89.0% completion. The remainder of the crude product was taken up in 5 mL methanol and 12 drops water, and was treated with about 20 mg anhydrous K_2CO_3 at room temperature for 3 hours to remove the acetate group. 1N HCl (5 mL) was added, and the mixture extracted with ether (3 x 20 mL). The combined organic phases were dried ($MgSO_4$) and the solvent removed. Flash chromatography of the resulting oil (1:9 EtOAc:hexane) afforded the pure allylic alcohol, which was silylated as above to give 20.0 mg of the TBDMS ether (about 55%, based on % completion and the removal of a t_0 sample). The t_0 sample was hydrolyzed and silylated in the same manner. Mass spec analysis of the ratio of diprotio to deuterated allylic alcohol was performed as described above. The reagents and results for the *m*CPBA epoxidations of the decenol acetates are summarized in the tables below.

Reaction	C2-d	C3-d	C2,C3-H	*m*CPBA
13	0.37		0.46	0.74
14		0.44	0.44	0.71
15	0.41		0.45	0.75
16		0.42	0.43	0.74

Reaction	% Completion	$[213]_0$	$[214]_0$	$[213]_p$	$[214]_p$	k_{rel}
13	89.0	96.04	100.00	100.00	98.82	1.029 ± 0.025
14	80.3	90.42	100.00	96.59	100.00	1.050 ± 0.025
15	81.1	94.56	100.00	99.56	100.00	1.038 ± 0.025
16	83.8	91.87	100.00	99.75	100.00	1.056 ± 0.025

8. Tartrate Analogues

Preparation of (2R,3S)-2,3-dihydroxy-3-phenylethylpropionate, 47.

Note: Preparation of the corresponding methyl ester by a more efficient route is presented below.

(2R,3S)-2,3-dihydroxy-3-phenyladamantylpropionate **49**, prepared by Dr. M. Takatani in approximately 80% ee, was recrystallized four times from absolute ethanol to constant melting point (85-86 °C, dl diol melts at 136.5-137°C). The product was determined to be >95% ee by nmr as discussed below. Optically pure **49** (170 mg, 0.537 mmol) in 3 mL ethanol was added to a solution of ca. 10 mg sodium metal in 5 mL ethanol at room temperature under N_2 atmosphere. The reaction was quenched by cannula transfer into 5mL of a 0.2 M solution of trifluoroacetic acid in ethanol. The reaction mixture was evaporated under reduced pressure to yield a clear oil. Flash chromatography (1:1 EtOAc:hexane) provided 32.0 mg (28%) pure **47** as a clear oil.

^{1}H NMR ($CDCl_3$) δ7.29 (m, 5H), 4.95 (d, J = 4 Hz, 1H), 4.35 (d, J = 4 Hz, 1H), 4.22 (q, J = 7 Hz, 4H), 3.50 (s, 2H), 1.25 (t, J = 7 Hz, 6H); IR (CH_2Cl_2) 3400 (br), 2910, 2840, 1740 cm^{-1}; $[\alpha]_D^{23}$ +7.22° (c 2.1, CH_2Cl_2).

Determination of Optical Purity of 49.

To a solution of 48 mg (0.152 mmol) **49** in 15 mL THF was added 40 mg (0.25 mmol) carbonyl diimidazole, followed by a small amount (ca 10 mg) of KH in mineral oil. After stirring for 2 h at room temperature, the solvent was removed and the residue taken up in 15 mL ether and washed with water (15 mL). The organic layer was dried ($MgSO_4$) and solvent removed to yield a white solid. Medium pressure liquid chromatography (18:82 EtOAc:hexane) provided 29 mg (56%) of pure carbonate **50**. A sample of carbonate from the racemic diol adamantyl ester was also prepared.

Data for **50**:

^{1}H NMR (C_6D_6) δ7.21 (m, 5H), 5.25 (d, J = 4.9 Hz, 1H), 4.26 (d, J = 4.9 Hz, 1H), 2.01 (m, 6H), 1.95 (m, 3H), 1.42 (m, 6H); IR (KBr) 2980, 2920, 2860, 1830 (s), 1760 (m), 1735 (m), 1380, 1350, 1150, 1115 cm^{-1}; IR (CH_2Cl_2) 2970, 2910, 2850, 1830 (s), 1755 (m), 1730 (m), 1440, 1378, 1348, 1275, 1198, 1147, 1113 (s), 1043 cm^{-1}; $[\alpha]_D^{23}$ -11.11° (c 4.3, EtOH).

Upon addition of a total of 36 mg (0.13 mmol, 3.5 equivalents) of the

chiral solvating agent (+)-2,2,2-trifluoro-1-(9-anthryl)-ethanol to 12 mg of **50** in C_6D_6, the C-2 methine proton doublet shifts to a single doublet resonance at 4.45 δ. Identical analysis of a sample of the racemic carbonate produces doublets at 4.46 and 4.40 δ, indicating a >95% enantiomeric excess for **50**.

Preparation of (2R,3S)-2,3-dihydroxy-3-phenylmethylpropionate, 15.

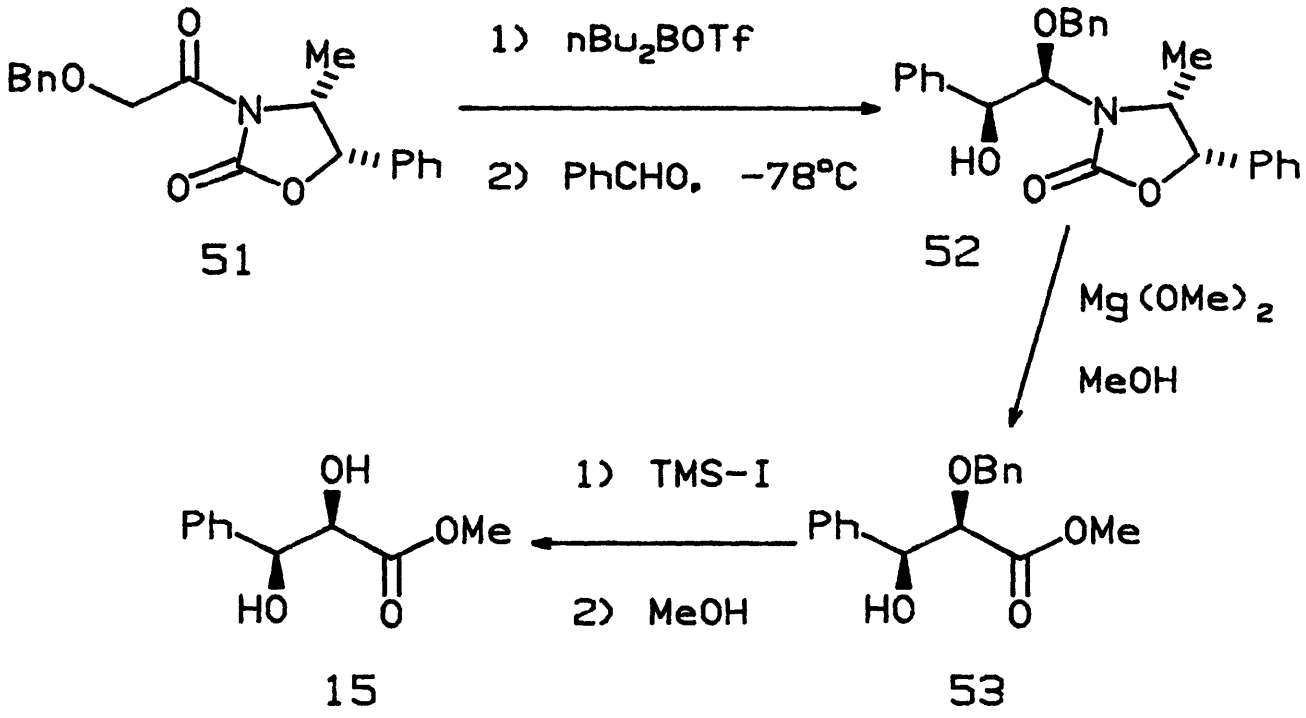

This synthesis was performed by Ms. Pamela Shapiro.

Oxazolidinone **51** derived from norephedrine was kindly supplied by Mr. Steven Bender of the Evans group. The aldol condensation of **51** (2.999 g, 9.22 mmol) with benzaldehyde (1.27 g, 12.0 mmol) was performed in THF at -78°C mediated by $(n\text{Bu})_2\text{BOTf}$, according to the method of Evans.[132] Flash chromatography of the crude product (3:97 acetone:CH_2Cl_2) yielded 3.663 g (92%) of the adduct **52** as a clear oil. The nmr spectrum shows no evidence for more than one diastereomer. GC analysis (SE-30 capillary, 20 m, 150-220°C) showed only one peak.

^{1}H NMR ($CDCl_3$) δ 7.14-7.42 (m, 15H), 5.52 (d, J = 4.5 Hz, 1H), 5.08 (d, J = 6.9 Hz, 1H), 5.00 (t, J = 6.3 Hz, 1H), 4.60 (s, 2H, benzyl), 4.40 (m, 1H), 3.13 (d, 1H, -OH), 0.76 (d, J = 6.7, 3H).

While this particular aldol condensation reaction has not been reported by the Evans group, closely related reactions have been performed. In every case, the same sense of diastereoselectivity has been observed in high diastereomeric excess and good yield. We rely on this observed selectivity pattern to assign the absolute configuration of our product.

To 200 mL of methanol was added 0.252 g Mg turnings (10.4 mmol) and 0.0295 g I_2 (0.24 mmol) and the mixture was refluxed under Ar atmosphere until the Mg disappeared. The solution was cooled to 0°C and **52** (2.3 g, 5.3 mmol) in methanol (20 mL) was added. The reaction was stirred at 0°C for 30 minutes and then quenched by addition of 200 mL of 10% HCl (producing an orange color). Ether (200 mL) was added, the layers separated, and the aqueous phase extracted with ether (3 x 100 mL). The combined organic phases were dried over $MgSO_4$ and solvent removed to yield a dark orange oil. Flash chromatograhy (3:7 EtOAc:hexane, TLC visualization with p-anisaldehyde) provided the methyl ester **53** (1.318 g, 86%) as a clear oil.
^{1}H NMR ($CDCl_3$) δ 7.1-7.4 (m, 10H), 4.99 (t, J = 4.5 Hz, 1H), 4.68 (d, J = 10.8 Hz, 1H), 4.42 (d, J = 10.8 Hz, 1H), 4.07 (d, J = 4.5 Hz, 1H), 3.62 (s, 3H), 3.11 (d, J = 4.5 Hz, -OH).

The Mosher ester from (+)-MTPA-Cl showed 95.0% ee in the C-2 proton resonances at 6.31 (minor) and 6.24 (major):
^{1}H NMR ($CDCl_3$) δ 7.1-7.4 (m, 15H), 6.24 (d, J = 6.1 Hz), 4.67 (d, J = 11.2 Hz, 1H), 4.46 (d, J = 11.2 Hz, 1H), 4.27 (d, J = 6.2 Hz, 1H), 3.46 (s, 3H), 3.45 (q, J = 1Hz, 3H).

To a solution of **53** (1.20 g, 4.2 mmol) in $CHCl_3$ (10 mL) was added 0.775 mL Me_3SiI (1.09 g, 5.4 mmol) at room temperature. After stirring for 15 minutes, the brown-red reaction mixture was treated with 40 mL methanol and the solvent removed. The orange residue was taken up in ether and washed with 1N Na_2SO_3 until disappearance of color and then with saturated

$NaHCO_3$. The organic phase was dried over $MgSO_4$ and the solvent removed to give a pale yellow solid. Flash chromatography (1:1 EtOAc:hexane) produced 0.306 g (35%) of **15** as a white crystalline solid; m.p. 83-84°C; $[\alpha]_D^{25}$ +10.10° (c=1.57, $CDCl_3$).

^1H NMR ($CDCl_3$) δ 7.25-7.40 (m. 5H), 5.04 (dd, J_1 = 7.1, J_2 = 2.5 Hz, 1H), 4.39 (dd, J_1 = 7.1, J_2 = 2.5 Hz, 1H), 3.85 (s, 3H), 3.15 (d, J = 6.0 Hz, 1H, -OH), 2.79 (d, J = 6.0 Hz, 1H, -OH); IR ($CHCl_3$) 3540, 2960 (w), 1740 (s), 1440, 1390, 1270, 1220 (br), 1110, 1085, 1050, 700, 675 cm^{-1}. Anal. Calcd for $C_{10}H_{22}O_4$: C, 61.22; H, 6.16. Found: C, 61.48; H, 6.23.

A sample of **15** was peracetylated (Ac_2O, pyridine) to afford the diacetate **54** as a clear oil.

^1H NMR (C_6D_6) δ 7.25-7.40 (m, 5H), 6.67 (d, J = 3.7 Hz, 1H), 5.62 (d, J = 3.7 Hz, 1H), 3.38 (s, 3H), 1.75 (s, 3H), 1.70 (s, 3H).

Addition of 50 μL of $Eu(hfc)_3$ solution (76 mg/0.4 mL C_6D_6) to a solution of 5 mg **54** in 0.6 mL C_6D_6 shifted the acetate resonances to 2.47 and 2.29 . Singlets due to the minor enantiomer appeared at 2.56 and 2.37 δ; the enantiomeric excess was determined to be 93.5%.

Asymmetric epoxidation of (E)-α-phenylcinnamyl alcohol using ligand 15.

A solution of 27.6 mg (0.131 mmol) (E)-α-phenylcinnamyl alcohol and 25.1 mg (0.128 mmol) **15** in 20 mL dry CH_2Cl_2 was treated with 29.2 mg (0.103 mmol) $Ti(OiPr)_4$ under inert atmosphere. After standing at room temperature for 15 minutes, the reaction mixture was cooled to -23°C and 0.39 mmol TBHP (0.100 mL of a 3.87 M solution in toluene) was added by syringe. The reaction mixture was allowed to stand at -20°C overnight, after which 10 mL of aqueous $FeSO_4$/tartaric acid quench solution was added with vigorous shaking. The aqueous phase was extracted with ether and the combined organic phases dried ($MgSO_4$) and evaporated. The crude product was flash chromatographed (1:9 EtOAc:hexane) to yield 23.0 mg (77%) of epoxy alcohol. HPLC analysis on a chiral Pirkle column showed the product to be 80% ee, enriched in the 2S enantiomer.

Kinetic Resolution of 1-cyclohexyl-(E)-2-buten-1-ol using ligand 15.

The kinetic resolution was performed in the usual way, using 38.9 mg

(0.252 mmol) 1-cyclohexyl-(E)-2-buten-1-ol, 15.9 mg pentadecane as internal gc standard, 45.7 mg (0.233 mmol) **15** 56.1 mg (0.197) $Ti(OiPr)_4$, and approximately 0.15 mmol TBHP (19 uL of an approximately 7.7 M solution in CH_2Cl_2), at -20°C. After 3 h, gc analysis on the 15 m Carbowax-20M capillary column (temperature program: 70°C, 4 min, 16 deg/min, 220°C, 4 min) showed 65.2 % of the allylic alcohol to be consumed. Normal workup including peracetylation of the crude reaction product and subsequent flash chromatography produced 13.8 mg allylic acetate (27.9%, 80% based on percent completion). NMR analysis in C_6D_6 using chiral shift reagent $Eu(hfc)_3$ showed the product to have 16% ee. By comparison to the NMR shift pattern of allylic acetate resolved using (+)-DIPT, the product is assigned the R configuration, the same as the slower reacting enantiomer from the L-(+)-tartrate mediated resolution.

Kinetic Resolution of 1-cyclohexyl-(E)-2-buten-1-ol using ligand 47.

The reaction was performed as above using a 1.2:1 ratio of ligand to $Ti(OiPr)_4$, at -20°C in CH_2Cl_2. After 50% completion, the recovered allylic acetate had a 7% ee of the R enantiomer. The epoxy acetate product was found by gc to be a 41:59 ratio of erythro:threo diastereomers.

Preparation of (2R,3S)-2,3-dihydroxy-3-cyclohexylethylpropionate, 48.

The crude product from transesterification of the adamantyl ester **49** (142 mg, ca. 0.68 mmol) was dissolved in 15 mL methanol and 8 drops glacial acetic acid. To this solution was added 100 mg of 5% Rh on alumina powder, and the mixture was hydrogenated at 50 psi with vigorous shaking for three days. The reaction mixture was filtered and evaporated to a white solid. Chromatography (3:7 EtOAc:hexane) yielded 28 mg unreacted starting material plus about 100 mg of a mixture of starting material and product. Medium pressure chromatography (3:7 EtOAc:hexane) produced 75.4 mg (ca. 65%) pure **48** as a white solid; $[\alpha]_D^{23}$ -11.5° (c 5.03, $CDCl_3$).
^1H NMR ($CDCl_3$) δ 4.28 (m, 3H, ester methylene and C-2 proton), 3.55 (br t, 1H, C-3 proton), 3.14 (br d, 1H), 2.00 (m, 1H), 1.5-1.8 (m, 4H), 1.32 (t, J = 7 Hz, 3H), 1.0-1.35 (m, 6H); IR ($CDCl_3$) 3400, 2980, 2950, 1735 cm^{-1}.

Kinetic Resolution of 1-cyclohexyl-(E)-2-buten-1-ol using ligand 48.

Kinetic resolution was performed in the usual manner, using 40.5 mg

(0.262 mmol) of allylic alcohol, three drops of heptadecane as internal standard, 75.0 mg (0.347 mmol) **48**, 82 mg (0.29 mmol) $Ti(O\underline{i}Pr)_4$, and 0.16 mmol TBHP (0.047 mL of a 3.343 M solution in CH_2Cl_2). At 50% completion, peracetylation of the quenched reaction mixture shows the product epoxy acetates to be 77.8% erythro and 22.2% threo. The recovered allylic acetate (19.4 mg, 37.6%) was found to be 70% ee in the R enantiomer, indicating a k_{rel} of 6.1.

Preparation of (2R,3S)-2,3-dihydroxy-3-cyclohexylmethylpropionate, 16.

A 100 mL hydrogenation pressure flask was charged with 0.1138 g (0.592 mmol) of (2R,3S)-2,3-dihydroxy-3-phenylmethylpropionate **15**, 15 mL methanol, 10 drops acetic acid, and 0.300 g of Rh on alumina powder (5% Rh, Aldrich Chemical Co.). The mixture was hydrogenated at 53 psi with shaking on a Parr hydrogenator for four days. The reaction mixture was filtered and evaporated to a white solid. Chromatography (3:7 EtOAc:hexane) provided pure (2R,3S)-2,3-dihydroxy-3-cyclohexylmethylpropionate **16**, as a white crystalline solid; mp. 97.5-99 °C; $[\alpha]_D^{20}$ -20.8° (c 5.5, $CDCl_3$). ^1H NMR ($CDCl_3$) δ 4.27 (d, J = 5.5 Hz, 1H), 3.78 (s, 3H), 3.52 (br t, J = 8.5 Hz, 1H), 3.23 (d, J = 5.5 Hz, 1H), 2.17 (br d, J = 9.2 Hz, 1H), 2.00 (br d, J = 12 Hz, 1H), 1.7-1.4 (m, 4H), 1.2 (m, 4H), 0.99 (m, 2H); ^{13}C NMR ($CDCl_3$) 174.7, 76.8, 70.9, 52.7, 40.3, 29.1, 26.2, 25.8; IR (CH_2Cl_2) 3540 (br), 2920, 2850, 1738 (s), 1440, 1390, 1290 (br), 1230 (br), 1190, 1135, 1110 (s), 1085, 1040, 973, 925 cm^{-1}.

Asymmetric epoxidation of (E)-α-phenylcinnamyl alcohol using ligand 16.

A solution of 50.0 mg (0.238 mmol) (E)-α-phenylcinnamyl alcohol and 51.0 mg (0.252 mmol) **16** in 10 mL dry CH_2Cl_2 was treated with 0.064 mL (0.22 mmol) $Ti(O\underline{i}Pr)_4$ under inert atmosphere. After standing at room temperature for 10 minutes, the reaction mixture was cooled to -23°C and 0.45 mmol TBHP (0.120 mL of a 3.74 M solution in heptane) was added by syringe. The reaction mixture was allowed to stand at -20°C overnight, after which 10 mL of aqueous $FeSO_4$/tartaric acid quench solution was added with vigorous shaking. The aqueous phase was extracted with ether and the combined organic phases dried ($MgSO_4$) and evaporated. The crude product was flash chromatographed (1:9 EtOAc:hexane) to yield 48 mg (89%) of epoxy alcohol. HPLC analysis on a chiral Pirkle column showed the product to be greater

than 98% ee, enriched in the 2S enantiomer, as confirmed by coinjection with a sample of racemic epoxy alcohol.

9. Epoxidation of Secondary Allylic Alcohols by $Ti(OiPr)_4$ and (dl)-Tartrates

Epoxidations were performed in the usual manner at 0°C in CH_2Cl_2, employing the amounts (in mmoles) of reagents listed below in the table. For nonenol (**11**) the internal standard was pentadecane, and for (E)-1-cyclohexyl-2-buten-1-ol (**12**) the internal standard was α-bromotoluene.

Rxn.	**11**	(+)-DET	(-)-DET	(+)-DIPT	(-)-DIPT	$Ti(OiPr)_4$	TBHP
1	1.75	2.10	--	--	--	1.75	3.50
2	1.76	--	2.15	--	--	1.76	3.50
3	1.57	0.94	0.94	--	--	1.57	3.14
4	1.00	0.50	0.50	--	--	1.00	2.00
5	1.00	0.65	0.65	--	--	1.00	2.00
6	1.00	--	--	0.50	0.50	1.00	2.00
7	1.00	--	--	0.65	0.65	1.00	2.00
	12						
8	1.03	--	--	1.47	--	1.13	2.00
9	1.04	--	--	--	1.49	1.15	0.31
10	1.02	--	--	0.73	0.73	1.12	2.00
11	1.05	--	--	0.76*	0.76*	1.16	0.32

* (dl)-DIPT was prepared from commercially available (dl)-tartaric acid.

Reaction aliquots were quenched by transfer into a 0°C solution of an equivalent volume of acetone containing 0.5 mL water, and were stirred vigorously for 1 h while warming to room temperature. The reaction mixture was filtered through celite and evaporated to a faint yellow oil. The residue was taken up in 15 mL of ether and treated with 10 mL 1N NaOH in brine with vigorous stirring for 30 minutes at 0°C. The organic phase was dried ($MgSO_4$) and evaporated to an oil.

For the nonenol reactions, erythro/threo ratios were determined by gc analysis of the trimethylsilyl ethers prepared in situ by addition of trimethylsilyl imidazole to ethereal solutions of each product. Trimethylsilylimidazole was added to each sample until the ratio of erythro to threo products on the gc reached a constant value (usually only 2 additions of silyl reagent were needed). For **12**, erythro/threo ratios were determined by gc analysis of the acetylated epoxy alcohols (Ac_2O, pyridine).

10. Kinetic Resolution of (3R)-4-phenyl-1-penten-3-ol, **29**.

Preparation of 29.

To a suspension of 0.04 mol NaH (1.6 g of 60% dispersion in mineral oil) in 300 mL toluene under argon at room temperature was added trimethylphosphonoacetate (7.286 g, 0.040 mol) in 5 mL toluene with stirring over 20 minutes. After an additional 100 mL toluene was added to facilitate stirring, the reaction mixture was stirred for 30 minutes and then was cooled to -20°C. A solution of (dl)-2-phenylpropionaldehyde (5.367 g, 0.040 mol) in 10 mL toluene cooled to -20°C was then added over 15 minutes. The reaction mixture was allowed to warm gradually to room temperature while stirring overnight. Water (50 mL) was then added, the layers separated, and the organic phase washed with water (2 x 200 mL). The combined aqueous phases were extracted with ether (2 x 100 mL), and the combined organic phases were dried ($MgSO_4$) and the solvent removed to yield 8.19 g (107%) of crude (4-phenyl)-(E)-2-pentenylacetate, **55**. Only one compound was visible in the NMR, providing evidence for a >30:1 ratio of E:Z olefins.

Data for **55**: ^1H NMR ($CDCl_3$) δ 7.4-7.1 (m, 5H), 5.81 (d, J = 15 Hz, 1H), 5.80 (d, J = 15 Hz, 1H), 3.73 (s, 3H), 3.64 (heptet, J = 6.6 Hz, 1H), 1.45 (d, J = 6.6 Hz, 3H).

A solution of **55** (6.79 g, approximately 0.036 mol) in 20 mL CH_2Cl_2 was added to 100 mL of a DIBAL-H solution in CH_2Cl_2 (1.0 M, 0.10 mol) at 0°C by cannula. The reaction mixture was stirred for 4 h while warming to room tempeature. The reaction was quenched by dropwise addition of saturated NH_4Cl to give a gel, which was dissolved in 1 N H_2SO_4 and extracted with ether (2 x 150 mL). The organic phase was washed with 1 N H_2SO_4 (80 mL), saturated NaCl (100 mL), saturated $NaHCO_3$ (100 mL), and saturated NaCl (2 x 100 mL), dried ($MgSO_4$), and evaporated to afford a clear oil. Flash chromatography (1:4 EtOAc:hexane, 5 x 12 cm column) afforded 5.295 g (91%) of (E)-4-phenyl-2-penten-1-ol **56**, contaminated with approximately 20% 2-phenyl-1-propanol as a colorless oil.

Data for the major component of **56**: ^1H NMR ($CDCl_3$) δ 7.35-7.1 (m, 5H), 5.85 (dd, J_1 = 15, J_2 = 6.8 Hz, 1H), 5.61 (dt, J_1 = 15, J_2 = 5.5 Hz, 1H), 4.05 (m, 2H), 3.47 (heptet, J = 6.7 Hz, 1H), 1.90 (br s, 1H), 1.36 (d, J = 6.7 Hz, 3H).

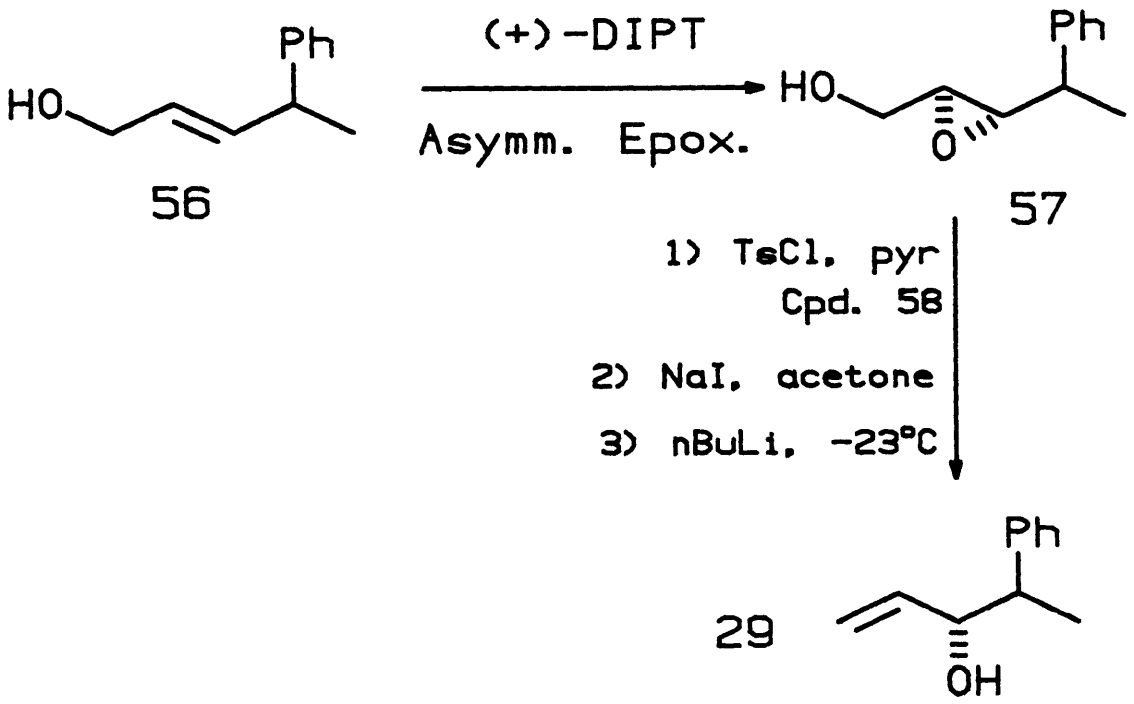

A portion of **56** (1.067 g, 0.00658 mol) was epoxidized in the usual way at -20°C using the following reagents: $Ti(OiPr)_4$ (1.83 mL, 1.75 g, 0.00616 mol), (+)-DIPT (1.733 g, 0.00740 mol), TBHP (1.66 mL of a 3.98 M solution in toluene, 0.0066 mol), in CH_2Cl_2 (65 mL). After 36 h at -20°C, 50 mL of the $FeSO_4$/tartaric acid quench solution was added with vigorous stirring for 15 minutes. The aqueous phase was extracted with ether (2 x 70 mL) and the organic phases were combined and evaporated *in vacuo*. The crude product was dissolved in 100 mL ether and stirred with 50 mL 1N NaOH in saturated NaCl for 2 h at room temperature. The aqueous phase was extracted with ether (60 mL) and the combined organic phases were dried ($MgSO_4$) and evaporated to an oil. Flash chromatography (3:7 EtOAc:hexane) yielded 0.784 g (2*S*, 3*S*)-2,3-epoxy-4-phenyl-1-pentanol **57** (76%), as an oil, in an approximately 1:1 diastereomeric ratio (epimeric at C-4).

^1H NMR ($CDCl_3$) δ 7.38-7.18 (m, 10H), 3.95-3.80 (ddt, 2H), 3.7-3.5 (m, 2H), 3.15-2.98 (m, 8H), 2.85 (m, 1H), 2.70 (m, 1H), 1.86 (m, 2H, -OH), 1.41 (d, J = 6.8 Hz, 3H), 1.34 (d, J = 6.8 Hz, 3H).

Mosher ester analysis showed **57** to be greater than 95% enantiomerically pure.

A solution of **57** (0.750 g, 0.00421 mol) in 10 mL CH_2Cl_2 was treated with Et_3N (1.0 g, 0.010 mol), 4,4-dimethylaminopyridine (ca. 20 mg), and p-toluenesulfonyl chloride (1.00 g, 0.00524 mol) at room temperature. After 1 h, the reaction was quenched by addition of 0.5 mL 3-dimethylaminopropylamine and the solvent was removed. Flash chromatography (1:4 EtOAc:hexane) of the crude product afforded 1.174 g (81%) of (2S, 3S)-2,3-epoxy-4-phenyl-pentan-1-ol tosylate **58**, as a colorless oil, again as a 1:1 diastereomeric mixture.

^1H NMR ($CDCl_3$) δ 7.76 (m, 4H), 7.35-7.15 (m, 14H), 4.23 (m, 1H), 4.17 (m, 1H), 4.05-3.85 (m, 2H), 3.1-2.9 (m, 4H), 2.82 (m, 1H), 2.67 (m, 1H), 2.45 (s, 6H), 1.36 (d, J = 6.7 Hz, 3H), 1.30 (d, J = 6.7 Hz, 3H).

A solution of tosylate **58** (1.12 g, 0.00337 mol) in 20 mL acetone was treated with 1.5 g NaI (0.0100 mol) with stirring overnight. The reaction mixture poured into a mixture of 30 mL ether and 40 mL aqueous $Na_2S_2O_3$ (0.56 M) with stirring. The organic layer was washed with $Na_2S_2O_3$ (30 mL) and then with saturated NaCl. The combined aqueous phases were extracted with ether (50 mL), and the combined organic phases then dried over $MgSO_4$ and evaporated to a yellow oil.

Following the procedure of Nicolaou;[133] after drying the oil on the vacuum line (0.1 mm) for 30 minutes, dry THF (35 mL) and a stir bar were added, and the solution cooled to -23°C under argon. To this solution was added 0.0085 mol nBuLi (5.3 mL of a 1.6 M solution in hexanes) dropwise by syringe. After 30 minutes, the reaction was quenched by addition of 30 mL ether followed by 15 mL saturated aqueous NH_4Cl. After warming gradually to room temperature with stirring, the organic layer was washed with saturated NaCl (30 mL) and the combined aqueous phases extracted with 40 mL ether. The combined organic phases were dried ($MgSO_4$) and evaporated. Flash chromatography (1:4 EtOAc:hexane) afforded 0.4408 (3R)-4-phenyl-1-penten-3-ol, (3R)-**29** (81%), as a colorless oil in a 1:1 diastereomeric mixture (epimeric at C-4).

^1H NMR ($CDCl_3$) δ 7.3-7.15 (m, 10H), 5.88 (m, 1H), 5.77 (m, 1H), 5.29 (dd, J_1 = 15 Hz, J_2 = 1 Hz, 1H), 5.21 (dd, J_1 = 15 Hz, J_2 = 1 Hz, 1H), 5.16 (dd, J_1 = 10 Hz, J_2 = 1 Hz, 1H), 5.11 (dd, J_1 = 8 Hz, J_2 = 1 Hz, 1H), 4.24 (m, 1H), 4.14 (m, 1H), 2.91 (m, 1H), 2.81 (m, 1H), 1.53 (d, J = 5 Hz, 2H, -OH),

1.33 (d, J = 6.7 Hz, 3H), 1.27 (d, J = 6.7 Hz, 3H).
As stated below, nmr analysis of the Mosher ester showed (3R)-**29** to be present in 95% enantiomeric excess.

A sample of racemic 4-phenyl-1-penten-3-ol, **59**, was prepared by addition of vinyl magnesium bromide to (dl)-2-phenylpropionaldehyde in THF at -78°C. The addition of MeMgBr to (dl)-2-phenylpropionaldehyde is known to give a 2.4:1 excess of the S,S/R,R diastereomer.[134] 4-Phenyl-1-penten-3-ol was isolated from the vinyl magnesium bromide addition in a 3.2:1 diastereomeric ratio; by analogy to the MeMgBr case (Cram's rule) the dominant diastereomer should be the S,S/R,R pair. Since the allylic alcohol (3R)-**29** is a mixture of R,S and R,R diastereomers, we can identify the peaks due to each isomer from the nmr spectrum of **59**: ^{1}H NMR ($CDCl_3$) δ 5.88 (R,S), 5.77 (R,R), 5.29 (R,S), 5.21 (R,R), 5.16 (R,S), 5.11 (R,R), 4.24 (R,R), 4.14 (R,S), 2.91 (R,R), 2.81 (R,S), 1.53 (-OH), 1.33 (R,R), 1.27 (R,S).

The (-)-MTPA ester of the racemic allylic alcohol **59** displayed four methoxide peaks, one pair 3.2 times as intense as the other, as expected from the presence of a racemic mixture of diastereomers. The (-)-MTPA ester of (3R)-**29** showed two of these peaks due to the major (3R) epimer, and two minor peaks due to the minor (3S) pair; the enantiomeric excess for the (3R) center was 95%. It is therefore possible, relying on the asymmetric epoxidation selection rule and Cram's rule, to assign the absolute configuration represented by each of the (-)-MTPA ester methoxide peaks: 3.49 (3R,4R), 3.47 (3S,4S), 3.33 (3R,4S), 3.17 (3S,4R).

Kinetic Resolution of (3R)-phenyl-1-penten-3-ol, (3R)-29.

Kinetic resolution of (3R)-**29** was performed at -20°C in the usual manner, with the following reagents: (3R)-**29** (0.1176 g, 0.725 mmol), n-heptadecane (57.6 mg), $Ti(OtBu)_4$ (0.2787 g, 0.819 mmol), (+)-DIPT (0.2659 g, 1.135 mmol), TBHP (0.115 mL of a 3.98 M solution in toluene, 0.458 mmol), and CH_2Cl_2 (10 mL). After 40 h, 30 mL of the $FeSO_4$/tartaric acid quench solution was added with vigorous stirring for 15 minutes. GC analysis revealed that 66% of the allylic alcohol had been consumed. The aqueous phase was extracted with ether (2 x 20 mL), and the combined

organic phases were dried ($MgSO_4$) and the solvent removed. After tartrate hydrolysis with 25 mL 1N NaOH/brine and 25 mL ether (room temperature, 90 minutes), flash chromatography (1:4 EtOAc:hexane) afforded 35.1 mg of the recovered allylic alcohol (88%) and 74.0 mg of the epoxy alcohol (57%).

The (-)-MTPA ester of the recovered allylic alcohol displayed the four methoxide peaks with the following integral intensities in parentheses (normalized to 100): 3.49, 3.47 (69.6 for both, 3.49 much larger than 3.47), 3.33 (26.5), and 3.17 (4.2). Since the 3.47 and 3.19 peaks arise from the 3S compounds (the slower reacting C-3 epimer for kinetic resolution), we assume that, to whatever extent they have reacted, they were consumed equally. This allows us to assign the integral intensity of the 3.47 peak to be 4.2 and the 3.49 peak to be 69.6-4.2 = 65.4. Recalling that the kinetic resolution went to 66% completion, we have the following amounts of isomers at the beginning and end of the kinetic resolution:

	3.49 (R,R)	3.47 (S,S)	3.33 (R,S)	3.17 (S,R)
Start	97.5	2.5	97.5	2.5
End	44.5	2.8	18.0	2.8

Notice that the amounts of the (S,S) and (S,R) isomers are unchanged (within experimental error), as expected for the slower reacting C-3 configuration. The rate of the epoxidation of the (3R,4S) allylic alcohol relative to that of the (3R,4R) alcohol is therefore:

$$k_{rel} = \ln(18.0/97.5) \,/\, \ln(44.5/97.5) = 2.15 \pm 0.1.$$

11. Preparation and Epoxidation of Digeranyl Tartrate

1.00 g L-(+)-DIPT (4.27 mmol) and 9.8 g geraniol (63.5 mmol) were combined in a dry 25 mL round-bottomed flask with stir bar. A small piece of sodium metal was added; after stirring overnight at room temperature, 30 mL of water was added followed by 70 mL ether. The organic phase was washed with water (50 mL) and the combined aqueous phases extracted with ether (50 mL). The combined organic phases were washed with saturated NaCl, dried ($MgSO_4$), and evaporated to yield a yellow oil. Excess geraniol was removed by Kugelrohr distillation at 95°C (4 mm Hg). Medium pressure liquid chromatography of the remaining yellow oil (11:89 EtOAc:hexane) produced pure (L)-digeranyl tartrate as a colorless oil.
^1H NMR ($CDCl_3$) δ 5.37 (br t, J = 6.8 Hz, 2H), 5.08 (m, 2H), 4.77 (d(AB), J_1 = 7.9, J_{AB} = 13 Hz, 4H), 4.56 (d, J = 7.2 Hz, 2H), 3.34 (d, J = 7.2 Hz, 2H, -OH), 2.08 (m, 8H), 1.73 (s, 6H), 1.69 (s, 6H), 1.62 (s, 6H); IR (CH_2Cl_2) 3500, 2960, 2920, 2850, 1735, 1440, 1375, 1250, 1110, 1080, 910 cm^{-1}; $[\alpha]_D^{21}$ -13.04° (c 13.6, $CHCl_3$); Anal. Calcd for $C_{24}H_{38}O_6$: C, 68.22; H, 9.06. Found: C, 67.97; H, 9.32.

That no epimerization of the tartrate occurred during the base-catalyzed transesterification was confirmed by the transesterification of a sample of digeranyl tartrate back to diethyl tartrate under identical conditions (EtOH, Na). The DET obtained had an identical optical rotation to DET used to make the digeranyl tartrate. This result is interesting since the isopropylidene-protected tartrate undergoes facile epimerization with NaOMe in methanol.

Epoxidation of Digeranyl Tartrate with 1 Equivalent $Ti(OiPr)_4$ and TBHP.

A 25 mL round-bottomed flask was charged with 0.1422 g digeranyl tartrate (0.337 mmol) and 15 mL dry CH_2Cl_2. $Ti(O\underline{i}Pr)_4$ (0.098 mL, 0.094 g, 0.33 mmol) was added by syringe and the mixture cooled to 0°C under inert atmosphere. After stirring for 20 minutes, the reaction was cooled to -23°C and TBHP (1.01 mmol, 0.242 mL of a 4.18 M solution in CH_2Cl_2) was added to begin the reaction. After two days at -20°C, TLC showed approximately 40% of the digeranyl tartrate to have reacted with no release of geraniol or geranyl epoxide. The reaction was quenched by addition of 7 mL of a $FeSO_4$/tartaric acid solution (3%/10% by weight) with vigorous stirring while warming to 0°C. The organic phase was dried ($MgSO_4$) and solvent

removed to afford a faint yellow oil.

Careful TLC at this stage again indicated that no geraniol or geranyl epoxide was present, i.e., that less than 5% transesterification had taken place. It is worth noting that in 3:7 EtOAc:hexane TLC showed digeranyl tartrate to have a higher R_f value than geraniol, whereas in 1:9 EtOAc:hexane (developed three times) the relative positions of geraniol and geranyl tartrate were reversed.

Hydrolysis of the tartrate was done with 10 mL 1N NaOH/brine and 15 mL ether at room temperature for 16 hours. Drying of the organic phase with $MgSO_4$, removal of solvent, peracetylation with 3 mL pyridine and 1.5 mL Ac_2O, and column chromatography (1:9 EtOAc:hexane) afforded 0.0248 g of geranyl epoxy acetate (18.8% of the maximum amount possible from complete epoxidation of digeranyl tartrate). NMR analysis in C_6D_6 in the presence of $Eu(hfc)_3$ indicated a >95% ee for this material, by comparison to (dl)-geranyl epoxy acetate prepared by mCPBA oxidation of geraniol. By comparison to geranyl epoxy acetate prepared from the product of asymmetric epoxidation, the product of the digeranyl tartrate oxidation was assigned the 2S configuration, the same as the product from asymmetric epoxidation using (+)-tartarte.

A similar reaction using 0.9 equivalents $Ti(OiPr)_4$ per equivalent of digeranyl tartrate was conducted at 0°C and produced geranyl epoxide of >90% ee, as determined from NMR of the (-)-MTPA ester in the presence of achiral shift reagent Resolve-Eu.

A similar reaction using 2.0 equivalents of $Ti(OiPr)_4$ per equivalent of digeranyl tartrate at -20°C provided a 77% yield of geranyl epoxide of 58% ee (2S) as determined by NMR of the acetate with $Eu(hfc)_3$.

12. Preparation and Epoxidations Using n-Butyl Hydroperoxide

n-Butyl hydroperoxide was prepared from n-butylmethane sulfonate by the method of Williams and Mosher.[135]

A 2.1 M solution of the hydroperoxide in CH_2Cl_2 was dried over activated 4A molecular sieves for 12-16 hours at 0°C. After the concentration was determined by iodometric titration, the hydroperoxide was employed in asymmetric epoxidations of two standard substrates. The hydroperoxide solution was then transferred by pipette to a fresh batch of sieves, and the titration and epoxidations performed again. This process

was repeated until the results of asymmetric epoxidation were reproduced twice in succession, thus employing the epoxidation reaction as an indicator of the water content of the hydroperoxide solution. The concentration of the hydroperoxide solution did not change with the sieve treatments.

Asymmetric epoxidations of (E)-α-phenylcinnamyl alcohol (**60**) and (E)-2-decen-1-ol (**36**) were performed under stoichiometric conditions in the usual manner at -20°C, using a 1:1.2 ratio of $Ti(OiPr)_4$:(+)-DIPT. The following table lists the enantiomeric excess of the product epoxy alcohols for the sequential molecular sieve treatments.

	Enantiomeric Excess (%)	
Reaction	**60**	**36**
1	--	4
2	75	18
3	94	70
4	90	75
5	92	75

13. Kinetic Resolution of α-Phenethyl Hydroperoxide, PHP

Three methods were employed to test the kinetic resolution of racemic hydroperoxide in the asymmetric epoxidation: (1) standard epoxidation of a prochiral substrate with 3-4 equivalents of PHP, (2) kinetic resolution of a racemic secondary allylic alcohol to 50% conversion, and (3) epoxidation of an enantiomerically pure secondary allylic alcohol (prepared by kinetic resolution using (+)-tartrate) by 3-4 equivalents of PHP and (-)-tartrate. In each case, the enantiomeric excess of the recovered phenethyl alcohol was determined by optical rotation and by nmr analysis of the MTPA ester. An example of each of these methods is given below, followed by a list of results.

Phenethyl hydroperoxide was purchased from Oxirane Corp. as a solution in ethylbenzene and phenethyl alcohol. The hydroperoxide was easily purified by flash or medium pressure chromatography on silica gel in CH_2Cl_2; no decomposition of the hydroperoxide was seen. Hydroperoxide concentration was determined by iodometric titration. Subjection of a known amount of purified hydroperoxide to the epoxidation workup conditions including column chromatography resulted in quantitative recovery of

hydroperoxide.

Enantiomerically enriched sec-phenethyl alcohol has been prepared and correlated by a number of workers;[136] the R configuration exhibits a positive optical rotation in methanol and CH_2Cl_2. For absolute configuration assignment of the MTPA esters of phenethyl alcohol, sec-phenethyl alcohol enriched in the S-enantiomer (72% ee) was prepared by the method of Mukiayama.[137] The MTPA ester of this material prepared from (R)-(+)-MTPA-Cl displays the following pattern of more intense resonances: methoxide singlet - downfield; methyl doublet - upfield; phenyl multiplet - upfield; methine quartet - upfield.

Method 1

In a dry 50 mL round bottomed flask, 0.1218 g (Z)-4-diphenylmethoxy-2-buten-1-ol (0.48 mmol) and 0.1541 g (-)-DET (0.75 mmol) were dissolved in 15 mL dry CH_2Cl_2 under inert atmosphere. The flask was cooled to -23°C and 0.1634 g $Ti(O\underline{i}Pr)_4$ (0.57 mmol) was added. The reaction mixture was allowed to stir for 20 minutes and then 0.298 g of phenethyl hydroperoxide was added by syringe (6.55 mL of a 0.329 M solution in CH_2Cl_2, 2.16 mmol). The reactions were stored in a -20°C freezer and quenched after 26 hours by cannula transfer into a solution of 0.5 mL water in 30 mL acetone with vigorous stirring. Filtration through celite, removal of solvent, tartrate hydrolysis in ether/1N NaOH in brine, drying, and removal of solvent gave a mixture of PHP, phenethyl alcohol, epoxy alcohol, and a small amount of unreacted starting material. Medium pressure chromatography (3:7 EtOAc:hexane) provided phenethyl hydroperoxide (0.217 g, 1.57 mmol, 93% based on complete consumption of allylic alcohol), phenethyl alcohol (0.0484 g, 0.400 mmol, 83%), and epoxy alcohol (0.111 g, 0.41 mmol, 86%).

Optical rotations were measured for each of the products:

Phenethyl hydroperoxide: $[\alpha]_D^{23}$ +3.09° (c 17.2, CH_2Cl_2)

Phenethyl alcohol: $[\alpha]_D^{23}$ -6.2° (c 3.23, CH_2Cl_2)

Epoxy alcohol: $[\alpha]_D^{25}$ +18.70° (c 5.55, CH_2Cl_2).

The enantiomeric excess of the epoxy alcohol was estimated by comparison with a sample of epoxy alcohol prepared by Dr. D. Tuddenham and determined by Mosher ester analysis to be 90% ee ($[\alpha]_D^{25}$ +18.62° (c 5.07, CH_2Cl_2)). In this case, the epoxy alcohol was estimated to also be 90% ee. NMR ($CDCl_3$) of the (+)-MTPA ester of the recovered phenethyl alcohol revealed a 16.2% ee in the S configuration, consistent with its direction

of optical rotation.

Method 2

A dry, 50 mL round-bottomed flask was charged with 0.1112 g (E)-1-cyclohexyl-2-buten-1-ol **61** (0.72 mmol), 0.2432 g (+)-DIPT (1.038 mmol), 0.2 mL of hexadecane as internal standard, and 25 mL CH_2Cl_2. After removal of a small amount of the solution as a t_0 gc sample, $Ti(OiPr)_4$ (0.2459 g, 0.87 mmol) was added at room temperature. After 10 minutes, the reaction mixture was cooled to -42°C, and 0.72 mmol of PHP was added (1.12 mL of a 0.646 M solution in CH_2Cl_2). The reaction mixture was allowed to warm to -30°C, whereupon the hexadecane dissolved. A 1 mL aliquot removed by cannula into a stirred $FeSO_4$/tartaric acid quench solution showed the reaction to be about 30% complete. After standing at -42°C for a further 25 minutes and then at -30°C for 20 minutes, the reaction was quenched by cannula transfer into a solution of 1 mL water in 30 mL acetone at 0°C, with vigorous stirring for 30 minutes. Addition of 2 g $MgSO_4$, filtration, evaporation, and tartrate hydrolysis in ether/1 N NaOH/brine afforded a faint yellow oil. GC of the crude product indicated 50% of the allylic alcohol was consumed. Medium pressure chromatography (1:4 EtOAc:hexane) afforded phenethyl alcohol (0.0402 g, 0.33 mmol, 92% based on 50% completion), phenethyl hydroperoxide (0.0467 g, 0.30 mmol, 83%), and unreacted allylic alcohol (0.0562 g, 0.36 mmol, 101% based on 50% completion).

NMR of the (+)-MTPA ester of **61** revealed a >95% enantiomeric excess in recovered allylic alcohol. NMR of the (+)-MTPA ester of recovered phenethyl alcohol revealed a 17% ee of the R enantiomer. For the recovered phenethyl hydroperoxide, $[\alpha]_D^{23}$ -14.4° (c 3.11, MeOH). Assuming that 50% of the hydroperoxide was consumed, a 17% ee in phenethyl alcohol product indicates that the resolved hydroperoxide should be 17% ee in the S enantiomer. Reduction of the hydroperoxide with triphenylphosphine (1.2 equivalents, ether, room temperature, 1 h) provides phenethyl alcohol of $[\alpha]_D^{23}$ +6.7° (c 2.68, MeOH). These results provide an absolute configuration assignment of S to the levorotatory enantiomer, and indicate a maximum optical rotation of approximately -14.4/0.17 = -85° for the homochiral hydroperoxide.

Method 3

A dry, 50 mL round-bottomed flask was charged with 0.1327 g of (R)-

(E)-1,3-dicyclohexyl-2-propen-1-ol (0.597 mmol), prepared in 93% ee by Dr. Victor Martin according to the published procedure.[3c] To this was added 0.2000 g (-)-DIPT (0.85 mmol) and 25 mL dry CH_2Cl_2. $Ti(OiPr)_4$ (0.187 g, 0.66 mmol) was added and, after standing for 10 minutes, the reaction mixture was cooled to -23°C. Phenethyl hydroperoxide (0.247 g, 1.79 mmol, 2.80 mL of a 0.646 M solution in CH_2Cl_2) was then by syringe to begin the reaction. After 16 h, the reaction was quenched by acetone/water, and the tartrate hydrolyzed by NaOH/brine, as noted above for Method 2. MPLC (15:85 EtOAc:hexane) afforded 12.2 mg of recovered allylic alcohol (0.055 mmol), 63.4 mg of phenethyl alcohol (0.52 mmol, 96% based on recovered allylic alcohol), 39.1 mg of the threo epoxy alcohol, and a mixture of the erythro epoxy alcohol and phenethyl hydroperoxide. NMR of the (+)-MTPA ester of phenethyl alcohol showed it to be racemic. However, a similar reaction using (-)-DMT provided phenethyl alcohol of 14% ee of the S enantiomer.

Allylic Alcohol	Method	Tartrate	PHP %ee (Config.)	Epoxy alcohol %ee
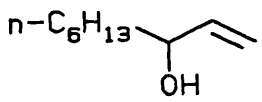	1	DIPT	11 (S)	> 95
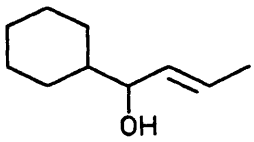	1	DET	18 (R)	> 95
	2	DIPT	17 (R)	> 95
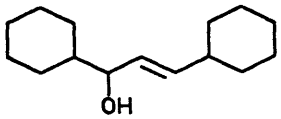	1	DIPT	0	> 95
	1	DMT	14 (R)	> 95
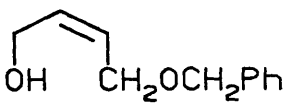	3	DET	5 (R)	75
	3	DIPT	4 (S)	75
	3	DNePT	8 (R)	62
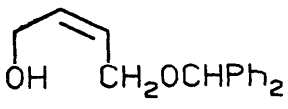	3	DET	16 (R)	90
	3	DIPT	0	90

14. Signer Molecular Weight Determinations.

Molecular weights were measured in solution by the isopiestic Signer method.[94] Tetra-n-butyl tin, purified by distillation, was used as the molecular weight standard.

A typical procedure for a molecular weight determination was as follows. In the drybox a 100 mL round-bottomed was charged with 0.164 g (+)-DIPT (0.700 mmol) and 0.199 g $Ti(O\underline{i}Pr)_4$ (0.700 mmol) in 10 mL CH_2Cl_2. After five minutes at room temperature, the solvent was removed in vacuo. CH_2Cl_2 was again added (5 mL) and removed under vacuum. Two more solvent/vacuum cycles were performed to yield a yellow foam, free of isopropanol (calculated 0.279 g). The Ti-tartrate complex was transferred to one bulb of the Signer apparatus with several CH_2Cl_2 washings to insure quantitative transfer; a total of approximately 5 mL CH_2Cl_2 was required. The other bulb of the Signer apparatus was charged with Bu_4Sn (107 mg, 0.308 mmol) and CH_2Cl_2 (about 3 mL). The sealed apparatus was removed from the drybox, and both solutions subjected to three freeze/pump/thaw cycles (0.1 mm). The apparatus was then allowed to warm slowly to room temperature and was stored at approximately 25°C until distillation of solvent from the standard (Bu_4Sn) bulb to the unknown was complete. Seven days were required to reach equilibrium; the volumes of each solution remained unchanged for four days after that. The Bu_4Sn bulb contained 3.98 mL solution; the bulb containing $Ti(DIPT)(O\underline{i}Pr)_2$ held 4.17 mL solution. Since equilibrium is achieved at the point at which the concentration of solute is the same in each bulb,

$$MW_{unknown} = \frac{(\text{grams unknown})(\text{MW std})(\text{mL std})}{(\text{grams std})(\text{mL unknown})}$$

$$= (0.279\ g)(347\ g/mole)(3.98\ mL) / (0.107\ g)(4.17\ mL)$$

$$= 864\ g/mole$$

The Signer apparatus was then opened in the drybox and a sample of each solution was removed and evaporated for nmr analysis. The nmr spectra showed each solution to be pure and without decomposition.

Occasionally, after equilibrium had been achieved, solvent was transferred from the unknown to the standard solution by bulb-to-bulb distillation (simply by cooling the standard solution with liquid

nitrogen), and the system was allowed to again distill to equilibrium. In every case, the equlibrium volumes were the same as the first determination. To demonstrate the stability of the complexes and the quality of the valve seals, in several instances the apparatus was allowed to stand for a month to six weeks after equilibrium was reached; the volumes of the solutions did not change. It should be noted that measurements in cyclopentane usually required two weeks to reach equilibrium; pentane, five to six days; CH_2Cl_2 and ether, a week to ten days. Experimental error can be considered to be approximately 10%.

Section VI
References

1. Rosten, Leo "The Education of Hyman Kaplan"; Harcourt Brace Jovanovich: San Diego, 1937 and 1965.

2. a. Morrison, J.D.; Mosher, H.S. "Asymmetric Organic Reactions"; Prentice-Hall: New York, 1971; reprinted by the American Chemical Society, 1976.
   b. Izumi, Y.; Tai, A. "Stereodifferentiating Reactions"; Academic Press: New York, 1977.
   c. Bartlett, P.A. Tetrahedron **1980**, 36, 2-72.
   d. Morrison, J.D.; Mosher, H.S. Science **1983**, 221, 1013-1019.

3. a. Katsuki, T.; Sharpless, K.B. J. Am. Chem. Soc. **1980**, 102, 5974-5976.
   b. Rossiter, B.E.; Katsuki, T.; Sharpless, K.B. J. Am. Chem. Soc. **1981**, 103, 464-465.
   c. Martin, V.S.; Woodard, S.S.; Katsuki, T.; Yamada, Y.; Ikeda, M.; Sharpless, K.B. J. Am. Chem. Soc. **1981**, 103, 6237-40.
   d. Sharpless, K.B.; Behrens, C.H.; Katsuki, T.; Lee, A.W.M.; Martin, V.S.; Viti, S.M.; Walker, F.J.; Woodard, S.S. Pure Appl. Chem. **1983**, 55, 589-604.
   e. Sharpless, K.B.; Woodard, S.S.; Finn, M.G. Pure Appl. Chem. **1983**, 55, 1823-1836.
   f. Hill, J.G.; Rossiter, B.E.; Sharpless, K.B. J. Org. Chem. **1983**, 48, 3607-3608.
   g. Gonnella, N.C.; Nakanishi, K.; Martin, V.S.; Sharpless, K.B. J. Am. Chem. Soc. **1982**, 104, 3775-3776.
   h. For an account of the events and reasoning leading up to the discovery of the asymmetric epoxidation process, see: Sharpless, K.B. Proc. Robert A. Welch Found. Conf. Chem. Res., **1984**, 27, Chapter III, 59-89.
   i. Hill, J.G.; Sharpless, K.B.; Exon, C.M.; Regenye, R. Org. Syn. **1984**, 63, 66-78.
   j. Schweiter, M.J.; Sharpless, K.B. Tetrahedron Lett. **1985**, 26, 2543-2546.
   k. Finn, M.G.; Sharpless, K.B. In "Asymmetric Synthesis"; Morrison, J.D., Ed.; Academic Press: New York; Volume 5, Chapter 8.

4. We believe that the asymmetric epoxidation reaction can therefore be very effective as an aid in assigning the absolute configuration of chiral molecules.

5. a. Rossiter, B.E. In "Asymmetric Synthesis"; Morrison, J.D., Ed.; Academic Press: New York; Volume 5, Chapter 7.
   b. For methods of regio- and stereospecific elaboration of 2,3-epoxy alcohols, see: Behrens, C.H.; Sharpless, K.B. Aldrichim. Acta **1983**,

16, 67-79. Caron, M.; Sharpless, K.B. J. Org. Chem. **1985**, 50, 1557-1560. Chong, J.M.; Sharpless, K.B. J. Org. Chem. **1985**, 50, 1560-1563.

6. a. Katsuki, T.; Lee, A.W.M.; Ma, P.; Martin, V.S.; Masamune, S.; Sharpless, K.B.; Tuddenham, D.; Walker, F.J. J. Org. Chem. **1982**, 47, 1373-1378.
   b. Ma, P.; Martin, V.S.; Masamune, S.; Sharpless, K.B.; Viti, S.M. J. Org. Chem. **1982**, 47, 1378-1380.
   c. Reed, L.A., III; Ito, Y.; Masamune, S.; Sharpless, K.B. J. Am. Chem. Soc. **1982**, 104, 6468-6670.

7. Nagaoka, H.; Kishi, Y. Tetrahedron **1981**, 37, 3873-3888.

8. From reference 84.

9. a. See reference 2a, Chapters 1-3 for a general review.
   b. For more detailed reviews, see: Boone, J.R.; Ashby, E.C. In "Topics in Stereochemistry"; Allinger, N.L.; Eliel, E.L., Eds.; Interscience Publishers: New York, 1979; Vol. 11 pp 53-95. Wigfield, D.C. Tetrahedron **1979**, 35, 449-462.
   c. Cram, D.J.; Abd Elhafez, F.A. J. Am. Chem. Soc. **1952**, 74, 5828-5835.
   d. Karabatsos, G.J. J. Am. Chem. Soc. **1967**, 89, 1367-1371.
   e. Cherest, M.; Felkin, H.; Prudent, N. Tetrahedron Lett. **1968**, 2199-2204. Cherest, M.; Felkin, H. Tetrahedron Lett. **1968**, 2205-2208.
   f. Prelog, V. Helv. Chim. Acta **1953**, 36, 308-319.
   g. For more recent transition state proposals, see: Anh, N.T.; Eisenstein, O. Nouv. J. Chim. **1977**, 1, 61-70. Cieplak, A.S. J. Am. Chem. Soc. **1981**, 103, 4540-4552. Paddon-Row, M.N.; Rondan, N.G.; Houk, K.N. J. Am. Chem. Soc. **1982**, 104, 7162-7166.

10. The role of stereoelectronic factors in enantioselective reactions is receiving wider attention. For example, Roush has recently discovered a highly enantioselective addition reaction of allyl and crotyl boronates to aldehydes, mediated by tartrate diesters. He postulates an asymmetric disposition of electron density (not steric bulk) about the metal, giving rise to an electrostatic repulsion as the enantioselective interaction (Roush, W.R.; Walts, A.E.; Hoong, L.K. J. Am. Chem. Soc., in press).
    As with asymmetric epoxidation, allylboronate additions are thought to proceed through a structurally restricted transition state. According to Roush, enantioselectivity in the chiral reaction is then a matter of the energy difference between two well-defined diastereomeric arrangements with very similar steric interactions, to which the relatively subtle electronic effects are able to contribute significantly. This idea of using interactions of relatively small magnitude to modify an already restricted transition state to achieve greater

selectivity is merely common sense, of course. (For example, in general no one expects great enantioselectivity from free radical reactions). For the most part, however, researchers have designed or invoked second-order steric interactions as the enantioselective elements (i.e., in nucleophilic additions to carbonyl compounds or in asymmetric aldol condensation reactions). Control elements that do not rely on van der Waals repulsion are now being identified in well-known reactions (as in Houk's work on additions to unsaturated systems) and hopefully will be routinely considered in the design of new stereoselective reactions.

11. a. Swern, D. In "Organic Peroxides"; Wiley-Interscience: New York, 1971, Vol. II, Chapter V.
    b. Berti, G. In "Topics in Stereochemistry"; Allinger, N.L.; Eliel, E.L., Eds.; Interscience Publishers: New York, 1973; Vol. 7, pp 93-251.
    c. Dryuk, G. Tetrahedron **1976**, 1-12.

12. a. Sheldon, R.A.; Kochi, J. "Metal-Catalyzed Oxidations of Organic Compounds"; Academic Press: New York, 1981; Chapter 9.
    b. Sheldon, R.A. J. Mol. Catal **1980**, 7, 107-126.
    c. Sheldon, R.A.; Kochi, J.K. Adv. Catal. **1976**, 25, 272-413.
    d. Lyons, J.E. Aspects Homogeneous Catal. **1977**, 3, 1-136.
    e. Sheldon, R.A.; Van Doorn, J.A. J. Catal. **1973**, 31, 427-37.
    f. Sharpless, K.B.; Verhoeven, T.R. Aldrichim. Acta **1979**, 12, 63-74.
    g. Parshall, G.W. J. Mol. Catal. **1978**, 4, 243-270.
    h. Mimoun, H. J. Mol. Catal. **1980**, 7, 1-29.

13. Gladiali, S.; Soccolini, F. Syn. Commun. **1982**, 12, 355.

14. a. Still, W.C.; Novack, V.J. J. Am. Chem. Soc. **1981**, 103, 1283-1285.
    b. Corey, E.J.; Chaykovsky, M. J. Am. Chem. Soc. **1965**, 87, 1353.

15. Prileschajew, N. Ber. **1909**, 42, 4811-4815.

16. a. Lynch, B.M.; Pausacker, K.H. J. Chem. Soc. **1955**, 1525-1531.
    b. Campbell, D.R.; Edwards, J.O.; Maclachlan, J.; Polgar, K. J. Am. Chem. Soc. **1958**, 80, 5308-5312.

17. a. Bach, R.D.; Wolber, G.J. J. Am. Chem. Soc. **1984**, 106, 1410-1415.
    b. Lang, T.J.; Wolber, G.J.; Bach, R.D. J. Am. Chem. Soc. **1981**, 103, 3275-3282.
    c. Bach, R.D.; Wolber, G.J.; Coddens, B.A. J. Am. Chem. Soc. **1984**, 106, 6090-6099.
    d. Bach, R.D.; Coddens, B.A., calculations on the mechanism of asymmetric epoxidation, submitted for publication, 1986.
    e. Rondan, N.G.; Rebek, Jr., J.; Houk, K.N., unpublished results.

18. Henbest, H.B.; Wilson, R.A.L. J. Chem. Soc. **1957**, 1958-1965.

19. Newman, M.S.; Gill, N.; Thomson, D.W. J. Am. Chem. Soc. **1967**, 89, 2059-2062.

20. Friedrich, L.E.; Fiato, R.A. J. Org. Chem. **1974**, 39, 416-418.

21. a. Chamberlain, P.; Roberts, M.L.; Whitham, G.H. J. Chem. Soc. B. **1970**, 1374-1381.
b. Johnson, M.R.; Nakata, T.; Kishi, Y. Tetrahedron Lett. **1979**, 4343-4346, 4347-4350. Hasan, I.; Kishi, Y. Tetrahedron Lett. **1980**, 4229- 4232.
c. Chautemps, P.; Pierre, J.-L. Tetrahedron **1976**, 32, 549-557.
d. Narula, A.S. Tetrahedron Lett. **1981**, 2017-2020.

22. Bartlett, P.D. Rec. Chem. Prog. **1950**, 11, 47-51.

23. a. Kwart, H.; Hoffman, D. J. Org. Chem. **1966**, 31, 419-425.
b. Kwart, H.; Starcher, P.S.; Tinsley, S.W. J. Chem. Soc., Chem. Commun. **1967**, 335-337.

24. For example, norbornene reacts approximately three orders of magnitude faster than cyclohexene in reactions that involve 1,3-dipolar mechanisms,[34a,24] but only 1.2 times faster in epoxidation by peracids[26] and just 1.9 times faster in epoxidation by the molybdenum-peroxo complex MoO_5·HMPA.[34a]
Also, cyclopropenes are epoxidized by peracid at the same rate as cyclobutenes, even though cyclopropene has twice the strain energy and is much more reactive toward 1,3-dipolar reagents than cyclobutene.[20]

25. Awasthy, A.K.; Rocek, J. J. Am. Chem. Soc. **1969**, 91, 991-996.

26. a. Bingham, K.D.; Meakins, G.D.; Whitham, G.H. Chem. Commun., **1966**, 445.
b. Swern, D. Org. Reactions **1953**, 7, 378.

27. a. Plesnicar, B.; Tasevski, M.; Azman, A. J. Am. Chem. Soc. **1978**, 100, 743-746.
b. Azman, A.; Borstnik, B.; Plesnicar, B. J. Org. Chem. **1969**, 34, 971-972.
c. Yonezawa, T.; Kato, H.; Yamamoto, O. Bull. Chem. Soc. Jpn. **1967**, 40, 307-311.
d. Bach, R.D.; Willis, C.L.; Domagala, J.M. In "Progress in Theoretical Organic Chemistry"; Csizmadia, I.G., Ed.; Elsevier: Amsterdam, 1977, Vol. 11, pp 221-229.

28. a. Corey, E.J.; Niwa, H.; Falck, J.R. J. Am. Chem. Soc. **1979**, 101,

1586-1587.
b. Bruice, T.C. J. Chem. Soc., Chem. Commun., **1983**, 14-15.

29. a. Sheng, M.N.; Zajacek, J.G. J. Org. Chem. **1970**, 35, 1839-1843.
b. Sheng, M.N.; Zajacek, J.G. Advan. Chem. Ser. No. 76 **1968**, 418-432.

30. a. Substitution of electron-withdrawing substituents on an alkylhydroperoxide (i.e. para-nitrocumene hydroperoxide vs. cumene hydroperoxide) increases the rate of epoxidation. See reference 29b.
b. The more electron-deficient the metal, the more reactive is the coordinated alkyl peroxide group to nucleophilic attack. See p 347 of reference 12c. See also Strukul, G.; Michelin, R.A.; Orbell, J.D.; Randaccio, L. Inorg. Chem. **1983**, 22, 3706-3713.
c. See Appendix 1 for the results of pseudo-first order kinetics using electron-deficient hydroperoxides.

31. a. Gould, E.S.; Hiatt, R.R.; Irwin, K.C. J. Am. Chem. Soc. **1968**, 90, 4573-4579.
b. Baker, T.N.; Mains, G.J.; Sheng, M.N.; Zajacek, J.G. J. Org. Chem. **1973**, 38, 1145-48.

32. Mimoun, H.; Seree de Roch, I.; Sajus, L. Tetrahedron **1970**, 26, 37-50.

33. Chong, A.O.; Sharpless, K.B. J. Org. Chem. **1977**, 42, 1587-1590.

34. a. Sharpless, K.B.; Townsend, J.M.; Williams, D.R. J. Am. Chem. Soc. **1972**, 94, 295-296.
b. It has also been shown by ^{17}O NMR measurements that a Mo(VI) oxo-peroxo complex does not undergo exchange of oxo and peroxo oxygen atoms: see reference 105.

35. Serjeant, E.P.; Dempsey, B. "Ionisation Constants of Organic Acids in Aqueous Solution"; IUPAC Chemical Data Series No. 23; Pergamon: Oxford; 1979.

36. a. Itoh, T.; Jitsukawa, K.; Kaneda, K.; Teranishi, S. J. Am. Chem. Soc. **1979**, 101, 159-169.
b. Dehnel, R.B.; Whitham, G.H. J. Chem. Soc., Perkin Trans. 1, **1979**, 953-955.
c. Itoh, T.; Kaneda, K.; Teranishi, S. J. Chem. Soc., Chem. Commun., **1976**, 421-422.

37. a. Narula, A.S.; Tetrahedron Lett., **1982**, 5579-5582.
b. Rossiter, B.E.; Verhoeven, T.R.; Sharpless, K.B. Tetrahedron Lett., **1979**, 4733-4766.
c. Mihelich, E.D. Tetrahedron Lett., **1979**, 4733-4736.
d. Sharpless, K.B.; Michaelson, R.C. J. Am. Chem. Soc. **1973**, 95, 6136-

6137.
e. Isobe, M.; Kitamura, M.; Mio, S.; Goto, T. Tetrahedron Lett. **1982**, 221-224.

38. Bruice, T.C.; Benkovic, S.J. J. Am. Chem. Soc. **1964**, 86, 418-426.

39. Lubben, T.V.; Wolczanski, P.T. J. Am. Chem. Soc. **1985**, 107, 701-703.

40. a. Mimoun, H.; Chaumette, P.; Mignard, M.; Saussine, L.; Fischer, J.; Weiss, R. Nouv. J. Chim. **1983**, 7, 467-475.
b. Van Asselt, A.; Bercaw, J.E.; unpublished results. We thank Professor Bercaw and Mr. Van Asselt for allowing us to quote these results.

41. Takai, K.; Oshima, K.; Nozaki, H. Tetrahedron Lett., **1980**, 1657-1660.

42. Mihelich, E.D.; Daniels, K.; Eickhoff, D.J. J. Am. Chem. Soc. **1981**, 103, 7690-7692.

43. Bortolini, O.; DiFuria, F.; Scrimin, P.; Modena, G. J. Mol. Catal. **1980**, 7, 59-74.

44. Rebek, Jr., J.; McCready, R. J. Am. Chem. Soc. **1980**, 102, 5602-5605.

45. a. Mimoun, H.; Charpentier, R.; Mitschler, A.; Fischer, J.; Weiss, R. J. Am. Chem. Soc. **1980**, 102, 1047-1054.
b. Mimoun, H. Angew. Chem., Int. Ed. Eng. **1982**, 21, 734-750.
c. Mimoun, H. J. Mol. Catal. **1980**, 7, 1-29.
d. Mimoun, H.; Machirant, M.M.P.; Seree de Roch, I. J. Am. Chem. Soc. **1978**, 100, 5437-5444.
e. Chaumette, P.; Mimoun, H.; Saussine, L.; Fischer, J.; Mitschler, A. J. Organomet. Chem., **1983**, 250, 291-310.

46. Sheldon, R.A.; Van Doorn, J.A. J. Organomet. Chem. **1975**, 94, 115-127.

47. Igersheim, F.; Mimoun, H. Nouv. J. Chim. **1980**, 4, 161-166.

48. Ledon, H.J.; Durbut, P.; Varescon, F. J. Am. Chem. Soc. **1981**, 103, 3601-3603.

49. We do not include the studies on other types of epoxidation reactions, such as by "oxenoid" (^{1}S) oxygen atoms[50] and metal-oxo groups.[51]

50. Pudzianowski, A.T.; Loew, G.H. J. Am. Chem. Soc. **1980**, 102, 5443-5449.

51. a. Rappe, A.K.; Goddard, III, W.A. J. Am. Chem. Soc. **1980**, 102, 5114-5115.

b. Rappe, A.K.; Goddard, III, W.A. Nature **1980**, 285, 311-312.
c. Sharpless, K.B.; Teranishi, A.Y.; Backvall, J.-E. J. Am. Chem. Soc. **1977**, 99, 3120-3128.

52. a. Jarvie, J.O.; Rauk, A.; Edmiston, C. Can. J. Chem. **1974**, 52, 2778-2784, and references cited therein.
b. Savariault, J.M.; Lehmann, M.S. J. Am. Chem. Soc. **1980**, 102, 1298-1303.
c. Busing, W.R.; Levy, H.A. J. Chem. Phys. **1965**, 42, 3054-3059.
d. Giguere, P.A. J. Chem. Ed. **1980**, 60, 399-401.

53. a. Hanzlik, R.P.; Shearer. G.O. J. Am. Chem. Soc. **1975**, 97, 5231-5233.
b. Secondary deuterium isotope effect in epoxidation of styrene by cytochrome P-450 (k_D/k_H = 1.08 for α-d, 1.01 for β,β-d_2): Hanzlik, R.P.; Shearer, G.O. Biochem. Pharmacol. **1978**, 27, 1441-1444.
c. Confirmation of -d result in reference a, plus secondary isotope determination for ozonolysis of styrene (k_D/k_H = 1.08 for both α-d and β,β-d_2): Choi, H.-S.; Kuczkowski, R.L. J. Org. Chem. **1985**, 50, 901-902.
d. Isotope effects in oxidation of 2-methylpropenes with triplet oxygen: Havel, J.J.; Hunt, C.J. J. Phys. Chem. **1976**, 80, 779-782.
e. Secondary deuterium isotope effects in epoxide opening reactions: Hanzlik, R.P.; Westkaemper, R.B. J. Am. Chem. Soc. **1980**, 102, 2464-2467.

54. a. David S.; Eisenstein, O.; Hehre, W.J.; Salem, L.; Hoffmann, R. J. Am. Chem. Soc. **1973**, 95, 3806-3807.
b. Dunning, T.H.; Pitzer, R.M.; Aung, S. J. Chem. Phys. **1972**, 57, 5044-5051.
c. Sweigart, D.A.; Turner, D.W. J. Am. Chem. Soc. **1972**, 94, 5599-5603.

55. For example,
a. Deslongchamps, P. "Stereoelectronic Effects in Organic Chemistry"; Pergamon Press: Oxford, 1983.
b. Deslongchamps, P. Tetrahedron **1975**, 31, 2463-2490.
c. Kirby, A.J. "The Anomeric Effect and Related Stereoelectronic Effects at Oxygen" Reactivity and Structure Concepts in Organic Chemistry. Vol. 15; Springer-Verlag: Berlin, 1983.
d. Noyori, R.; Kobayashi, H.; Sato, T. Tetrahedron Lett. **1980**, 2573-2576. Noyori, R.; Sato, T.; Kobayashi, H. Tetrahedron Lett. **1980**, 2569-2572.

56. a. Dunitz, J.D.; Seiler, P. J. Am. Chem. Soc. **1983**, 105, 7056-7058.
b. See reference 49c, chapters B.2 and C.1, and references cited therein.

57. Davis, F.A.; Harakal, M.E.; Awad, S.B. J. Am. Chem. Soc. **1983**, 105, 3123-3126.

58. Rebek, Jr., J.; Marshall, L.; Wolak, R.; McManis, J. J. Am. Chem. Soc. **1984**, 106, 1170-1171.

59. a. Henbest, H.B. Chem. Soc. Special Publ. **1965**, 19, 83-92.
b. Ewins, R.C.; Henbest, H.B.; McKervey, M.A. J. Chem. Soc., Chem. Commun., **1967**, 1085-1086.

60. a. Bowman, R.M.; Collins, J.F.; Grundon, M.F. J. Chem. Soc., Chem. Commun., **1967**, 1131-1132.
b. Bowman, R.M.; Grundon, M.F. J. Chem. Soc. (C), **1967**, 2368-2371.
c. Montanari, F.; Moretti, I.; Torre, G. Boll. sci. fac. Chim. ind. Bologna **1968**, 26, 113.
d. Montanari, F.; Moretti, I.; Torre, G. J. Chem. Soc., Chem. Commun. **1969**, 135-136.
e. Boyd, D.R.; Jerina, D.M.; Daly, J.W. J. Org. Chem. **1970**, 35, 3170-3172.
f. Bowman, R.M.; Collins J.F.; Grundon, M.F. J. Chem. Soc., Perkin Trans. 1 **1973**, 626-632.
g. Montanari, F.; Moretti, I.; Torre, G. Gazz. Chim. Ital. **1974**, 104, 7-15.
h. Grundon M.F.; McColl, I.S. Phytochemistry **1975**, 14, 143-150.

61. Pirkle, W.H.; Rinaldi, P.L. J. Org. Chem. **1977**, 42, 2080-2082.

62. a. Helder, R.; Hummelen, J.C.; Laane, R.W.P.M.; Wiering, J.B.; Wynberg, H. Tetrahedron Lett., **1976**, 1831-1834.
b. Wynberg, H.; Greijdanus, B. J. Chem. Soc., Chem. Commun., **1978**, 427-428.
c. Igarashi, M.; Midorikawa, H. Bull. Chem. Soc. Jpn. **1967**, 40, 2624-2627.
d. Marsman, B.; Wynberg, H. J. Org. Chem. **1979**, 44, 2312-2314, and references cited therein.

63. a. Julia, S.; Guixer, J.; Masana, J.; Rocas, J. J. Chem. Soc., Perkin Trans. 1, **1982**, 1317-1324.
b. Julia, S.; Masana, J.; Vega, J.C. Angew. Chem., Int. Ed. Eng. **1980**, 929-930.

64. Nanjo, K.; Suzuki, K.; Sekiya, M. Chem. Lett., **1978**, 1143-1144.

65. a. Hummelen, J.C.; Wynberg, H. Tetrahedron Lett., **1978**, 1089-1092.
b. Wynberg, H. In "Selectivity - a Goal for Synthetic Efficiency; Workshop Conferences Hoechst/Volume 14"; Bartmann, W.; Trost, B.M., Eds.; Verlag Chemie: Weinheim, 1983, 365-375, and references cited therein.
c. Banfi, S.; Colonna, S. Syn. Comm. **1983**, 13, 1049-1052.

66. Yamada, S.; Mashiko, T.; Terashima, S. J. Am. Chem. Soc. **1977**, 99, 1988-1990.

67. Michaelson, R.C.; Palermo, R.E.; Sharpless, K.B. J. Am. Chem. Soc. **1977**, 99, 1990-1992.

68. Coleman-Kammula, S.; Duim-Koolstra, E.T. J. Organomet. Chem. **1983**, 246, 53-56.

69. Kagan, H.B.; Mimoun, H.; Mark, C.; Schurig, V. Angew. Chem., Int. Ed. Eng. **1979**, 18, 485-486.

70. Tani, K.; Hanafusa, M.; Otsuka, S. Tetrahedron Lett. **1979**, 3017-3020.

71. Groves, J.T.; Myers, R.S. J. Am. Chem. Soc. **1983**, 105, 5791-5796.

72. Mansuy, D.; Battioni, P.; Renaud, J.-P.; Guerin, P. J. Chem. Soc., Chem. Commun. **1985**, 155-156.

73. Hanson, R.M.; Sharpless, K.B., submitted for publication.

74. a. Reed, III, L.A.; Ito, Y.; Masamune, S.; Sharpless, K.B. J. Am. Chem. Soc. **1982**, 104, 6468-6470.
    b. Sharpless, K.B., unpublished results.

75. a. Morgans, Jr., D.J.; Sharpless, K.B. J. Am. Chem. Soc. **1981**, 103, 462-464.
    b. Minami, N.; Ko, S.S.; Kishi, Y. J. Am. Chem. Soc. **1982**, 104, 1109.
    c. Corey, E.J.; Hopkins, P.B.; Munroe, J.E.; Marfat, A.; Hashimoto, S. J. Am. Chem. Soc. **1980**, 102, 7986.
    d. Roush, W.R.; Brown, R.J. J. Org. Chem. **1982**, 47, 1371.
    e. Roush, W.R.; Brown, R.J.; DiMare, M. J. Org. Chem. **1983**, 48, 5083.
    f. Roush, W.R.; Brown, R.J. J. Org. Chem. **1983**, 48, 5093.
    g. Arata, K.; Tanabe, K. Catal. Rev.-Sci. Eng. **1983**, 25, 365-420.

76. Ko, S.-Y.; Hollinshead, D.M.; Sharpless, K.B., unpublished results.

77. For example, application of equation (1) shows that a tartrate binding constant of 10^5 would leave about 0.5% of the total titanium as $Ti(O\underline{i}Pr)_4$ for a 5 mol% catalyst reaction that is 0.5 M in substrate and 1 M in hydroperoxide. Reducing the catalyst level to 1 mol% would liberate 2.3% of the titanium as $Ti(O\underline{i}Pr)_4$. (For simplicity's sake we treat hydroperoxide and allylic alcohol as the same monodentate alcohol and we ignore species like $Ti_2(tartrate)(OR)_6$.) Under stoichiometric conditions, only 0.06% of the titanium would be found as $Ti(O\underline{i}Pr)_4$.

78. Woodard, S.S., Ph.D. Dissertation, Stanford University, Stanford, Ca., 1981.

79. a. Bradley, D.C.; Mehrotra, R.C.; Gaur, D.P. "Metal Alkoxides"; Academic Press: New York, 1978, Chapter 4.
b. Clark, R.J.H. "The Chemistry of Titanium and Vanadium"; Elsevier: Amsterdam, 1968.
c. Clark, P.J.; Kays, M.J.; Edwards, J.D.; Reiger, P.O. J. Chem. Soc., Chem. Commun., **1976**, 429-430.

80. Seebach, D.; Hungerbühler, E.; Naef, R.; Schnurrenberger, P.; Weidmann, B.; Zuger, M. Synthesis, **1982**, 138-141.

81. Preliminary pseudo-first order kinetics measurements showed an α-hydroxy ester to be transesterified at 20-40 times the rate of an unfunctionalized ester (methyl-2-hydroxyisobutyrate vs. methyl enanthate). That transesterification of tartrate is much slower than epoxidation was shown by Woodard's observation of reproducibly different kinetic behavior for epoxidation with DET and DIPT under pseudo-first order conditions (a large excess of isopropanol).

82. In fact, kinetic resolution was responsible in a sense for the discovery of the asymmetric epoxidation process in 1980. The Ti-tartrate complex was tested first on the secondary allylic alcohol 4-methyl-1-penten-3-ol in a screening process for unusual diastereoselectivity. In that first experiment, it was found that the reaction stopped after only half the substrate was consumed (in spite of excess TBHP), and that the product epoxy alcohol was highly enriched in the erythro isomer. These two facts taken together strongly implicated an efficient kinetic resolution coupled with an asymmetric epoxidation. If the slow reacting enantiomer had not been quite so unreactive, the reaction might have gone to completion and an unspectacular erythro/threo ratio observed -- with nothing to suggest the presence of an asymmetric epoxidation process. See reference 3h.

83. Schweiter, M.J., S.M. Dissertation, Massachusetts Institute of Technology, Cambridge, Ma., 1984.

84. Lu, L.D.-L.; Johnson, R.A.; Finn, M.G.; Sharpless, K.B. J. Org. Chem. **1984**, 48, 728-731.

85. Miyano, S.; Lu, L.D.-L.; Viti, S.M.; Sharpless, K.B. J. Org. Chem. **1983**, 48, 3608-3611.

86. For example, the IR spectrum of Ti(DIPT)(O*i*Pr)$_2$ + 1.0 *N*-methylephedrine shows only a 1740 cm^{-1} band in the C=O stretching region, indicating that the β-hydroxy amine is an effective bidentate ligand.

87. a. Pitchen, P.; Kagan, H.B. Tetrahedron Lett., **1984**, 1049-1052.
b. Pitchen, P.; Dunach, E.; Deshmulch, M.N.; Kagan, H.B. J. Am. Chem. Soc. **1984**, 106, 8188-8193.

88. Hoff, C.; Lopez, R. University of Miami, private communication to K.B. Sharpless.

89. While K_1 and K_2 for binding of TBHP to $Ti(OiPr)_4$ are approximately 3.0, hydroperoxide should be a poorer ligand for dimeric complexes such as $Ti(OiPr)_3$(allylic alcohol) or $Ti(OiPr)_2$(allylic alcohol)$_2$. Comparing Hoff's results and our K_{eq} determinations for hydroperoxide, we conclude that alkylperoxide is a poorer bridging ligand than primary alkoxide.

90. Halpern, J. In "Asymmetric Synthesis"; Morrison, J.D., Ed.; Academic Press: New York; Volume 5, Chapter 2, and references cited therein.

91. Pedersen, S.F.; Burns, D.B.; Sharpless, K.B., unpublished results. Triphenylmethyl hydroperoxide is also effective for kinetic resolution of secondary allylic alcohols and is a convenient oxidant for some small-scale asymmetric reactions since it is a crystalline solid that is easy to handle and purify.

92. Indeed, molecular sieve powder has been shown to be the dessicant of choice for drying many organic solvents, often equalling or surpassing traditional methods such as distillation from Na or $LiAlH_4$. See reference 126.

93. Schowen, R.L. Prog. Phys. Org. Chem. **1972**, 9, 275-332.

94. Clark, E.P. Ind. Eng. Chem., Anal. Ed. **1941**, 13, 820-821.

95. a. Tapscott, R.E.; Belford, R.L.; Paul, I.C. Coord. Chem. Rev. **1969**, 4, 323-359
b. Robbins, G.L.; Tapscott, R.E. Inorg. Chem. **1976**, 15, 154-159.
c. Tapscott, R.E. Inorg. Chim. Acta **1974**, 10, 183-189.
d. Marcovich, D.; Tapscott, R.E. J. Am. Chem. Soc. **1980**, 102, 5712-5717.
e. Hahs, S.K.; Tapscott, R.E. J. Chem. Soc., Chem. Commun. **1974**, 701-702.
f. Hahs, S.K.; Ortega, R.B.; Tapscott, R.E.; Campana, C.F.; Morosin, B. Inorg. Chem. **1982**, 21, 664-672.
g. A similar dimeric Ni(II) complex of tartaric acid has been described: Bostelaar, L.J.; DeGraaff, R.A.G.; Hulsbergen, R.B.; Reedijk, J.; Sachtler, W.M. Inorg. Chem. **1984**, 23, 2294-2297.

96. a. Williams, I.D.; Pedersen, S.F.; Sharpless, K.B.; Lippard, S.J. J. Am. Chem. Soc. **1984**, 106, 6430-6431.
b. Pedersen, S.F.; Dewan, J.; Sharpless, K.B., unpublished results; x-ray crystal structures of **13c**, **13d**, and **13e**.

97. Sandstrom, J. "Dynamic NMR Spectroscopy"; Academic Press: New York, 1982.

98. Gordon, A.J.; Ford, R.A. "The Chemist's Companion"; Wiley: New York, 1972; page 314.

99. Klemperer has published many papers on ^{17}O nmr spectroscopy; those listed here are only those specifically referenced for other reasons in the text.
a. Besecker, C.J.; Klemperer, W.G. J. Am. Chem. Soc. **1980**, 102, 7598-7600.
b. Klemperer, W.G.; Shum, W. J. Am. Chem. Soc. **1978**, 100, 4891-4893.
c. Klemperer, W.G.; Shum, W.J. J. Am. Chem. Soc. **1977**, 99, 3545-3546.
d. Klemperer, W.G.; Shum, W.J. J. Chem. Soc., Chem. Comm., **1979**, 60-61.

100. Hillhouse, G.L.; Bercaw, J.E. J. Am. Chem. Soc. **1984**, 106, 5472-5478.

101. Balakrishnan, P.; Baumstark, A.L.; Boykin, D.W. Tetrahedron Lett. **1984**, 25, 169-172.

102. Balakrishnan, P.; Baumstark, A.L.; Boykin, D.W. Org. Magn. Res. **1984**, 22, 753-756.

103. See reference 79a.

104. Russo, W.R.; Nelson, W.H. J. Am. Chem. Soc. **1970**, 92, 1521-1526.

105. a. Postel M.; Brevard, C.; Arzoumanian, H.; Reiss, J.G. J. Am. Chem. Soc. **1983**, 105, 4922-4926.
b. Curci, R.; Fusco, G.; Sciacovelli, O.; Triosi, L. J. Mol. Catal. **1985**, 32, 251-257.
c. Zimin, Y.S.; Stepanov, A.G.; Nekipelov, V.M. React. Kinet. Catal. Lett. **1985**, 28, 145-152. Coordination of cumyl hydroperoxide to tris-amino alcohol complexes of Cr(III); manuscript unavailable at this time. CA Abstracts: 103(22):188455z.
d. Harrison, A.T.; Howarth, O.W. J. Chem. Soc., Dalton Trans. **1985**, 1173-1177.

106. The difference in electron-withdrawing capacity of benzyl and isopropyl groups is highlighted by the ^{17}O chemical shift of benzyl alcohol (-6.8 ppm) vs. isopropanol (+21.7 ppm). Another example is

offered by the proton chemical shifts of methyl groups in ethylbenzene (1.2 ppm) and methylcyclohexane (0.9 ppm). The pK_a of benzyl alcohol is 3.8 units lower than t-butanol and 1.7 units below that of isopropanol (15.4 vs. 19.2 vs. 17.1).[35]

107. Bercaw reported J_{O-H} = ca. 80 Hz.[100] Curci, et. al. also report the downfield resonance of TBHP to be slightly (50 Hz. wider than the upfield band).[105c]

108. Kropf, H.; Bernert, C.R.; Dahlenburg, L. Tetrahedron **1970**, 26, 3279-3287.

109. The O^{17} resonance of ethylene oxide is found at -64 ppm relative to ether; propylene oxide at -31 ppm, and styrene oxide at -23 ppm. Increasing the electron donating ability of substituents on the epoxide carbons pushes the O^{17} resonances downfield. Sauleau, A.; Sauleau, J.; Faure, R.; Monti, J.P. Org. Magn. Res. **1983**, 21, 483-484. See also: Iwamura, H.; Sugawara, T.; Kawada, Y.; Tori, K.; Muneyuki, R.; Noyori, R. Tetrahedron Lett. **1979**, 3449-3452.

110. See reference 90.

111. Ko, S.-Y. and Sharpless, K.B., unpublished results. The epoxidation of allyl alcohol was performed with 5% $Ti(OiPr)_4$, 6% DIPT, and 200% cumyl hydroperoxide, relative to allyl alcohol, in CH_2Cl_2. After complete epoxidation as monitored by gc, the reaction mixture was treated with $Ti(OiPr)_4$ and thiophenol to afford 3-thiophenoxy-1,2-propanediol in 90% isolated yield and 89% ee.

112. Martin, V.S.; Woodard, S.S.; Sharpless, K.B., unpublished results.

113. This assumes that the slower-reacting enantiomer produces only threo epoxy alcohol, thus providing a lower limit on the diastereomeric excess in the abnormal direction for epoxidation of the faster-reacting enantiomer.
Since (Z)-4-undecen-3-ol is epoxidized at a slower rate than usual, it is of course possible that the epoxidation takes place by a different mechanism entirely. The reasonable level of kinetic resolution observed in this case, however, makes it appropriate to apply our transition state model. This result represents a mismatched combination of diastereomeric selectivity imposed by the catalyst (which favors the formation of erythro products) and the inherent diastereomeric selectivity of the substrate (which favors the formation of threo epoxy alcohols with achiral Ti(IV) and V(V) catalysts). In this case the substrate-imposed selectivity is slightly stronger (erythro/threo = 4/6). (Z)-3-penten-2-ol is a similar substrate that undergoes good kinetic resolution (k_{rel} = ca. 20) in which the catalyst-imposed

diastereomeric selectivity dominates to the extent of an 81:19 ratio of erythro:threo epoxy alcohols.[3c]

114. In reference 3j, we mentioned only Professor Eschenmoser in this context. Professor Whitesell had sent us the same suggestion earlier, but we remembered it only after reference 3j was published; we apologize to Professor Whitesell for this omission.

115. Roof, A.A.M.; Winter, W.J.; Bartlett, P.D. J. Org. Chem. **1985**, 50, 4093-4098. This paper explores the epoxidation of syn- and anti-sesquinorbornene by peracid, substrates that restrict the transition state geometry to a planar one. So, the possibility of (but not the preference for) a planar arrangement is confirmed by this work, and such a reaction is shown to have an early transition state.

116. The preferred ground state conformation of allyl alcohol itself appears to be the rotamer in which the allylic C-O bond is nearly coplanar with the olefin system:
    a. Microwave spectrum: Murty, A.N.; Curl, Jr., R.F. J. Chem. Phys. **1967**, 46, 4176-4180.
    b. Photoelectron spectra: Brown, R.S.; Marcinko, R.W. J. Am. Chem. Soc. **1978**, 100, 5721-5727.
    c. Microwave spectrum in a low-temperature matrix (the preferred conformation appears to depend on whether Ar or N_2 is the matrix used): Silvi, B.; Froment, F.; Corset, J.; Perchard, J.P. Chem. Phys. Lett. **1973**, 18, 561-562.
    d. Ab initio calculation in which the cis conformation is slightly favored: Grunde, R.; Azman, A. J. Mol. Struct. **1975**, 27, 212-215.

    Bach has calculated that the energy level of the bond in allyl alcohol is 10 kcal/mole lower for a dihedral angle of 90° than for the planar (0°) rotamer. For the allylic alkoxide anion, on the other hand, very little energy difference is found for dihedral angles between 0 and 90° (though the 180° conformation is 9 kcal/mole lower in energy than the 0° conformation): Bach, R.D.; Wolber, G.J.; Coddens, B.A., submitted for publication.

117. Houk, K.N.; Moses, S.R.; Wu, Y.-D.; Rondan, N.G.; Jager, V.; Schohe, R.; Fronczek, F.R. J. Am. Chem. Soc. **1984**, 106, 3880-3882.

118. Hill, J.G.; Sharpless, K.B., unpublished results.

119. The carbonyl groups of amides are significantly more basic than those of esters. See Gutmann, V. "Coordination Chemistry in Non-Aqueous Solutions"; Springer-Verlag: Wien, 1968, p 19. Gutmann, V. Chemtech **1977**, 255-263.

120. Serjeant, E.P.; Dempsey, B. "Ionisation Constants of Organic Acids in

Aqueous Solution"; IUPAC Chemical Data Series No. 23; Pergamon: Oxford; 1979.

121. Burns, D.B.; Sharpless, K.B., unpublished results.

122. Peacock, R.D.; Stewart, B. Coord. Chem. Rev. **1982**, 46, 126-157.

123. See footnote 10 in reference 3c.

124. Still, W.C.; Kahn, M.; Mitra, A. J. Org. Chem. **1978**, 43, 2923.

125. Martin, C.A.; Sharpless, K.B., unpublished results.

126. a. Burfield, D.R.; Lee, K.-H.; Smithers, R.H. J. Org. Chem. **1977**, 42, 3060-3065.
b. Burfield, D.R.; Smithers, R.H. J. Org. Chem. **1978**, 43, 3966-3968.
c. Burfield, D.R.; Smithers, R.H.; Tan, A.S.C. J. Org. Chem. **1981**, 46, 629-631.
d. Burfield, D.R.; Smithers, R.H. J. Org. Chem. **191983**, 48, 2420-2422.

127. a. Van Rheenan, V.; Kelly, R.C.; Cha, D.Y. *Tetrahedron Lett.* **1976**, 1973-1976.
b. For a review of catalytic osmylations, see, Schroder, M. Chem. Rev. **1980**, 80, 187-213.

128. Ott, D.G. "Syntheses with Stable Isotopes"; Wiley-Interscience: New York, 1981.

129. Mitsunobu, O. Synthesis **1981**, 1-28.

130. Fieser, L.F.; Fieser, M. "Reagents for Organic Synthesis"; Wiley-Interscience: New York, page 584.

131. Corey, E.J.; Katzenellenbogen, J.A.; Posner, G.H. J. Am. Chem. Soc. **1967**, 89, 4245-4247.

132. a. Evans, D.A.; Bartroli, J.; Shih, T.L. J. Am. Chem. Soc. **1981**, 103, 2127-2129.
b. Evans, D.A.; Bartroli, J. Tetrahedron Lett. **1982**, 23, 807-810.
c. For a review, see: Evans, D.A. Aldrichimica Acta **1982**, 15, 23-32.

133. Nicolaou, K.C.; Duggan, M.E.; Ladduwahetty, T. Tetrahedron Letters **1984**, 25, 2069-2072.

134. Reference 2a, page 92, Table 3.1.

135. Williams, H.R.; Mosher, H.S. J. Am. Chem. Soc. **1954**, 76, 2984-87.

136. Jacques, J.; Gros, C.; Bourcier, S. "Stereochemistry, Fundamentals and Methods"; Kagan, H.B., Ed.; Georg Thieme Publishers: Stuttgart; Volume 4, p 229b, 1977.

137. Asami, M.; Ohno, H.; Kobayashi, S.; Mukaiyama, T. Bull. Chem. Soc. Jpn. 1978, 51, 1869-1873.

Biographical Note

The author was born on October 23, 1958, in Atlantic City, New Jersey. He graduated from the California Institute of Technology in 1980, receiving an Eastman Kodak Scholarship from 1977-1980. Following a summer research position at the Eastman Kodak Company in Rochester, New York, he enrolled at the Massachusetts Institute of Technology in 1980, joining the Sharpless research group. He will pursue postdoctoral studies in the laboratory of Professor James P. Collman at Stanford University, funded by a postdoctoral fellowship from the National Institutes of Health.